The biomechanics of collective neural crest cell chemotaxis

Adam Shellard

A thesis submitted in partial fulfilment for the degree of Doctor of Philosophy

University College London

December 2018

I, Adam Shellard, confirm that the work presented in this thesis is my own. Where information has been derived from other sources, I confirm that this has been indicated in the thesis.

Abstract

Collective cell migration underlies various events in development, regeneration and disease. In most cases *in vivo*, collective migration occurs by collective cell chemotaxis, the directed migration of cell groups along gradients of soluble chemical cues. Despite this, the mechanisms of collective cell chemotaxis are poorly understood. Here I use *Xenopus* and zebrafish neural crest, a highly migratory embryonic stem cell population whose behaviour has been likened to malignant invasion, to study collective chemotaxis *ex vivo* and *in vivo*. I show that the neural crest exhibits a tensile actomyosin ring at the edge of the migratory cell group that contracts in a supracellular fashion. This contractility is polarized during collective cell chemotaxis: it is inhibited at the front but persists at the rear of the cell cluster. Combining computational simulations with optogenetic and laser ablation experiments, I show that this differential contractility drives directed collective cell migration *ex vivo* and *in vivo* through intercalation of rear cells. Rear cell intercalation triggers a wave of cellular anterograde movement through the middle of the cluster that drives the whole group forward. The mechanically coupled cells at the edge of the group are pulled to the rear by the actomyosin contractility. This novel mechanism of collective cell chemotaxis can be conceptually visualized as squeezing a tube of tooth paste at the back, which pushes the toothpaste forward. Thus, in neural crest cells, the engine for collective chemotaxis is at the rear of the cell group.

Surprisingly, many of the cell behaviours that I describe here for the whole cell cluster have an equivalent in directional migration of single cells. For example, contraction of rear cells within a cluster is equivalent to actomyosin contraction at the back of single cells during directional migration; retrograde movement of cells in the periphery of the cluster could correspond to the surface/cortex retrograde flow observed in single cells; and rear intercalation and forward movement of cells at the centre of the cluster is analogous to rear endocytosis and forward movement of vesicles in single cells. In summary, I have discovered a novel mechanism of collective cell migration in which we can consider the whole cluster as a single ‘supracell’.

Impact statement

In this thesis, the mechanism underlying collective neural crest cell chemotaxis is studied. The cranial neural crest contributes to the majority of skeletal and connective tissues in the face, meaning the tissues of the craniofacial complex are primarily derived from the neural crest. Craniofacial malformations are observed in ¾ of human birth defects and are typically recognised by abnormalities in the underlying structure of the face. Therefore, craniofacial abnormalities are usually attributed to problems in neural crest cell development, including its migration. For example, perturbed neural crest migration can result in babies with small noses, jaws and ears as well as cleft palate. These phenotypes are characteristic of Treacher Collins syndrome. Given the variety of craniofacial abnormalities, it is therefore essential to understand the mechanisms that regulate the migration of cranial neural crest as a prelude to understanding the origins of birth defects and their prevention or repair.

An understanding into the mechanisms of collective cell migration and collective cell chemotaxis has relevance for a variety of pathologies in which cell motility is aberrant. A prominent example is cancer invasion, to which neural crest migration has been compared. In this thesis, I study the migration of the cranial neural crest, which moves in a highly collective manner. Similarly, many cancer cells use collective migration as a strategy to move from the primary tumour along blood vessels to new tissues. Specifically, in this thesis I study the mechanism by which cranial neural crest undergoes collective chemotaxis; external chemotactic signals are essential for their normal development. Likewise, various signalling pathways have been implicated in the metastatic spread of a multitude of human tumours. Tumour cells frequently express chemokine receptors, which allows them to become migratory and respond to external cues, and tumour cells can express chemokines themselves which promotes tumour cell growth, angiogenesis and the formation of immunotolerant microenvironments. Given most cancer-related deaths come from metastasis, and collective migration occurs commonly in many types of cancer metastasis, uncovering details of neural crest migration informs a general understanding of collective cell migration, including that which occurs during cancer metastasis; and such knowledge could be implicated in the prevention and treatment of metastatic tumours, such as melanomas.

Acknowledgements

Disaster was well averted in my PhD thanks to invaluable contributions from so many. Of course, first and foremost I thank my supervisor, Prof. Roberto Mayor, for the upmost guidance and supervision through my time in the lab. Next, I want to give a big thank you to Dr. András Szabó, who generated the computational model that is laid out in this thesis and who helped with PIV analysis. Our Friday discussions lasted eternally, but despite my craving to get to drink-o'clock Fridays, it was well worth it!

Very many thanks are owed to colleagues-turned-friends past and present members of the Mayor lab. I'd like to thank Isabel Bahm (for letting me mock and distract her during her daily dispersion analysis), Maria Kotini (for, despite her fearsomeness, not kicking me), Jon Leslie (for supervising me in my rotation, and for your warnings), András Szabó (for always fixing my FIJI), Melissa Turan (for stealing my biscuits and chair), Alfredo Sansone (for vaffanculo), Alice Roycroft (for her endless levels of optimism and cheeriness), Elena Scarpa (for her supervision, in spite of the knowledge of my incompetence at dissection), Elias Barriga (for the Jägerbombs, Embryology Party playlist, and for breaking my finger), Becky Jones (for the memes and gifs), and Nil Ege (for exchanging stupid YouTube videos).

Next, thanks to Xavier Trepat for the optogenetic constructs, to my thesis committee, Dr. Masa Tada and Prof. David Wilkinson, and to the Wellcome Trust for funding.

A thank you goes to my course mates, Scott Haston and Rosalyn Flower. Friday night jokes, drinks and chats with you quickly became an imperative part of my week that allowed me to survive this journey. Thanks for taking me with you and for keeping me grinning when things have been going badly (or, occasionally, well)! Lots of really great times were spent at the plethora of pubs and bars around UCL, who I thank for enthusiastically serving me over the years. I thank my out-of-lab friends with whom I routinely rehabilitated, including David Dylus, Antonio Ferreira and Flavie Lespat.

By the same token, I thank everyone who has helped, supported and encouraged me over the course of my PhD, particularly my parents.

Moving onto the next stages of academic life, I eagerly await the next challenging, bullish adventure; wish me luck!

Table of contents

List of figures

List of tables

List of movies

Movie 1. Photoablation and recoil of the actin (LifeAct, magenta) cable in an edge neural crest cells of an explant expressing at the edge of an explant. Ablation occurs at t = 0 s. Membrane is cyan. Scale bar, 5 μm.

Movie 2. Simulated clusters with uniform contractility: high contractility at both the front and rear (left), or rear contractility only (right). Inner cells are green; outer cells are yellow (contractile) or grey (non-contractile). Movie is 10,000 simulated time-points.

Movie 3. Simulated cluster with high rear contractility. Left, the cells of the centred cluster with colour indicating the direction of motion. Right, the centre of mass of the cluster. Note the forward moment of cells down the middle and rearward movement of cells at the cluster edge. Movie is 5000 simulated time-points.

Movie 4. Simulated cluster with no relaxation (continuous rear contraction). Inner cells are green; outer cells are yellow (contractile) or grey (non-contractile). Movie is 5,000 simulated time-points.

Movie 5. Neural crest grafts (magenta) *in vivo* in wild-type host embryos. Grafts are expressing or not expressing optoGEF-contract (right and left, respectively), and a membrane marker. The green box represents the area of optogenetic activation with the 488-nm laser. Ventral migration is down. Scale bar, 100 μm.

Movie 6. Neural crest grafts (magenta) *in vivo* in wild-type host embryos. Grafts are expressing or not expressing optoGEF-relax (right and left, respectively), and a membrane marker. The green box represents the area of optogenetic activation with the 488-nm laser. Ventral migration is down. Scale bar, 100 μm.

Movie 7. Neural crest grafts (magenta) *in vivo* in SDF1-morphant host embryos expressing or not expressing optoGEF-contract (right and left, respectively), and a membrane marker. The green box represents the area of optogenetic activation with the 488-nm laser. Ventral migration is down. Scale bar, 100 μm.

List of abbreviations

ABP	Actin-binding protein
ADAM	A disintegrin and metalloproteinase
ADF	Actin-depolymerising factor
ANOVA	Analysis of variance
AP	Alkaline phosphatase
aPKC	Atypical protein kinase C
Arp	Actin related protein
BA	Branchial arch
BCIP	5-bromo-4-chloro-3-indoyl-phosphate
BCR	Blastocoel roof
BMP	Bone morphogenetic protein
BSA	Bovine serum albumin
C3a	Complement component 3a
C3aR	Complement component 3a receptor
CA-MLC	Constitutively active myosin light chain
Cdc42	Cell division control protein 42 homologue
CIL	Contact inhibition of locomotion
Cx	Connexin
CXCL	C-X-C motif ligand
CXCR	C-X-C motif ligand receptor
DEPC	Diethylpyrocarbonate
DFA	Danilchick’s Medium for Amy
Dig	Digoxigenin
DMSO	Dimethyl sulfoxide
E-Cadherin	Epithelial cadherin

ECM	Extracellular matrix
EMT	Epithelial-to-mesenchymal transition
F-actin	Filamentous actin
FAK	Focal adhesion kinase
FDX	Fluorescein-dextran
FGF	Fibroblast growth factor
FGFR	Fibroblast growth factor receptor
FRET	Förster resonance energy transfer
G protein	GTP binding protein
G-actin	Globular actin
GAP	GTPase-accelerating protein
GDP	Guanosine diphosphosphate
GEF	Guanine-nucleotide exchange factor
GFP	Green fluorescent protein
GPCR	G-protein coupled receptor
GSK3β	Glycogen synthase kinase 3β
GTP	Guanosine triphosphate
HGF	Hepatocyte growth factor
HIF	Hypoxia-inducible factor
ISH	*in situ* hybridisation
LPA	Lysophosphatidic acid
LPAR	Lysophosphatidic acid receptor
LPD	Lamellipodin
MAPK	Mitogen-activated protein kinase
MDCK	Madin-Darby Canine Kidney
MEM	Minimum essential medium

MEMFA	Minimum essential medium with formaldehyde
MET	Mesenchymal-to-epithelial transition
MLC	Myosin light chain
MLCK	Myosin light chain kinase
MMP	Matrix metalloproteinase
MMR	Marc’s modified Ringer’s
MO	Morpholino oligomer
mRNA	Messenger ribonucleic acid
MTOC	Microtubule-organising centre
MYPT	Myosin phosphatase targeting protein
NAM	Normal amphibian medium
NBT	4-nitro blue-tetrazolium-chloride
N-Cadherin	Neuronal cadherin
NCAM	Neural cell adhesion molecule
NRG	Neuregulin
NT	Neurotrophin
NTP	Nucleoside triphosphate
Par	Partitioning-defective
PBS	Phosphate buffered solution
PBT	Phosphate buffered solution with Triton-X
P-Cadherin	Placental cadherin
PCP	Planar cell polarity
PCP	Planar cell polarity
PDGF	Platelet-derived growth factor
PDGFR	Platelet-derived growth factor receptor
PGC	Primordial germ cell

$PI(3,4)P_2$	$Phosphoinositide(3,4)P_2$
PI3K	Phosphoinositide-4,5-bisphosphate 3-kinase
PIP_3	$Phosphoinositide(3,4,5)P_3$
PIV	Particle image velocimetry
PLLp	Posterior lateral line primordium
pMLC	Phospho-myosin light chain
PMSG	Pregnant serum mare gonadotrophin
PtdIns	Phosphoinosidies
PTEN	Phosphatase and tensin homologue
PTEN	Phosphatase and tensin homology
PVF	PDGF/VEGF related factor
PVR	PDGFR/VEGFR related factor
r	Rhombomere
RA	Retinoic acid
Rac	Ras-related C3 botulinum toxin substrate
RDX	Rhodamine-dextran
Rho	Ras homologue
ROCK	Rho-associated protein kinase
SCF	Stem cell factor
SDF	Stromal cell-derived factor
TBS	Tris-buffered saline
TGF	Transforming growth factor
UAS	Upstream activating sequence
VE-Cadherin	Vascular endothelial cadherin
VEGF	Vascular endothelial growth factor
VEGFR	Vascular endothelial growth factor receptor

WASP	Wiskott-Aldrich syndrome protein
WAVE	WASP-family verprolin-homologous protien
ZO	Zona occludens

Introduction

Note that parts of the introduction have been used or adapted from Shellard & Mayor, 2016.

1 Cell migration

1.1 Introduction to cell migration

Cell motility is an evolutionarily ancient process that is essential in many aspects of life. Cell migration refers to the process whereby a cell changes its location from one position to another. Migratory phenomena are apparent in aerobic and anaerobic conditions, prokaryotic and eukaryotic organisms, and in unicellular and multicellular organisms. Prokaryotes use structures like flagellum to performing rotating movements or pili for ameboid-like movement, while others use their cell body to generate sliding movements. Cells exploit migratory behaviour in search for food or to avoid hostile and unfavourable conditions, as observed in bacterial and protozoan locomotion (Baker et al., 2006, Netotea et al., 2009). Unicellular eukaryotic cells, such as the social amoeba *Dictyostelium discoideum* can also migrate, as can most cells in multicellular organisms, which are able to move during defined phases of tissue formation, maintenance, regeneration and wound healing (Cattaruzza and Perris, 2005), and immune defence (Bleul et al., 1996, Aiuti et al., 1997). In this manner, cell migration is a fundamental morphogenetic process; it is crucial for tissue and organ formation. Furthermore, cells employ migratory capabilities in a multitude of diseases such as chronic destructive inflammation (failed immune cell migration), osteoporosis (failed mesenchymal stem cell migration), atherosclerosis (monocytes and smooth muscle cells migrate to the sites of vascular injury), mental retardation (defective neuronal migration) and cancer metastasis (recapitulation of migratory capacity) (Ewald et al., 2008, Nieto and Cano, 2012, Davis et al., 2014).

Cell migration is a highly complex and intricate process, relying on numerous coordinated events. Moreover, it is becoming increasingly evident that cells are highly plastic in their ability to migrate in different modes depending on context. This chapter will first discuss fundamental processes that underlie single cell migration, and then evaluate how these features are used by groups of cells that move together by collective cell migration.

1.2 Single cell migration

1.2.1 Introduction

Single cell migration, in which cells move solitarily, is important for development, immune surveillance and cancer metastasis *in vivo* (Ridley et al., 2003, Friedl and Weigelin, 2008). Most knowledge on the mechanisms of cell migration have derived from studying single cell migration *in vitro* on 2D substrates.

1.2.2 Focal adhesion-dependent cell migration

1.2.2.1 The migration cycle

Cell migration is an integrated multistep process (Ridley et al., 2003). Migrating cells are highly polarised with complex regulatory pathways that spatially and temporally integrate various processes. In general, cell migration can be conceptualised as a cyclic process (Lauffenburger and Horwitz, 1996). First, the cell must polarise, meaning it has distinct regions. In the case of cell migration, this means generating a front-rear polarity. Polarity is generated in response to migration-promoting factors such as diffusible chemical signals, extracellular matrix (ECM) stiffness gradients or molecules comprising the ECM (Etienne-Manneville and Hall, 2003). Other times, cells can polarise randomly without the need of external signals established in a gradient. Polarised cells extend protrusions, such as lamellipodia, filopodia and invadopodia, which are driven by actin polymerisation, in the direction of migration (Ananthakrishnan and Ehrlicher, 2007), or via the formation of blebs, which are small, roundish protrusions generated by hydrostatic pressure and initially devoid of F-actin (Paluch and Raz, 2013). Protrusions are stabilised via adherence to the ECM through focal adhesions, or to adjacent cells. In both cases, external components are linked to cell's intracellular cytoskeleton. Propulsive force for forward movement is generated through traction on these adhesion sites, which allows the cell to move forward (Geiger et al., 2001). Constant assembly and disassembly of adhesion sites at the front and rear, respectively, permits continual cell locomotion.

These fundamental processes occur in various cell types, although there are exceptions. For example, focal adhesion-free mechanisms of cell migration have been recently described (Section 1.2.3). Moreover, the molecular mechanisms can vary greatly. Distinct observation of these processes can be identified in slow-moving cells such as fibroblasts whereas fast-moving cell like neutrophils seem to glide over the substrate. It is also becoming apparent that cells are highly plastic and able to adopt different modes of motility depending on their environment. Many somatic and cancer cells have different protrusion dynamics, migration speeds and cytoskeletal activities different in *in vitro* and *in vivo* situations (Knight et al., 2000, Friedl and Wolf, 2003).

1.2.2.2 The protrusive machinery

In most classical modes of migration, the forward movement of a cell is driven by the polymerisation of actin filaments (filamentous actin; F-actin) at the leading (front) edge (Blanchoin et al., 2014). F-actin is a self-assembling filamentous structure of semi-flexible polymers consisting of actin monomers (globular actin; G-actin) that produces double-helix microfilament structures measuring 7 nm in diameter with the helix repeating every 37 nm (Gittes et al., 1993). F-actin has intrinsic polarity that results in, primarily, unidirectional growth; it has a fast-growing 'barbed' end and a slow-growing 'pointed' end. Organised assembly of actin filaments at the cell edge thereby drives membrane protrusion (Pollard and Borisy, 2003). The protrusion itself occurs by an 'elastic Brownian ratchet' mechanism. Filamentous actin stores thermal energy, which causes it to bend. When the filament is bent away from the plasma membrane at the cell edge, the addition of G-actin causes the filament to extend and release elastic energy that straightens the filament; in doing so, providing the force for membrane protrusion (Pollard and Borisy, 2003).

Actin nucleation, is the rate-limiting step of polymerisation (Krause and Gautreau, 2014, Welch and Mullins, 2002, Pollard and Borisy, 2003). The most studied nucleation proteins are the Arp2/3 complex (actin-related proteins 2 and 3), and the formin family proteins; other actin nucleators include spire, cordon-bleu, LMOD and JMY (Firat-Karalar and Welch, 2011). The rate-limiting step of actin nucleation is trimer formation (adding one G-actin monomer to the Arp2/3 complex). The Arp2/3 complex facilitates the formation of new F-actin by binding to the sides of pre-existing filaments and initiating the growth of daughter filaments at a 70^{o} angle from the mother filament. The Arp2/3 complex is highly active at the cell edge because it localises to molecular scaffolds including Wiskott-Aldrich syndrome protein (WASP)/WASP-family verprolin-homologous protein (WAVE) family members, which are themselves activated at the cell membrane (Welch and Mullins, 2002). The rate and organisation of actin polymerisation is regulated by actin-binding proteins (ABPs) which affect the pool of available monomers and free ends (Pollard and Borisy, 2003, Dos Remedios et al., 2003). A multitude of ABPs have been identified with varying functions (Fig. 1.1B), including nucleation, regulation of actin filament growth, stability and disassembly, monomer-binding, actin bundling and crosslinking, cytoskeletal linkers, membrane anchors and myosins which contract cross-linked actin filaments. Actin polymerisation is also coordinated by Ras homologue (Rho) family small guanosine triphosphate (GTP)–binding proteins, GTPases, which are conformationally regulated by GTP and guanosine diphosphate (GDP). On/off Rho GTPase activity is

coordinated by guanine nucleotide exchange factors (GEFs) and inactivated by GTPase activating proteins (GAPs). The Rho GTPases Rac (Ras-related C3 botulinum toxin substrate) and Cdc42 (cell division control protein 42 homologue) are required for the formation of lamellipodial and filopodial protrusions, by mediating actin polymerisation through activation of the WASP/WAVE family of Arp2/3 complex activators (Welch and Mullins, 2002), which also provide feedback to Rac and Cdc42 by binding to GAPs and GEFs (Soderling et al., 2002, Cory et al., 2002, Hussain et al., 2001). WAVE/WASP proteins can also be controlled by proteins involved in other aspects of cell activity, such as Src, Nck and WIP which regulate focal adhesions (Pollard and Borisy, 2003, Cory et al., 2002, Suetsugu et al., 2002, Higgs and Pollard, 2001, Moreau et al., 2000, Sasahara et al., 2002). Hence, actin polymerisation and cell protrusion are highly regulated processes.

The organisation of F-actin causes the formation of different types of cellular protrusions. Filopodia are organised into long parallel bundles thanks to filament bundling (Welch and Mullins, 2002). The tips of filopodia are enriched in Ena/VASP proteins, which antagonise capping and branching at the (growing) barbed end (Welch and Mullins, 2002). Fascin bundles adjacent F-actin polymers (Welch and Mullins, 2002). By contrast, lamellipodia are formed because of branched nucleation. Lamellipodial protrusions have F-actin in a branched dendric network, which gives the structure a fan-like shape (Pollard and Borisy, 2003). They are regulated by proteins such as the Ena/VASP binding protein lamellipodin (Krause et al., 2004), which promotes 3D and *in vivo* cell migration via its Ena/VASP and SCAR/WAVE interactions (Carmona et al., 2016, Law et al., 2013). The structural designs of lamellipodia and filopodia endows them with the capacity to perform distinct functions; filopodia act as exploratory sensors, whereas lamellipodial geometry allows the cell the crawl over a large surface.

1.2.2.3 Polarisation

Polarisation, the division of molecular processes within a cell, is essential for cell migration. Specifically, cells are polarised along the front-rear axis in a highly complex and regulated manner (Fig. 1.1A). The establishment and maintenance of polarity is required so that the cell is able to segregate molecules that are involved at the front of the cell, those that are involved at the rear, and everywhere in between. In doing so, persistent forward locomotion can be ensured. Cell polarity can arise cell-autonomously through a combination of local positive feedback loops and global inhibitors which amplifies tiny, stochastic variations (Wedlich-Soldner and Li, 2003),

although . Often, polarity is established in response to extracellular stimuli such as chemokines, ECM molecules or gradients in extracellular mechanical stiffness (Ladoux et al., 2016).

Cdc42 is a master regulator of cell polarity that localises specifically to the front of migratory cells (Itoh et al., 2002). It spatially confines where lamellipodia form (Srinivasan et al., 2003), and, by acting through the Par3/Par6/aPKC (Par defective, Par; atypical protein kinase C, aPKC) complex, localises the microtubule-organizing centre (MTOC) and Golgi apparatus in front of the nucleus. This further coordinates polarised migration by enabling the microtubule-mediated delivery of vesicles to the front, thereby allowing recycling of cellular components, such as membrane molecules (Etienne-Manneville and Hall, 2002, Rodriguez et al., 2003). Accordingly, inhibition of Cdc42 strongly abrogates persistent forward movement (Etienne-Manneville and Hall, 2002). There is extensive cross-regulation between Cdc42 and targets downstream of GTP-binding protein (G protein)–coupled receptors (GPCRs) and integrins, which are responsive to chemotactic cues and the ECM, respectively, which together contribute to generating and maintaining high Cdc42 activity at the leading edge (Li et al., 2003, Etienne-Manneville and Hall, 2002, Etienne-Manneville and Hall, 2001). In the case of single cell chemotaxis (the movement of cells in response to gradients of soluble chemical cues), signal cross-talk and amplification is essential for efficient directed migration, because diffusion often renders chemotactic gradients very shallow. The spatial limitations of a cell mean a recognition between high and low chemotactic levels (through GPCR activation on its membrane) at the front and rear is challenging. Amplification of signal into steeper intracellular signalling gradients, which generate the cellular response of chemotaxis allows cells to respond in a highly directional manner (Devreotes and Janetopoulos, 2003). The amplification process involves the localised activation of phosphoinositide-4,5-bisphosphate 3-kinase (PI3K) at the front, and phosphatase and tensin homologue (PTEN) at the rear. This response is evident in *Dictyostelium* (Devreotes and Janetopoulos, 2003, Merlot and Firtel, 2003), which undergo chemotaxis to cAMP. PI3K and PTEN control the levels of the phosphoinositides PtdIns(3,4,5)P_3 (PIP_3) and PtdIns(3,4)P_2 [PI(3,4)P_2] (Devreotes and Janetopoulos, 2003, Merlot and Firtel, 2003). Cells with modified PI3K or PTEN exhibit a reduced ability to undergo chemotaxis, illustrating the importance of this amplification.

Cdc42 and PI3K regulate polarity through activation of the actin polymerisation machinery required for active protrusions. This is achieved by local activation or delivery of Rac GEFs (Welch et al., 2003). Active Rac maintains directional

protrusions by stimulating recruitment and activation of PI3K to the plasma membrane, positively regulating microtubule polymerisation and recruitment and clustering of activated integrins to the edge of lamellipodia (Srinivasan et al., 2003, Welch et al., 2003, Rodriguez et al., 2003, del Pozo et al., 2000, Kiosses et al., 2001, Shattil, 1995). All of these factors positively regulate Rac as well, thereby maintaining the front polarity.

In contrast to Rac, Rho (described in more detail in Section 1.2.2.4) preferentially localises at the cell rear and is also involved in maintaining front-rear polarity. However, RhoA can also be locally and dynamically activated at the leading edge, contributing to lamellipodial dynamics (Heasman et al., 2010). Rho promotes myosin II activity, which in turn binds to actin filaments (then termed actomyosin), which contracts the actin cytoskeleton in an ATP-dependent manner. Accordingly, inhibition of Rho leads to deformation in cell shape; often, migrating cells are elongated because the rear can no longer contract. Rho is also involved in microtubule stabilisation (Rodriguez et al., 2003, Small and Kaverina, 2003). Both events promote focal adhesion turnover specifically at the cell rear. Rac and Rho are mutually antagonistic, repressing each other's activity (Evers et al., 2000), meaning no protrusions are generated other than at the front (Worthylake and Burridge, 2003, Xu et al., 2003). Hence, front and rear zones of different protein pools are generated in polarised migratory cells. However, active Rac has been implicated in detachment at the rear of migrating cells (Gardiner et al., 2002), and also Rho can lead to Rac activation (Tsuji et al., 2002) so it is clear that generation and maintenance of cell polarity is a highly complex process.

Cell polarity is maintained by a combination of the above molecular-based feedback mechanisms, and through physical forces. In regions of protrusion, the membrane is stretched, and the tension exerted upon it is transmitted across the rest of the cell membrane to inhibit actin assembly and Rac activation, thereby maintaining front-rear polarity (Houk et al., 2012). In migrating neutrophils, increasing membrane tension interferes with actin nucleation (Houk et al., 2012) through phospholipase and MTOR signalling (Diz-Munoz et al., 2016). Membrane tension also regulates the speed and geometry of actin polymerisation by acting as a physical barrier; when membrane tension is high, a dense, branched actin network forms, whereas a less dense network forms when membrane tension is lower, with filaments forming perpendicular to the membrane (Mueller et al., 2017). Conversely, low membrane tension triggers actin assembly, and enhances cell spreading and polarisation (Raucher and Sheetz, 2000). Thus, membrane tension serves as an essential regulator of cell polarity.

Interestingly, although individual cell migration by definition means cells are not moving while bound to each other, components of the cadherin-catenin complex, normally associated with cell-cell adhesions, function to stabilise front-rear polarity in mouse neural crest cells and glioblastoma cells to promote directional solitary migration; β- and αE-catenins are transported from the lamellipodium to perinuclear regions (Vassilev et al., 2017). αE-catenin determines perinuclear localisation of RhoA via RhoGEF regulation, and perinuclear RhoA supports myosin-IIB assembly to stabilise cells' front-rear polarity (Vassilev et al., 2017).

1.2.2.4 Integrins and adhesion

Actin polymerisation drives the formation of protrusions at the cell front. Actin flows away from the cell backwards with respect to the substrate, in a process known as retrograde flow, that is driven by actin polymerisation and myosin motors (Cramer, 1997, Lin et al., 1997, Watanabe and Mitchison, 2002). Actin flows provides a means for the cells to stay in contact with the substrate. The developing protrusion can be anchored to the substrate: cell-matrix adhesions cross-link the ECM to the intracellular actin cytoskeleton, reducing actin retrograde flow, and meaning cell-matrix adhesions act as 'molecular clutches' through their ability to couple retrograde flow to the substrate. This coupling promotes protrusive growth due to the continuous actin polymerisation, suppresses membrane contraction and transmits contractile forces to the substrate which causes the cell to be pulled forward (Alexandrova et al., 2008, Parsons et al., 2010, Gardel et al., 2010). Together, protrusion formation and traction force help drive cell migration. Hence, not only is stabilisation of protrusions achieved by attachment to the surroundings, but also the interaction between the cell and the ECM represents the primary source of force generation for cellular migration. That being said, actin retrograde flows do not necessarily need to be coupled to the substrate via integrin-dependent adhesions for cell migration (non-adhesive migration is discussed in Section 1.2.3). Cells that are in confinement and lacking cell-ECM adhesions utilise strong actin retrograde flow for the forces of motility; such frictional forces resisting retrograde flow maintain the cell body in place and as myosin contractility on the actin network drives contraction (Bergert et al., 2015, Paluch et al., 2016).

Cell-matrix adhesions are large dynamic transmembrane multi-protein complexes that indirectly crosslink the ECM to the intracellular cytoskeleton. This coupling allows them to generate both a physical and a regulatory connection in which mechanical and chemical signals are transduced that can result in force generation, cytoskeletal

rearrangements and the activation of many signalling pathways that regulate cell behaviour (Wolfenson et al., 2013). In doing so, cells can respond to the stiffness and composition of the ECM (Boettiger, 2012, Dabiri et al., 2012).

Integrin-based cell-matrix adhesions are the most common and widely studied form of cell-matrix adhesions, although other forms of cell-matrix adhesions such as those composed of syndecan and selectin also exist (Tedder et al., 1995, Carey, 1997, Woods and Couchman, 2001, Barthel et al., 2007). Integrin heterodimers, consisting of an α and a β subunit, are transmembrane receptor proteins that connect the ECM to the cytoskeleton via large ligand-binding extracellular domains and short cytoplasmic domains (Tamkun et al., 1986). The many different α and β subunits result in a wide range of possible combinations. For example, humans have 18 different α subunits and 8 different β subunits, which together can form a minimum of 24 different combinations. These different combinations give rise to the specificity for various ECM components, such as different laminins, collagens or fibronectin, and thereby facilitate migration of cells to the correct location during embryogenesis and tissue morphogenesis (Bokel and Brown, 2002).

Integrin-mediated adhesion is a tightly regulated process. Activated integrins (Fig. 1.1B) undergo conformational changes that can be driven by different mechanisms (Wehrle-Haller, 2012). Fundamentally, binding of integrin to either the ligand in the ECM or intracellular talin/kindlin at sites of actin polymerisation causes a conformational change in the integrin dimer that allows it to bind to intracellular or extracellular components. These mechanisms are referred to as ‘outside-in’ or ‘inside-out’ activation, respectively. Once integrins are crosslinked to both the ECM and the cytoskeleton, they aggregate together (Fig. 1.1B). Clustering of active integrins is critical to form large multiprotein complexes that facilitate strong anchoring due to the low binding affinity of integrin for the ECM. Integrin clustering is triggered by the binding of talin to the cytoplasmic tail of activated integrin (Cluzel et al., 2005). Actomyosin-driven contractile forces lead to further clustering of integrin to enhance the size and strength of cell-matrix adhesions (Yu et al., 2011). Active and clustered integrins initiate diverse intracellular signalling pathways that, among other jobs, regulate further formation and strengthening of adhesion sites (Geiger et al., 2001). Integrin clustering is less evident in faster moving cells, which have less time to aggregate. For instance, neutrophils form ‘focal complexes’ which do not have extensive integrin clustering, but tend to not mature into ‘focal adhesions’. By contrast, slower moving cells have more time to aggregate strongly clustered focal adhesions. The generation of focal adhesions requires the recruitment of many associated

proteins. Some enter adhesions in preformed cytoplasmic complexes (Webb et al., 2002), whereas other components enter adhesions with distinct kinetics. Components are also differentially recruited based on adhesion maturity; for example, paxillin is present in focal complexes, whereas α-actinin is more prominent in older adhesions (Webb et al., 2002). Therefore, assembly of the exact composition of focal adhesions is highly regulatory.

Integrins do not have any catalytic activity themselves; signals are rather transmitted via its direct and indirect interactions. While they bind directly to ECM ligands, they are only coupled to F-actin via adapter proteins such as talin (Horwitz et al., 1986), α-actinin (Otey et al., 1990), paxillin (Liu et al., 1999) and vinculin (Burridge and Mangeat, 1984, Johnson and Craig, 1995). In addition to this coupling role, adapter proteins also have other functions. They can act as scaffolders; for example, p130Cas can bind to many other proteins and facilitate several of the downstream functions of cell-matrix adhesions (Wozniak et al., 2004, Mitra et al., 2005). Adapter proteins can also recruit signalling proteins, such as the tyrosine kinases, focal adhesion kinase (FAK) and Src. These signalling proteins can activate integrins and other downstream targets (Klinghoffer et al., 1999), and recruit GEF and GAP proteins, which regulate small GTPases. Hence, Src and FAK, among others, are key components of cell-matrix adhesions and crucial for their regulation as well as their function. Integrins are also regulated by post-translational modifications. For instance, phosphorylation of α4 integrin in migrating cells promotes the release of bound paxillin, thereby stabilising lamellipodia. Activated integrins preferentially localize to the leading edge to form new adhesions (Kiosses et al., 2001) due to the regulation of integrin's affinity for external ECM molecules by its intracellular interactions. For example, the GTPase Rap 1, PKC, and talin increase integrin activity, whilst Raf-1 kinase suppresses its activation (Fig. 1.1B) (Kinbara et al., 2003).

The extensive signalling capabilities of focal adhesion complexes allows them to act as mechanosensors, conveying information on the physical state of the ECM via mechanically-induced conformational changes in focal adhesion-associated proteins and altered cytoskeletal dynamics (Lauffenburger and Horwitz, 1996, Beningo et al., 2001, Galbraith et al., 2002). Moreover, highly regulated signalling at focal adhesion complexes means cells can coordinate traction generation correctly in a manner that will permit efficient locomotion. Optimal migration is achieved at intermediate levels of actin retrograde flow and traction force because migrating cells must be able to detach from the underlying substrate and simultaneously exert traction; hence, migration speed is a biphasic function of the strength of cell attachment

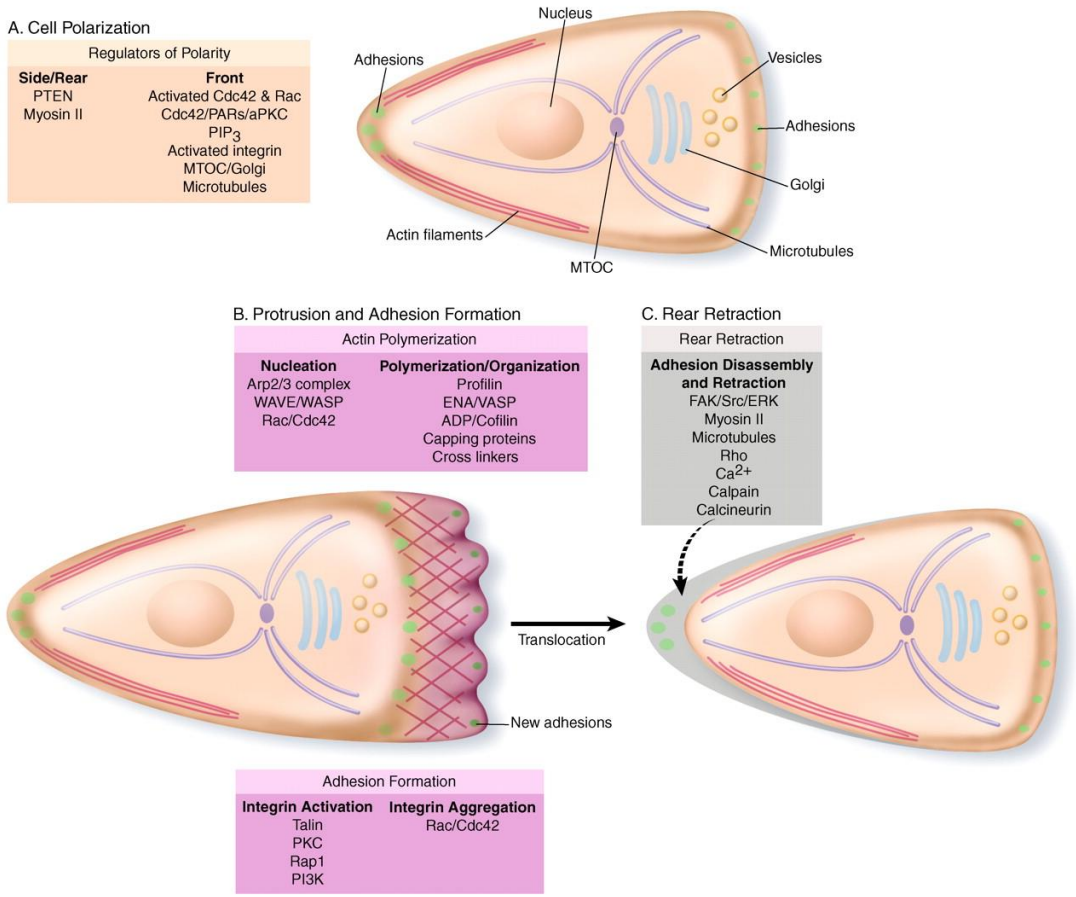

Fig. 1.1. Features of cell migration. (A to C) Diagrams and boxes illustrating some of the main regulators of cell polarity (A), protrusion (B, upper box), adhesion (B, lower box) and rear retraction (C).

Adapted from (Ridley et al., 2003).

(Gardel et al., 2008). The propulsive forward force derived from focal adhesion is based on the interaction of myosin II with the actin cytoskeleton. Myosin is a motor protein that contracts actin in adenosine triphosphate (ATP)-dependent manner. Myosin II is comprised of two heavy chains, two regulatory light chains and two essential light chains that form a head domain that binds F-actin and uses ATP hydrolysis to 'walk' towards the barbed end, a linker neck domain and a tail domain that mediates interaction with other molecules (Vicente-Manzanares et al., 2009). Myosin bound to actin allows myosin to function as a motor that drives F-actin filament sliding in this 'walking' mechanism, thereby contracting bundles or networks of actin (Murrell et al., 2015). Myosin II activity is regulated by myosin light-chain (MLC) phosphorylation, controlled by various kinases (e.g. MLC kinase, MLCK; Rho kinase, ROCK) and phosphatases (e.g. MLC phosphatase, which it inhibited by ROCK) (Agarwal and Zaidel-Bar, 2018). These upstream activators are themselves controlled in different ways; for example, ROCK is regulated by Rho, and MLCK is regulated by phosphorylation and intracellular calcium (Riento and Ridley, 2003). MLC phosphorylation activates myosin, resulting in increased contractility and transmission of tension to sites of adhesion, by enabling the myosin cross bridge to bind to the actin filament (Vicente-Manzanares et al., 2009).

At the migratory front, cell-matrix adhesions disassemble as new protrusions are formed (Webb et al., 2002). This disassembly is controlled by many molecules, including FAK, Src, Cas and Crk which together activate Rac-specific GEFs and ERK signalling that promote adhesion turnover (Larsen et al., 2003, Turner et al., 2001, Brahmbhatt and Klemke, 2003). Microtubules have also been implicated in focal adhesion dynamics (Stehbens and Wittmann, 2012). Hence, FAK and Src are used to assemble focal adhesions at the leading edge, before contributing to its disassembly through activation of Rac and ERK. However, some adhesions persist and mature into larger, more stable, mature and strongly adhesive structures. These focal adhesions are disassembled at the cell rear through actomyosin-mediated contractile forces (Fig. 1.1C). Also, the tension generated from the long tail to the anchor point can physically break the link between the integrin and the actin cytoskeleton. Interestingly, this tension is sufficient to open stretch-activated calcium channels (Lee et al., 1999), which can target calcineurin, calpin and ERK to cleave focal adhesion proteins including integrins, talin, vinculin, and FAK (Hendey et al., 1992, Glading et al., 2002). Local calcium can also activate myosin II activity through Calmodulin, which promotes MLCK activity. Indeed, myosin II is essential for the migration of the majority of cell types. In *Dictyostelium*, monocytes and neutrophils,

perturbed Rho, ROCK or myosin II activity impairs retraction of the cell rear, and spoils polarity, with multiple pseudopodia along the sides of the cell and actin organisation compromised (Chung et al., 2001, Worthylake and Burridge, 2003, Xu et al., 2003).

1.2.2.5 Rear-driven migration

The processes described above suggest that cell migration is a step-wise cyclical process in polarised cells; first protrusions are formed, next they are stabilised by focal adhesions and then rear retraction is mediated by contractility. However, there is significant evidence to suggest that initial polarisation and movement can also be driven by the rear, and not just from the front.

Contraction at the rear can initiate single cell migration. For example, in fibroblasts, actin depolymerisation-based force can retract the cell rear to polarise cells (Mseka and Cramer, 2011). Myosin II contractility, in this context, is initially required for aligning actin bundles that are needed for polarisation and later to maintain bundle length that ensures directed protrusion at the cell front (Mseka and Cramer, 2011). Initiation of single cell migration can also be driven from the front or rear depending on response to external chemotactic signals. In *Dictyostelium*, cells exposed to the chemoattractant cAMP break symmetry with a protrusion at the front, whereas cells exposed to the chemorepellent 8CPT break symmetry with rear retraction, which is myosin II-dependent (Cramer et al., 2018), meaning different chemotactic cues can initiate migration by distinct cytoskeletal mechanisms. Furthermore, in keratinocytes, immediately before the initiation of cell motility, actin network flow increases at the prospective cell rear in a myosin II-dependent manner (Yam et al., 2007).

Local stimulation of myosin II activity in stationary cells can even induce directed motility initiation away from the site of stimulation, suggesting it may be sufficient to start migration (Yam et al., 2007). Moreover, rear contraction is sufficient for migration in some adherent cells. Human breast adenocarcinoma cells invade based on a mechanism in which RhoA/ROCK/Myosin II is active at the cell rear in a uropod-like structure, transmitting traction forces via β1 integrin to the cell cortex (Poincloux et al., 2011), a specialised cytoplasmic layer on the inner face of the cell membrane enriched in F-actin, myosin and ABPs. In mitotic HeLa cells, the cortex is ~190 nm thick but this may vary in other cell types (Clark et al., 2013). Inhibition of actomyosin contractility abrogates invasion because contractile convergent retrograde forces are required to pull on the matrix in a rearward direction, generating forward movement of the cell that pushes the matrix at the front (Poincloux et al., 2011). Interestingly,

lamellipodial extension and the Arp2/3 complex are dispensable for the invasion of these cells. However, this contraction-based model is dependent on focal contacts, particularly at the lateral and rear edges, to transmit contractile forces to the substrate (Poincloux et al., 2011); therefore, it is distinct from migratory modes that are integrin-independent (Section 1.2.3).

1.2.3 Adhesion-independent cell migration

There is a comparatively high level of understanding of the molecular mechanisms involved in the classical mode of cell migration described above (Section 1.2.2). This has, in part, been enabled thanks to the ease of imaging single cell migration on 2D substrates *in vitro*. However, with the development of *in vivo* imaging tools and models, and *in vitro* technologies to study 3D migration, it has become increasingly clear that there are various modes of cell migration, and the stepwise process of 2D cell crawling does not represent the variety of migration styles found in 3D (Even-Ram and Yamada, 2005, Friedl and Brocker, 2000).

One such key difference is the requirement for substrate attachment. Many cell types have been shown to be able to undergo migration in an adhesion-independent manner (Paluch et al., 2016). These include leucocytes, various cells of the developing embryo and some cancer cells *in vivo* (Lammermann et al., 2008, Lammermann et al., 2013, Woolf et al., 2007, Bergert et al., 2015, Liu et al., 2015, Ruprecht et al., 2015, Kardash et al., 2010, Cattin et al., 2015). As they migrate, these cells are normally rounded, albeit their shape changes are highly dynamic, and they have weak or no cell-substrate adhesion, all while maintaining front-rear polarity. These features are characteristic of amoeboid cells. Moreover, there is convincing evidence that many migratory cell types are highly plastic, and able to switch between adhesion-dependent and adhesion-independent modes of migration, depending on the context (Liu et al., 2015, Ruprecht et al., 2015).

During amoeboid migration, cell confinement secures the plasma membrane surface to allow it to migrate without cell-matrix adhesions (Friedl et al., 2001). Indeed, physical confinement is sufficient to switch neutrophils from integrin-dependent to integrin-independent mode of locomotion; interestingly, despite the loss of propulsive traction forces, cells speed up (Toyjanova et al., 2015), because they are no longer adhered to a surface. Likewise, confinement promotes breast cancer invasion via adhesion-independent motility (Balzer et al., 2012).

Mechanistically, little is known about adhesion-independent migration, but a few different modes of force transmission have been proposed (Paluch et al., 2016).

Under confinement, cells can ‘push’ off the walls to retain cell shape and high actomyosin cortical contractility at the rear and protrusion expansion at the front drives cell movement (Hawkins et al., 2009). This type of migration can explain why some cell types, like leucocytes, can migrate only under confinement and not on flat surfaces (Lammermann et al., 2008). Another mechanism of confined cell migration is by contractile retrograde flows of the actomyosin cortex, which generates friction forces against the substrate that push the cell forward (Bergert et al., 2015). In the absence of confinement, cells can produce protrusions into the gaps of their microenvironment that help cells, like cancer cells, move in complex matrix geometries (Tozluoglu et al., 2013). Alternatively, in the absence of confinement, or surrounding cells/ECM, cells can ‘swim’ by generating propulsive forces that couple deformations in the membrane to the surrounding fluid (Barry and Bretscher, 2010, Leshansky et al., 2007, O'Neill et al., 2018, Lim et al., 2013). Although this mode of migration has been recently demonstrated experimentally by cells suspended in liquid (O'Neill et al., 2018), the *in vivo* relevance of this type of motility is unclear.

Mechanistically, in all these modes, amoeboid migration relies on strong actomyosin contractility, which is crucial for generating propelling forces; strong contractions at the cell rear generates cytoplasmic flows (Fig. 1.2B) (Friedl, 2004, Lammermann and Sixt, 2009, Pankova et al., 2010, Madsen and Sahai, 2010, Wolf and Friedl, 2006). Cortical contractility also favours a rounded cell shape and may therefore directly counteract adhesion. For example, myosin II knockout leads to impaired migration and increased spreading of T cells (Jacobelli et al., 2010), whereas increase cortical contractility favours a rounded amoeboid-like shape and non-adhesive migration (Bergert et al., 2012, Liu et al., 2015). Likewise, increasing contractility induces adhesion-independent migration of early germ layer progenitors in confinement (Ruprecht et al., 2015).

Hence, many cell types use or can switch to an amoeboid-style of migration by increasing cortical contractility, enhancing confinement and reducing substrate adhesion (Fig. 1.2A). However, this does not necessarily mean that all cell types are able to undergo integrin-independent migration. For example, while a number of cells including zebrafish early progenitors, cancer cells and fibroblasts can migrate effectively under confinement in the absence of integrins, other cell types like T cells seem to rely on cell-matrix adhesions (Overstreet et al., 2013). In the case of zebrafish primordial germ cells, cadherin-based interactions with neighbouring cells are used to transduced force (Kardash et al., 2010). Altogether it is clear that cell

migration, let alone collective migration, is a highly complex process, with varying modes and mechanisms to achieve effective cell motility.

1.3 Introduction to collective cell migration

1.3.1 An overview

Along with single cell migration, cells can also migrate while remaining in cohorts, which is referred to as collective cell migration (Friedl and Gilmour, 2009). During collective migration, cells remain connected as they move. This connection adds a layer of complexity to the group because cells must cooperate and coordinate their activity to move efficiently while remaining in contact. Thus, in different contexts, there are varying degrees of tissue organisation (Vaughan and Trinkaus, 1966, Friedl et al., 2004, Montell, 2008). Collective migration is particularly prevalent during embryonic morphogenesis, driving the formation of many complex tissues and organs and a comparable behaviour is recapitulated during tumour invasion. Collective cell migration is fundamental to many morphogenetic processes, and exhibited in wound healing and diseases like cancer metastasis (Vaughan and Trinkaus, 1966, Friedl et al., 2004, Friedl and Gilmour, 2009, Scarpa and Mayor, 2016). Although the key aspects of single cell migration are well established (Section 1.2) (Ridley et al., 2003, Nobes and Hall, 1999, Mattila and Lappalainen, 2008, Friedl and Wolf, 2009), the mechanisms underlying different forms of collective migration are much less well understood.

1.3.2 Defining collective cell migration and models

The primary hallmark characterising collective cell migration is that the cells remain mechanically and functionally coupled. Arguably, this is the only feature necessary for migration to be defined as collective. In the case of epithelial collective migration, intercellular adhesions are stable and preserved during movement, whereas in mesenchymal collective cell migration the junctions are transient (Friedl et al., 2004, Montell, 2008, Carmona-Fontaine et al., 2008b). A second hallmark characteristic of collective migration is that the cluster exhibits supracellular polarity and organisation of its cytoskeleton. This means that there is organisation at the level of the cluster. By consequence, the forces exerted through protrusions and focal adhesions are organised in a manner to generate movement of an entire tissue mass. Hence, collective migration is normally not simply multiple cells acting as much like individuals that are connected to one another, as this would often lead to disorganisation (Mayor and Etienne-Manneville, 2016). Instead, through some means of cell-cell interaction and communication, processes are re-arranged to achieve the movement of the entire

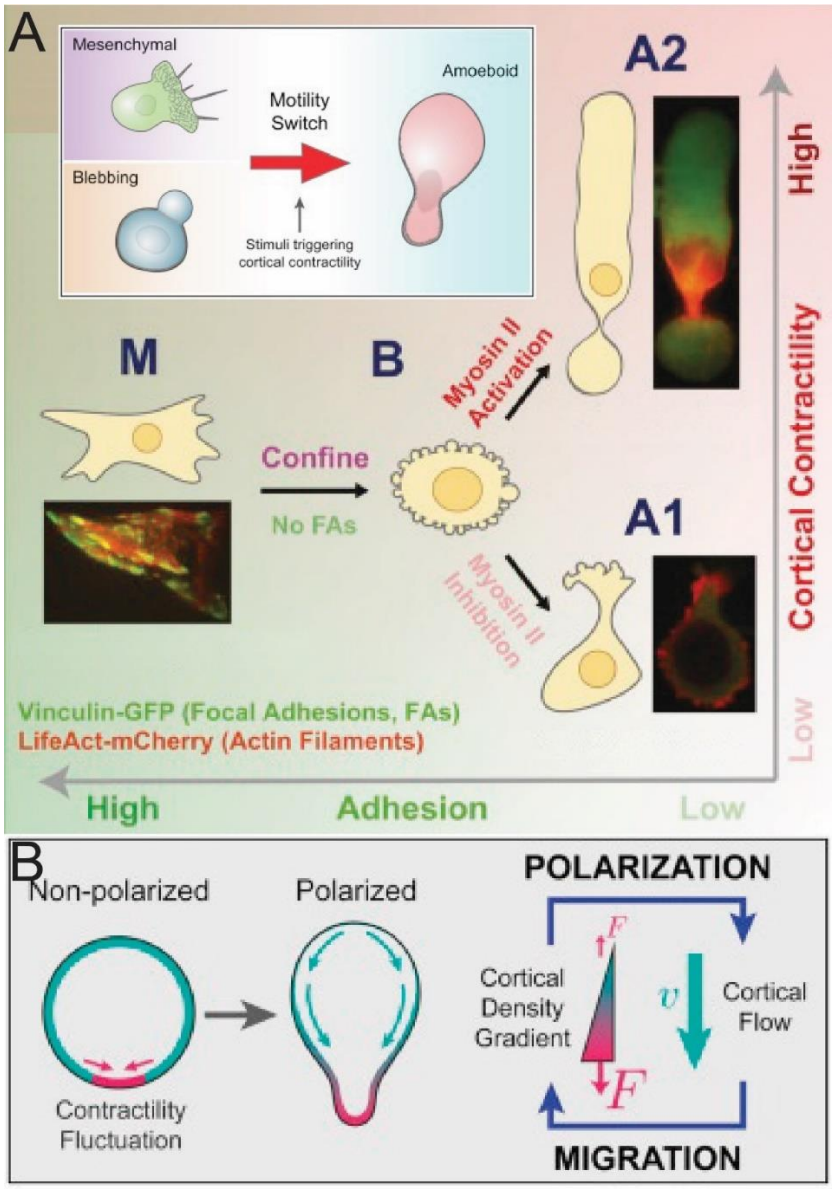

Fig. 1.2. Controlling modes of single cell migration. (A) Inset: embryonic progenitor cells transform into a prototypic ameboid migration mode by induction of cortical contractility. Physical confinement and low adhesion induce the mesenchymal-amoeboid transition. A large range of slow mesenchymal cell types can display fast ameboid-lie migration. A fast mode (A1) and faster and more conserved contractile mode (A2) were observed. A2 migration could be an ancestral migratory behaviour shared among eukaryotes. **(B)** In non-adhesive cells, polarisation is driven by the cell cortex. Actomyosin cortical flows drive fast and and persistent cell motility in confined 3D environments.

Adapted from (Ruprecht et al., 2015, Liu et al., 2015).

group. Inevitably, this usually means functional segregation of roles. Such differences are often seen when analysing those cells at the front (leaders) and the cells behind (followers) (Mayor and Etienne-Manneville, 2016), for example.

Efforts to understand the processes underlying collective cell migration has led to a variety of *in vitro* and *in vivo* experimental models. Through this, several types of collective migration have been found. 2D *in vitro* models, such as scratch wound assays in which a confluent epithelial sheet is wounded, and the subsequent migration toward the wound margin, is a popular model for wound healing and collective epithelial migration. These assays have been used to investigate polarisation, force generation and transmission (Nobes and Hall, 1999, Farooqui and Fenteany, 2005, Simpson et al., 2008), and have demonstrated that one common mode of collective migration is by a sheet moving across a tissue surface (Fig. 1.3A).

Finger-like multicellular strands that collectively invade 3D ECM is another mode of collective migration (Fig. 1.3, B and C). This can be modelled *in vitro* using multicellular spheroids in scaffolds like Matrigel (Wolf et al., 2007, Lee et al., 2007). Strand invasion is evident in processes like mammary gland development during branching morphogenesis, vascular sprouting during angiogenesis. head mesoderm migration of amphibian embryos (Bell and Waizbard, 1986, Winklbauer et al., 1992, Nabeshima et al., 1998), mucosa epithelial migration upon renewal. *Drosophila* is a popular model organism to perform genetic studies of tracheal branching morphogenesis (Affolter et al., 2003, Affolter and Caussinus, 2008). Vascular sprouting can be observed *in vivo* via intravital imaging of injured cornea or retina in mice (Becker et al., 1998, Hellstrom et al., 2007), and also studied using the Matrigel plug assay, which leads to *de novo* blood vessel invasion (Kibbey et al., 1992). The imaging capabilities of zebrafish mean they are also used for vascular morphogenesis studies, using the intersegmental vessels as a model (Siekmann and Lawson, 2007). Strand invasion is also evident during cancer invasion (Fig. 1.3D), such as in carcinomas. In the case of collective cancer migration, histopathology and injection of cancer spheroids into mice, and subsequent observation through a window chamber has been used (Alexander et al., 2008, Christiansen and Rajasekaran, 2006).

Isolated cell groups or clusters can also undergo collective migration. For example, cranial neural crest cells migrate collectively after delaminating form the neural tube. Likewise, border cells in the *Drosophila melanogaster* egg chamber detach from the epithelium before migrating a long distance as a small unit (Fig. 1.3E). In zebrafish

embryos, the lateral line primordium migrates as a cluster under the skin, periodically depositing neuromasts that form the future mechanosensory lateral line organ, and acts as a model for a cell population that becomes organised during migration (Lecaudey and Gilmour, 2006). Cluster migration is also identified in metastatic cancers like melanoma, that penetrate the tissue stroma (Fig. 1.3F) (Day et al., 1981, Haas and Gilmour, 2006). Such stromal cells and their secreted factors can be taken into account through explanation of tissue into 2D or 3D culture; for example, patterns of cancer invasion or morphogenetic processes like vascular sprouting have be studied in this manner (Friedl et al., 1995).

Some cell collectives migrate in streams, such as the many subpopulations of the neural crest and in a variety of species (e.g. chick, *Xenopus*, zebrafish), as well as the mammalian endoderm (Hegerfeldt et al., 2002, Teddy and Kulesa, 2004, Matthews et al., 2008, Carmona-Fontaine et al., 2008b). The neural crest, the model used in this thesis, is particularly useful because it can be dissected out of *Xenopus* embryos and cultured in *ex vivo* conditions where they retain many of the mechanisms they perform *in vivo* (Alfandari et al., 2003, Carmona-Fontaine et al., 2008b, Barriga et al., 2018). Hence, detailed cellular and molecular analysis can be performed using combined *ex vivo* and *in vivo* approaches. In other cases, cells can migrate in chains. This has been described for the *Drosophila* myoblasts, the squamous cell carcinoma (Richardson et al., 2007, Gaggioli et al., 2007), some neural crest cell populations (Simkin et al., 2013), and for *Dictyostelium* upon starvation (Weijer, 2009).

Each of these distinct forms of collective migration serve different purposes and are variations of the same fundamental process. For instance, cell monolayer migration, which are often comprised of a relatively homogeneous cell population, can be constitutively motile or induced, can be a normal developmental process or a reconstituted one, such as collective migration of the gut intestinal epithelial or wound closure, respectively. On the other hand, sprouting ducts and glands include distinct cell types that move together to form a ductal tree or network. Hence, collective migration, although hugely diverse and highly complex processes, are nonetheless variants on a similar theme.

1.3.3 Mechanisms of collective migration

Irrespective of the immense diversity of migratory modes, and diversity in the underlying molecular pathways, collective migration always requires cell-cell cohesion, collective cell polarity, and coordination of supracellular cytoskeletal

activity, whereby cytoskeletal dynamics is shared between multiple cells to function as a single unit to jointly generate force. These aspects are particularly oriented in response to guidance by extracellular chemical and physical signals which coordinate collective cell migration (Mayor and Etienne-Manneville, 2016). In some cases, collective migration also involves interaction with accessory stromal cells and ECM remodelling (Friedl and Gilmour, 2009).

Interestingly, because collective migration ensures many cells migrate at a similar speed and in the same direction, whereas they would otherwise be stationary or migrate in different directions, cells moving together is more efficient than solo motility. The reasons behind this include the emergence of supracellular polarity (Mayor and Etienne-Manneville, 2016) and supracellular organisation of the cytoskeleton (Ladoux and Mege, 2017, Ladoux et al., 2016) that enable the persistent coordination locomotion. That being said, cells moving in the same direction and at a similar speed is more common in epithelia or otherwise cell groups with strong cell-cell adhesions, whereas there is more cell interchange and 'supracellular' behaviour in collective mesenchymal migration (Malet-Engra et al., 2015, Theveneau et al., 2010). The complexity of collective behaviour emerges in the fact that cell groups undergo more persistent, albeit slower, migration than single cells (Malet-Engra et al., 2015, Theveneau et al., 2010), indicating that there is intricate communication within the group. Indeed, it can be concluded that one role of cell-cell contacts is not only to maintain the group but also to coordinate its constituent members.

In this section I will discuss how the principles of single cell migration (Section 1.2) scale up to the multicellular platform, from the point of view of leader and follower cells; by virtue of their respective positions, they inherently tend to have differing roles to play for the efficient coordination of a large interconnected cell group. Importantly, most research has been aimed to understanding how collective cell migration is achieved by focusing on processes at the front of the cell cluster. However, recent evidence shows that followers perform an essential role for cluster migration, including supracellular polarisation, controlling leader polarisation and in the participation of gradient sensing and chemotaxis.

1.3.3.1 Cell–cell cohesion and coupling

The key difference between single and multicellular migration is that cells maintain contact with one another when moving collectively. Cell–cell adhesion is mediated in a number of ways, but primarily by adherens junction proteins (Niessen, 2007), which mechanically couples the cytoskeletons of adjacent cell via cadherins and

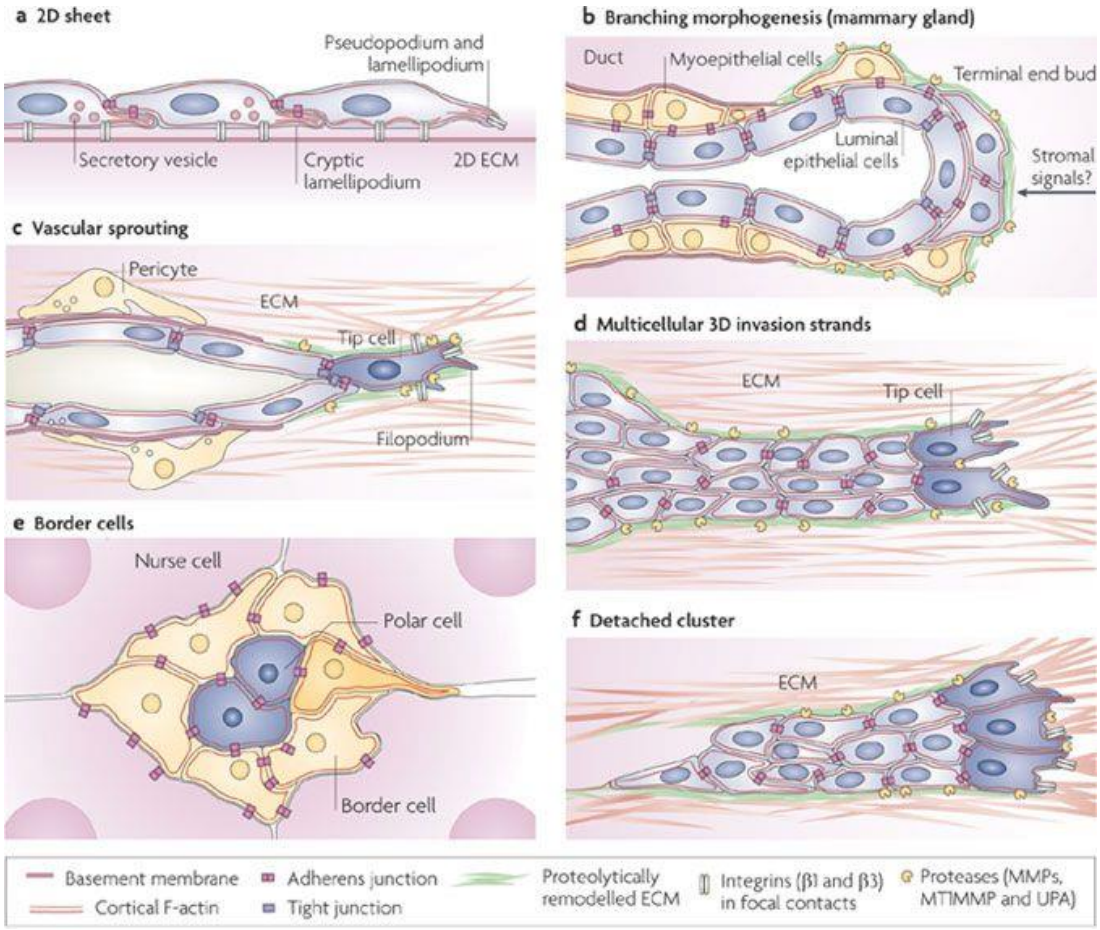

Fig. 1.3. Examples of collective cell migration. (A) Epithelial monolayer with protrusive leader cells. Follower cells are connected by adherens junctions. All cells are involved in force generation via focal adhesions with the ECM. *In vivo*, they remodel this substrate. **(B)** Terminal end bud sprouting during branching morphogenesis. The end bud is induced by factors from the stroma, the ECM is remodelled, basement membrane is deposited. **(C)** Vascular sprouting in developing or regenerating vessels. The tip cell is highly protrusive and guides the collective forward. Pre-existing pericytes act as a guidance track. **(D)** Multicellular 'strand-like' cancer invasion **(E)** *Drosophila* border cell cluster consisting of mobile outer cells and two less mobile polar cells migrating along cell–cell junctions of nurse cells in the egg chamber. **(F)** Collective invasion of detached cancer cells.

Adapted from (Mayor and Etienne-Manneville, 2016).

immunoglobulin superfamily members. This tight association with the cytoskeleton means adherens junction are essential for maintaining the integrity and cohesion of the migrating cell population, preventing cell dispersion or tissue disruption. Cadherins are the main transmembrane components of adherens junctions. They bind in a calcium-dependent homophilic manner between adjacent cells, interacting with and controlling the actin and microtubule networks via p120-, α- and β-catenins (Etienne-Manneville, 2011). Epithelia or epithelial-like cells can migrate as collectives in spite of their highly stable E-Cadherin (epithelial cadherin)-based contacts. Indeed, in many contexts E-Cadherin is essential for collective cell migration (Suffoletto et al., 2018); such stable contacts exist during epithelial formation and sheet wound healing. Likewise, VE-Cadherin (vascular endothelial cadherin) is necessary in endothelial cells during angiogenesis. However, adherens junctions can also be rapidly remodelled to allow cells to sort and exchange positions (Kametani and Takeichi, 2007, Yamada and Nelson, 2007). For instance, at stromal cell-cell contacts in mesenchymal populations, like the neural crest, N-Cadherin (neuronal cadherin) is dynamic (Kuriyama et al., 2014). Likewise, some cancer cells can also move together by using diverse mechanisms that rely on either stable or transient contacts, and there is increasing evidence that collective migration is a very common form of cancer metastasis (Cheung and Ewald, 2016).

Impairing cadherin function dramatically alters collective cell dynamics (Bazellieres et al., 2015). In cancer, collective cancer cell migration can be inhibited by reducing N-Cadherin junctions and disrupting actin cytoskeletal filament bundles (Yue et al., 2018). In some systems, cells detach and migrate separately upon abrogation of normal cadherin activity (Camand et al., 2012, Liu et al., 2011, Wilson et al., 2007). The loss of E-Cadherin to promote cell motility is the classical mechanism of epithelial-to-mesenchymal transition (EMT; Section 2.2.3) as seen in morphogenesis and cancer models. This normally happens to leader cells, which are those cells generally at the front of the migratory unit, ‘leading’ the collective’s movement by responding to external cues, such as soluble factors, the ECM and neighbouring cells. By contrast, in other systems, cell migration is totally blocked without any dissociation of the cell cluster e.g. border cells which lose E-Cadherin (Niewiadomska et al., 1999). This happen because the border cells lose their protrusions (Niewiadomska et al., 1999) due to a loss of polarisation (Cai et al., 2014). Therefore, tight regulation of cadherin function is essential for normal collective behaviour, otherwise rendering the group immobile, or leaving the cells

to migrate individually, which is highly inefficient (Malet-Engra et al., 2015, Theveneau et al., 2010).

Overall, cadherins are implicated as the dominant mediators of collective cell interactions, the loss of which may or may not be compensated for by other cell–cell adhesion pathways (Gavert et al., 2008, Grunert et al., 2003, Lee et al., 2006, Thompson and Williams, 2008). For instance, border cells use nurse cells as a substrate to move along. Their interaction is dependent on E-Cadherin and other cadherins cannot compensate for its loss. Contacts between border cells and nurse cells are essential for supracellular polarisation of the border cell group and efficient movement across the egg chamber (Cai et al., 2014). By contrast, overexpression of E-cadherin in nurse cells inhibits collective migration and increases the polarization of border cells in the direction of the oocyte (Cai et al., 2014). Likewise, mechanically active heteroetypic E/N-Cadherin adhesion between cancer associated fibroblasts and cancer cells enables cooperative tumour invasion by collective cell migration (Labernadie et al., 2017).

Another reason why cadherins cannot necessarily compensate for each other is that different cadherins can have different mechanotransductive properties. For example, in epithelial tissues, E-Cadherin-mediated junctions are reinforced when submitted to pulling forces meaning that E-Cadherin predicts the rate at which intercellular force builds up. By contrast, P-Cadherin (placental cadherin) is not involved in the adaptation of tension but predicts the level of intercellular force (Bazellieres et al., 2015). In carcinoma and aggressive sarcomas, P-Cadherin induces polarisation through an increase in mechanical forces via β-PIX and Cdc42 (Plutoni et al., 2016). This results in collective migration and correlates with aggressive tumours (Plutoni et al., 2016). While cadherins may not easily compensate for one another, in many cases the expression of a weaker, more dynamically behaving cadherin results in new cluster behaviour. For example, reduced E-Cadherin leads to collective migration of mammary carcinoma cells via upregulation of N-Cadherin, promoting cancer invasion and metastasis (Elisha et al., 2018). Likewise, a switch from E-Cadherin to N-Cadherin is required for collective cranial neural crest migration (Scarpa et al., 2015). Therefore, how cell clusters behave is highly dependent on the molecular composition of the adherens junction, including the balance between different cadherins (Bazellieres et al., 2015).

By extension, fine-tuned cadherin levels have a role to play in maintaining cluster cohesion and cooperation. In some collectively migrating populations, cells retain their relative positions to one-another, especially in epithelial cell types, such as during epithelial wound healing. In other cases, such as mesenchymal cell populations, the high turnover of, and unstable, cadherin-dependent contacts allows cells to change positions within the group, generating a more supracellular behaviour. For example, *in Xenopus* cranial neural crest, N-Cadherin endocytosis allows the group to behave as a liquid (Kuriyama et al., 2014). Therefore, the maintenance and dynamic control of cell–cell contacts controls cell leadership and preserves cluster cohesion. Indeed, in migrating cell populations, adherens junctions are often not highly stable structures. In wound healing assays, adherens junctions continuously move rearwards along the side of collectively migrating cells (Peglion et al., 2014). This junctional retrograde flow is driven by actomyosin and ends with dissociation of the cell-cell interaction, and recycling of the junctional components by endocytosis, such as N-Cadherin in fibroblasts, and trafficking toward the front, resulting in the formation of new junctions (Peglion et al., 2014). Polarised 'treadmilling' of adherens junctions is controlled by a front-to-rear gradient of p120-catenin phosphorylation, which regulates N-Cadherin trafficking, and junctional stability impacts polarity and speed of leaders during collective migration (Peglion et al., 2014). This dynamic 'treadmilling' of adherens junctions represents an additional way of making intercellular contacts malleable, while continuing to maintain maintaining the mechanical strength of adherens junctions between adjacent cells during migration.

Often, adherens junctions between leaders are not simply connected to a sparse intracellular actin cytoskeleton, but rather to thick actin cables, with these cells displaying a stretched morphology, suggesting that strong forces are exerted between neighbours (Peglion et al., 2014, Omelchenko et al., 2003). In this manner, adherens junctions can synchronise the dynamics of the actin retrograde flow in multiple adjacent front cells. Contractile actomyosin cables connected by cadherins junctions at the wound edge cell sheet is involved in closing the wound hole by functioning as a 'purse string' (Jacinto et al., 2002). Also in epithelial sheets, α-catenin controls the anisotropic force distribution of cell junctions to enable cooperative movements of epithelial cell sheets (Matsuzawa et al., 2018). It does this by activating RhoA at cell-cell junctions, which stabilises α-catenin; the consequential stabilisation of directional alignment of multiple cells permits efficient collective cell migration (Matsuzawa et al., 2018).

Contractile cables are also formed at the edge of some collectively migrating cell populations. In cancer cells, one function of the peripheral actomyosin cable is to maintain cluster integrity and prevent cell dispersion (Hidalgo-Carcedo et al., 2011), whereas in MDCK 'finger-like' collective migration, one large leader cell drags the rest of the cluster forward and an actomyosin cable prevents the initiation of a new leader cell by follower cells (Reffay et al., 2014, Hidalgo-Carcedo et al., 2011).

In addition to their important mechanical role in leader cells, cadherins can also regulate leader-to-follower transitions in more non-discrete cell groups. In the zebrafish lateral line, cadherin 2 is expressed across the entire tissue, but functional junctions are first assembled in the transition zone between the front and rear cells and become progressively more stable along the front-rear axis (Revenu et al., 2014). Hence, relocation and stabilisation of cadherins can help determine cell roles.

Cadherin-mediated adherens junctions are also required for collective cell chemotaxis (detailed further in Section 1.3.3.5), suggesting that no individual cell, even a leader cell, can interpret the chemotactic gradient without interacting with its neighbours. Although directionality is thought to be primarily coordinated by extracellular signals such as chemotactic gradients (Section 1.3.3.5), cell adhesion molecules also contribute to directionality; in *Drosophila* larval epidermal cells, levels of the atypical cadherin Daschous varies along the axis of migration, which polarises Daschous at cell boundaries (Arata et al., 2017). This polarity coordinates the migratory direction by acting with the unconventional myosin Dachs and another atypical cadherin, Fat, to restrict lamellipodia to the opposite end of the cell (Arata et al., 2017). Fat also directs collective migration of the *Drosophila* follicular epithelium, which rotate and elongate the egg chamber, with equal contribution from each individual cell (Cetera and Horne-Badovinac, 2015). Fat2 and Lar, which are involved in planar polarised actin protrusive activities (Squarr et al., 2016), localise to juxtaposing membrane domains and promote tissue motility (Barlan et al., 2017). Fat2 signals from the trailing edge (Viktorinova and Dahmann, 2013) to induce protrusions in the cells behind and stabilises Lar's localisation at the leading edge of the cell behind (Barlan et al., 2017). Lar signals from the leading edge to promote rear retraction in the cell ahead (Barlan et al., 2017). Hence, Fat2 and Lar define a basally localised planar signalling system for controlling CCM (Barlan et al., 2017). In the collective migration of endothelial cells, engulfed cadherin fingers serve as polarised junctional structures and engulfment occurs along with the formation of lamellipodia-like zone of low actomyosin contractility, in a VE-

Cadherin/catenin and Arp2/3-dependent manner (Hayer et al., 2016). Lateral accumulation of cadherin fingers in follower cells precedes collective turning, and increased contractility can initiate cadherin extension as well as engulfment by a neighbour cell to promote follower behaviour; cadherin fingers therefore serve as guidance cues that direct collective migration (Hayer et al., 2016). Additionally, the relationship between cell-cell and cell-adhesion contacts is often antagonistic (Dupin et al., 2009, Borghi et al., 2010, Burute and Thery, 2012), meaning intercellular adhesions are required for the correct polarization of the cells and for directed movement. In fact, anisotropic distribution of adherens junctions is sufficient to promote cell polarization and directed migration (Dupin et al., 2009, Desai et al., 2009). When adherens junctions are lost, cells experience polarisation defects with randomly directed protrusions, and integrins are constitutively engaged with the ECM along the entire cell periphery (Camand et al., 2012).

Although cadherins are the dominant mediators of cell-cell adhesion in collectively migrating populations, other types of contacts are also important. The immunoglobulin family members, neural cell adhesion molecule (NCAM) proteins, ALCAM and L1CAM mediate cell-cell contact (van Kempen et al., 2000, Gavert et al., 2008, Lehembre et al., 2008, Schreiber et al., 2008). These alternative, homophilic N-cadherin and non-cadherin adhesion systems are often upregulated during EMT. In doing so, they promote cluster cohesion and prevent dispersion, resulting in increased collective motility (Grunert et al., 2003, Lee et al., 2006, Schreiber et al., 2008, Lehembre et al., 2008, Wei et al., 2004, Massoumi et al., 2009). Through cross-signalling, integrins can also contribute to cell-cell cohesion. For example, cell cohesion is promoted by the binding of α5β1 integrin to fibronectin (Salmenpera et al., 2008) or by the binding of α6β1 integrin to laminin (Belvindrah et al., 2007). Desmosomes are another means of cell-cell adhesion in migrating cohorts. Branching epithelia, sprouting vessels and epithelial cancers all contain desmosomal proteins, such as desmocollins, the loss of which results in dispersion (Khan et al., 2006, Chidgey and Dawson, 2007). Likewise, migrating cells often express tight junction-related proteins (e.g. claudin 1, claudin 4, occludin and ZO1 in epithelia) (Langbein et al., 2003, Smalley et al., 2005) and are important for collective migration (Manda et al., 2018). Furthermore, although their mode of contribution to collective migration is unknown, the gap junction proteins, connexin (Cx) 43 and Cx26 are present in cell-cell junctions of neural crest, sprouting epithelia and invasive cancers (Ito et al., 2006, Defranco et al., 2008, Czyz, 2008, Lo et al., 1997).

1.3.3.2 Polarity mechanisms

The translocation of non-polarised, randomly moving cells that fill the open space from the edge by collective random walk is very inefficient (Simpson et al., 2008, Vitorino and Meyer, 2008). Therefore, instead, cell cohorts use several mechanisms to polarise the cluster in a supracellular manner such that leaders are different from followers (Vitorino and Meyer, 2008). In comparison to follower cells, front cells display distinct, polarised morphologies, with large protrusions oriented in the direction of migration, and they detect extracellular guidance cues (by virtue of being closest to the source) and have a highly dynamic cytoskeleton (Fig. 1.4A) (Vitorino and Meyer, 2008).

In some cases, polarity works by genetically determined differentiation. For example, in angiogenesis, asymmetric cell division results in the generation of protrusive tip cells and less dynamic stalk cells (Gaggioli et al., 2007, Hellstrom et al., 2007, Siekmann and Lawson, 2007). Other mechanisms of generating polarity include the asymmetric stiffening of cortical actomyosin networks mediated by Rho GTPases and myosin II (Vitorino and Meyer, 2008, Fischer et al., 2009); and polarized remodelling of the ECM (Section 1.3.3.4) (Wolf et al., 2007, Nabeshima et al., 2000, Palmieri et al., 2008). For example, in branching morphogenesis, cells are confined (Friedl and Wolf, 2008) but must degrade extracellular ECM components and chemokines, and deposit basement membrane components to lay the tracks for future migration (Smola et al., 1998, Schmidt et al., 2007). In this manner, supracellular polarity is conferred upon the group. Indeed, there are emergent collective migratory modes for epithelia under tubular confinement and, as well as mesenchymal cells under confinement, such as the neural crest (Szabo et al., 2016, Xi et al., 2017).

Collectives can also be polarised by external inductive signals (Fig. 1.4B), including chemokines such as stromal cell-derived factor 1 (SDF1; also known as CXC ligand 12, CXCL12) and growth factors like members of the fibroblast growth factor (FGF) and transforming growth factor-β (TGFβ) families (Lecaudey and Gilmour, 2006, Vitorino and Meyer, 2008, Valentin et al., 2007) that might be either freely diffusing or tethered to the ECM (Shintani et al., 2008), which results in chemotaxis (Section 1.3.3.5) or haptotaxis, respectively, when they are found in gradients. Such inductive factors can be produced by other cells in a paracrine manner (Orimo et al., 2005) or released by the migratory cell group themselves in a juxtacrine or autocrine fashion (Aman and Piotrowski, 2008).

Collective polarity can also be conferred on migrating clusters through differential expression of ECM-binding proteins. For instance, comparatively greater integrin expression by leader over followers can generate polarised attachment to the ECM, thereby defining the group's front (Farooqui and Fenteany, 2005, Vitorino and Meyer, 2008, Hegerfeldt et al., 2002, Haas and Gilmour, 2006). Hence collective polarity can be driven by genetics or by a temporary functional state based on the cell's position within the group. Either way, supracellular polarity renders the cell collective more responsive and adaptive to the environment than the individual cell.

A further way in which the cluster can polarise is by the induction of follower cells on leaders. In some systems, cells undergo the phenomenon of contact inhibition of locomotion (CIL), which is the complex process by which contacting cells collapse their protrusions at the site of contact, repolarise and form new protrusions away from the contact and then separate and migrate away in a new direction (Mayor and Carmona-Fontaine, 2010, Roycroft and Mayor, 2016, Theveneau et al., 2010, Abercrombie and Heaysman, 1953, Stramer et al., 2013, Abercrombie, 1970). Thus, CIL is a mechanism that polarises cells in a contact-dependent manner (Mayor and Carmona-Fontaine, 2010, Roycroft and Mayor, 2016). This phenomena was first described by Abercrombie and Heaysman (Abercrombie and Heaysman, 1953) in which fibroblasts were observed to reduce their speed upon collision with other cells, and then ceasing their movement before dispersing in other directions. They further noticed that fibroblasts avoid migrating on top of each other, but rather align and tend to form a monolayer. These observations were attributed to CIL (Abercrombie and Heaysman, 1953, Abercrombie and Dunn, 1975). In further work, it was observed that cell protrusions are retracted upon contact and extended in another part of the cell (Abercrombie and Ambrose, 1958). CIL has since been identified in numerous cell types including embryonic fibroblasts, haemocytes and neural crest cells and is the driving force behind various phenomena including collective cell migration and cell dispersion.

During many forms of collective cell migration, CIL ensures the absence of protrusions at points of cell–cell contacts (i.e. in the middle of the group) and promotes the formation and maintenance of protrusions in the leader cells away from their contacts with follower cells (Mayor and Carmona-Fontaine, 2010, Theveneau and Mayor, 2011c). Indeed, in most examples of collective cell migration *in vivo*, major protrusions are observed at the leading edge, pointing away from the contact with the follower cells, which is the hallmark of cell polarization induced by CIL (Abercrombie, 1970, Mayor and Carmona-Fontaine, 2010, Stramer et al., 2013). Thus, CIL between

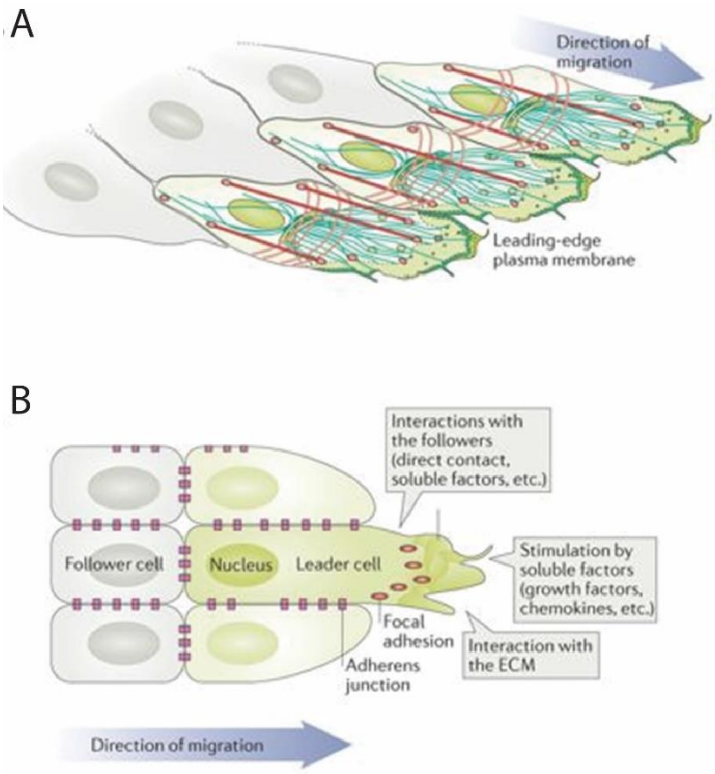

Fig. 1.4. Polarisation in collectively migrating cells. (A) In most systems, leader (front) cells are highly polarised along the direction of migration, suggesting mesenchymal front-rear phenotypic polarity. Epithelial apico-basal polarity is lost during EMT. Leader cells are connected to follower by intercellular adhesions. They have dynamic protrusions at the front edge e.g. lamellipodia and filopodia and have a polarised cytoskeleton that permits the secretion of ECM-degrading protease-capsulated vesicles and the transmission of biomechanical forces to the group e.g. across longitudinal actomyosin cables. **(B)** Leaders are responsive to external signals such as chemokines and the ECM which guide their migration, and all cells are connected by intercellular adhesion sites. Adherens junctions restrict the localization of focal adhesions to the cell front, by locally inhibiting their formation and maintenance.

Adapted from (Mayor and Etienne-Manneville, 2016).

leader and follower cells seems to be a fundamental aspect of collective cell migration.

Although the fundamental steps of CIL are the same in different contexts, the molecular basis is different depending on the cell type. Various cell-cell adhesion molecules, including cadherins, ephrins, Eph receptors and many members of the PCP pathway have been implicated in CIL (Theveneau et al., 2010, Becker et al., 2013, Barriga et al., 2013, Astin et al., 2010, Batson et al., 2014, Villar-Cervino et al., 2013, Carmona-Fontaine et al., 2008a, Shnitsar and Borchers, 2008, Mayor and Theveneau, 2014). Likewise, cell-matrix components including syndecans and integrins are involved (Matthews et al., 2008). Upon collision, cadherins and ephrins undergo homophilic or heterophilic interactions. In the case of cadherins, engagement leads to the recruitment of Par3 (Moore et al., 2013). In some cases, like for syndecan, the precise role neighbourly interactions is unknown, but nonetheless PCP components accumulate at sites of cell contact (Carmona-Fontaine et al., 2008a, Matthews et al., 2008, Witzel et al., 2006, Bin-Nun et al., 2014, Hayes et al., 2013, Peradziryi et al., 2011, Becker et al., 2013). The engagement of these cell-cell contacts leads to activation of intracellular signalling pathways. Activated molecules include the small GTPases RhoA, Rac1 and Cdc42 (Astin et al., 2010, Batson et al., 2014, Carmona-Fontaine et al., 2008a, Moore et al., 2013, Desai et al., 2013), as well as downstream proteins like calponin2 (Davis et al., 2015, Ulmer et al., 2013). Specifically, RhoA becomes active at contact sites, whereas Rac1 and Cdc42 are inhibited at the contact and activated away from it. Since these small GTPases are dynamic regulators of protrusion formation (Section 1.2.2.3) (Krause and Gautreau, 2014), CIL causes this repolarisation; also, microtubules and microfilaments collapse (Moore et al., 2013, Davis et al., 2015) and focal adhesions disassemble at intercellular adhesion sites (Theveneau et al., 2013). This is accompanied by an increase in tension at the cell–cell contact followed by a rapid actomyosin contraction (Davis et al., 2015), causing protrusion collapse. In terms of forces, cell-matrix adhesions are rapidly disassembled upon cell contact, driven by Src and FAK downstream of the N-Cadherin in neural crest (Roycroft et al., 2018). Hence, a build-up of tension at the contact drives separation. Overall, the result is that new protrusions are formed away from the cell contact by the small GTPase Rac1, with RhoA building up at the prospective rear, and the front and rear of the cell becomes uncoupled (Martin et al., 2014, Roycroft and Mayor, 2016). The strong experimental evidence of the importance of CIL for collective cell migration is also supported by

various mathematical models (Desai et al., 2013, Woods et al., 2014, Li and Lowengrub, 2014).

1.3.3.3 Cytoskeletal organization and force generation

Collective migration relies on extracellular interactions to generate the force for forward movement. In some cases, force generation can also be provided by means intercellular interactions with surrounding tissues (Geisbrecht and Montell, 2002). For example, border cells migrate on nurse cells using relatively weak E-Cadherin-based junctions; they simultaneously adhere relatively strongly to neighbouring border cells with E-Cadherin, and these identical component adhesions distinguished by differential expression levels (and thus cell-cell adhesion strength) by the two cell populations (Cai et al., 2014). Also, E/N-Cadherin adhesions between cancer and associated fibroblasts enables collective tumour cell invasion (Labernadie et al., 2017). Thus, distinct receptor–ligand pairs mediate collective force coupling to the actin cytoskeleton in different contexts. However, mostly, integrin-mediated signalling is used, which allows cells to respond to the composition and stiffness of the ECM, generate the force required for collective movement, and the ECM provides directional cues for multicellular streams (Alexander et al., 2008, Ventre et al., 2012). The molecular principles of actin turnover and polarised force generated by moving cell groups are similar to those in the migration of individual cells (Section 1.2.2.4), but they are shared and coordinated between cells at different positions. For instance, the cortical actin network in the cell group shows supracellular organization, such that anterior protrusion activities and posterior retraction dynamics involve many cells (Friedl et al., 1995, Vitorino and Meyer, 2008, Hegerfeldt et al., 2002, Kolega, 1981). The high level of organisation in the actomyosin cytoskeleton reinforces cell behaviour (e.g. leaders remain and function as leaders) (Fig. 1.5, B and C), although many of the mechanisms involved in supracellular cytoskeletal organisation have not yet been understood. They likely arise through the united actions of gap junction coupling, cadherin-based contacts and paracrine release of growth factors and cytokines (Röper, 2013, Mayor and Etienne-Manneville, 2016).

During sheet migration, Cdc42 and Rac control the formation of lamellipodia, pseudopodia and filopodia, which are formed by multiple front cells that drive the leading edge forward (Vaughan and Trinkaus, 1966, Nobes and Hall, 1999, Farooqui and Fenteany, 2005, Mattila and Lappalainen, 2008). Calcium pulses can control local cycles of lamellipodia retraction and adhesion along the front of

collectively migrating endothelial cells (Tsai and Meyer, 2012). Integrins activate a huge number of effector molecules (Section 1.2.2.4) that induce forces that support the formation of protrusions (Krause and Gautreau, 2014) and microtubule network polymerisation (Etienne-Manneville, 2013) that supports the front by providing new and recycled components like receptors and membrane. The leading edge forms strong, mature integrin-dependent focal adhesion complexes (Nobes and Hall, 1999, Zaidel-Bar et al., 2007). These, and the extensive leader protrusions together result in an intracellular cytoskeleton and polarised morphology that is typical of leader cells (Etienne-Manneville and Hall, 2001), and these combined signalling pathways contribute to stabilisation of these features (Etienne-Manneville, 2013). The traction forces generated by leader cells is sufficient to pull and coordinate migration persistence of five to ten cells behind the front edge, dragging the followers behind (Vitorino and Meyer, 2008, Caussinus et al., 2008). These strong traction forces that are generated at the wound edge are generated thanks to the association of focal adhesions with high levels of RhoA, which maintains longitudinal actomyosin cables (Reffay et al., 2014). These promote contraction of the cell body and the associated pulling forces are transmitted to many follower cells behind (Reffay et al., 2014, Li et al., 2012). In primary astrocytes, intermediate filaments promote directed collective migration by restricting traction forces to the front of leader cells, preventing aberrant traction in the followers and by contributing to maintenance of lateral cell-cell interactions (De Pascalis et al., 2018). However, in general, little is known about intermediate filaments in collective migration, including what potential role they might play in neural crest migration.

In *Drosophila* border cells, although the cell most responsive to EGF/PVF signals becomes the leader, protrusions are also regulated by the insulin and Hippo pathways (Ghiglione et al., 2018, Chang et al., 2018) and actomyosin forces are necessary for initial cluster detachment from the source epidermis and subsequent migration (Sharma et al., 2018). Intercellular tension decreases from the front of the cluster to the rear (Cai et al., 2014), meaning that the leader(s) could drag the follower cells forward during collective migration, akin to epithelial monolayers. Any such ‘drag’ or pulling forces requires force transmission, which is an essential feature of collective cell migration. This capacity of follower cells to respond to the forces exerted by the preceding cells depends on mechanosensing (Ladoux and Nicolas, 2012, Pruitt et al., 2014) and relies on force-induced conformational changes of mechanotransducers whose activity is modified thanks to force-induced accessibility of new binding domains. For example, talin and α-catenin are mechanotransducers in focal

adhesions and adherens junctions, respectively. When stretched, α-catenin undergoes a conformational change that stabilises its binding to actin, and allows vinculin to bind to it, thereby increasing junctional stability (Yonemura et al., 2010, Buckley et al., 2014, Leckband and de Rooij, 2014). Indeed, force-dependent binding of vinculin to α-catenin regulates cell-cell contact stability and collective cell migration in MDCK cells (Seddiki et al., 2018). Forces transmitted from the ECM to cells can inform about matrix rigidity that affects collective behaviour. In the case of *Xenopus* cranial neural crest, for example, an integrin-dependent vinculin-talin-paxillin complex is essential for collective migration because this complex is used to sense the stiffness of the underlying mesoderm, which is necessary and sufficient for migration of the cell group (Barriga et al., 2018). Matrix rigidity can also induce collective migration via EMT; for example, tumour metastasis is promoted in a Twist-dependent mechanotransductive pathway that responds to high ECM stiffness (Wei et al., 2015).

Forces must also be transmitted between mechanically coupled cells to achieved coordinated movement (Fig. 1.5A). The cell–cell contact-associated protein Merlin is involved in mechanotransduction during collective migration (Das et al., 2015). When leader cells exert pulling forces on their neighbours, Merlin translocates from sites of intercellular contacts to the cytoplasm, where it supports the polarisation of Rac1 activation and lamellipodium formation, thereby defining the front side of the following cell (Das et al., 2015). Merlin therefore controls polarised Rac1 activation and protrusion formation on the multicellular scale (Das et al., 2015). In addition, tension exerted on C-Cadherin-mediated junctions via cadherin-integrin crosstalk strengthens desmosomes (Weber et al., 2012, Bjerke et al., 2014). Hence, proper collective movement requires efficient cross-signalling of cell-cell and cell-ECM adhesions within and between cells. During tissue invasion like in sprouting blood vessels or invading cancer strands, tip cells protrude with actin-rich pseudopodia and filopodia (Wolf et al., 2007, le Noble et al., 2008, Ribeiro et al., 2002, Caussinus et al., 2008) that establish directionality by sensing and attaching to tissue structures at the front (Fig. 1.6A). This cell-matrix signal is transmitted to follower cells through E-Cadherin (le Noble et al., 2008, Vasioukhin et al., 2000). Engagement of these adherens junctions components including p120-catenin enhances its interaction with cortactin, an Arp2/3 recruiter, that simultaneous reinforces leading edge protrusions and strengthens cell-cell junctions by facilitating and stabilising nucleation sites for actin branching (Boguslavsky et al., 2007). Border cells sense directionality in a similar way, as they respond to EGF

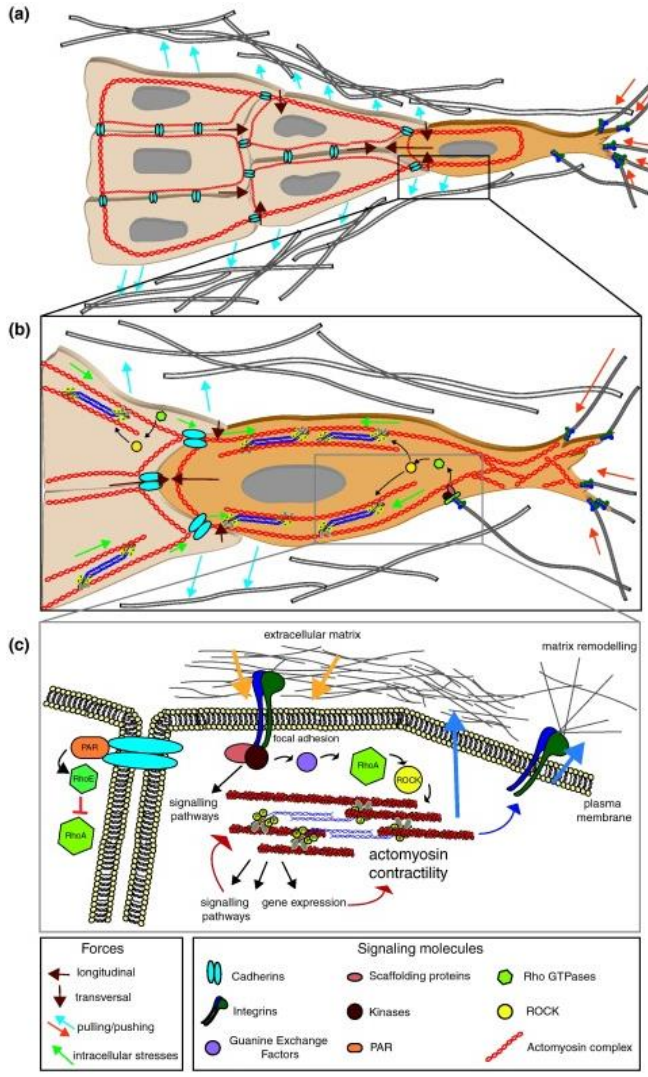

Fig. 1.5. Actomyosin mechanosensing during collective migration. (A) In more epithelial-like cases, leader-ECM connections result in pulling forces, which are transmitted to the cell and other cells via the actomyosin cytoskeleton. **(B)** The actomyosin cytoskeleton polarised and highly organised, which maintains leader phenotype. There is low contractility at cell-cell junctions whereas peripheral actomyosin cables result in intracellular stresses which aid in collective cohesiveness. **(C)** Actomyosin contractility is tightly regulated and involved in force transduction, and matrix remodelling.

Adapted from (Pandya et al., 2017)

and PVR which induces one primary highly protrusive leader which generates much of the traction force, with contributions from the other followers (Fig. 1.6B) (Duchek et al., 2001, Wang et al., 2010b). By contrast, mesenchymal cells like the neural crest exhibit CIL which means traction in a supracellular manner around the edge of the cluster, so front cells perform most of the force transduction (Fig. 1.6C) (Scarpa et al., 2015). By contrast, the lateral line is steered from the rear because cells at the back express the SDF decoy receptor, CXCR7, which, after endocytosis, results in the formation of a self-generated gradient with responsive CXCR4-expressing front cells (Fig. 1.6D) (Valentin et al., 2007, Boldajipour et al., 2008, Dambly-Chaudiere et al., 2007).

While the above would suggest that in most cases, leader cells are the primary force generators in migrating cohorts, in some moving cell sheets (e.g. epithelia), follower cells also develop polarized lamellipodia, which help maintain the coordinated translocation of the group (Farooqui and Fenteany, 2005, Boguslavsky et al., 2007). Follower cells can also directly participate in generating pulling forces (Haas and Gilmour, 2006, Trepat et al., 2009). During epithelial monolayer migration, stress primarily builds up several cell rows behind the leading edge and extends across large distances. (Trepat et al., 2009). Therefore, although leader cells are important for local guidance, the forces they generate are only a small part of a global ‘tug-of-war’, involving cells far behind, thanks to long-range force transmission across cell-cell adhesions (Trepat et al., 2009, Trepat and Fredberg, 2011, Tambe et al., 2011).

Mechanical interactions among follower cells regulate the selective emergence of leader cells at the wound margin of epithelial sheets by manifesting locally increased traction and monolayer stresses, which pull on the presumptive leaders to elect them to their fate (Vishwakarma et al., 2018). Moreover, leader cell and single-cell speed are insufficient to explain wound edge dynamics (Vig et al., 2017). Altogether, these results suggest that force generation depends on both leader and follower cells, which both play an important part in organising collective cell migration.

ECM composition can also promote collective behaviour and different migratory modes of the same cell type. At low collagen concentrations, tumour cells move individually whereas higher collagen levels results in the formation of cell clusters with high invasive capacity (Plou et al., 2018). In addition, when the concentration of TGF-β in the microenvironment is lower, cancer cell aggregates adopts a spheroid-like morphology and peripheral actin localisation; in contrast, higher concentrations of

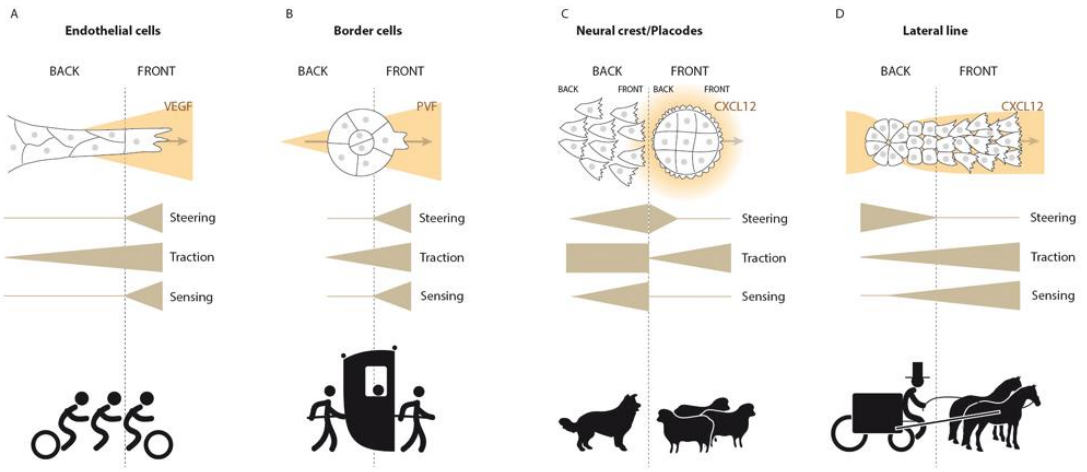

Fig. 1.6. Cooperative behaviour to steer groups. (**A**) In endothelial cells, VEGF activates protrusive lamellipodia in a tip cell, which senses and steers the group toward the chemotactic signal. Traction is generated by multiple members of the group. (**B**) In *Drosophila* border cells, the most responsive to PVF becomes the leader which directs and drags the followers forward, although there is also some contribution in traction from the followers. (**C**) The neural crest is attracted to SDF1-producing placodal cells, which guide their migration. Although neural crest cells have intrinsic motility, directionality is conferred to the group by this chemotactic process (SDF1 activating CXCR4 on neural crest cells). Traction forces are generated at the edge of the neural crest cell group but not in the middle due to CIL. The neural crest move toward the placodes, and the placodes are repelled away by CIL between the two cell populations. Thus, the neural crest 'chases' the placodal cells and the placode cells 'run' away by CIL. (**D**) Zebrafish lateral line primordium cells are directed by SDF1 in a self-generated gradient thanks to differential expression of receptors (CXCR4 at the front, decoy receptor CXCR7 at the rear). Rear cells are necessary for steering the group because laser ablation to separate these cells results in a non-motile front due to the inability to self-generate a chemotactic gradient.

Adapted from (Theveneau and Linker, 2017).

TGF-β induces the formation of clusters with higher invasive capacity, resulting in clear strand-like collective cell migration (Plou et al., 2018).

Interestingly, whereas adhesion-independent mechanisms of solitary single cell migration have been described, there is almost no evidence yet of collective systems that move while lacking cell-ECM connections. In the case of ductal morphogenesis, multicellular pushing forces from a stalk cells force the terminal bud to protrude into soft tissue in the apparent absence of force-generating adhesion complexes (Ewald et al., 2008).

1.3.3.4 ECM remodelling and accessory cells

Collective invasion *in vivo* occurs through or along ECM or other tissues. Owing to their size, groups of migrating cells are more spatially constrained than individually migrating cells, meaning the cell groups, compared to individual cells, have a higher propensity to carve out a path that they can take or otherwise use preformed tracks. To achieve this, hollow tube-like ECM tubes can be formed, and there can be secondary modification of the extracellular microenvironment, such as via the deposition of basement membrane components upon which the group can migrate. *In vivo*, the cell collectives can degrade the ECM and carve out the path of least resistance upon which it can move, and these tactics are sometimes essential for efficient collective cell migration (Gaggioli et al., 2007, Wolf et al., 2007). The modification and enlargement of the path of migration is usually performed by the leader cells. For example, traction (from leaders) exerted on the ECM can affect the shape of the matrix fibres, and the ECM can promote directional guidance depending on the orientation and organisation of its constituent components (Alexander et al., 2008, Ventre et al., 2012).

ECM degradation, through secretion of matrix metalloproteinases (MMPs) is performed primarily by leader cells, to provide a region into which the cell group can move. For instance, tip cells (the leaders) use the surface-localized protease MMP14 to degrade interstitial fibrillar collagen, and the empty area is then enlarged by additional ECM degradation by follower cells (Friedl and Wolf, 2008, Yana et al., 2007). FGF-stimulated leader tracheal cells in *Drosophila* secrete MMP2, which contributes to the inhibition of FGF receptor (FGFR)–MAPK signalling in followers, thereby allowing synchronous group movement forward. In embryos lacking MMP2, leader phenotype is unstable; instead, followers are stimulated to become new tip cells, resulting in tracheal defects due to collective disorganisation (Ghabrial and Krasnow, 2006, Wang et al., 2010a). Alternatively, collective invasion can occur along

pre-formed tracks that have low mechanical resistance. This is common in instances such as pre-existing basement membrane, vascular tracks or even the lumen of lymph vessels (Hendrix et al., 2003). This is one way in which carcinoma invasion is promoted; stromal fibroblast leaders generated migratory tracks that exert the least resistance to migration (Gaggioli et al., 2007) and carcinoma collective migrative is guided by fibronectin (Gopal et al., 2017).

In addition to ECM degradation, cells can perform secondary matrix remodelling. Leader cells secrete ECM components that dramatically alter the ECM composition, thereby allowing follower cells to migrate on a favourable substrate. For example, epithelial sheets, strands and tubes deposit basement membrane components, including collagen IV, perlecan and laminin to generate a smooth scaffold track between the migratory group and the ECM (Gudjonsson et al., 2002, Brachvogel et al., 2007). The formation of a basement membrane allows cells to migrate easily forward with little resistance (Farooqui and Fenteany, 2005, Schmidt et al., 2007) and the changes in substrate composition and consequential integrin activation and signalling affect the migratory behaviour of the followers, increasing the polarised organisation of the cell group (Peng et al., 2013, Nguyen et al., 2000).

During collective migration, there is often extensive communication between the migrating cohort and surrounding cells. In many cases, they can provide a supporting role for collective migration e.g. stromal cells such as fibroblasts, pericytes and myoepithelial cells. During skin regeneration, epidermal keratinocytes interact with dermal fibroblasts to build the basement membrane by jointly depositing collagen IV, nidogens, and laminins 1 and 5 (Smola et al., 1998, Nischt et al., 2007). Likewise, in sprouting blood vessels, the basement membrane is jointly deposited by endothelial cells and pericytes and serves as a guidance track for the moving multicellular vessel (Brachvogel et al., 2007). During collective cancer cell invasion, fibroblasts cooperate with the leading edge to remodel the ECM and guide the cancer cells along the newly formed track (Gaggioli et al., 2007). Furthermore, whereas fibroblasts use actomyosin contractile forces to remodel the ECM via secretion of MT1MMP, cancer cells depend on Cdc42 to follow the tracks (Gaggioli et al., 2007). Hence, distinct programmes of collective migration exist (Gaggioli et al., 2007).

1.3.3.5 Chemotaxis

Cell migration is fundamental to many processes in development and disease, including embryonic morphogenesis, wound healing and the immune response

(Friedl and Gilmour, 2009). This often involves cells responding to specific signals that guide their movement, either from mechanical stimuli, molecules bound to the extracellular matrix or soluble external factors (Ricoult et al., 2015, Cai et al., 2014, Das et al., 2015, Gardel et al., 2010, Riahi et al., 2015, Roca-Cusachs et al., 2013, Charras and Sahai, 2014). Cell migration in response to gradients of the latter, called chemotaxis, has been widely studied and it is a well-established and very important mechanism that provides directionality and persistence to migrating cells (Roca-Cusachs et al., 2013, Roussos et al., 2011, Swaney et al., 2010). Indeed, most long-range directional migration *in vivo* occur by chemotaxis (Dona et al., 2013, Theveneau et al., 2010, Majumdar et al., 2014, Haeger et al., 2015, Roca-Cusachs et al., 2013). The chemotactic response of cells, in part, involves the polymerisation of actin at the leading edge and the accompanying formation of protrusions, and myosin-II-mediated contraction at the rear (Kay et al., 2008).

The first description of chemotaxis was made by Engelmann and Pfeffer in bacteria over a century ago (Pfeffer, 1884, Engelmann, 1882). Since then, repulsive (Yang et al., 2002, Butler and Dodd, 2003) and attractive cues have been found for a variety of processes (Friedl and Gilmour, 2009, Roussos et al., 2011). However, most factors are multifunctional on cell behaviour, which makes definitive demonstration of chemoattractant behaviour *in vivo* difficult. Nevertheless, some attributes of chemoattractants may be summarised as follows. Chemoattractants are generally transcribed, translated and secreted by the target tissue itself to where the responsive cells are migrating. These responding cells are required to express a receptor for the chemoattractant when temporally appropriate. Loss of the chemoattractant or its receptor should lead to failure of cells reaching the target region; instead, non-directional migration can be expected. *In vitro*, localised chemoattractants should cause chemotaxis and *in vivo*, cells should be diverted from their normal path by ectopic, localised sources of chemoattractant. Chemotaxis should be rescued by an exogenous ligand when the endogenous chemoattractant is lost, if placed into the region the cells would normally migrate toward. Chemotaxis requires that cells migrate up a concentration gradient of a soluble factor, so sufficient and consistent changes in the chemoattractant's concentration should be found to give rise to a detectable gradient. This last point is perhaps the most difficult to demonstrate due to technical limitations and that in some cases the gradient is generated *in situ* by the migrating cell (Cai and Montell, 2014). Nonetheless, a fulfilment of these criteria is important to show that not only are the cells capable of being chemotactic towards the factor, but also that chemotaxis is actually happening *in vivo*. Altered migration in

response to the external factor would otherwise demonstrate chemokinesis, the process by which factors simply promote or support migration, rather than providing directionality to the movement as in the case of chemotaxis, as seen in various cell types in physiology and throughout development (Roussos et al., 2011, Kay et al., 2008).

Most collective migration *in vivo* relies on cell groups responding to soluble factors such as chemokines or growth factors, many of which are used as models of collective cell chemotaxis. Chemokines and growth factors help confer supracellular polarisation on migratory groups and act as directional cues. For instance, collective migration of endothelial cells is driven by chemotaxis toward vascular endothelial growth factors (VEGFs), FGF2, nitric oxide and other cytokines (Priya et al., 2015), which initiates the directional migration of tip cells and blood vessel formation (Lamalice et al., 2007, Chauvet et al., 2013) (Fig. 1.7, B and B'). Leader cells sense these chemical cues and promote the whole group's chemotaxis, meaning they direct collective migration. Branching morphogenesis of the *Drosophila* trachea displays similar characteristics; leader-directed chemotaxis to Bnl and FGF (Fig. 1.7, A and A'). In the case of *Drosophila* border cells which undergo chemotaxis toward PVF (platelet-derived growth factor-, PDGF, and VEGF- related factor) (Montell et al., 2012), the cell that has highest receptor-mediated signalling (i.e. the most responsive to the chemotactic agents) becomes the leader of its group, with large forward-directed protrusions (Fig. 1.7, E and F).

Mechanistically, the effect of chemotactic signalling is the induction of cell polarisation and the formation and maintenance of protrusions via those signalling pathways described previously to promote actin polymerisation (Section 1.2.2.2); Cdc42 and Rac are activated and recruited in a polarised manner via phosphoinositide signalling (Kolsch et al., 2008). For instance, SDF1 binding to CXCR4 in front cells of the lateral line primordium drives actin polymerisation and protrusion via the G protein subunit Gβ1 (Xu et al., 2014). Likewise, protrusions are oriented in a PDGF-dependent manner during head mesendoderm collective cell chemotaxis (Fig. 1.7, I and J). The intracellular signalling induced from chemotactic signals also cross-talks with cell-ECM signalling (Guo and Giancotti, 2004, Shen et al., 2012), for example, FGF2 and VEGF affect integrin signalling by regulating integrin expression or FAK phosphorylation (Le Boeuf et al., 2006, Avraham et al., 2003, Sieg et al., 2000). Thus, chemotactic signals regulate cell-substrate adhesions. Inhibition of cell-substrate interactions in *Dictyostelium*, for example, prevents its chemotaxis toward SDF1 because it perturbs cell-cell

interactions (Wang et al., 2014). Conversely, integrin signalling generally potentiates growth factor receptor activity (Byzova et al., 2000, Kuwada and Li, 2000). Expression α6β4 integrin in pancreatic cancer cells encourages cancer spreading and metastasis by promoting hepatocyte growth factor (HGF)-induced activation of Rac1 (Cruz-Monserrate and O'Connor, 2008).

In the longer term, chemotactic signals control gene expression, thereby regulating the heterogeneity of the migratory cell population. In tracheal cells, soluble FGF enhances the expression of its own receptor, and also increases expression of Delta1 to regulate FGF's downstream signalling, altogether reinforcing the leader phenotype (Ghabrial and Krasnow, 2006, Pocha and Montell, 2014, Vincent et al., 1998, Ikeya and Hayashi, 1999). Similar genetic effects are observed during vascular sprouting (Hellstrom et al., 2007, Siekmann and Lawson, 2007) and tumour angiogenesis (Noguera-Troise et al., 2006, Ridgway et al., 2006), ensuring the stability of leader cell characteristics.

Just as how follower cells, in addition to leaders, have a role in supracellular polarity and force generation, they likewise play an important role in collective cell chemotaxis. For example, neural crest cell chemotaxis is far more efficient as a collective than as individually dissociated cells (the cluster is more directional and persistent, and a group of *n* cells will reach their target whereas only a few *n* individual moving cells will reach their destination), suggesting that leaders need followers in order to respond properly (Theveneau et al., 2010, Malet-Engra et al., 2015). The cranial neural crest undergo chemotaxis toward SDF1, and other chemokines and growth factors *in vivo* via stereotypical streams or chains (Section 2.4.2) (Fig. 1.7, G and H). CIL between cells, including followers, is essential for supracellular polarisation and therefore allows for collective behaviour.

Because chemotactic signals determine directionality, clusters have an advantage over single cells in that their larger size means they can better detect a gradient, so long as they can cooperate over the entire distance. A consequence of this is that a cluster is more persistently polarised along the front-rear axis than individual cells (Theveneau et al., 2010). However, a fundamental problem with the 'source and sink' model in which cells endocytose the chemotactic signal and migrate up the gradient is that, whereas externally-imposed gradients are effective at short ranges, they work dramatically less well at longer ranges. Moreover, in externally-imposed gradients, all cells respond similarly. Instead, it is now thought that most chemotactic events work in which the migratory cell group self-generates a

chemotactic gradient. In the case of the zebrafish lateral line, cells respond to uniform external SDF1 rather than a gradient (David et al., 2002, Wilson et al., 2007). In addition, while front cells express CXCR4b, rear cells express CXCR7 (Aman and Piotrowski, 2008); SDF1 binding to receptors of the latter allow the group to sense a gradient by acting as a sink (Fig. 1.7, C and D) (Dambly-Chaudiere et al., 2007, Valentin et al., 2007, Dona et al., 2013, Aman and Piotrowski, 2010). Hence, the lateral line self-generate an SDF1 gradient across the primordium (Fig. 1.8A). Similarly, melanoma cells self-generate a gradient of lysophosphatidic acid (LPA) which encourages tumour metastasis (Muinonen-Martin et al., 2014) (Fig. 1.8B). During E-Coli CCT along a self-generated gradient, cells migrate as a coherent group by spontaneously sorting themselves such that difference between individual chemotactic abilities are compensated by differences in the local steepness of the traveling gradient each individual must navigate (Fu et al., 2018). In *Xenopus*, cranial neural crest undergo collective chemotaxis toward SDF1-producing placode cells (Theveneau and Mayor, 2012b, Mayor and Theveneau, 2013), but CIL between the cell populations boosts placode migration further forward, meaning a distance of effective chemotactic gradient is maintained as the two cell populations move (Fig. 1.8C) (Section 2.4.8) (Theveneau et al., 2013). CIL could also help maintain efficient collective chemotaxis of other cell populations by this mechanism too; such as metanephric mesenchyme chemotaxis toward glial cell line-derived neurotrophic factor (GDNF) (Costantini and Kopan, 2010), CIL between front and rear regions of the lateral line by FGF (Nogare et al., 2014), and/or between tumour cells and fibroblasts (Bhowmick et al., 2004, Pietras and Ostman, 2010, Szabo and Mayor, 2015). Furthermore, cell-cell communication enhances the capacity of cell groups to sense shallow gradients during morphogenesis (Ellison et al., 2016), although there are limits to the precision of gradient sensing with spatial communication and temporal integration (Mugler et al., 2016).

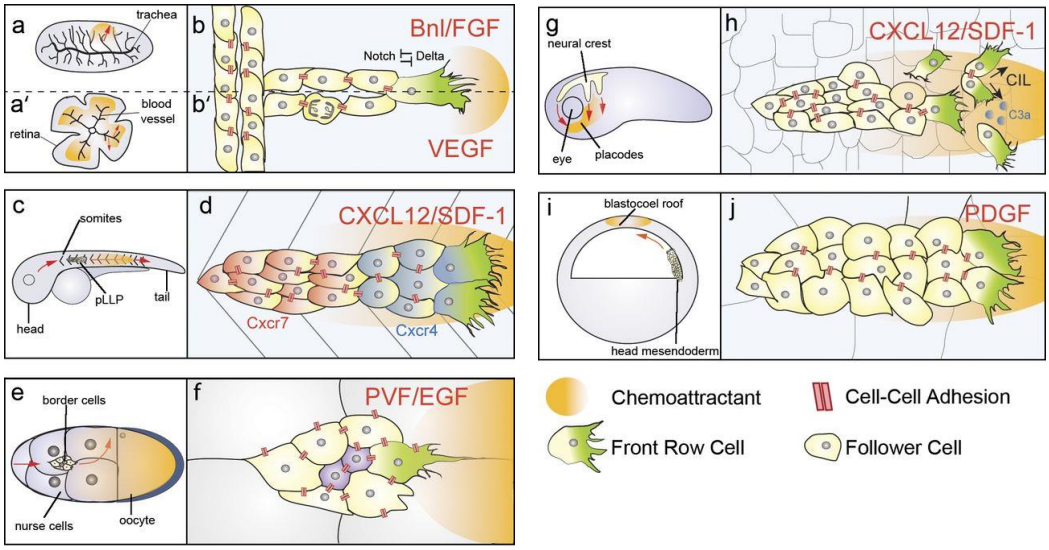

Fig. 1.7. Examples of collective cell chemotaxis. (**A to B'**) Branching morphogenesis of *Drosophila* trachea and sprouting morphogenesis of mouse retina toward Bnl or VEGF, respectively. Both are examples of the chemoattractant inducing tip and stalk cell fates via Notch-mediated lateral inhibition. (**C and D**) Caudal migration of the zebrafish lateral line primordium toward SDF1, which binds CXCR4 on front cells and CXCR7 on rear cells. Front cells respond by forming protrusions, while followers endocytose SDF1. (**E and F**) *Drosophila* border cells migrate posteriorly and then dorsally in the egg chamber between nurse cells in response to PVR and EGF, with the most responsive cell having large forward-directed protrusions. They are in contact with polar cells (purple) during migration. (**G and H**) Neural crest migrate ventrally across the *Xenopus* head toward SDF1. Collective migration requires CIL to polarise front cells and co-attraction via C3a/C3aR to prevent dispersion. (**I and J**) Collective migration of head mesendoderm toward the blastocoel roof (BCR), which is a source of PDGF in *Xenopus*. Protrusions are oriented in a PDGF and cell–cell contact–dependent manner.

Adapted from (Scarpa and Mayor, 2016).

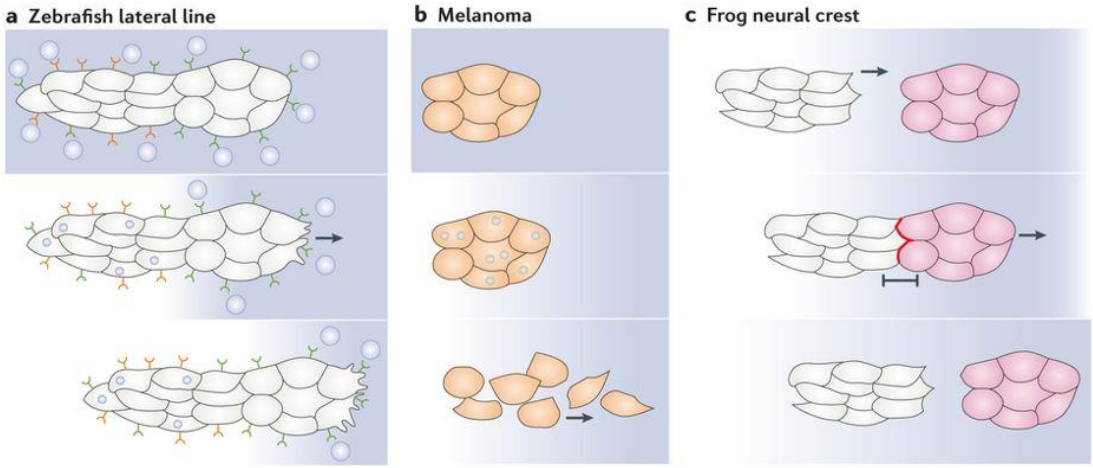

Fig. 1.8. Self-generated chemoattractive gradients during collective cell migration. (A) The front of the zebrafish lateral line primordium expresses CXCR4 (green), whereas the rear expresses CXCR7 (red). SDF1 is initially uniformly expressed and binds to both receptors. But while activated CXCR4 results in protrusion formation, CXCR7 acts as a decoy receptor that becomes internalised upon SDF1 binding. Thus, the lateral line self-generates an SDF1 gradient which can be followed. **(B)** LPA is initially heterogeneously distributed in the ECM. Melanoma cells degrade LPA, thereby self-generating a gradient due to low local LPA levels. Thus, the undergo self-generated chemotaxis to LPA. **(C)** *Xenopus* neural crest cells (grey) undergo collective chemotaxis towards SDF1 that is secreted by placode cells (pink). Upon contact, they trigger CIL which forces the placodes to move away. This 'chase and run' mechanism (Section 2.4.8) allows for continue movement along the gradient.

Adapted from (Mayor and Etienne-Manneville, 2016).

2 Neural crest

2.1 Introduction to neural crest

2.1.1 A brief history

The neural crest, first identified exactly 150 years ago, is the name given to the fold of neural ectoderm at the junction between neural and epidermal ectoderm in neural-stage vertebrate embryos. It was first discovered by Wilhem His in 1868 as a cell population between the dorsal neural tube and the dorsal epidermal ectoderm and the source of spinal and cranial ganglia (His, 1868). His named this cell population 'Zwischenstrang', the intermediate cord, which was later renamed neural crest by Arthur Milnes Marshall in 1879 (Marshall, 1879). Most initial research was performed in amphibian embryos (Hörstadius 1950), before cell labelling techniques such as radioisotopic labelling with tritiated thymidine, rhoadamine-lysinated dextra, the vital dye dil, and the quail-chick marking system (Le Douarin, 1969) allowed researchers to visualise neural crest through development. Now, a wide variety of techniques are utilised to study the neural crest *in vitro* and *in vivo* and in a variety of species.

2.1.2 A brief overview

The neural crest is a highly migratory, transient, multipotent embryonic stem cell population found exclusively in vertebrates. Indeed, it has been proposed that the emergence of the neural crest was central to the evolution of vertebrates (Northcutt and Gans, 1983, Gans and Northcutt, 1983), accounting for the acquisition of greater complexity in the vertebrate head (Munoz and Trainor, 2015). It is initially induced at the neural plate border, before migrating toward more dorsal regions of the developing embryo. During migration or upon arrival at their destination, the neural crest differentiates into various cell types, contributing extensively to many different tissues. For this reason, the neural crest has been called 'the fourth germ layer'.

The neural crest is a diverse cell population; their position in the embryo, their origin, their behaviour including migratory method, and cell type they will differentiate into differs from one species to another, from one subpopulation to another and even from one cell to another within the same subpopulation.

2.2 Neural crest formation

2.2.1 Induction/specification

The neural crest is initially induced at late blastula stages at the neural plate border as a result of the interaction between the ectodermal neural plate and the non-neural,

ectodermal epidermis (Duband et al., 2015) (Fig. 2.1). Neural crest can be induced whenever a border between these two tissues forms (Mancilla and Mayor, 1996, Selleck and Bronner-Fraser, 1995, Bronnerfraser, 1994, Sauka-Spengler and Bronner-Fraser, 2008).

In *Xenopus* and zebrafish, induction is driven by a reduction of bone morphogenetic protein (BMP) signalling in the ectoderm (Marchant et al., 1998, Nguyen et al., 1998). In other vertebrates, such as chick and mouse, induction appears to be driven by the confrontation of BMP-expressing ectoderm with non-BMP-expressing ectoderm (Streit and Stern, 1999). In addition to BMP signalling, Wnt activity, FGF signalling, retinoic acid and Notch signalling all play an important role in the induction and maintenance of the neural crest; these signals are produced by neighbouring regions and in particular by the neural plate, the epidermal ectoderm and the underlying mesoderm (Milet and Monsoro-Burq, 2012, Prasad et al., 2012). The precise combination of these signalling molecules controls neural crest specification (Steventon et al., 2005) by regulating the expression of transcription factors at the neural epidermal border belonging to the *Msx*, *Pax* and *Zic* families (Tribulo et al., 2003, Woda et al., 2003, Luo et al., 2002). These transcription factors in turn upregulate neural crest-specific transcription factors such as *Slug/Snail*, *SoxE/Sox9/Sox10*, *FoxD3*, *AP-2* and *c-Myc* (Sasai et al., 2001, Mayor et al., 2000, LaBonne and Bronner-Fraser, 2000, del Barrio and Nieto, 2002, Aybar et al., 2003, Honore et al., 2003, Meulemans and Bronner-Fraser, 2004) that activate target genes responsible for further neural crest development. All three levels of interaction shape a system of tightly controlled relationships that create the neural crest gene regulatory network; and in *Xenopus*, all of these neural crest specifiers are necessary and/or sufficient for the expression of all of the other specifiers, demonstrating the existence of extensive cross-regulation (Sauka-Spengler and Bronner-Fraser, 2008, Bronner-Fraser, 2005, Basch et al., 2004, Huang and Saint-Jeannet, 2004, Meulemans and Bronner-Fraser, 2004).

2.2.2 Maintenance

Neural crest identity is maintained during neurulation and is driven by Wnt and BMP activity from the intermediate mesoderm (Steventon et al., 2009). A gene regulatory network, including the above described transcription factors such as Snail1 and Snail2, which are members of the SNAI family of transcription factors, are expressed by the neural crest where further development is required (del Barrio and Nieto, 2002, Shi et al., 2011, LaBonne and Bronner-Fraser, 2000). Snail promotes the expression

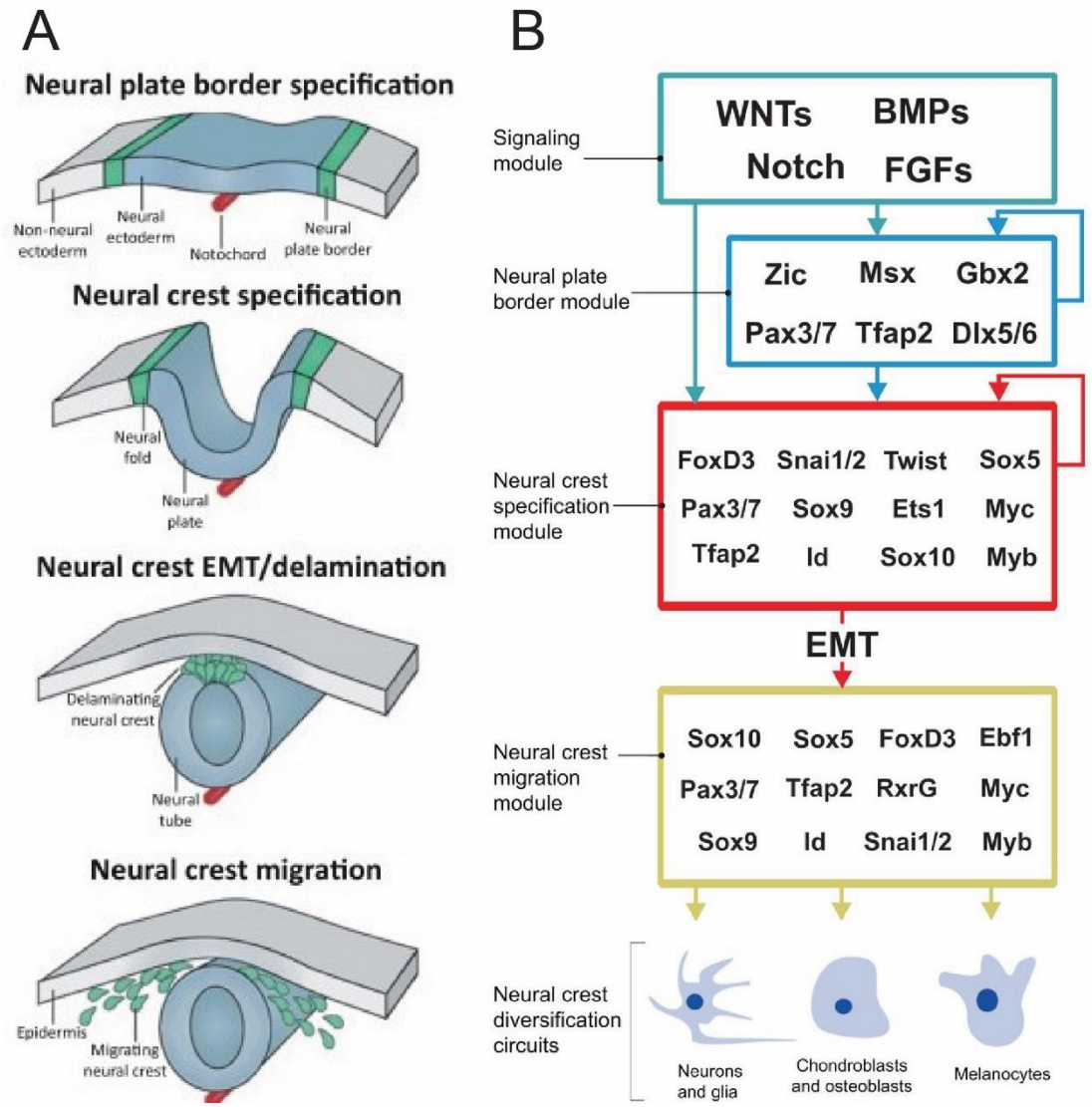

Fig. 2.1. Overview of neural crest development. A, The neural crest form by a series of regulatory events: induction at the neural plate border, specification, delamination from the neural tube, migration throughout the embryo and differentiation into many derivatives. **B**, a gene regulatory network controls neural crest development. Inductive signals pattern the ectoderm and induce the expression of neural plate border specific genes, which define plate border territory. These genes engage in positive regulation and drive neural crest specification, which results in activation of EMT machinery to allow the neural crest to become migratory. Migratory neural crest express genes that allow them to remain motile and eventually initiate different differentiation programmes.

Adapted from (Simoes-Costa and Bronner, 2015) and (Martik and Bronner, 2017)

of other maintenance genes, such as *Twist*, *FoxD3* and *Sox9* and *Sox10* (Aybar et al., 2003). Twist, a basic helix-loop-helix (bHLH) transcription factor, and Id, a direct target of c-Myc, are also important for the maintenance of neural crest stem cell identity. These maintenance genes are required to ensure the steady state of the population of the neural crest by acting as survival factors through inhibition of apoptosis and proliferation (Sauka-Spengler and Bronner-Fraser, 2008, Vega et al., 2004, Tribulo et al., 2004). Altogether, they ensure that an appropriate number of neural crest precursors are maintained before the beginning of migration.

2.2.3 Delamination and epithelial-mesenchymal transition (EMT)

After induction and specification, the neural crest is initially a highly cohesive but non-migratory population of cells with epithelial characteristics. They leave the border of the neural plate through a process of delamination. Delamination is defined as the separation of tissue into different populations, in this case the neural crest cells separating from the surrounding tissue (Theveneau and Mayor, 2012b). This process involves the neural crest going through a full or partial epithelial-mesenchymal transition (EMT), which refers to a series of events coordinating a change from an epithelial to mesenchymal phenotype (Lamouille et al., 2014).

Prior to delamination, presumptive neural crest cells are initially anchored to neighbouring cells by tight junction proteins such as occludin and cell adhesion molecules such as NCAM and E-Cadherin (Kandel, 2013). Dorsally expressed BMPs initiate delamination through upregulation of factors that are also involved in neural crest induction, such as the zinc finger transcription factors snail1, snail2, slug, twist, FoxD3 and sox9 and sox10 (Sanes, 2012, Cheung et al., 2005). When Sox9, Snail2 and FoxD3 are overexpressed together they are able to induce ectopic neural crest cells (Cheung et al., 2005). A transient inhibition of Wnt signalling may also be required for delamination (Rabadan et al., 2016). These signals coordinate changes in the structure of the neural plate cells, causing fusion of the neural folds, and resulting in the formation of a closed neural tube and of neural crest on its dorsolateral aspect on each side (Duband et al., 2015, Theveneau and Mayor, 2012b). Both the prospective neural plate and the prospective epidermis contribute to the neural crest (Mancilla and Mayor, 1996, Selleck and Bronner-Fraser, 1995). Hence the neuroectoderm splits into two populations, the neural tube and the neural crest (Theveneau and Mayor, 2012b).

Prior to delamination, the neural crest are epithelial. Epithelial cells are tightly bound together, highly stable, organised in sheets, supported by a basal lamina and display

apico-basal polarity. Mesenchymal cells, on the other hand, are loosely associated with their neighbours and are highly motile. The change from epithelial to mesenchyme type is known as EMT (Nieto and Cano, 2012, Thiery et al., 2009). EMT therefore marks a change from a non-migratory epithelial-tissue with stable cell adhesions to a mesenchymal migratory population with transient or looser connections. EMT plays a key role in development; it is required for various processes including formation of the mesoderm during gastrulation, heart morphogenesis and the formation of the sclerotome (Larue and Bellacosa, 2005). In addition, the invasiveness of cancer cells is associated with cells undergoing EMT (Angela Nieto, 2013, Thiery et al., 2009, Thiery and Morgan, 2004). EMT is a reversible process and cells can revert to epithelia by mesenchymal-epithelial transition (MET) (Chaffer et al., 2007).

EMT is characterised by a loss in apico-basal polarity markers, a gain in front-rear polarity, a reduction in intercellular adhesions and increased motility converting highly cohesive epithelial cells to the loosely connected mesenchymal cells (Hay, 1995). This switch requires many cellular changes, including actin reorganisation, cell-cell adhesion disassembly and changes to cell-matrix adhesions.

For neural crest, partial or full EMT is important for their delamination and essential for their subsequent migration. During EMT in neural crest cells, epithelial cell-cell junction proteins such as E-Cadherin, gap junction components and tight junction components are downregulated (Vandewalle et al., 2005, Kirby and Hutson, 2010). Many of the regulators of EMT in neural crest are those involved during its induction, maintenance and delamination. For example, BMP signalling, in addition to its inductive and delamination-inducing roles, activates Sip1 (van Grunsven et al., 2007), a transcriptional repressor and known promoter of EMT (Thiery et al., 2009, Kang and Massague, 2004, Kerosuo and Bronner-Fraser, 2012), in neural crest cells (Rogers et al., 2013). Sip1 specifically targets genes involved in epithelial cell-cell junctions, inhibits the expression of E-Cadherin (Rogers et al., 2013, Vandewalle et al., 2005) and its absence from neural crest cells prevents normal migration *in vivo* (Van de Putte et al., 2003). Many of the transcription factors involved in delamination, such as slug, snail and twist, also repress the expression of E-Cadherin and other epithelial junction components during EMT (Taneyhill et al., 2007, Nieto et al., 1994, Kang and Massague, 2004, Carl et al., 1999), which leads to the reconstruction of cell junctions (Barriga et al., 2013, Bolos et al., 2003). These factors also reduce the expression of occluding and promote modification of NCAMs with polysialic acid residues to decrease adhesiveness (Sanes, 2012, Taneyhill, 2008). HIF-1 also plays a role in

promoting EMT in the neural crest by promoting the expression of *Twist*, which represses *E-Cadherin* (Barriga et al., 2013).

As described above, a key feature of EMT is a cadherin switch where the expression of one type of cadherin is repressed and another is promoted. In addition to the reduction of E-Cadherin and tight junction components, weaker cadherins are upregulated. The cranial neural crest initially switches from expressing E-Cadherin to N-Cadherin, which is essential for its efficient migration (Rogers et al., 2013, Scarpa et al., 2015, Dady et al., 2012). The switch from E-Cadherin to N-Cadherin in cranial neural crest cells coincides with neural induction (Dady et al., 2012, Nandadasa et al., 2009, Rogers et al., 2013). Consequently, neural crest cells leave the closing neural tube and start expressing N-Cadherin (Bronnerfraser et al., 1992, Xu et al., 2001a, Theveneau et al., 2010) through the action of Sip1, and the transcription factors *Ets1*, *LSox5* and p53 (Perez-Alcala et al., 2004, Theveneau et al., 2007, Rinon et al., 2011, Rogers et al., 2013, Van de Putte et al., 2003). This upregulation in N-Cadherin in the cranial neural crest is essential for their migration (the role of N-Cadherin for migration is described in detail in Section 2.4) (Rogers et al., 2013, Scarpa et al., 2015, Van de Putte et al., 2003). Some type II cadherins are also expressed during migration, such as cadherin-7 and cadherin-11 (Cheung et al., 2005, Hadeball et al., 1998, Nakagawa et al., 2001), and residual levels of E-Cadherin also continue to be expressed (Barriga et al., 2013).

In contrast to cranial neural crest, the cadherin switch is not sufficient to promote EMT and delamination from the neural tube in trunk neural crest; instead, the cadherins switch again from N-Cadherin to cadherin-6 and cadherin-7 (Nakagawa and Takeichi, 1995, Park and Gumbiner, 2012, Clay and Halloran, 2014), which is controlled by the transcription factors *Snail/Slug*, *Foxd3* and *Sox9/10* (Cheung et al., 2005). Hence, these factors mediate a change in the neural crest from strong adhesions to weak ones.

In addition to the change in cell-cell adhesion components, neural crest cells also acquire a migratory phenotype during EMT. This involves the expression of intermediate filament proteins, the flattening of the cells and the ability to generate lamellipodia and filopodia to facilitate migration. The onset of migration in the neural crest is characterised by blebbing in the membrane, a process mediated by myosin II and ROCK activity (Berndt et al., 2008). Once the neural crest have separated from the neural tube the cells start to produce more robust lamellipodia and filopodia (Berndt et al., 2008).

Neural crest cells also begin expressing proteases capable of degrading cadherins such as a distintegrin and metalloproteinase 10 (ADAM10) (Mayor and Theveneau, 2013) and MMPs that degrade the overlying basal lamina of the neural tube to allow neural crest cells to escape (Kandel, 2013). They also express integrins that associate with ECM proteins, including collagen, fibronectin, and laminin, during migration (Sauka-Spengler and Bronner-Fraser, 2008). Once the basal lamina becomes permeable the neural crest cells can begin migrating throughout the embryo.

The processes of EMT and delamination are intimately linked, and the onset of these two processes relative to each other varies for different population of the neural crest along the anterior-posterior axis and for different species (Theveneau and Mayor, 2012b). In the cranial neural crest of *Xenopus*, the model used in this thesis, delamination occurs prior to the onset of EMT and the neural crest all delaminate at once as a collective whilst the neural tube is still open (Sadaghiani and Thiebaud, 1987), allowing the tissue to start its migration as group (Theveneau and Mayor, 2012b). As cells lose epithelial polarity, strong cell-cell and cell-matrix adhesions and acquire motility, they can leave the neuroepithelium of the dorsal neural tube and become highly migratory (Theveneau and Mayor, 2012b). Similar delamination is observed in mouse cranial neural crest (Nichols, 1981, Nichols, 1987) but chick cranial neural crest delaminate only upon fusion of the neural folds (Duband and Thiery, 1982). By contrast, trunk neural crest cells delaminate gradually one at a time as single cells after the neural tube has closed (Clay and Halloran, 2010, Duband, 2010, Erickson and Weston, 1983, Sela-Donenfeld and Kalcheim, 2000, Berndt et al., 2008, Clay and Halloran, 2014), demonstrating the fact that delamination and EMT are two distinct processes that corresponds to separate events. For the avian trunk neural crest, asymmetric localisation of DLC1 promotes their directional delamination and individual cell migration (Liu et al., 2017). Inhibition of delamination by preventing cells to enter the S-phase does not affect the EMT programme and the expression of *Snail2* (Burstyn-Cohen et al., 2004). Furthermore, ectopic expression of *Sox9* can induce neural crest but not EMT (Cheung and Briscoe, 2003). However, in some cases, the two processes intertwine; the transcription factor *Sox9*, apart from controlling neural crest specification and survival, can also trigger EMT in coordination with Snail2 (Cheung et al., 2005).

Overall EMT is a intricate process that requires change in cellular architecture driven by small GTPases, cytoskeletal re-organisation, cell junctional alterations and changes in supracellular polarity. The neural crest therefore undergoes dramatic

changes during EMT that facilitate them for their next migratory phase. Indeed, because EMT is a hallmark of metastasis in cancer and the neural crest have been compared to cancer cells (Fig. 2.2), the neural crest is often used as a model to investigate the molecular mechanisms driving the process (Kulesa et al., 2013, Kerosuo and Bronner-Fraser, 2012, Powell et al., 2013, Gallik et al., 2017).

2.3 Neural crest differentiation

The neural crest are multipotent stem cells, able to differentiate into many cells types and extensively contribute to numerous tissues (Fig. 2.3A) (Dupin et al., 2006). Their specification is a multistep process that occurs during and after cell migration. Neural crest cells receive paracrine inductive signals from the neural tube, paraxial mesoderm and the overlying ectoderm as they migrate that specify their fate, and their fate is determined by the time at which they migrate, their origin, the stream in which they are found and their destination (Rogers et al., 2012, Le Douarin and Teillet, 1974, Stemple and Anderson, 1993, Le Douarin et al., 1993, Le Douarin, 2004).

Based on their position of origin along the anterior-posterior axis, the region into which they migrate and the tissues that they contribute to, the neural crest can be sub-divided into four populations: cranial or cephalic, vagal and sacral, truncal and cardiac. The neural crest differentiates into a vast number of cell types that include ectomesenchymal cells and non-ectomesenchymal cells. The cranial neural crest migrates dorsolaterally through the embryo into the pharyngeal arches. They colonise the face and neck, contributing to the craniofacial mesenchyme, which includes cartilage, bone, dermis,, smooth muscle, teeth, cranial neurons, glia and connective tissue (Hall, 2008, Theveneau and Mayor, 2011c). Trunk neural crest migrates in one of two directions. Those that migrate dorsolaterally over the somites give rise to the melanocytes, while those that migrate ventrolaterally between somites and the neural tube become glia, dorsal root ganglia, part of the sympathetic nervous system, and neurons of the peripheral nervous system and epinephrine-producing cells of the adrenal gland depending on how far they migrate. The vagal and sacral neural crest migrate ventrally into the splanchnic and parasympathetic ganglia of the enteric nervous system in the gut. The cardiac neural crest migrate into the pharyngeal arches developing into melanocytes, cartilage, connective tissue and pharyngeal arch neurons, contributing to heart valves and arteries. Some migrate beyond the pharyngeal arches (also known as the branchial arches) to the cardiac outflow tract where they contribute to the arteries and the cardiac septum of the cardiovascular system.

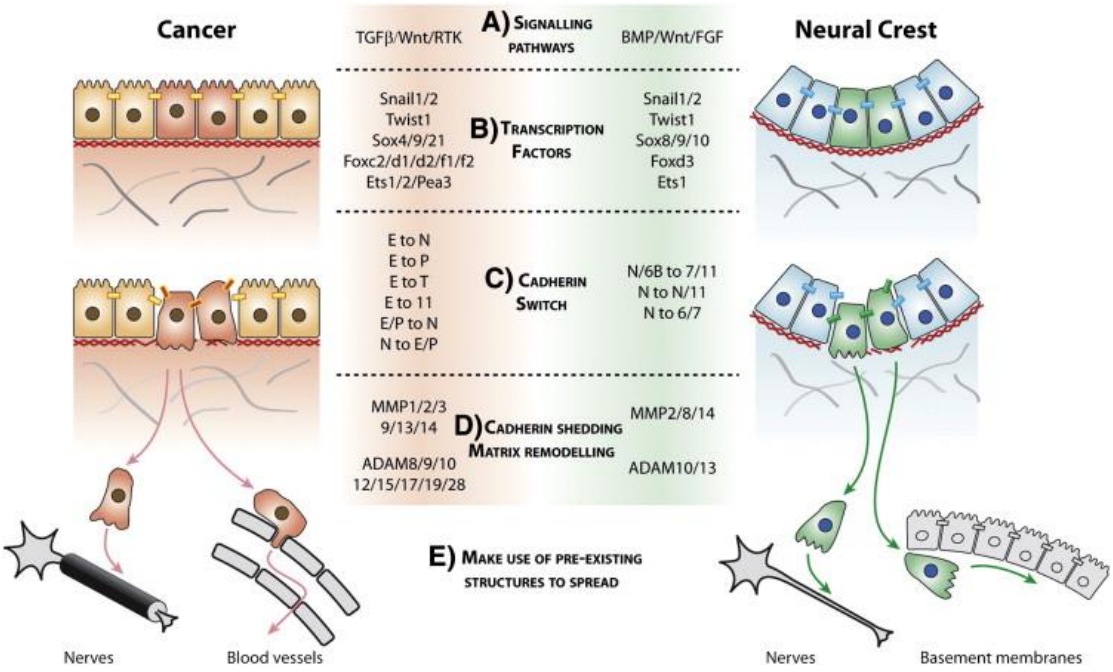

Fig. 2.2. Cancer and neural crest development. A, Pre-migratory neural crest and benign tumours express high levels of the indicated signalling pathways which induce expression of similar transcription factors (B) that initiate EMT. During EMT, similar changes in adhesion proteins are observed that allow cells to escape from their original tissue (C), as well as matrix remodelling proteins (D). E, neural crest migrate in a solitary of collective fashion, like neural crest, depending on context.

Adapted from (Theveneau and Mayor, 2012b)

2.4 Neural crest migration

2.4.1 Introduction

After undergoing EMT, the neural crest becomes a highly migratory cell population, often likened to invasive cancers (Theveneau and Mayor, 2012b, Kulesa et al., 2013, Theveneau and Mayor, 2011b, Kerosuo and Bronner-Fraser, 2012). Neural crest cell migration has been studied in a variety of vertebrate animal models, including *Xenopus*, zebrafish, chick, mouse (Barriga et al., 2015) and even non-classical model organisms such as lamprey (Nikitina et al., 2008), hagfish (Ota et al., 2007) and turtle (Gilbert et al., 2007, Cebra-Thomas et al., 2013). The neural crest migrate ventrally down the embryo, initially as a continuous wave away from the neural tube, but quickly splitting into discrete streams along stereotypical pathways to various sites (Fig. 2.3A). The cranial neural crest migrates along dorsolateral routes between the ectoderm and underlying paraxial mesoderm (Tosney, 1982, Kuo and Erickson, 2010). In chick and mouse, early trunk neural crest migrates ventrolaterally through the anterior sclerotome (Bronner-Fraser, 1986, Rickmann et al., 1985, Loring and Erickson, 1987, Teillet et al., 1987). Trunk neural crest migrating later, which will become melanocytes, follow the dorsolateral path between the dermomyotome and dorsal ectoderm, with their migration affected by the structure of the somites (Rawles, 1948, Collazo et al., 1993, Kelsh et al., 2009). However in zebrafish and *Xenopus*, melanocytes use both ventromedial and dorsolateral pathways.

In this thesis, the cranial neural crest of *Xenopus* and zebrafish embryos have been used as a model system for studying collective cell migration and collective cell chemotaxis, because they migrate collectively and in response to external chemotactic signals both *in vivo* and *ex vivo*, after dissection and culture of the neural crest (Alfandari et al., 2003). Hence the details below, unless otherwise stated, refer to the *Xenopus* and zebrafish crania neural crest, rather than other neural crest cell populations. This section will outline the multiple factors known to be involved in neural crest migration, including physical constraints, cell-cell and cell-matrix interactions, and chemotaxis (Woods et al., 2014, Theveneau and Mayor, 2012c, Perris, 1997).

2.4.2 Formation of streams

As the neural crest begin migration, they are gathered into characteristic streams. The cranial neural crest initially splits into three distinct stereotypical streams: the mandibular, hyoid and branchial. The loosely associated neural crest cells that make

up these streams migrate large distances along established routes ventrally to invade the segmented branchial arches (BAs). In these streams, the neural crest cells migrate large distances, confined between the basal lamina beneath the epidermis and the developing dermomyotome along the dorso-ventral axis of the developing head. In the head, inhibitory cues such as Semaphorin-3F (Gammill et al., 2007) and versican (Szabo et al., 2016), and others, are expressed in the epibranchial placode cells surrounding the migratory streams originating from the hindbrain (Section 2.4.3). In addition, EphA4, EphB1 and ephrin-B2 are expressed in the neural crest and matching mesoderm (Smith et al., 1997). Blocking the function of these inhibitors impairs the correct formation of neural crest streams (Gammill et al., 2007, Smith et al., 1997), suggesting that the neural crest streams are shaped by a pre-existing environmental pattern of inhibitors that funnels the neural crest into correct migratory pathways (Golding et al., 2000). However, prior to migration the inhibitors are not patterned along the presumptive neural crest streams in the epibranchial region as they are expressed as a continuous band adjacent to the neural crest. Therefore, how the initial formation of the neural crest streams is established remains unknown.

Other sources of pre-pattern have been suggested at late stages of migration when the neural crest streams enter the pharyngeal arches, a series of composite structures segmenting the head (Graham and Smith, 2001, Shone and Graham, 2014). The pattern of the arches is established through patterned expressions of BMP/FGF in the endoderm independently of the neural crest (Veitch et al., 1999) which might control the establishment of the neural crest stream pattern (Cerny et al., 2004). However, while this could explain the separation of the cranial neural crest streams at the late migratory stages, it is unclear how the neural crest streams in the ectoderm would be guided by the distant endoderm. Furthermore cranial streams of the neural crest have been observed prior to pharyngeal arch morphogenesis (Schilling and Kimmel, 1994, Kimmel et al., 2001). Consequently, one idea is that the initial establishment of the neural crest streams results from the dynamic interactions of the neural crest and placodal tissues, which are known to occur in neural crest migration (Theveneau et al., 2013) (Section 2.4.8).

2.4.3 Restrictive signals

The fate of the neural crest cells is determined by the stream they are in. For this reason, and to promote neural crest invasion itself, it is important that the cells maintain their streams. There are a variety of factors promoting and maintaining the restriction of the streams. The death of some neural crest cells in specific areas is

thought to contribute to the initial formation of the streams by creating the crest-free regions between the streams (Kirby and Hutson, 2010). Negative cues define and maintain the neural crest-devoid regions between the separate streams as the neural crest migrate through permissive areas. However, whether they help establish the streams is unclear (Section 2.4.2). The repulsion is driven by a number of inhibitory molecules.

The repulsive signals of ephrins and class 3 semaphorins are the major two family groups acting as restrictive signals between neural crest streams (Fig. 2.3B) (Yu and Moens, 2005). The formation of these ligand/receptor complexes result in bidirectional signalling that repels the neural crest, by protrusion collapse which is observed at the interface between neural crest and neighbouring tissue (Theveneau and Mayor, 2012c). Semaphorins 3A, 3F and 3G are expressed in the crest-free area between the streams; and their cognate receptors, neuropilins 1 and 2, and the co-receptor plexin A1, are expressed by the cranial neural crest (Koestner et al., 2008, Yu and Moens, 2005, Osborne et al., 2005, Eickholt et al., 1999, Gammill et al., 2007, Vastrik et al., 1999). Neural crest cells expressing these receptors are repulsed by the presence of the semaphorins and therefore do not migrate on the regions where they are present (Eickholt et al., 1999, Chilton and Guthrie, 2003, McLennan and Kulesa, 2007). Likewise, class 3 semaphorins contribute to neural crest segregation in the head, trunk and caudal regions of the sclerotome (Eickholt et al., 1999, Gammill et al., 2007, Gammill et al., 2006, Osborne et al., 2005, Yu and Moens, 2005, Toyofuku et al., 2008) by acting through plexin–neuropilin complexes expressed by the neural crest (Gammill et al., 2006, Gammill et al., 2007, Osborne et al., 2005, Yu and Moens, 2005). Perturbed semaphorin signalling results in ectopic migration of cranial neural crest cells between the normal streams in mouse (Gammill et al., 2007), and migration of the trunk neural crest also relies on repulsive semaphorin signalling (Gammill et al., 2006).

The Eph/Ephrin family also restrict migration of the neural crest to distinct streams. A variety of Ephs and ephrins are expressed by and around the cranial neural crest, respectively, of many different model organisms and although the exact expression is not conserved across species, the role they play is always inhibitory (Wang and Anderson, 1997, Smith et al., 1997, Davy and Soriano, 2007, Mellott and Burke, 2008, Adams et al., 2001, Davy et al., 2004, Winning et al., 1996). There is a similar role for Eph/Ephrins in chick trunk neural crest migration (Santiago and Erickson, 2002). This includes preventing neural crest cells from invading non-neural crest tissue and the caudal half of somites, thereby restricting them to the rostral half of somites in chick

embryos (Kuriyama and Mayor, 2008, Gammill and Roffers-Agarwal, 2010). Perturbation of Eph/Ephrin signalling results in the formation of non-distinct streams with the neural crest either invading surrounding tissue or migrating across to the wrong stream (Smith et al., 1997). For instance, ephrin-B2 is expressed in the second branchial arch and is a repulsive cue for neural crest cells that migrate to the third and fourth branchial arches, as they express EphA4 and EphB1 (Smith et al., 1997). The mixing of neural crest from different streams is also prohibited because neural crest belonging to different streams express complementary Eph receptors and ephrin ligands (Theveneau and Mayor, 2012b).

Other signals that restrict neural crest migration involve Slit/Robo interactions. The receptors Robo1 and Robo2 are expressed by early migrating trunk neural crest cells and respond to Slit2, which is expressed in the dorsolateral pathway (Jia et al., 2005, Giovannone et al., 2012). Additionally, the extracellular matrix proteoglycan, versican, is also expressed by the region between the streams and its presence confines the migration of the neural crest to versican-free regions (Szabo et al., 2016). The BMP anagonist, DAN, is expressed in mesoderm that becomes absent along migratory pathways, restrains cell speed thereby inhibiting uncontrolled neural crest (and also metastatic melanoma) invasion (McLennan et al., 2017). Moreover, restricting the neural crest to streams *in silico* facilitates their migration (Szabo et al., 2016, Woods et al., 2014), similar to other migrating cell types (Liu et al., 2015, Xi et al., 2017, Chen et al., 2018, Denais et al., 2016, Monzo et al., 2016, Lautscham et al., 2015) in which cells are funnelled down corridors.

2.4.4 Cell-cell contacts and collective cell migration

The neural crest displays a range of migratory behaviours depending on species and location within the embryo. Some exhibit a more individual migratory behaviour (Kulesa et al., 2004), whereas most of neural crest cells migrate together, either as chains, groups or even single sheets, in spite of the fact that neural crest go through EMT (Friedl and Gilmour, 2009, Theveneau and Mayor, 2011b, Rorth, 2009, Kulesa et al., 2010, Thiery et al., 2009). For example, cephalic neural crest cells maintain short and long-range cell–cell interactions during migration both *in vitro* (Erickson, 1985) and *in vivo* (Kulesa and Fraser, 1998, Kulesa and Fraser, 2000, Teddy and Kulesa, 2004). This kind of movement has been called collective cell migration, which can be defined as the coordinated migration of cells as tight clusters or loose groups (as in the case of neural crest), where cooperation between cells contributes to their

overall directionality (Theveneau and Mayor, 2012b, Rorth, 2009, Friedl et al., 2012, Revenu et al., 2014, Etienne-Manneville, 2014, Theveneau and Mayor, 2012a).

Overall directionality during collective cell migration is higher than during single cell migration, indicating that intercellular interactions promote the directionality of migrating neural crest (Kulesa and Fraser, 1998, Kulesa and Fraser, 2000, Teddy and Kulesa, 2004). Unlike epithelial cells, which move slowly and have tightly formed intercellular adhesions, the collective mass of the mesenchymal neural crest is a cohesive unit linked by transient contacts, such as N-Cadherin adhesions (Nakagawa and Takeichi, 1995, Pla et al., 2001, Taneyhill, 2008, Kulesa and McLennan, 2015). Cadherin levels, such as cadherin-11 and N-Cadherin, are tightly regulated as their presence is required for migration and too high or low levels can prevent migration (Kashef et al., 2009, Theveneau et al., 2010, Becker et al., 2013, Kuriyama et al., 2014, Vallin et al., 1998, Borchers et al., 2001). N-Cadherin dynamics is regulated by LPA receptor 2 (LPAR2), prompting N-Cadherin endocytosis which leads to an increase in tissue plasticity (Kuriyama et al., 2014). This plasticity allows neural crest cells to migrate under physical constrains without abolishing cell cooperation (Kuriyama et al., 2014). Hence, cell contacts are maintained but allow transient connections with a more fluid-like phenotype. N-Cadherin also controls re-organisation of the tissue and acquisition of migratory features through its induction of CIL via its inhibition of Rac1 (Section 2.4.6). The protocadherin PCNS is also expressed in migrating neural crest and is required for its migration (Rangarajan et al., 2006), although its role is not known.

Cell-cell communication is also necessary for efficient neural crest migration. Cx43, a gap junction protein that facilitates cell-cell communication, is important in regulating the speed and directionality of the neural crest; reduced expression results in reduced migration (Huang et al., 1998). Neural crest cells with reduced Cx43 expression have more protrusive activity and have less polarised migration. Also, cells lacking Cx43 fail to retract in response to Semaphorin (Xu et al., 2006). Further to its role in cell-cell communication, Cx43 is also involved in regulating adhesion through interactions with N-Cadherin (Xu et al., 2001b, Xu et al., 2001a). Moreover, semaphorin and ephrin inhibitory signals ensure NC remain in streams (Section 2.4.2), and short-range chemotaxis (Section 2.4.7.2) promotes collectiveness of the group.

2.4.5 Cell-substrate interactions

The neural crest migrates via permissive substrates containing extracellular matrix (ECM) proteins. In *Xenopus*, cranial neural crest express $\alpha5\beta1$ integrin which allows

it to migrate on fibronectin, its migratory substrate (Epperlein et al., 1988), which surrounds the migrating neural crest streams (Alfandari et al., 2003). However, in other populations, such as trunk neural crest from chick, other ECM proteins are involved, such as collagen, laminin or vitronectin (Bilozur and Hay, 1988), and so different integrins are required (Testaz and Duband, 2001). Cranial neural crest also express the proteoglycan, Syndecan-4 which binds to fibronectin (Matthews et al., 2008) and is important for the formation of focal adhesions (Woods et al., 2000). *In vivo*, collective neural crest migration relies on stiffening of the underlying head mesoderm, which triggers EMT (Barriga et al., 2018). Mechanosensation is detected by an integrin-vinculin-talin complex, which is necessary and sufficient for neural crest migration (Barriga et al., 2018).

Apart from receiving signals from local environment, neural crest cells alter their local milieu via ECM degradation. This is achieved through expression of various MMPs, (Giambernardi et al., 2001, Cai and Brauer, 2002, Duong and Erickson, 2004, Cantemir et al., 2004, Tomlinson et al., 2009), endopeptidases that process cell surface molecules. Also, various ADAMs – cell-surface-bound glycoproteins that participate in cell-cell adhesion by cleaving transmembrane proteins – are expressed (Alfandari et al., 1997, Cai et al., 1998), including ADAM13 which cleaves matrix glycoproteins (Alfandari et al., 2001). Both MMPs and ADAMs degrade a wide range of molecules from the ECM that are implicated in invasive behaviour during cell migration (Sternlicht and Werb, 2001, Edwards et al., 2008). TIMP2, a regulator of the activity of matrix metalloproteinases, is also required for neural crest migration (Cantemir et al., 2004). Expression of the glycoprotein Tenascin C is critical for neural crest migration (Tucker, 2001).

The totality of intrinsic and external input guide the neural crest as a collective through distinct streams in a directional manner. How these various cues are integrated and interpreted at the level of the cell and of the cluster is not well understood, though.

2.4.6 Contact inhibition of locomotion and directional migration

The importance of directional migration for the neural crest lies with the fact that they must reach and populate specific target regions. Directional migration requires cell polarisation, in order to specify a front that has localised actin polymerisation and a rear that is able to contract (Kay et al., 2008, Krause and Gautreau, 2014).

As discussed previously (Section 1.3.3.2), CIL can polarise cells in a contact-dependent manner (Mayor and Carmona-Fontaine, 2010, Roycroft and Mayor, 2016).

CIL has been since identified in neural crest cells and is the driving force behind phenomena including cell dispersion and collective cell migration.

CIL affects the behaviour of individual neural crest cells and the neural crest cell group. For single cells, it encourages cell dispersion by forcing colliding cells to migrate away from each other. For the group, CIL between cranial neural crest cells is required for collective directional migration *in vitro*, *in vivo*, and *in silico* (Carmona-Fontaine et al., 2008b, Theveneau et al., 2010, Theveneau et al., 2013, Woods et al., 2014). The signalling components responsible for CIL in neural crest cells appear to converge to regulate the small/Rho GTPases, Rac, Cdc42 and Rho, which are responsible for cell polarisation and cell migration including directionality (Ridley et al., 2003). Non-canonical (planar cell polarity, PCP) Wnt signalling is necessary for CIL in neural crest cells, by activating RhoA at sites of intercellular contact, which in turn suppresses the generation and maintenance of lamellipodia through its target ROCK (Carmona-Fontaine et al., 2008b, Carmona-Fontaine et al., 2008a). Specifically Wnt11 binds to Frizzled7 of a neighbour cell, which leads to the recruitment of Dischevelled at the cell-cell contacts, which activates a variety of molecules including RhoA (Matthews et al., 2008). Moreover, the proteoglycan syndecan-4, expressed by neural crest cells, cooperates with non-canonical Wnt and N-Cadherin signalling to inhibit Rac activity at the cell–cell contact (Carmona-Fontaine et al., 2008a, De Calisto et al., 2005, Matthews et al., 2008). Together, mutually exclusive zones of Rac1 and RhoA activity are generated in neural crest cells, meaning that protrusions are formed only at sites where there is no homotypic neural crest contact, because RhoA activation at the contact site results in reorganisation of actin cytoskeleton, which in turn leads to collapse of protrusions at the contact site and concurrent inhibition of Rac1. Meanwhile, Rac is promoted at the free edge. This asymmetric distribution of RhoA at the contact and Rac1 at the free edge leads to a change in cell polarity and in the direction of migration. Perturbation of components from the Wnt-PCP pathway inhibits neural crest migration *in vivo* and *in vitro* (De Calisto et al., 2005, Carmona-Fontaine et al., 2008a). Likewise, perturbed N-Cadherin expression results in an increase in Rac1 levels at the contact (Theveneau et al., 2010). The presence of E-Cadherin however suppresses CIL, indicating that the switch from E- to N-Cadherin during EMT controls contact inhibition of locomotion in neural crest cells (Scarpa et al., 2015). Moreover, CIL is controlled tissue-autonomously through the PDGFA/PDGFRα/PI3K/Akt signalling axis that controls N-Cadherin upregulation during EMT (Bahm et al., 2017). The tight junction complex protein Par3 also plays a role in CIL in the neural crest (Moore et al., 2013).

Most neural crest cells migrating *in vivo* maintain close proximity and move in compact groups. Therefore, the polarity required for directional migration is established because at the free edge of the cell cluster, due to the lack of neural crest cell–neural crest cell contact (Fig. 2.3B, purple protrusions), cells become polarized and generate protrusions such as lamellipodia away from the group (Carmona-Fontaine et al., 2008b, Mayor and Carmona-Fontaine, 2010, Petrie et al., 2009), whilst no protrusions are formed in the middle of the cluster. Hence, directional migration is an emergent property of NC cells that depends on cell–cell interactions (Groeger and Nobes, 2007, Astin et al., 2010, Dumortier et al., 2012). Rather than acting simply as an intrinsic force that promotes single cell migration, shifts in CIL probabilities can underlie transitions between solitary cell migration and collective cell migration (Desai et al., 2013). However, CIL alone is not sufficient to explain directional migration, as it would promote cell dispersion on its own. Significant evidence supports the presence and requirement of chemoattractants for neural crest migration *in vitro* and *in vivo* (Section 2.4.7).

2.4.7 Chemotaxis

2.4.7.1 Long-range chemoattractants

Various chemoattractants have been proposed for the neural crest (Shellard and Mayor, 2016), including SDF1/CXCL12 (Theveneau et al., 2010, Killian et al., 2009, Belmadani et al., 2005, Rezzoug et al., 2011), FGF (Creuzet et al., 2004, Sato et al., 2011, Kubota and Ito, 2000), VEGF (McLennan et al., 2010, Bron et al., 2004, McLennan et al., 2015, McLennan and Kulesa, 2010), PDGF (Tallquist and Soriano, 2003, Eberhart et al., 2008, Kawakami et al., 2011, Bahm et al., 2017), stem cell factor (SCF) (Rovasio et al., 2012), neurotrophin 3 (NT-3) (Zanin et al., 2013), GDNF (Mwizerwa et al., 2011, Young et al., 2001, Goto et al., 2013), neuregulin 1 (NRG1) (Saito et al., 2012) and TGFβ (Saika et al., 2001). However, whether chemotaxis mediates the long-range directional migration of neural crest *in vivo* has not been conclusively demonstrated. Chemoattractants do not seem necessary for directional migration *in vitro* and *in silico*, where it has been suggested to be a self-organising property of the neural crest (Theveneau et al., 2010, Woods et al., 2014, Alfandari et al., 2003) as discussed in Section 2.4.6. Furthermore, many neural crest cells begin migration prior to full development of the target tissue and it is unclear how different neural crest subpopulations would be able to share common

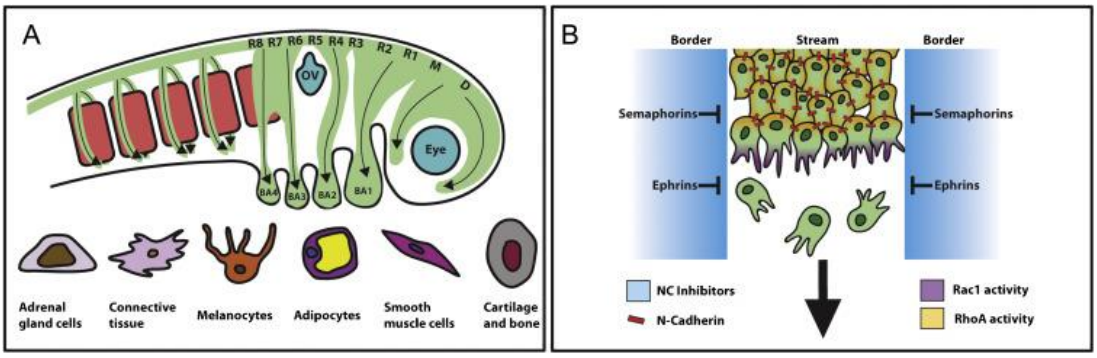

Fig. 2.3. Neural crest migration. (**A**) Migration routes of the neural crest (green) in a representative vertebrate embryo. D, diencephalon; M, mesencephalon; R, rhombomere; OV, otic vesicle; BA, branchial arch; red squares, somites. Below, examples of some of the cell types to which neural crest differentiate. (**B**) Representation of neural crest migrating in a cephalic stream. Neural crest cells migrate in distinct streams, mostly as a collective. Lateral migration is restricted by inhibitory signals at the borders (blue). Directional migration is an emergent property from CIL, whereby Rho (orange) is upregulated at sites of N-Cadherin-based contact (red) between cells; only leaders can generate Rac-dependent protrusions (purple). This leads to a polarised group of neural crest cells. Migration is inefficient by individual cells because polarity is not generated by CIL, a process dependent on cell interactions. NC, neural crest.

Adapted from (Shellard and Mayor, 2016).

migratory routes and invade different target regions using a limited number of chemoattractants. Conversely, some factors fill many of the criteria discussed 1.3.3.5, including appropriate expression patterns and chemotactic behaviour of neural crest toward them. Here we will examine the current evidence of the four most studied potential chemoattractants, which have the most convincing data.

Stromal cell-derived factor 1 (SDF1)

SDF1 regulates many directional migration events during embryonic development, including migration of the zebrafish posterior lateral line primordium (PLLp), primordial germ cells (PGCs) and various neural crest-derived cells (Belmadani et al., 2005, David et al., 2002, Boldajipour et al., 2008, Ding et al., 2013, Haas and Gilmour, 2006, Valentin et al., 2007). In many model organisms, SDF1 is expressed along the path taken by neural crest cells (Killian et al., 2009, Belmadani et al., 2005, Saito et al., 2012, Escot et al., 2013, Rehim et al., 2008, Kasemeier-Kulesa et al., 2010) that express the corresponding receptor, CXCR4 (Killian et al., 2009, Belmadani et al., 2005, Kasemeier-Kulesa et al., 2010, Belmadani et al., 2009, Chong et al., 2007, Chong et al., 2001). In some of these cases, chemotactic activity of the neural crest to SDF1 has not been properly tested, and how chemotaxis would be achieved in chick, where SDF1 is not found as a gradient, is unclear (Escot et al., 2013, Rehim et al., 2008). But there are some examples of chemotaxis to SDF-1 that are supported by experimental evidence. For example, CXCR4-expressing neural crest are chemotactic to SDF1 *in vitro* (Belmadani et al., 2005, Braun et al., 2002) and SDF1 misexpression diverts these neural crest cells away from their normal path, causing major defects such as cardiovascular abnormalities in many organisms (Escot et al., 2013, Kasemeier-Kulesa et al., 2010, Belmadani et al., 2009, Braun et al., 2002, Knaut et al., 2003, Svetic et al., 2007, Dona et al., 2013, Venkiteswaran et al., 2013), although mice neural crest behave rather differently in that SDF1 and CXCR4 mutants display only mild abnormalities (Tachibana et al., 1998, Nagasawa et al., 1996). In *Xenopus*, chick and zebrafish, perturbed SDF1 signalling disrupts neural crest cell migration (Killian et al., 2009, Rezzoug et al., 2011, Kasemeier-Kulesa et al., 2010, Belmadani et al., 2009), and some of the downstream components of this pathway have been identified. For example, the GEF Ric-8A is required for neural crest chemotaxis to SDF-1 *in vitro* (Fuentealba et al., 2013), but its mechanism of action is unclear. The regulation of the CXCR4 receptor has also been shown to be important for neural crest migration, as the transcription factor HIF-1α controls chemotaxis to SDF1 by regulating CXCR4 expression (Barriga et al., 2013).

In *Xenopus*, cell–cell interactions are essential for the collective chemotaxis of neural crest cells toward placodal-produced SDF1 (Theveneau et al., 2010). SDF-1 is only able to stabilize cell polarity in cells already polarized by cell–cell contacts, and therefore cannot attract non-polarized individual neural crest cells (Theveneau et al., 2010). Mathematical modelling has shown that cell contact enhances the chemotactic response (Coburn et al., 2013), consistent with the experimental evidence that SDF-1 stabilises and amplifies cell protrusions promoted by cell contact (Theveneau et al., 2010), similar to the chemotactic response of *Drosophila* border cells EGF and PVF (Prasad and Montell, 2007).

One major long-standing question is how neural crest segregates into different regions to colonize and differentiate into distinct tissues and organs. It has been proposed that different neural crest subpopulations express different receptors (Lumb et al., 2014). Indeed, it has been shown that differential response to SDF1 and neuregulin by distinct neural crest subpopulations determines whether these cells will migrate into the sympathetic ganglia or the dorsal root ganglia (Saito et al., 2012, Kasemeier-Kulesa et al., 2010).

Vascular endothelial growth factor (VEGF)

By the onset of neural crest migration, VEGF is expressed in the head ectoderm of avian embryos, specifically overlaying the dorsolateral migratory path of the rhombomeric 4 (r4) cranial neural crest, which expresses its canonical receptor, VEGFR2 (VEGF receptor 2), and co-receptor, neuropilin-1 (McLennan et al., 2010, Anderson-Berry et al., 2005, McLennan and Kulesa, 2007). VEGF expression later extends to the second branchial arch (BA2), and seems to be reduced in the on-route ectoderm (McLennan et al., 2010). During the initial stages of migration, VEGF is uniformly expressed in the overlying ectoderm, rather than as a gradient (McLennan et al., 2010). Nonetheless, both VEGFR2 and neuropilin-1 receptors are required for VEGF-mediated migration to BA2 (Bron et al., 2004, McLennan and Kulesa, 2010). *In vitro*, cranial neural crest are attracted to BA2 and VEGF (McLennan et al., 2010) and *in vivo*, r4 neural crest can be diverted from their normal path by ectopic VEGF (McLennan et al., 2010, McLennan et al., 2015). Perturbed VEGF/VEGFR2/neuropilin-1 signalling does not affect directional migration toward the BA2 entrance, but prevents invasion of BA2 at later stages (McLennan et al., 2010, McLennan and Kulesa, 2010, McLennan and Kulesa, 2007).

It is not clear how VEGF can control directional neural crest migration, as no VEGF gradient has been demonstrated so far. A mathematical model of neural crest

migration has proposed that the VEGF signal is diluted through the proliferation of neural crest cells which self-generate a VEGF gradient by the endocytosis of the ligand (Fig. 2.4A) (McLennan et al., 2012). This model posits that only leader cells respond to VEGF, whereas trailing cells respond to a second, unknown signal produced by leader cells (McLennan et al., 2012). However, a recent publication suggests that trailing cells can indeed respond to VEGF (McLennan et al., 2015). Moreover, there are key assumptions that are still awaiting experimental evidence: the consumption of VEGFA, the short-range signals transmitted from leader to follower cells, and the exclusive response of leader cells to VEGFA. It is unlikely that the neural crest self-generate a gradient in mice, because murine neural crest express VEGFA themselves (Wiszniak et al., 2015).

Fibroblast growth factor (FGF)

FGF8 is expressed in the pharyngeal arch ectoderm and endoderm during neural crest migration through the arches (Walshe and Mason, 2003, Abu-Issa et al., 2002) and it is not expressed by the neural crest (Frank et al., 2002). Its expression is partly dependent on Notch in mouse, and on the presence of the neural crest cells themselves in chick (Creuzet et al., 2004, High et al., 2009, Creuzet et al., 2002). Migration of different neural crest populations to their targets is dependent on FGF8 (Abu-Issa et al., 2002, Frank et al., 2002, High et al., 2009, Trokovic et al., 2003, Cavanaugh et al., 2015a, Trokovic et al., 2005). However, there is varying evidence of chemotaxis between different neural crest subpopulations and species. In some cases, the neural crest have been shown to express FGF8's cognate receptors, FGFR1 and FGFR3, and there is evidence that neural crest can be diverted from their usual paths by ectopic FGF8 beads (Creuzet et al., 2004, Sato et al., 2011). For other cases, there is only evidence that FGF8 is important for neural crest migration, but not for chemotaxis (Trokovic et al., 2003, Trokovic et al., 2005, Cavanaugh et al., 2015a). Species differences in neural crest migration can be illustrated in cardiac development, where neural crest chemotaxis to FGF8 is critical for heart development in chick and mouse (Abu-Issa et al., 2002, Kirby et al., 1983, Macatee et al., 2003), unlike in zebrafish where FGF signalling is redundant for neural crest contribution to the heart (Cavanaugh et al., 2015b).

FGF2 has also been proposed as a chemoattractant for neural crest. FGF2 is locally expressed and under the control of FGF8 in the mandibular mesenchyme (Kubota and Ito, 2000). Mesencephalic mouse neural crest cells express FGFR1 and FGFR3,

but although these neural crest are chemotactic to FGF *in vitro*, there are no functional studies of FGF2 chemotaxis *in vivo* (Kubota and Ito, 2000).

Platelet-derived growth factor (PDGF)

PDGFRα (PDGF receptor) is expressed in the migrating neural crest of many species (Cebra-Thomas et al., 2013, Eberhart et al., 2008, Takakura et al., 1997, Ho et al., 1994, Orrurtreger et al., 1992, Schatteman et al., 1992, Bahm et al., 2017) and in non-neuronal derivatives of the cranial neural crest (Kirby et al., 1983, Orrurtreger et al., 1992, He and Soriano, 2013). PDGFRα protein also localises to neural crest, although its expression is not exclusive to neural crest and neural crest-derived tissues (Kawakami et al., 2011). Patch heterozygotes, in which PDGFRα is deleted, have defects in pigment cells derived from neural crest (Morrison-Graham et al., 1992). Patch homozygotes have abnormalities suggestive of defective cardiac neural crest (Soriano, 1997, Kirby and Hutson, 2010) and PDGFRα mutants exhibit cleft palate, which results from failed neural crest development (Schatteman et al., 1992, Soriano, 1997, Robbins et al., 1999). PDGFRα's cognate ligands, PDGFA and PDGFC, are found in the ectoderm, otic vesicle and pharyngeal endoderm (Eberhart et al., 2008, Ho et al., 1994, He and Soriano, 2013, Tallquist et al., 2000, Ding et al., 2000), which are neural crest targets. In mouse, both PDGFRα and PDGFRβ are required for the normal migration of cardiac neural crest (Richarte et al., 2007). Although some neural crest derivatives are capable of chemotaxis to PDGFA *in vitro* (He and Soriano, 2013), which ligand is required for signalling through PDGFRβ, and whether it acts chemotactically on neural crest cells *in vivo*, is unknown. Exogenously implanted PDGF-AA is able to attract PDGFRα-expressing neural crest *in vivo* (Eberhart et al., 2008, Tallquist and Soriano, 2003, Kawakami et al., 2011). In zebrafish, it appears that PDGF-AA pre-localised to where the PDGFRα-expressing NC cells migrate (Eberhart et al., 2008). Interestingly, the expression pattern of a PDGFRα negative regulator, the microRNA Mirn140, is identical to PDGFRα, and it has been proposed that this mechanism of PDGFR signalling modulation mediates the chemotaxis of cranial neural crest to the oral ectoderm, since overexpression of Mirn140 phenocopies PDGFRα mutants (Eberhart et al., 2008).

In conclusion, although there is some evidence that suggest that SDF1, VEGF, PDGF and FGF could work as neural crest chemoattractants, none of these molecules have been shown to be present in a gradient along the neural crest migratory pathways; the development of new tools to visualise gradients *in vivo* would resolve this (Rizza et al., 2017). Instead of precluding these molecules to be classified as neural crest

chemoattractant, the mechanism to sense a chemoattractant could be more complex than simply reading a long range gradient. However, what is clear is that in many cases, neural crest do require external chemotactic signals for normal directional migration.

2.4.7.2 Co-attraction

As mentioned previously, CIL (Section 2.4.6) is essential for directional collective cell migration but it is not sufficient alone, otherwise it would drive cell dispersion. To counteract this, short-range chemotaxis is used to maintain the cohesion of groups of cells during migration, as suggested in cancer (Hoelzinger et al., 2007, Jechlinger et al., 2006) and demonstrated in *Dictyostelium* (Kay et al., 2008). Despite having weak cell adhesion complexes, most neural crest cells migrate collectively rather than as individuals (Theveneau and Mayor, 2011b, Kulesa et al., 2010, Kulesa and Fraser, 2000). Short-range chemotaxis is used to maintain collectiveness in neural crest groups during directional migration. Neural crest cells produce the complement factor C3a, and express its receptor, C3aR (Carmona-Fontaine et al., 2011). Therefore, high levels of C3a are found where neural crest cells are abundant, and cells that lose contact with their neighbours are able to migrate back to the group, following this chemotactic gradient. This mutual attraction is a process termed co-attraction. Mechanistically, C3a signalling leads to Rac1 activation which is sufficient to polarise escaping neural crest back to the group (Fig. 2.4C) (Carmona-Fontaine et al., 2011). This mechanism of short-range chemotaxis is termed co-attraction. Co-attraction counterbalances CIL, which is required for directional migration but promotes cell dispersion (Carmona-Fontaine et al., 2011, Carmona-Fontaine et al., 2008b), by keeping the cells together as a collective as their migration requires this nature (Theveneau et al., 2010, Woods et al., 2014).

Accordingly, inhibition of C3 or its receptor reduces collectiveness, as cells are forced apart by CIL and can no longer efficiently migrate towards a chemoattractive source (Carmona-Fontaine et al., 2011, Woods et al., 2014). C3a and C3aR have also been found in cephalic neural crest cells in mouse (Lambris and Mayor, unpublished) and chick (Bronner and Mayor, unpublished), and in the mesoderm of *Xenopus* embryos (McLin et al., 2008). Neural crest migration in avian and zebrafish embryos also suggest a co-attractive behaviour, although the molecular mechanisms are unknown. The importance of short-range chemotaxis to hold groups of cells together is supported by mathematical models, where co-attraction and CIL are necessary and sufficient for generating directional migration of groups in confined streams (Carmona-Fontaine et al., 2011, Woods et al., 2014).

2.4.8 Chase and run

Many examples of paracrine chemotaxis, to enhance migration and for cell guidance, have been described in development and cancer (Kulesa et al., 2010, Erickson, 1985, Boldajipour et al., 2008). *Xenopus* and zebrafish neural crest cells, which express CXCR4, also undergo paracrine chemotaxis in response to SDF1 secreted by placodal cells *in vitro* (Theveneau et al., 2013). Cranial placodes are thickened regions of ectoderm that contribute to the development of cranial sensory structures (Steventon et al., 2014). Reciprocal interactions between the neural crest and placodal cells are required for normal morphogenesis of both populations (Steventon et al., 2014). Mechanistically, CIL generates polarised neural crest (Carmona-Fontaine et al., 2008b) whose protrusions are stabilised by SDF1 which enhances and maintains the polarity (Theveneau et al., 2010). Upon contact with neural crest cells a transient but functional N-Cadherin-based adhesion complex is formed between neural crest and placodal cells (Theveneau et al., 2013). Migratory neural crest explants normally generate traction forces around the edge (Scarpa et al., 2015), but at the point of N-Cadherin engagement focal adhesions and protrusions are downregulated as CIL is induced (Theveneau et al., 2013). Consequently, neural crest repolarise and separate from the placodal cells, whilst loss of focal adhesions and collapse of protrusions in the rear of the placode cluster causes the placodal cells to move away from the NC. This process has been termed ‘chase and run’ in which neural crest chase placodal cells by short-range chemotaxis, whereas the placode runs away from neural crest by CIL (Fig. 2.4B). The bidirectional interactions between neural crest and placodal cells coordinate highly efficient directional migration of both populations towards lateral and ventral regions.

CIL appears to play a two-fold role in neural crest migration. In addition to the homotypic CIL found between neural crest cells, heterotypic CIL also occurs between the neural crest and placodes (Theveneau et al., 2013). The neural crest are attracted to the placodes by the chemokine SDF1. When neural crest cells collide with the placodes CIL occurs and both the protrusions of the neural crest and the placodes collapse. The placodes then repolarise and migrate away from the contact, due to CIL. This generates a ‘chase and run’ mechanism whereby the placodes move away from the neural crest when they collide and the neural crest chase after them, once their protrusions have recovered, due to the placodes providing a chemoattractive source (Theveneau et al., 2013). Thus, the migration of the placodes depends on the neural crest and vice-versa.

Because of the wide variety of tissues to which they contribute, mutations that affect neural crest development can lead to congenital diseases defined as neurocristopathies (Etchevers et al., 2007) and research into the mechanisms of neural crest development may give an important contribution to the understanding of these pathological conditions may indicate potential therapeutic strategies.

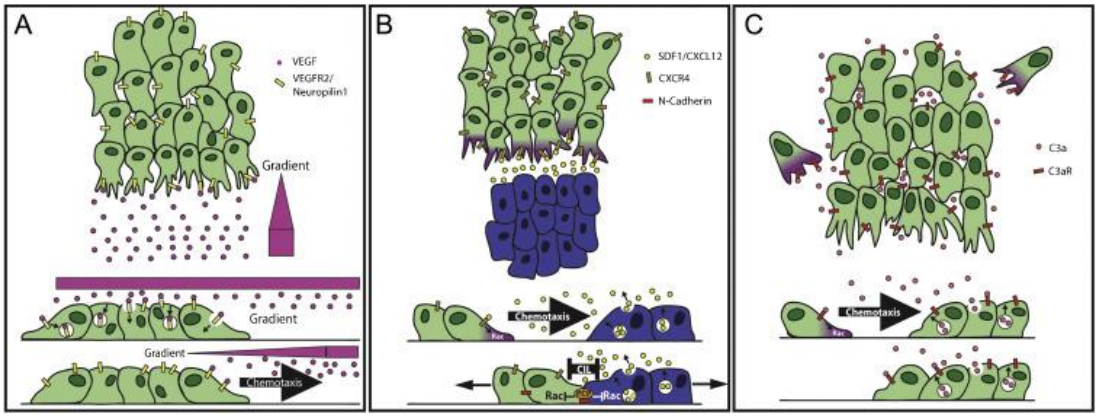

Fig. 2.4. Mechanisms of neural crest cell chemotaxis. (**A**) Proposed model for a neural crest self-generated gradient of VEGF (pink) from an initially uniform expression of VEGF in the overlying ectoderm. VEGF is consumed by neural crest, potentially by its endocytosis when bound to VEGFR2/neuropilin-1 (purple). Leaders are able to respond to unconsumed VEGF in front, relaying a signal to its followers. The diffuse VEGF signal from a source means that there is always some VEGF to which the front cells can respond. (**B**) Neural crest undergo short-range chemotaxis to placodal cells (blue) via placodal-secreted SDF1 (yellow) which binds CXCR4 (olive) on neural crest. CIL through PCP signalling and a transient N-Cadherin adhesion mediates repulsion between neural crest and placodes, leading to the placode moving away (run) from the neural crest, while the neural crest still follow (chase) the placode due to chemotaxis. This is referred to as 'chase and run'. Thus, movement of both cell populations is interdependent. (**C**) Neural crest co-attraction. Neural crest co-expresses the chemoattractant C3a and its cognate receptor C3aR. Neural crest-produced C3a binds to C3aR on neural crest cells, causing activation of Rac. In this manner, C3a promotes cohesion of the neural crest cluster; cells that move away by CIL return to the high concentration of C3a present in the cluster.

Adapted from (Shellard and Mayor, 2016)

Hypothesis

Directed migration orchestrates important events in development, homeostasis and disease (Friedl and Gilmour, 2009, Roca-Cusachs et al., 2013, Mayor and Etienne-Manneville, 2016, Haeger et al., 2015). Chemical and mechanical external cues are essential for long-range directed migration (Majumdar et al., 2014, Roca-Cusachs et al., 2013), which have been best understood in individually migrating cells but less studied during the prominent collective migration of cells.

Collective cell migration by durotaxis, whereby cell groups follow gradients in the stiffness of the extracellular matrix, has recently been explained on the cellular level (Sunyer et al., 2016). However, most collective cell migration *in vivo* occurs by chemotaxis, whereby cell groups follow gradients of soluble chemical cues (Silver and Montell, 2001, Montell, 2003, Dona et al., 2013, Gilmour et al., 2017, Haas and Gilmour, 2006, Theveneau et al., 2010). Leader cells of collective cell migration have been studied extensively; they have highly dynamic actin-based protrusions (Theveneau et al., 2010, Friedl and Gilmour, 2009), form interactions with follower cells and with the extracellular matrix, and are responsive to chemotactic signals (Mayor and Etienne-Manneville, 2016, Cai et al., 2014, Wang et al., 2010b). Despite this, how the action of the leaders would be transmitted to the group and how the entire group responds collectively to the chemoattractants remains unexplained.

This thesis addresses the biomechanics of collective cell chemotaxis *ex vivo* and *in vivo*, using the cranial neural crest, an embryonic mesenchymal stem cell population that migrates large distances by collective chemotaxis towards SDF1 (Theveneau et al., 2010) in a manner similar to cancer cells (Kerosuo and Bronner-Fraser, 2012). Although the contractile forces involved in single cell migration are comparatively well understood, very little is known about how they act in collective cell migration.

The hypothesis is that cells at the group's rear, to which little attention has been paid, may contribute to collective cell chemotaxis by providing contractile forces.

The cranial neural crest is ideal to address this question. Epithelial sheets, a common model for collective migration, has no back and uses no chemotactic signals. In other models of collective chemotaxis, such as border cells or the lateral line, analysis of their forces is difficult because they cannot be studied *in* vitro. By contrast, the neural crest has a clear front and rear, and can be studied both *ex vivo* and *in vivo*.

Materials and methods

3.1 Solutions

3.1.1 Marc's modified ringer's (MMR)

100 mM NaCl, 2 mM KCl, 1 mM $MgSO_4$, 2 mM $CaCl_2$, 5 mM HEPES, 0.1 mM EDTA, pH 7.6.

3.1.2 Normal amphibian medium (NAM 1/10)

11 mM NaCl, 0.2 mM KCl, 0.1 mM $Ca(NO_3)_2$, 0.1 mM $MgSO_4$, 10 mM EDTA, 0.2 mM NaH_2PO_4, 0.1 mM $NaHCO_3$, pH 7.5, 50 μm/mL streptomycin.

3.1.3 Cysteine solution

2% L-cysteine (Sigma, C7352) in H_2O with 50 mM NaOH.

3.1.4 Ficoll solution

3% polysucrose (Ficoll, Sigma) in NAM 3/8.

3.1.5 NAM 3/8

40.7 mM NaCl , 0.74 KCl, 0.37 mM $Ca(NO_3)_2$, 0.37 mM $MgSO_4$, 37 μM EDTA, 0.37 mM NaH_2PO_4, 0.1 mM $NaHPO_4$, pH 7.5, 50 μm/mL streptomycin.

3.1.6 MEMFA

100 mM MOPS, 1 mM $MgSO_4$, 2 mM EGTA, 3.7% formaldehyde.

3.1.7 Phosphate buffer saline (PBS)

137 mM NaCl, 2.7 mM KCl, 4.3 mM Na_2PO_4, 1.4 mM H_2PO_4, pH 7.3.

3.1.8 PBS with Tween (PBT)

1X PBS with 0.1% Tween-20.

3.1.9 Bleaching buffer

20% H_2O_2, 2.5% 20X SSC, 5% formamide.

3.1.10 20X saline-sodium citrate buffer (SSC)

3 M NaCl, 0.3 M tri-sodium citrate, pH 7.0.

3.1.11 Hybridisation buffer

50% formamide, 5X SSC, 1X Denhardt's solution, 1 mg/mL ribonucleic acid, 100 μg/mL heparin, 0.1% CHAPS, 10 mM EDTA, 0.1% Tween-20, pH 5.5.

3.1.12 Washing buffer 1

50% formamide, 10% 20X SSC, 0.1% Tween-20.

3.1.13 Washing buffer 2

25% formamide, 10% 20X SSC, 0.1% Tween-20.

3.1.14 Washing buffer 3

12.5% formamide, 10% 20X SSC, 0.1% Tween-20.

3.1.15 Washing buffer 4

10% 20X SSC, 0.1% Tween-20.

3.1.16 Washing buffer 5

1% 20X SSC, 0.1% Tween-20.

3.1.17 Maleic acid buffer (MAB)

100 mM maleic acid, 100 mM NaCl, 0.1% Tween-20, pH 7.6.

3.1.18 Anti-digoxigenin-alkaline phosphatase (AP) buffer

100 mM NaCl, 50 mM MgCl2, 100 mM Tris-HCl, pH 9.8, 0.1% Tween-20.

3.1.19 Danilchick's medium for Amy (DFA)

53 mM NaCl, 5 mM Na_2CO_3, 4.5 mM K-Gluconate, 32 mM Na-Gluconate, 1 mM $MgSO_4$, 1 mM $CaCl_2$, 0.1% bovine calf serum albumin (BSA; Sigma, A4503), pH 8.3 adjusted with bicine.

3.1.20 E3 medium

5 mM NaCl, 180 μM KCl, 330 μM $CaCl_2.2H_2O$, 400 μM $MgCl_2.6H_2O$, pH 7.2 adjusted with NaOH, 2 μL of 1% methylene blue (Sigma-Aldrich) per 1 L.

3.1.21 Tricaine solution

20 mM tricaine methanesulfonate (Tricaine, or MS-222)

3.1.22 Clearing mix

Two volumes benzyl alcohol, 1 volume benzyl benzoate (Sigma-Aldrich).

3.1.13 Diethylpyrocarbonate water (DEPC)

0.1% diethylpyrocarbonate.

3.1.14 Mowiol

25% glycerol, 10% Mowiol 4-88 (Sigma, 81381), 50% 0.2 M Tris HCl, pH 8.5.

3.2 Embryological and histological procedures

3.2.1 Animal care

Adult *Xenopus laevis* (Nasco, and Xenopus Resource Centre) were kept in standard conditions (water temperature: 17ºC; room temperature: 20ºC; water conductivity 1600 μS, water pH 6.8) in the animal facilities of University College London. They were used in accordance with the regulations of the Animals (Scientific Procedures) Act 1986, as described previously (Steventon et al., 2009). Animal licenses were approved by University College London and the UK Home Office.

Adult zebrafish strains were maintained according to standard procedures, described previously (Westerfield, 2000).Three transgenic zebrafish strains are used in this thesis: Tg(Sox10:GFP) (Carney et al., 2006), which labels neural crest cytoplasm; Tg(Sox10:mG) (Richardson et al., 2016), which labels neural crest nuclei and cell membrane; Tg(Sox10:nuclearRFP-Gal4) (Cavanaugh et al., 2015a, Moore et al., 2013), which labels neural crest nuclei. These transgenic lines drive fluorescent expression from the Sox10 promoter, which is specifically expressed by neural crest cells during their migration.

3.2.2 Preparation and staging of embryos

Xenopus laevis embryos were obtained as previously described (Barriga et al., 2018). Briefly, ovulation of mature *Xenopus laevis* females was induced by subcutaneous injection of 100 IU pregnant mare serum gonadotrophin hormone (PMSG; Intervet) into females 2-5 days before a second injection of 500-750 IU of chorionic gonadotrophin hormone (Chorulon; Intervet), which was performed ~16 hours before the planned fertilisation. Egg-laying females were kept in MMR at 17ºC, which maintains the naturally laid mature oocytes inactivated until collection. Testes were obtained from male *Xenopus laevis* by anaesthetisation in Tricaine solution for 40 min, and then culling by pithing. The testes were dissected and stored in Leibovitz L-15 medium (Invitrogen, 11415-064) with added streptomycin (5 μg/mL, Sigma, 85886) at 4ºC. Mature oocytes were fertilised *in vitro* in a 100 mm tissue culture dish (Falcon 734-0006) with 500 μL MMR which had a small piece of testes crushed in it.

After 10 min, NAM 1/10 was added to the dish. Fertilised eggs were de-jellied no earlier than the 1-cell stage in cysteine solution. Embryos were raised at 14.5ºC in NAM 1/10 and staged according to the normal table of *Xenopus* development (Nieuwkoop and Faber, 1967).

Zebrafish were bred according to standard procedures (Westerfield, 2000). They were fed prior to pairing male and female adults with a divider in a breeding box ~16 hours before mating. The divider was removed and 0.5-1 h later, embryos were collected in a 9 cm Petri dish with Fish H_2O and methylene blue (a disinfectant). Embryos were cleaned under tap water to remove dead embryos and debris. Embryos were raised at 28ºC and staged according to the normal table of zebrafish development (Kimmel et al., 1995).

3.2.3 Embryo microinjections

Xenopus laevis and zebrafish embryos were injected using a Narishige IM300 microinjector under a LeicaMZ6 or a Nikon SMZ645 dissecting microscope. Needles were made from 0.58 mm borosilicate glass capillaries (Intracel, 01-001-06; or Harvard Apparatus) using a Narishige PC-10 dual-stage needle puller. The puller was set to the two-step mode with the first step set to 88ºC and second step adjusted to 99.4ºC. Needles were calibrated with an eyepiece graticule to inject a volume of 5 nl or 10 nl per injection for *Xenopus*, or 5 nl per injection for zebrafish.

For *Xenopus*, embryos were injected with mRNA, DNA or morpholino (or their combination). Ficoll is a highly branched hydrophobic polysaccharide used to preserve the integrity of the embryo during microinjection. Fluorescein-dextran (FDX; Invitrogen, D1821, 20 ng) or rhodamine-dextran (RDX; Invitrogen, D1824, 20 ng) were used as tracers, where appropriate. Embryos were injected at the 4-cell stage: once into the dorsal blastomere and once into the ventral blastomere on one side of the embryo. For injection of morpholinos, or to more precisely target the neural crest, embryos were injected into the animal ventral blastomere at the 8-cell stage on one side. For cell labelling, embryos were injected with mRNAs for nuclear RFP and/or membrane GFP and/or membrane RFP and/or membrane eBFP2. Injection quantities and form are shown in Table 3.1. Alternatively, Hoescht 33342 (1:1000, Leica B2251) was added to the imaging solution to stain nuclei for live imaging. 1-16 h post-injection embryos were transferred to NAM 1/10 and kept at 14.5ºC. Alternatively, embryos were kept between 14ºC and 18ºC to change the speed of development.

For zebrafish, embryos were injected with DNA in fish H_2O at the 1-cell stage and kept at 28°C. Alternatively, embryos were maintained between 27°C and 31°C to change the speed of development and maintained in fish H_2O or E3 medium. For Gal4/UAS transactivation with UAS:MLC-GFP, zebrafish were grown to 8 hpf (75% epiboly) before being incubated in a solution containing 5 μM Tamoxifen (Sigma-Aldrich, T5648). Note that MLC refers to myosin regulatory light chain II.

Construct	**Injection form**	**Injection quantity per embryo**
Nuclear-RFP	mRNA	300 pg
Membrane-RFP/GFP/eBFP2	mRNA	300 pg
OptoGEF-RhoA	mRNA	1.3 ng
CIBN-GFP-CAAX	mRNA	2.6 ng
Mito-GFP-CAAX	mRNA	2.2 ng
MLC-GFP/Cherry	mRNA	50 pg
N-Cadherin or N-Cadherin-RFP	mRNA	800 pg or 200 pg, respectively
E-Cadherin	mRNA	800 pg (Roycroft et al., 2018, Scarpa et al., 2015)
LifeAct-Ruby	mRNA	300 pg
MYPT	mRNA	300 pg
MLCK	mRNA	300 pg
CA-MLC	mRNA	300 pg
SDF1	Morpholino	8 ng (Theveneau et al., 2010)
CXCR4	Morpholino	8 ng
MLC-GFP-UAS	DNA	50 pg

Table 3.1. Construct microinjections

3.2.4 Whole mount *in situ* hybridisation

In situ hybridisation was performed as described previously (Fawcett and Klymkowsky, 2004, Harland, 1991). Briefly, after fixing the embryos at the appropriate stage in MEMFA for 1 hr, embryos were dehydrated in 100% methanol and stored at

-20ºC. Embryos were rehydrated with successive washes of 75% methanol/PBT, 50% methanol/PBT, 25% methanol/PBT and PBT. Embryos were then bleached in bleaching buffer for 10-15 min until white, washed three times in PBT and re-fixed in 3.7% formaldehyde in PBS for 30 min. After further washing in PBT, embryos were transferred to hybridisation buffer and incubated at 62-65ºC for 1 hr. They were then incubated overnight in hybridisation buffer containing digoxigenin-labelled *Twist* probe (Hopwood et al., 1989) at 62-65ºC. Embryos were washed in a series of solutions: washing buffer 1, washing buffer 2, washing buffer 3, washing buffer 4 for 10 min each at 62ºC. A last wash in washing buffer 5 lasted 30 min at 62ºC. All solutions used up to this point were made with DEPC-treated water (autoclaved solution of 0.1% diethylpyrocarbonate in H2O) to prevent RNase contamination, which could otherwise degrade the RNA probe.

Embryos were washed with PBT, MAB and blocked in 2% Boehringer Mannheim Blocking Reagent (BMBR; Roche, 11096176001) in MAB for 2 h at RT. Embryos were incubated overnight at 4ºC with an AP-conjugated antibody (Roche, 11093274910) at a 1:3000 dilution in 2% BMBR/MAB. Excess antibody was removed by five 30 min washes in MAB. Embryos were transferred to AP buffer and developed using 175 μg/mL 5-bromo-4-chloro-3-iodoyl-phosphate (Roche, 11585002001) and 150 μg/mL 4-nitro blue tetrazolium chloride (Roche, 11383213001) in dark. The reaction was stopped by washing in PBT and background staining was removed by a 20 min wash in 100% methanol. Embryos were fixed in 3.7% formaldehyde/PBS and kept until they were photographed.

3.2.5 Whole mount immunostaining

Immunostaining of flat-mounted *Xenopus* embryos was performed as previously described (Barriga et al., 2018). Briefly, the vitelline membrane was removed from embryos in NAM 3/8 using fine forceps (Dumont #5 Inox 11 cm, World Precision Instruments, 500342). After 15 min, embryos were fixed with 2% trichloroacetic acid (TCA), dorsal halves dissected, washed in PBS, blocked with 10% normal goat serum (NGS) for 40 min and stained with anti-phospho-myosin (ab2470, Abcam, 1:100) and anti-fibronectin (1:40, 4H2, Developmental Studies Hybridoma Bank) overnight at 4ºC. Embryos were washed in PBS, incubated with Alexa Fluor (Thermo-Fischer) secondary antibodies (1:350) and DAPI (1:1000) and excess antibody removed by washing with PBS. Embryos were then flat-mounted in a clearing mix.

For whole mount immunostaining of zebrafish, embryos were dechorionated using fine forceps and fixed in 4% PFA overnight at 4ºC at 16 hpf (15 somites). Embryos

were permeabilized for 15 min in 0.5% TritonX:PBS, blocked with 10% NGS:05% TritonX:PBS and stained with anti-phospho-myosin (1:100, 3674, Cell Signaling or 1:100, ab2470, Abcam) overnight. After extensive washing, embryos were incubated overnight in secondary antibodies, DAPI and Phalloidin, as above, washed and then mounted in 1% soft agarose/PBS.

3.2.6 Neural crest dissection and grafts

Xenopus neural crest dissections and transplants were carried out as previously reported (De Calisto et al., 2005). Briefly, after the vitelline membrane was removed with fine forceps, neural crest was dissected at stage 19 using blunt forceps and an eyebrow hair knife to first remove the epidermis and then explant the neural crest, for either cell culture (detailed further in section 3.3.1) or to be used as donor neural crest in a graft. Alternatively, pre-migratory neural crest was dissected at stage 14-15 (Scarpa et al., 2015). For grafts, the epidermis of host embryos was not detached from the embryo prior to neural crest removal. Host embryos were then held in modelling clay and graft neural crest was transferred into the position of where the host neural crest was removed. The epidermis was then manipulated to cover the graft, and a glass coverslip used to maintain it. After 1 h, the coverslip was removed.

Neural crest from embryos injected with 20 ng of fluorescein-dextran (FDx, Invitrogen, D1820) (donors) was dissected and transferred into host embryos at the place that NC was removed from. The whole procedure was performed in NAM 3/8. Then embryos were raised until stage 24 in NAM 3/8 in which they were photographed.

3.3 Cell biology

3.3.1 Neural crest cultures

Plastic dishes (Falcon, 351006) or glass dishes (μ-Dish, 35 mm high, Ibidi, or FluoroDish, FD35-100) were incubated with 10 μg/mL or 1 μg/mL fibronectin (Sigma, F1141) in PBS, respe5ctively, for 1 h at 37ºC. After washing with PBS, dishes were blocked with 0.1% BSA/PBS for 30 min at 37ºC, washed again with PBS and filled with Danilchick's for Amy Medium (DFA) with added 50 μg/ml streptomycin. Neural crest cultures were performed as previously described (Borchers et al., 2000, Alfandari et al., 2003). Neural crest explants dissected from *Xenopus* embryos were cut into similar size pieces and plated on the fibronectin-coated dishes in DFA, and left to attach for 45-60 min. To acquire single cells, neural crest explants were first incubated for 3-10 min in a Ca^{2+}- and Mg^{2+}-free solution of DFA and mechanically dissociated with a hair knife, and then transferred and plated as above. All procedures

and live imaging were carried out at 18°C. For incubation in uniform SDF1, explants were incubated in a solution containing 10 ng/mL SDF1. For incubation in blebbistatin explants were incubated in a solution containing 100 μM. For live imaging of cell nuclei, where nuclei markers had not been microinjected, Hoescht 33342 (1:1000, Leica B2251) was added to the imaging solution. Treatments were applied only after cluster attachment.

3.3.2 Chemotaxis assay

Chemotaxis assays were performed as previously described (Theveneau et al., 2010, Theveneau and Mayor, 2011a). Briefly, acrylic heparin beads (Sigma, H5263) were incubated with 1 mg/mL purified human stromal cell-derived factor-1 (SDF1; Sigma) overnight at 4°C. Alternatively, platelet-derived growth factor A (PDGF-A) was used. Lines of high vacuum silicon grease were applied to fibronectin-coated dishes and SDF1 beads immobilised in the grease using a hair knife and fine forceps. Neural crest explants were plated approximately 300 μm (two diameters) away from the bead (Theveneau and Mayor, 2011).

3.3.3 Dispersion assay

Dispersion assays were performed as previously described (Carmona-Fontaine et al., 2011). Briefly, neural crest was explanted into a fibronectin-coated dish and allowed to disperse. Dispersion was recorded by time-lapse microscopy.

3.3.4 Explant immunostaining

Immunostaining was performed on neural crest explants as previously described with few modifications (Matthews et al., 2008). Briefly, explants were fixed in 4% formaldehyde (PFA; Sigma, P6148)/PBS for 30 min, washed three times in PBS and permeabilised in 0.1% Triton X-100/PBS for 10 min. After washing the explants thoroughly in PBS, they were blocked with 3% foetal calf serum (FCS)/5% BSA in PBS for 30 min. Primary antibody diluted in 3% FCS/5% BSA/PBS solution was applied overnight at 4°C. Following extensive washes in PBS, secondary antibody diluted in 3% FCS/5% BSA/PBS solution was applied for 1 h at RT. 1 μg/mL 4'6-diamidino-2-phenylindole (DAPI; Sigma, D9542) and 1 mg/mL phalloidin tetramethylroadmin-b-isothiocyanate (PhR; P1951) were used together with the secondary antibody where appropriate. Samples were thoroughly washed in PBS and mounted in Mowiol.

3.4 Molecular biology and biochemistry

3.4.1 Synthesis of mRNA probe for *in situ* hybridisation

For *in vitro* transcription of antisense RNA, plasmid DNA was cut at a 5' restriction site with the appropriate endonuclease. Plasmids were linearised and purified as described above. Antisense RNA transcription was carried out by mixing 1 μg of linearized DNA, 4 μL of 5x buffer, 2 μL of 10x DTT, 2 μL of NTP-Dig, 0.5 μL of ribonuclease inhibitors and 1 μL of RNA polymerase and making the solution up to 20 μL with RNase free water. The NTP mix contains digoxigenin-labelled UTP, so the resulting RNA was labelled with digoxigenin. All reagents were obtained by Promega. The mixture was incubated at 37°C for 2 hr. From this, 1 μL was replaced with 1 μL of DNase to degrade the DNA template. The RNA concentration was measured using a Nanodrop spectrophotometer (ND-1000). Quality of RNA probes was assessed with agarose gel electrophoresis. Probes were diluted in hybridisation buffer to working concentrations. *Twist* was diluted to 700 ng/mL.

3.4.2 Synthesis of mRNA for microinjection

mRNA templates were generated as previously described (Barriga et al., 2018). For synthesis of sense mRNA, plasmid DNA was linearized by cutting at a 3' restriction site with an appropriate restriction endonuclease. A 100 μL reaction of 10 μg plasmid DNA, 10 μL of appropriate 10x buffer and 1 μL of enzyme in water was incubated for 2 hr at 37°C. Enzymes and buffers were obtained from Promega. 1 μL of digested DNA was kept for agarose gel analysis. The rest of the digested plasmid was purified using Qiagquick PCR Purification kit (Qiagen, 28104) and concentration of purified digested plasmid was measured using a Nanodrop spectrophotometer (ND-1000). 1 μg of 3' linearised plasmid DNA was added to the transcription mixture. Synthetic capped mRNA was transcribed using the SP6 or T3 Ambion mMESSAGE mMACHINE kit (Invitrogen, AM1340 and AM1344, respectively). 1 μL of the reaction mixture was replaced with 1 μL of DNase and the mixture was incubated for a further 1 hr at 37°C in order to degrade template DNA. Sense mRNA was purified using the RNeasy kit (Qiagen, 74104) and resuspended in RNase free H_2O. RNA concentration was measured using a Nanodrop spectrophotometer (ND-1000). Quality of mRNA transcript and efficiency of the protocol was assessed by agarose gel electrophoresis. Thus, 1 μL of linearized and purified DNA, 1 μL of transcription mixture before addition of DNase, 1 μL of purified sense mRNA were run on 1% agarose (Fisher Scientific, BP1356-100) gel in TEA (20 mM acetic acid, 1 mM EDTA, 40 mM Tris, pH 7.6).

3.4.3 Oligomorpholinos

Oligomorpholinos were synthesised and provided by GeneTools. Two morpholinos were used for this thesis: SDF1 (8 ng, 5'-CAATGCCACCAGAAAACCCGTCCAT-3') (Theveneau et al., 2010), CXCR4 (5'-CAATGCCACCAGAAAACCCGTCCAT-3'). Equimolar concentrations of a standard control morpholino (ControlMO, 5'-CCTCTTACCTCAGTTACAATTTATA-3') was used.

3.4.4 Cloning

Membrane-eBFP2 was made by cloning eBFP2 downstream of a membrane sequence in pCS2+ vector, with AgeI and SnaBI sites using the primers: Fw: CTGTAAACCGGTGATGGTCTCCAAGGGAGAG; Rv: CCACGGTACGTATTACTTGTACAGCTCGTC.

The UAS:MLC-GFP construct was made using a UAS:GCaMP6 plasmid (Walker et al., 2013), removing GCAMP6 and cloning in MLC-GFP downstream of the UAS-encoding region by using BglII and NotI sites with the primers: Fw: GGCGGCAGATCTATGTCGAGCAAAAAGGCAAAG; Rv: TGTTGTGCGGCCGCCTTGTACAGCTCGTCCATGCC.

Optogenetic constructs (optoGEF-RhoA, CIBN-GFP-CAAX, mito-GFP-CAAX) were subcloned from their original vectors (Valon et al., 2017) to pCS2+.

3.5 Microscopy

3.5.1 Imaging of embryos fixed for *in situ* hybridisation

Images of fixed embryos after *in situ* hybridisation or whole mount immunostaining were collected using a MFZLIII Leica immunofluorescence stereomicroscope equipped with a FDC420 Leica camera controlled by Leica IM50 software.

3.5.2 Imaging of neural crest cells *in vitro*

To capture *in vitro* neural crest migration, single cell migration and chemotaxis, time-lapse cinematography was performed as described before (Carmona-Fontaine et al., 2008b, Theveneau et al., 2010). Compound microscopes equipped with motorized stages, either an Eclipse 80i Nikon microscope with a Hamamatsu Digital camera or a DMRXA2 Leica microscope with a Hamamatsu Digital camera controlled by Simple PCI program, were used. 10x/0.3NA dry lens was used. Fibronectin-coated petri dishes containing cultured neural crest cells were filled with DFA and closed so that no air bubbles were present.

When addition of various compounds in the culture medium was required (e.g. experiments with blebbistatin, NSC23766), then neural crest cells were cultured in up to four wells of a four-well dish. These were filled with DFA and sealed with a 22 mm x 22 mm cover slip smeared with high-vacuum grease (Dow Corning), over which the dish lid was fixed. These were inverted, and the cells imaged through the plastic. Images were acquired every 3-5 min for a period of 12 h.

Images for chemotaxis and dispersion assays were acquired every 3 min and 10 min, respectively, at 18^{o}C using a compound (DM5500, Leica) microscope.

3.5.3 Confocal microscopy

Xenopus ex vivo and *in vivo* live cell imaging was performed on a Perkin Elmer Ultraview VOX spinning disc confocal with NIKON TiE microscope or LSM880 Multiphoton microscope. Filters, shitters and image acquisition were controlled by Volocity or Olympus software, respectively. For actomyosin movies a 60X/1.4 NA oil immersion objective, or a 100X/1.4 NA oil immersion objective was used. Fixed cells were imaged using a 63X/1.4 NA oil immersion objective and a Leica TCS SPE confocal microscope controlled by LAS-AF software.

For graft experiments and zebrafish imaging, time-lapse images were acquired every 10 min on a confocal microscope (SP8vis, Leica). Images for immunostained explants were acquired on a confocal microscope (Leica SPE1 or LSM880 Multiphoton). Images for immunostained flat-mounted embryos were acquired on a confocal microscope (FV1000 Olympus). Images for immunostained zebrafish were acquired on a confocal microscope (SP8vis, Leica).

3.5.4 Laser photoablation

The actomyosin cable or cytosol was laser ablated using a confocal microscope (LSM880 Multiphoton). A 740 nm laser at 80% power was used for ablation on one *z* plane at 40-60X magnification in regions of interest. Images were acquired every 1-3 min between ablations to track cluster movement. For long-term ablation experiments, multiple repetitive ablations were performed, for both many cells (10 cells per explant, on average) and for the same cell due to the dynamic reformation of the actomyosin cable. For cell-cell junction control ablations, repetitive ablations were not performed because there was no reformation of the junction after initial ablation. All rear cells or front cells were targeted for ablation where indicated; 4-5 central cells were targeted for cell junction ablation. To measure recoil after ablation, images were acquired every 1 second and the size of the resulting gap in in the actin

cable (g(t)) and the distance between the lateral sides of the cell (w(t)) were measured over time. The presented strain was calculated as $s_g(t) = -g(t)/c(t=0)$, $s_w(t) = w(t) / w(t=0)$, where c(t=0) is the length of the actomyosin cable just before ablation.

3.5.5 Optogenetics

Images were acquired, and optogenetic activation was performed, on a confocal microscope (SP8vis, Leica). Prior to imaging, explants or embryos were protected from light with foil for 45 min. The 488-nm laser at 100% power was used to illuminate a region of interest for translocation of optoGEF-RhoA. For *ex vivo* explants, the region of interest corresponded to a single row of cells (between 6 to 15 cells) at the front or back of the explant; for *in vivo* photoactivation the region of interest corresponded to a 30% of the labelled neural crest stream, either at the front or back of the graft. For controls, cell non injected with the optoGEF-RhoA were illuminated with the 488-nm laser at 10% power, or optoGEF-RhoA injected cells were not illuminated.

3.5.6 Fluorescence resonance energy transfer (FRET)

FRET was performed as previously described (Scarpa et al., 2015). Briefly, DNA for the FRET probes, Raichu-Rac (Itoh et al., 2002) or RhoA (Pertz et al., 2006) were injected into eight-cell stage *Xenopus* embryos. After dissection and culture of neural crest, explants were fixed with 4% PFA. FRET was detected by excitation of CFP and collection of emission with 530 nm long-pass filters. Images were corrected for bleed through between channels prior to background subtraction, and data analyzed with the ImageJ plugin, RiFRET (Roszik et al., 2009). Acceptor photobleaching was performed as previously described (Matthews et al., 2008).

3.6 Data analysis

3.6.1 *In vivo* migration

Analysis of neural crest migration *in vivo* was performed by measuring the distance that the neural crest cells travelled along the dorsal-ventral (D-V) axis of the *Xenopus* embryo as revealed by the neural crest marker *Twist* by *in situ* hybridisation. Neural crest migration *in vivo* was estimated as a proportion of the D-V distance of the injected side to the D-V distance of the uninjected side for embryos that were injected with morpholinos or other constructs. This was repeated at three locations. For each embryo and the average proportion calculated. For embryos treated with blebbistatin, neural crest migration was estimated by the proportion of D-V distance of treated embryos to the length of the head at the stream.

If there is no impairment in migration, then the migration value estimated by the experimental data should approach 1.

In vivo migration = D-V distance injected side/D-V distance uninjected side.

3.6.2 Motility

From low-magnification time-lapse movies, individual cells were tracked using the ImageJ Manual Tracking plug-in. This method requires manual identification of each cell at each time point. The ImageJ Chemotaxis Tool plug-in was then used to analyse speed and directionality of cell migration. Cell speed is estimated based on the equation speed = dx/dt. The distance travelled (dx) within a period of time (dt corresponding to the time within two frames) is calculated by the ImageJ plug-in Migration and Chemotaxis Tool using the coordinates dx, dy from the cell tracks. Directionality is calculated as the Euclidian distance between the start and end of migration divided by the actual distance migrated. Tracking of single cells lasted 3-4 hours. Any cells that contacted another cell during this time were not included in the analysis. The mean speed and directionality was calculated per cell, from which the mean velocity and persistence of the population was calculated.

Intercalation percentage was calculated by: (R-I)/N, where R is the number of rear cells intercalating forward, I is the number of inner cells moving to the rear, and N is the total number of rear cells. These values were measured over 2 h.

3.6.3 Chemotaxis

To calculate the Chemotaxis Index (also called Forward Migration Index), the coordinate system was rotated to have the y-axis passing through the source of the chemoattractant at the top and the cells at the bottom. For neural crest chemotaxis, the centre of the mass of teach explant was tracked or individual cells from explants using the ImageJ Manual Tracking plug-in. The ImageJ Chemotaxis tool plug-in was then used to analyse the chemotaxis index, which corresponds to the net displacement divided by the distance travelled by each explant or cell. A chemotaxis value of 1 means that the cluster or cells or a cell is directly going towards the chemoattractant. The combined Manual Tracking and Chemotaxis Tool plugins were used for tracking *ex vivo*, *in vivo* and *in silico* to calculate distance travelled (Eucledian distance; positive values refer to movement forward; negative values refer to movement backward, relative to the start position), directionality, motility (accumulated distance), velocity/speed and forward migration index (also called chemotaxis index, or ventral migration index, where appropriate). *Ex vivo* cluster

tracks show ten representative clusters each, and *in vivo* tracks show five representative clusters each. Quantification of distance travelled was calculated at 70 min (Fig. 4.19D), 90 min (Fig. 4.18L) or 100 min (Fig. 4.18, F and I), 30 min (fig 4.18C).

3.6.4 Dispersion

The dispersion of neural crest explants was analysed using a custm-made ImageJ Delaunay Triangulation plug-in, to calculate the distance between neighbour cells. For a set of points (cell nuclei) in a plane, Delaunay triangulation requires that the circumferences of all the triangles are empty (no point is found at their interiors). For each explant at each time-point, the Delaunay triangulation connects each cell (cell nucleus) with its closest neighbours (other cell nuclei) in such a way that a network of triangles covers the entire explant and the areas of the triangles are measured. To analyse neural crest explant dispersion the area of triangles was measured and averaged. This was repeated for at least 15 explants within three different experiments for each condition.

3.6.5 Protein analysis

The ImageJ line tool was used to measure actomyosin length. Actomyosin contraction was defined by a 25% or greater reduction in actomyosin length over 30 s. Relaxation was defined by a 33% increase in actomyosin length over 10 min. Cell clusters were separated into front, rear and lateral segments relative to PBS- or SDF1-coated beads. ImageJ region of interest selectors were used to quantify protein levels. For protrusions displayed in Fig. 4.15 the Image Calculator tool on ImageJ was used to subtract membrane images from one another during time-lapse microscopy for protrusion analysis.

For immunostaining analysis, the region of interest measured plot intensity was normally to the intensity plot of the cell cytoplasmic region.

3.6.6 Cell movements

To measure cell movements within groups *ex vivo*, particle image velocimetry (PIV) was applied using a publicly available ImageJ plugin (https://sites.google.com/site/qingzongtseng/piv). Flow fields *in silico, ex vivo* and *in vivo* were calculated by subtracting the movement of the cluster to the individual cell or particle tracks. Flow fields were obtained by analyzing PIV on consecutive time frames with time interval of 30 sec to ensure tracking accuracy and median-filtered. To show the flow field, positions of virtual particles on a grid were traced through 14 consecutive PIV fields using custom scripts; fields from 5 independent samples, each

containing a contraction event, are binned, median-filtered, and averaged together. For *in silico* measurements, cell displacements were calculated from cell tracks over 200 time steps including a contraction. The displacement fields were binned and averaged over 100 contractions. To illustrate the time evolution of the displacement field, speed profiles from the back along the midline of the groups were averaged in a 140 μm wide band from consecutive displacement fields. To demonstrate cellular flow *in vivo*, cells were tracked manually using the ManualTracker ImageJ plugin; cells in zebrafish were tracked at 5 min intervals over 2.5 h; cells in *Xenopus* were tracked at 10 min intervals over 5 h.

3.6.7 Statistical analysis

Normality in the spread of data was tested using the Kolmogorov-Smirnov, d'Agostino-Pearson or Shapiro-Wilk test in Prism7 (GraphPad). Significances for datasets displaying normal distributions were calculated in Prism7 with unpaired Student's *t*-test (two tailed, unequal variances). Significances for non-normal distributed data were calculated in Prism7 using the Mann-Whitney *U* test (two-tailed). For cell values, *n* refers to cells from different clusters. For testing significance between multiple datasets simultaneously, analysis of variance (ANOVA, one-way) was performed if the data was normally distributed, or Kruskal-Wallis test if the data was not normally distributed.

3.7 Computational Model

Cells in the model are represented by their position and velocity on a two-dimensional plane and state (either 'contractile' or 'normal' state). Their movement is governed by an overdamped secondary dynamics; for cell 'a' the velocity and position is determined by:

$$\frac{\Delta v_a}{\Delta t} = \sum_n f_i(a,n) + f_p(a) + f_n - \delta v_a$$

$$\frac{\Delta r_a}{\Delta t} = v_a$$

The velocity is determined by direct interactions between cells ($f_i(a,n)$), self-propulsion ($f_p(a)$), stochastic noise ($f_n = F_n \cdot \xi$, where ξ is a zero-mean Wiener process and F_n is a model parameter setting the relative level of noise), and dampening (δ). Cells interact with their Voronoi neighbours locally through a central and symmetric interaction:

$$f_i(a,n) = [f_r(|r_n - r_a|) + \sigma(a)\sigma(n)F_c] \cdot \frac{r_n - r_a}{|r_n - r_a|}$$

Here $\sigma(a)$ indicates the state of cell 'a' with value 1 if the cell is contractile and 0 if normal, and F_c is a model parameter setting the strength of contraction. Function $f_r(r)$ is a piecewise linear function of distance between cells:

$$f_r(r) = \begin{cases} F_{rep} \cdot \dfrac{r - r_{core}}{|r_{core}|}, if\ r < r_{core} \\ 0, if\ r_{core} \le r < r_{neutral} \\ F_{att} \cdot \dfrac{r - r_{neutral}}{|r_{adhesion} - r_{neutral}|}, if\ r_{neutral} \le r < r_{adhesion} \\ F_{att} \cdot \dfrac{r_{reach} - r}{|r_{reach} - r_{adhesion}|}, if\ r_{adhesion} \le r < r_{reach} \\ 0, if\ r_{reach} \le r \end{cases}$$

Here F_{rep} and F_{att} are model parameters setting the strength of cell-cell repulsion and attraction, respectively. Propulsion of cell 'a' is described by:

$$f_p(a) = F_p(s - |v_a|)\frac{v_a}{|v_a|}$$

Model parameters s and F_p set the speed and relative strength of propulsion.

Equations are discretized and integrated using the forward Euler method with fixed dt time steps. The state of each cell is updated after each iteration. To determine if a cell is at the edge of the cluster, all Voronoi neighbours are considered that are within r_{reach} distance of the cell. A cell is considered to be at the edge if the direction of any two of its consecutive neighbours is more than $\alpha = 3\pi/4$ apart. Edge cells that are behind the center of the cluster (rear contractility simulations) are switched to 'contractile' state for 100 time steps, and switched back to 'normal' state for 100 time steps. In simulations of uniform contractility all edge cells are switched with the same periodicity. Intercalation is reduced in simulations by increasing the adhesion parameter F_{att} up to 6-fold.

Cells are initialized with zero velocities and non-overlapping randomly selected positions within a predefined rectangular area and initial state set to 'normal'. An initial contraction cycle is simulated with uniform contraction around the perimeter of the cluster before the start of the simulation experiments to enhance coherence of the group and reduce noise of the initial random cell placement. Time steps were chosen as dt=2.16 seconds, and $r_{core} = 10\,\mu m$ corresponds to a typical cell radius. Parameters used for the simulations were: $r_{neutral} = 1.500\,r_{core}; r_{adhesion} = 1.534\,r_{core}; r_{reach} = 1.834\,r_{core}; F_n = 5; F_c = 5;\ F_{rep} = 10; F_{att} = 0.5; F_p = 5; s = 2; \delta = 0.1$. Simulations are run for 10 000 steps, corresponding to 6 h time.

Parameters for the model as follows:

global_ranges = [6., 9., 9.2, 11.]

These are, in order, the distance at which the cells start to push each other away, at which they stop attracting each other, at which their attraction is maximal, and at which their interaction starts. These correspond correspond to the known cellular interaction ranges from experimental data. These values can be converted to microns based on one cell diameter being 20 mm.

Parameters controlling cell behaviour are:

global_speed = 2 # target speed of cells
global_velDampening = 0.1 # velocity dampening, or friction of movement (less than 1)
global_contraction_time = 100 # minimum duration of contractions
global_relaxation_time = 100 # minimum time between contractions

The contraction and relaxation times are a simplification, and the speed and velocity dampening are approximated to be consistent with the known behaviour of individual neural crest cells.

Interaction strengths (negative = attraction):
global_I_rnd = 5 # random movement strength of cell
global_I_spp = 5 # self-propulsion strength of cell
global_I_rep = 10 # core cell repulsion strength
global_I_contact = -0.5 # cell-cell adhesion strength

global_I_contraction = -5

These are terms of the cell-cell interaction and of the cell movement and are devised to produce a realistic cell behaviour in the model.

The model is downloadable from the following link, which includes instructs on use and parameters:

https://github.com/AndrasSzabo/shellard_model-2018_science

Further parameters and justifications are as follows:

Parameter	**Model/conversion**	**Experimental data/validation**
Cell size	1 cell = 20 μm diameter	Middle cells, which constitute most of a cluster, are 20 μm *ex vivo*

Simulation time run	10,000 steps = 6 h	Normal chemotaxis *ex vivo* takes 4-6 h
Contraction region	Rear half contractile; front half not contractile	Frequency distribution of contractility *ex vivo* suggests most contraction happens in the rear half.
Contraction frequeny	100 time steps contractile, 100 time steps not contractile	Not based on experimental data.
Number of synchronously contracting cells	All cells in the contraction zone will contract.	Based on the observation of multicellular synchronous contraction; albeit, experimentally, there is variability in the number of cells synchronously contracting.

Table 3.2. Modelling parameters

Results

4.1 Characterisation of actomyosin in neural crest

Various processes are already known about collective migration of *Xenopus* cranial neural crest cells (henceforth called neural crest cells, unless otherwise specified), and their collective chemotaxis to SDF1. A balance of CIL and short-range C3a-dependent chemotaxis (coattraction) is sufficient for collective cell migration. CIL inhibits stable internal protrusions and permits protrusions at the edge of the cell cluster, away from cell-cell contacts (Fig. 4.1, red). However, chemoattractive agents like SDF1 are essential for long-range directional movement; when SDF1 is inhibited, clusters fail to migrate in any particular direction (Theveneau et al., 2010). SDF1 stabilises protrusions at the front of the cluster during chemotaxis (Fig. 4.1, dark red) but, again, it is not clear that this is critical for collective chemotaxis. By contrast, the role of rear cells (Fig. 4.1, black dotted box) in the collective migration, and collective chemotaxis, of neural crest cells as other collectively migrating cell populations has not been studied. Likewise, little is known about the role of myosin-based contractile forces in collective cell migration, despite contractility being heavily involved in the migration of single cells, both through the initiation of migration and in the ongoing migratory process itself. Moreover, actomyosin is important in single cell chemotaxis.

To determine whether actomyosin contractility is important for neural crest migration constitutively active myosin light chain (CA-MLC), myosin light chain kinase (MLCK), and/or myosin phosphatase targeting protein (MYPT) was overexpressed in *Xenopus* embryos, and migratory stage embryos were fixed for *in situ* hybridisation with a Twist probe, which is expressed specifically by the neural crest. MLCK is an activator of myosin contractility, whereas MYPT is a subunit of myosin phosphatase, which inhibits myosin contractility. MYPT is the myosin targeting subunit of myosin light chain phosphatase that has an essential role as a targeting and regulatory subunit to confer substrate specificity and subcellular localisation on the catalytic subunit of myosin phosphatase (Grassie et al., 2011). Neither CA-MLC nor MLCK overexpression affected *in vivo* migration (Fig. 4.2, A and B), as measured by neural crest stream length, but MYPT overexpression inhibited neural crest migration *in vivo* (Fig. 4.2, C and D). The effect of MYPT could be rescued with CA-MLC or MLCK, indicating that the constructs were working (Fig. 4.2, C and D). In these experiments, the myosin constructs are active in both the neural crest and non-neural crest populations. Neural crest migration was also inhibited in embryos bathed in the myosin ATPase inhibitor, blebbistatin (Fig. 4.2, E and F), a drug which, in this

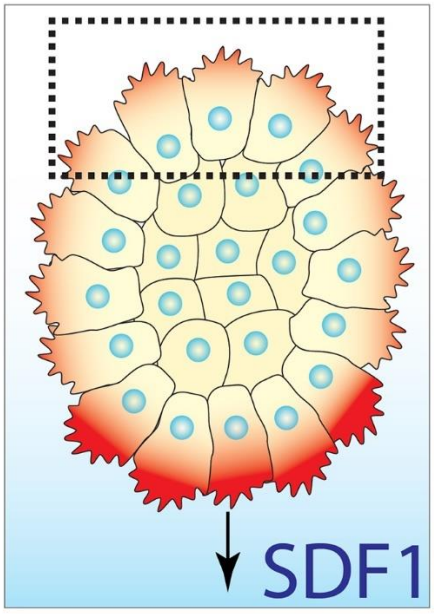

Fig. 4.1. The current model of collective neural crest cell chemotaxis. Neural crest with protrusions (red) at the edge undergoes chemotaxis to SDF1. Protrusions are found at the edge of the cell group (including both front and rear cells), and not in the middle, due to contact inhibition of locomotion (Carmona-Fontaine et al., 2008b). SDF1 stabilizes the protrusions at the front (darker red) (Theveneau et al., 2010). It is not known what role rear cells (dotted square) have in collective cell chemotaxis.

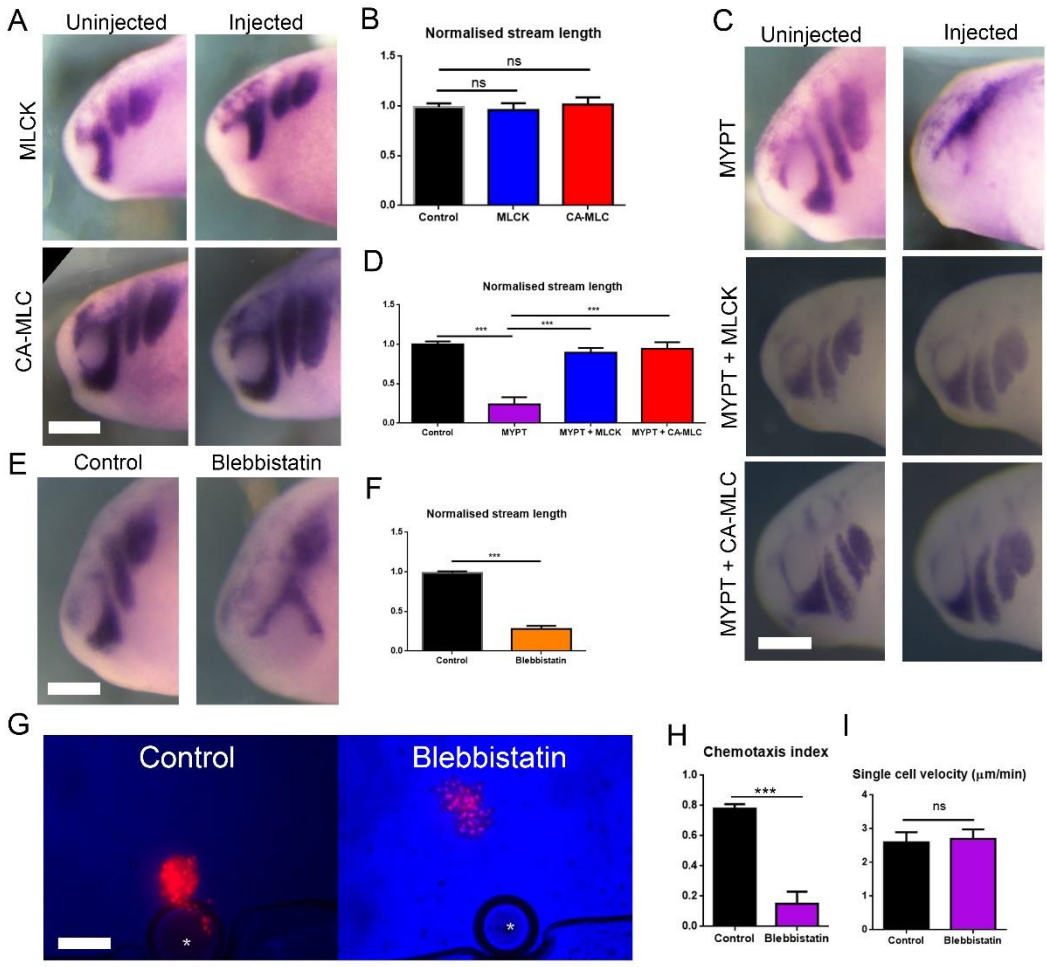

Fig. 4.2. Myosin contractility is important for collective migration. (**A to F**) *In situ* hybridisation with a probe for Twist in migratory stage *Xenopus* embryos and quantification of stream length (means ± SEM). Twist marks the neural crest. Dorsal is top, ventral is bottom. Note that activation of MYPT inhibits neural crest migration *in vivo*. Migration can be rescued with MLCK or CA-MLC, but these alone do not have any effect on overall neural crest migration. Blebbistatin treatment also inhibits neural crest migration *in vivo*. *n* = 50 embryos each; *N* = 3 experiments. Scale bar, 1 mm. For B and D, ***$P \leq 0.001$ (one-way ANOVA); ns, not significant. For F, ***$P \leq 0.001$ (two-tailed Student's *t*-test). (**G to I)** *Ex vivo* neural crest explants undergoing collective chemotaxis to SDF1 (G). Scale bar, 100 μm. The white Asterix indicates the SDF1 bead. Nuclear RFP mark the neural crest cells. Image shows 4 hrs post-plating. Note that the control explant has undergone chemotaxis normally but incubation with blebbistatin has inhibited chemotaxis, which is quantified in H (means ± SEM). At this concentration, blebbistatin inhibits chemotaxis without affecting single cell velocity (means ± SEM), as determined by cell tracking of dissociated neural crest cells (I). For H and I, ***$P \leq 0.001$ (two-tailed Student's *t*-test); ns, not significant.

experiment, acts on the whole embryo. Altogether, these results indicate that actomyosin contractility is important for neural crest migration. However, it cannot be determined whether it is myosin contractility of the neural crest cell populations, or in other cell types, that is necessary for *in vivo* migration. Indeed, the neural crest require stiff underlying mesodermal cells to migrate *in vivo* (Barriga et al., 2018). To test whether actomyosin contractility of the neural crest was important for collective chemotaxis, explants were exposed to an SDF1 chemotactic gradient *ex vivo* and incubated with blebbistatin. Unlike control explants, which underwent chemotaxis normally, blebbistatin treatment inhibited chemotaxis without affecting single cell motility (Fig. 4.2, G and I), indicating that actomyosin contractility of the neural crest is important for collective chemotaxis.

To understand the role of actomyosin in collective cell migration, fluorescently-tagged myosin regulatory light chain II (MLC) and LifeAct-Ruby were expressed into *Xenopus* embryos. Embryos were raised, and neural crest were dissected out and cultured to visualise the activity of filamentous actin and myosin. Live imaging revealed that actomyosin localises as a multicellular ring or cable around the edge of the neural crest cluster, both in the absence and presence of an SDF1 gradient (Fig. 4.3, A and B). To confirm that this localisation was not due to overexpression, neural crest explants were immunostained for phospho-myosin light chain (pMLC) to visualise endogenous protein. Myosin light chain phosphorylation, normally through Rho/ROCK, potentiates contraction by stimulation myosin ATPase activity (Waxman, 2018), and by controlling conformation of the myosin heavy chain (Kampourakis and Irving, 2015). In the absence of an SDF1 gradient, neural crest explants have pMLC localised around the edge of the cell group (Fig. 4.3C), showing a similar localisation to the overexpression. In both the absence and presence of SDF1, the myosin ring remained dynamic around the edge of the explant (Fig. 4.3D).

Neither actin nor myosin are transmembrane proteins, which explains the ‘dashed’ rather than continuous myosin appearance along the cluster periphery. To determine what proteins might be connecting the multicellular actomyosin cable between adjacent cells, neural crest explants overexpressing fluorescently tagged N-Cadherin, MLC and a membrane marker and immunostained with Phalloidin were imaged at high magnification. N-Cadherin is one of the major cell junction components of neural crest. The periphery of the neural crest explant shows a continuous actin cable, with myosin accumulating along it, particularly in the central regions of the cell away from the cell-cell contact (Fig. 4.4, A to C). N-Cadherin is enriched near the actomyosin cable at the cell junction (Fig. 4.4, A to D), suggesting that this cable is supracellular,

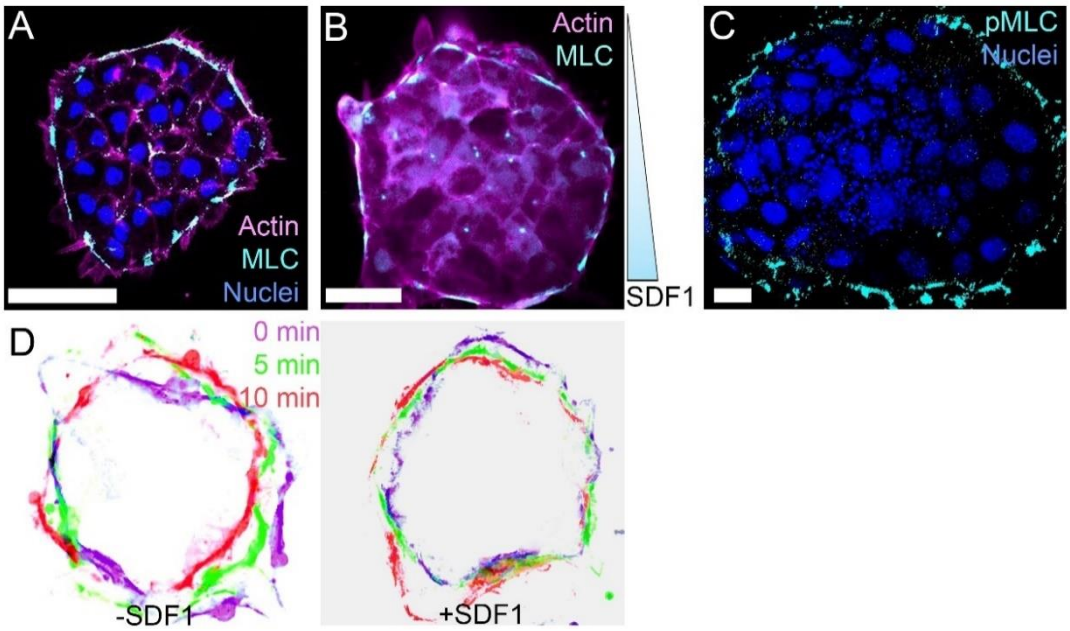

Fig. 4.3. *Xenopus* neural crest clusters exhibit a contractile actomyosin ring. (**A**) Fluorescence of a neural crest explant in the absence of SDF1 expressing MLC: myosin light chain (MLC-GFP), LifeAct-Ruby and stained with Hoescht. Representative example shown from *n* = 30 clusters from *N* = 5 experiments. Scale bar, 50 μm. (**B**) A neural crest explant expressing fluorescently-tagged myosin (MLC-GFP) and actin (LifeAct-Ruby) whilst undergoing chemotaxis to SDF1. MLC: myosin light chain. Representative example from *n* = 100 clusters from *N* = 10 experiments. Scale bar, 50 μm. (**C**) Immunostaining against phospho-myosin light chain (pMLC) of neural crest explant in the absence of SDF1. Representative example from *n* = 30 clusters from *N* = 3 experiments. Scale bar, 25 μm. (**D**) The myosin ring of neural crest explants pseudocoloured at the indicating time points in the absence (left) or presence of a SDF1 chemotactic gradient during live imaging. Representative examples from *n* = 100 clusters from *N* = 10 experiments.

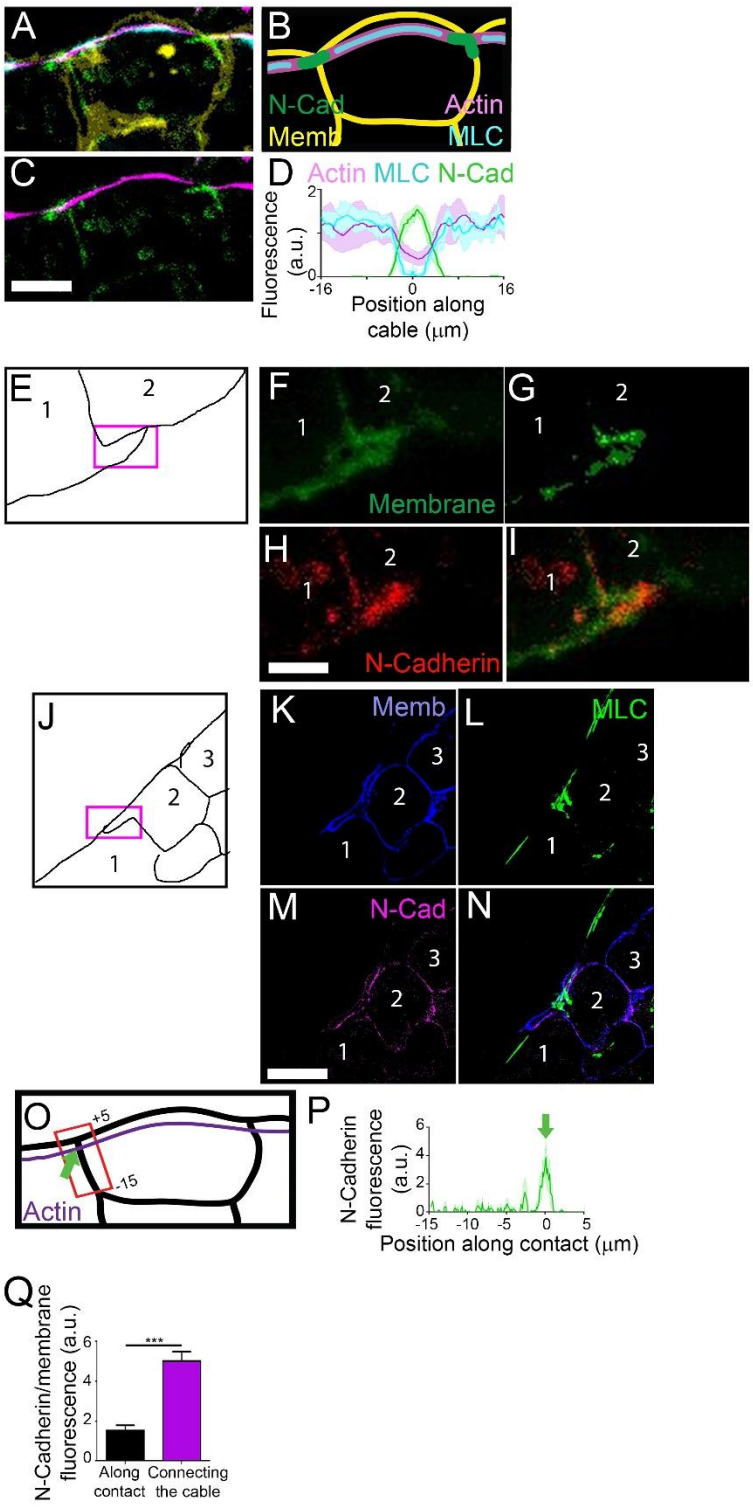

Fig. 4.4. N-Cadherin connects the actomyosin cable between adjacent cells. (**A to D**) Immunofluorescence of a cell at the edge of a neural crest explant (A and C) and diagram (B). Memb: membrane. Representative example from *n* = 10 cells each randomly selected from a different cluster, from *N* = 3 experiments. Scale bar, 10 μm. (D) Protein fluorescence levels (means ± SEM) along the actin cable. Position 0 μm represents the cell contact. *n* = 8 cells each randomly selected from 8 different

clusters, from *N* = 3 experiments. (**E to I**) Immunofluorescence of the cell-cell contact at the edge of a neural crest explant. A diagram is shown in E. Black lines are the cell edges. Numbers represent different cells. The pink box is the area of interest. Free space is in the bottom right. Membrane is shown in two different contrasts (F and G). Note that N-Cadherin, a cell-cell adhesion protein, strongly accumulates parallel to the cluster edge, rather than perpendicular to it, where you would expect the two edge cells to contact. When imaged at a single *z* plane (F to I) the membrane is also observed to be skewed parallel to the cluster edge, suggesting that the membrane is mechanically 'pulled' by one cell upon its neighbour. Representative image shown from *n* = 15 cells each randomly selected from 15 different clusters, from *N* = 3 experiments. Scale bar, 20 μm. (**J to N**) Immunofluorescence of a cell at the edge of a neural crest explant. J is the diagram, black lines represent cell edges, pink box is the area of interest, and numbers are different cells. Free space is at the top left of the picture. Note how the membrane is elongated/stretched toward its cell neighbour (between cells 1 and 2), N-Cadherin accumulates along this part and MLC fills in the gaps of the cable. This observation suggests tension is transmitted supracellularly by the actin cable from one cell to another, enough so that it can transmit tension to the cell contact/membrane. Representative image shown from *n* = 15 cells each randomly selected from 15 different clusters, from *N* = 3 experiments. Scale bar, 20 μm. (**O and P**) Diagram (O) showing the region along the cell contact (red box) quantified for N-Cadherin fluorescence (means ± SEM) (P); arrow (position 0 μm) indicates the intercellular contact in the actomyosin cable where N-Cadherin is accumulated. *n* = 6-7 cells each randomly selected from 6-7 different clusters from *N* = 3 experiments. Note that the diagram, M, is based on images A to C. Position along contact measured is the contact in the red rectangle. (**Q**) N-Cadherin fluorescence levels relative to cell membrane fluorescence (means ± SEM), showing that accumulation of N-Cadherin in the actomyosin cable at the contact is not due to an accumulation of cell membrane. *n* = 10 cells each randomly selected from 10 different clusters, from *N* = 3 experiments. ****P* ≤ 0.001 (two-tailed Student's *t*-test).

and may be connected to adjacent peripheral cells by N-Cadherin. Interestingly, when imaged on single *z* planes, rather than as a projection, the membrane is observed to be skewed laterally toward neighbour edge cells at the exact location that the cable crosses and that N-Cadherin has accumulated (Fig. 4.4, E to L). This suggests that the actomyosin cable may be under tension and is mechanically pulling on the cell membrane. N-Cadherin accumulation on the membrane as a connector of the actomyosin cable was not entirely due to just this membrane extension, though, because N-Cadherin levels normalised to membrane still showed a higher level at the point of actomyosin cable contact (Fig. 4.4, M to O).

The neural crest undergoes EMT prior to migration. One of the fundamental features of this process is a downregulation of E-Cadherin and upregulation of N-Cadherin, which, in part, causes the cell to behave in a less epithelial manner and in a more mesenchymal fashion (Scarpa et al., 2015). EMT and the switch of cadherin expression is essential for neural crest migration, as pre-migratory neural crest do not migrate *in vivo*, and the switch of cadherins leads to CIL via repolarisation of forces from the cluster's centre to its edge (Scarpa et al., 2015).

To determine whether this cadherin switch might be important in the formation of the actomyosin cable, and the forces it may contribute to migration, pre-migratory neural crest were imaged alongside migratory neural crest *ex vivo*. Whilst the migratory neural crest exhibited a peripheral actomyosin cable, pre-migratory neural crest tended to accumulate myosin internally at stress fibres and along the cell-cell contact (Fig. 4.5, A and B). To determine whether the E- to N-Cadherin switch was important for this delocalisation, explants over-expressing E-Cadherin were immunostained for pMLC. Unlike control explants, which have pMLC at the cluster periphery, overexpressing E-Cadherin caused a dramatic delocalisation of pMLC into inner cells of the cell cluster (Fig. 4.5, C and D). Furthermore, similar quantification of MLC through live imaging of E-Cadherin-expressed and N-Cadherin-overexpressed explants revealed that this change in localisation was only apparent when E-Cadherin levels were increased (Fig. 4.5E). These data suggest that the switch of cadherin expression during EMT may be required for the formation of the actomyosin cable.

The fact that myosin accumulates on an actin cable suggests that it may be contractile and/or under tension. To study this, the actin cable was photoablated and imaging was acquired at high temporal resolution. Cable ablation results in recoil of both the actomyosin cable and of the cell-cell junctions over the course of a few seconds (Fig. 4.6, A and B, and Movie 1). This suggests that the cable is under high tension.

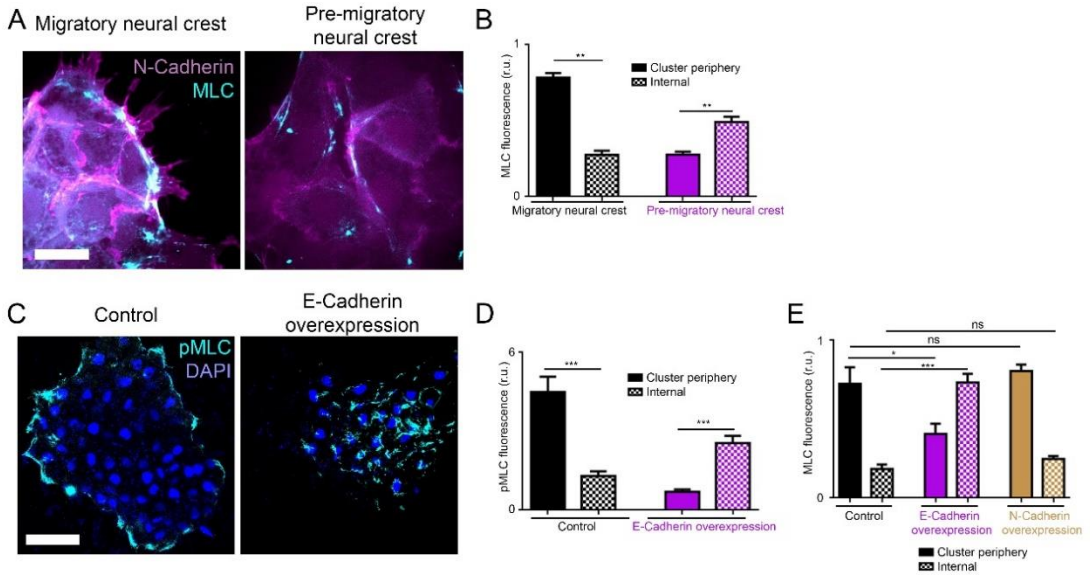

Fig. 4.5. E-Cadherin suppresses formation of a peripheral actomyosin cable. (**A and B**) Pictures of migratory (left panel) or pre-migratory (right panel) neural crest explants expressing fluorescently-tagged N-Cadherin and MLC (myosin light chain) (A), and quantification of myosin fluorescence (means ± SEM) at the cluster's periphery and cluster's centre (B). Note that in migratory neural crest most of the actomyosin is accumulated in the peripheral cable, whereas in pre-migratory neural crest no cable is observed and the actomyosin is present mainly in the centre of the cluster. *n* = 6 cells from 6 different clusters. ***P* ≤ 0.05 (two-sided Mann-Whitney *U*-test). Scale bar, 10 μm. (**C and D**) Immunostaining against pMLC (phospho-myosin light chain) in migratory neural crest in control (left panel) or E-Cadherin overexpression (right panel) conditions (C) and quantification of pMLC fluorescence (D) (means ± SEM). *n* = 8-11 cells from 8 different clusters. ****P* ≤ 0.001 (two-tailed Student's *t*-test). Scale bar, 50 μm. Note that the presence of E-cadherin impairs the formation of the actomyosin cable leading to accumulation of pMLC in the centre of the cluster, similar to the distribution observed in pre-migratory neural crest shown in fig. S1, F and G. (**E**) Myosin light chain (MLC) fluorescence (means ± SEM) when E-Cadherin or N-Cadherin is overexpressed. Note that the shift in actomyosin accumulation from the peripheral cable to the centre of the cluster is only induced by E-cadherin overexpression, but not by N-cadherin. *n* = 8-11 cells from 8 different clusters. **P* ≤ 0.05, ****P* ≤ 0.001 (one-way ANOVA); ns, not significant. Together these results suggest that the E- to N- cadherin switch during neural crest EMT is involved in the formation of the actomyosin cable in the periphery.

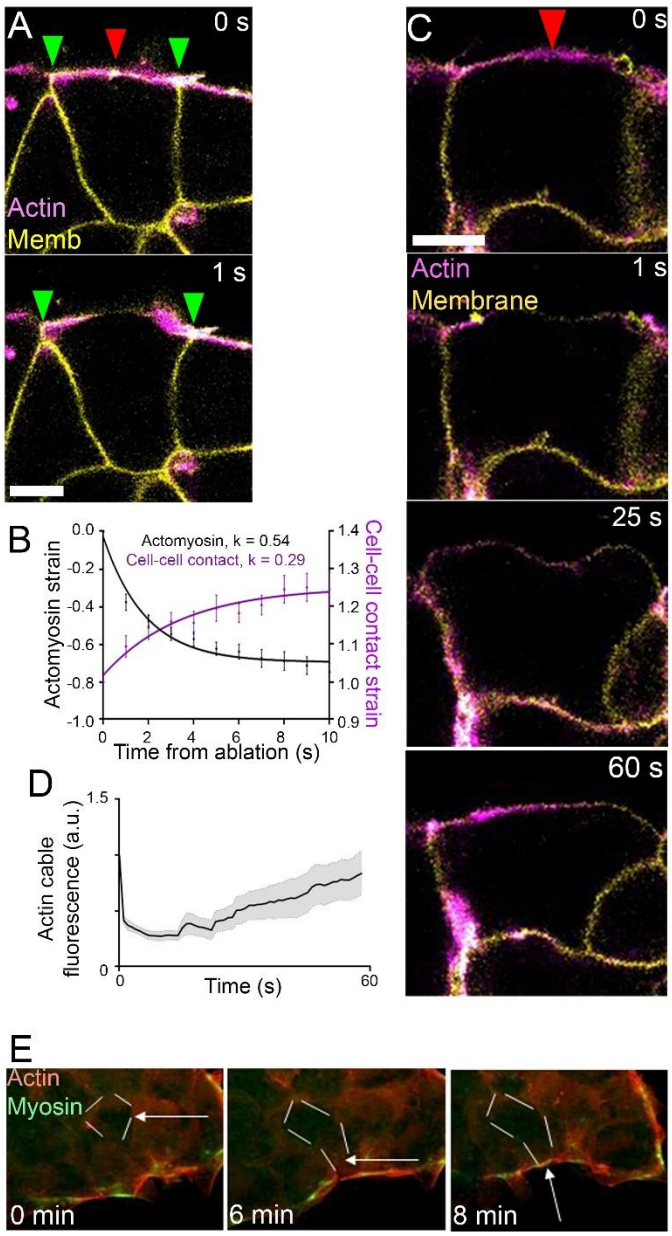

Fig. 4.6. The actomyosin cable is under tension. (**A**) Laser photoablation of the actomyosin cable (red arrowhead) in the absence of SDF1. Green arrowheads represent cell-cell contacts. Scale bar, 10 μm. Note the recoil of the cable and of the cell-cell junctions. Representative example from *n* = 30 cells from 25 different clusters, *N* = 5 experiments. (**B**) Strain of the actomyosin cable and of the cell-cell junctions (means ± SEM) after laser ablation of the actomyosin cable after ablation at t = 0 s. Lines indicate exponential fit, y = 0.07*exp(-0.54x) + 0.02 for actomyosin; y = -0.23*exp(-0.29x) + 0.03 for cell-cell contact. *n* = 8-10 cells, each from 8 different clusters, *N* = 3 experiments. (**C and D**) Regeneration of the actomyosin cable after laser ablation (C) and fluorescence quantification (means ± SEM) (D). Ablation is at 0 s. *n* = 6 cells each from 6 different clusters, *N* = 3 experiments. Scale bar, 10 μm. (**E**) Example of a cell exchanging its position. The cell (outlined in white dashes)

moves from the centre to the cell cluster periphery. Note how the actomyosin cable is preserved at the edge. LifeAct is red, myosin light chain is green. This is a representative example from many cells and clusters, *N* = 10 experiments. No quantification is associated with this.

Interestingly, the sometimes-dramatic changes in cell shape suggest that actin cable tension is transmitted across the entire cell membrane (Fig. 4.6C). The actin cable reforms itself quickly at the edge of the cluster following ablation (Fig. 4.6, C and D). The dynamic formation and reformation of the cable is further exemplified by cells at the periphery that leave the cluster or move around within the cluster (Fig. 4.6E); the cable assembles or disassembles such that it is always a multicellular structure at the cluster's edge. Moving of cells to or from the cell edge impeded supracellular cable connection only momentarily; although not quantified, the cable was generally observed to be re-established within seconds.

Because the actomyosin cable is under high tension, it is likely to be a contractile structure. To assess whether the actomyosin cable is contractile, we measured the length of the cable in individual cells. This revealed frequent shortening in the actomyosin cable, independent of SDF1 (Fig. 4.7, A and B). The fact that the ring is multicellular suggests that contractility may be synchronous. Indeed, these pulsed contractions were multicellular as adjacent cells contracted synchronously (Fig. 4.7, C and D). Note that the fact that cells synchronously contract mean quantifications throughout this thesis are performed on only one or two cells per cluster.

To further assess the supracellular nature of the actomyosin cable, two ablations were performed: a first ablation of the actomyosin cable in one cell to dissipate tension, followed by the immediate ablation of the actomyosin cable in a second cell, a few cells away from the first within the same cluster (Fig. 4.7E). The recoil of the cable was recorded in both cells. The recoil of the cable caused by the second ablation was reduced compared to the first (Fig. 4.7F), indicating that tension of the cable is transmitted between cells.

The existence of an actomyosin ring, as shown here, is not the first example that has been found in collectively migrating cell groups. In epithelial cells, the presence of an actomyosin cable seems to inhibit protrusion formation (Reffay et al., 2014). However, the mesenchymal neural crest cells form protrusions independent of the presence of the actomyosin ring (Fig. 4.7, G and H). Cells at the edge of the cluster occasionally, but rarely (~ <5% of the time), had an actomyosin cable that would transiently disappear during live imaging. On these occasions, the cable would reform very quickly (in less than one minute). The significance of this phenomena was not further studied, because of the rarity in which it occurs.

Whilst exposure to SDF1 gradients did not affect the magnitude of actomyosin contractions (Fig. 4.7B), contractions occurred less frequently in front cells during

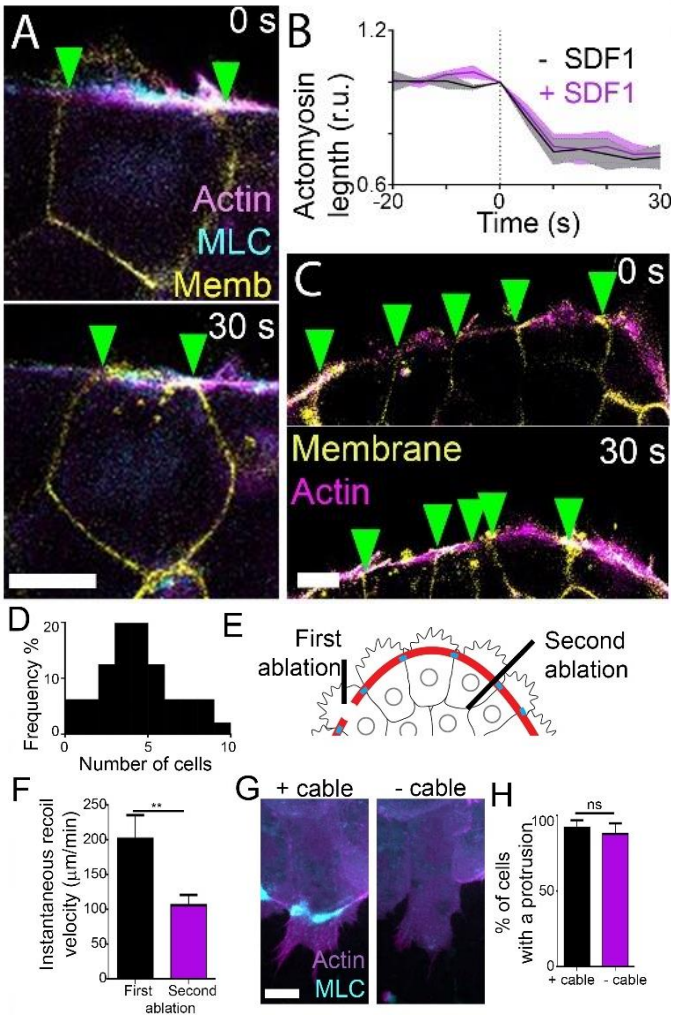

Fig. 4.7. The actomyosin cable is tensile and contractile in a supracellular manner. (**A**) Spontaneous contraction of the actomyosin cable. Green arrowheads: cell-cell contacts. Scale bar, 10 μm. (**B**) Actomyosin length (means ± SEM) measured over time. Contractions start at 0 s. *n* = 20 cells, each from 20 different clusters, *N* = 5 experiments. (**C**) Multicellular contraction of the actomyosin cable. Scale bar, 10 μm. (**D**) Histogram of the number of adjacent cells synchronously contracting. *n* = 48 sets of contractions from 10 clusters, *N* = 5 experiments. (**E**) Drawing representing the analysis of supracellular contractility in panel G. (**F**) Black bar: recoil velocity (means ± SEM) of the actomyosin cable after one cell's ablation; magenta bar: recoil velocity (means ± SEM) of the actomyosin cable in a cell ablated within 5 cells' distance away from the fist ablation. Note the diminished recoil velocity in the second ablation, indicating the supracellular nature of the actomyosin cable. *n* = 9 pairs of cells, each from different clusters, *N* = 3 experiments. ***P* ≤ 0.01 (two-tailed Student's *t*-test). (**G**) Images of a cell with and

without the actomyosin cable. Note the presence of protrusions in both cases. Scale bar, 10 μm. (**H**) Graph quantifying the percentage of cells exhibiting protrusions when the cell has or doesn't have an actomyosin cable (means ± SEM). *n* = 20 clusters, from *N* = 5 experiments. (two-tailed Student's *t*-test); ns, not significant.

collective chemotaxis without affecting cells at the rear (Fig. 4.8, A and B). A similar inhibition of front contractions was observed with the chemoattractant, PDGF-A (Bahm et al., 2017) (Fig. 4.8C). It should be noted that contraction frequency, as analysed here and in later experiments, is not necessarily a read-out of tension; this would be best analysed by laser ablation, or perhaps traction force microscopy.

To understand the mechanism by which SDF1 might inhibit front cell contractility, Rac1 FRET was performed on neural crest explants, because Rac1 is known to be activated by SDF1 (Theveneau et al., 2010) and Rac often has a mutually antagonistic relationship with Rho, an activator of contractility (Ridley, 2015). Cells and the cluster edge in the absence of SDF1 had similarly low Rac1 FRET efficiency as rear cells of clusters exposed to an SDF1 gradient (Fig. 4.9, A and B). By contrast, Rac1 FRET efficiency was increased in front cells during chemotaxis (Fig. 4.9C), indicating that SDF1 activates Rac1 in front cells. This supports previous data that SDF1 is an activator of Rac1 through its cognate receptor, CXCR4 (Theveneau et al., 2010). Next, a RhoA FRET construct was used to determine regions of high or low RhoA activity. RhoA FRET was high in edge cells in the absence of SDF1, but low in front cells when exposed to an SDF1 gradient (Fig. 4.9, C and D), indicating that RhoA and Rac1 levels are negatively correlated. To determine whether Rho is inhibited through SDF1-dependent Rac activation, explants were exposed to the Rac1 pharmacological inhibitor, NSC23766, during chemotaxis to SDF1. RhoA levels were significantly higher in front cells when exposed to the Rac1 inhibitor, suggesting that SDF1 activates Rac1, which in turn inhibits RhoA in front cells but not rear cells. Our data showed a difference in front-rear contractility during chemotaxis (Fig. 4.8). The FRET images in Fig. 4.9, A and B, are projections. In the future, it would be useful to separate out the *z* planes and identify the actin cable (with another marker), because Rho should be enhanced at the region of the actomyosin cable if it contributes to myosin contractility at the rear of neural crest explants during chemotaxis. To further assess whether SDF1 inhibits contractility in front cells, explants were immunostained for pMLC. Unlike control explants, cluster exposed to SDF1 had reduced levels of pMLC at the front (Fig. 4.9, E and F). pMLC levels could be alternatively activated by using an optogenetic form of RhoA (Fig. 4.14), described in detail in section 4.2. Exposure of clusters to the myosin ATPase inhibitor, blebbistatin, inhibited neural crest contractility (Fig. 4.9H). Finally, to determine whether SDF1 was signalling primarily through front cells and not rear cells, chemotaxis assays were performed in which neural crest clusters were composed of control and CXCR4 morphant cells, in a mosaic fashion. Chemotaxis was more

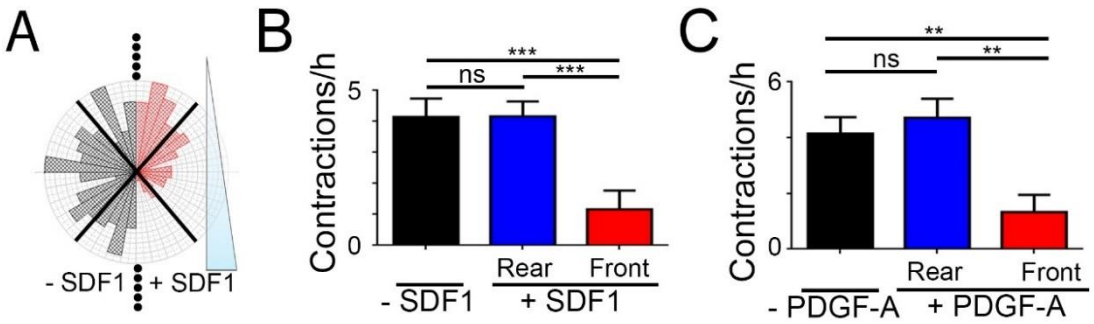

Fig. 4.8. Actomyosin contractility is inhibited at the front during collective chemotaxis. (**A**) Distribution of actomyosin contractility at different angles without (-SDF1) or with (+SDF1) an SDF1 gradient. *n* = 150 contractions, from 15 different clusters, *N* = 5 experiments. (**B and C**) Actomyosin contraction frequency (means ± SEM) of cells exposed to a gradient of the neural crest chemoattractants SDF1 (B), or PDGF-A (C). *n* = 15 cells (A) or 7 cells (B), randomly selected from different clusters, *N* = 3 experiments. ****P* ≤ 0.001 (one-way ANOVA); ns, not significant (B). ***P* ≤ 0.01 (Kruskal-Wallis test); ns, not significant (C). Note that SDF1 and PDGF-A inhibit contractions at the front of the explant.

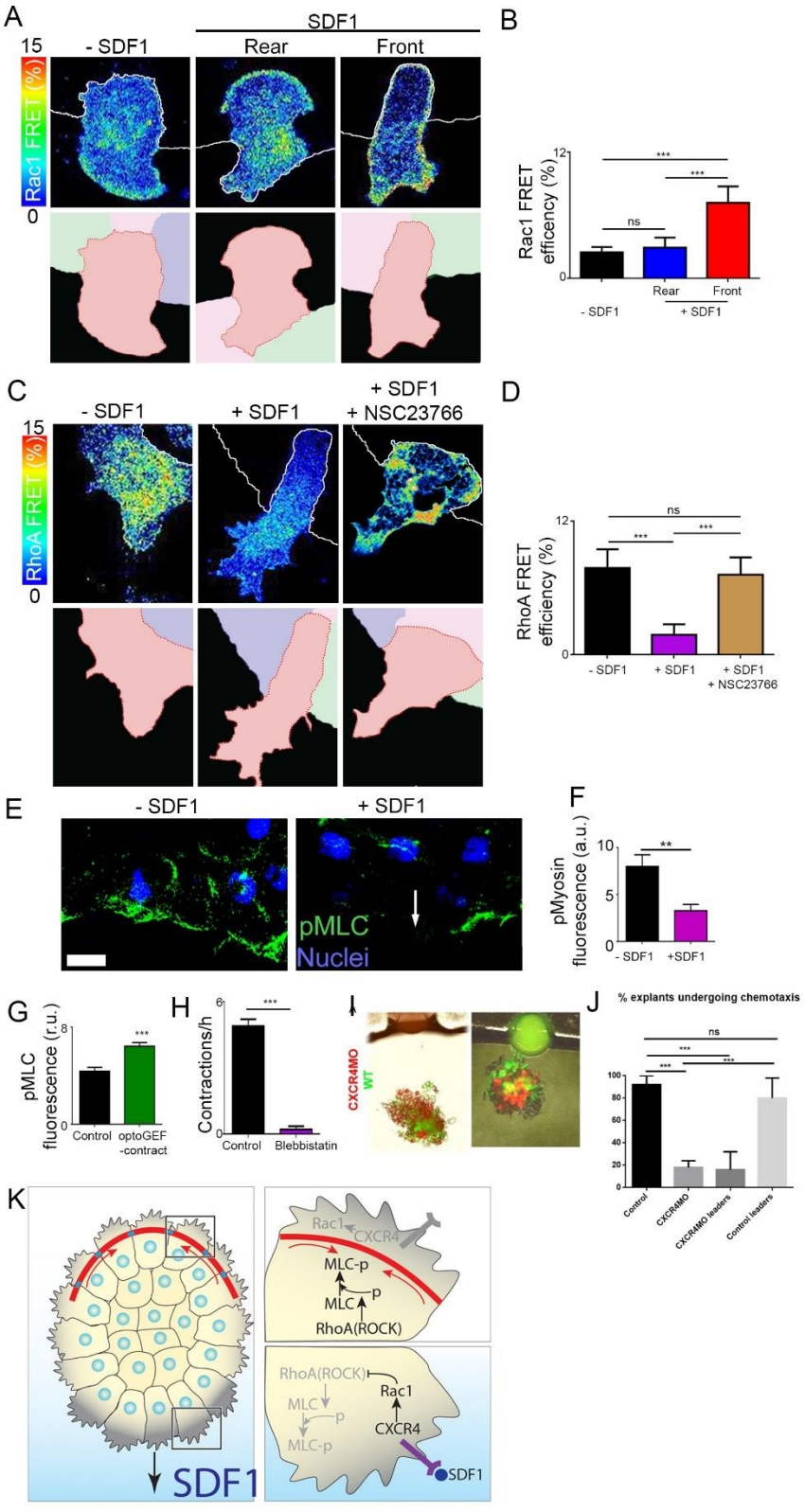

Fig. 4.9. Rac1/RhoA regulated by SDF1 inhibits contractions at the front. (**A to D**) Rac1 and RhoA FRET probes were expressed in mosaic in *Xenopus* neural crest explants. Top panels (A and C) show the FRET efficiency for the indicated treatments, bottom panels (A and C) show the cells within the cluster in different colours and black

represents the cell free space at the edge of the cluster. In each panel front is at the bottom. Rac1 FRET efficiency in cells at the front or rear of neural crest explants exposed to no SDF1 or to an SDF1 gradient (A), and the quantification of FRET efficiency (means ± SEM) (B). *n* = 10 cells from 10 different clusters, *N* = 3 experiments. ***$P \leq 0.001$ (one-way ANOVA); ns, not significant. Scale: 20 μm. Note that SDF1 leads to Rac1 activation only in front cells. RhoA FRET efficiency in cells at the front of neural crest explants exposed to no SDF1 or to an SDF1 gradient, with our without the Rac1 inhibitor, NSC23766 (C), and the quantification of FRET efficiency (means ± SEM) (D). *n* = 10 cells from 10 different clusters, *N* = 3 experiments. ***$P \leq 0.001$ (one-way ANOVA); ns, not significant. Scale: 20 μm. Note that SDF1 inhibits RhoA activity at the front of the cluster in a Rac1-dependent manner. (**E and F**) Immunostaining of the front of explants exposed to no SDF1 or to an SDF1 gradient (E) and quantification of phospho-myosin light chain (pMLC) levels (means ± SEM) (F). Scale bar, 20 μm. Arrow indicates loss of pMLC. *n* = 30 cells from 14 different clusters, *N* = 3 experiments. **$P \leq 0.01$ (two-tailed Student's *t*-test). (**G**) Quantification of phospho-myosin light chain (pMLC) (means ± SEM) after immunostaining explants illuminated or not illuminated while expressing optoGEF-contract. *n* = 10 cells each randomly selected from different clusters, *N* = 3 experiments. ***$P \leq 0.001$ (two-tailed Student's *t*-test). Note that activation of RhoA (optoGEF-contract) leads to an increase in MLC phosphorylation. (**H**) Frequency of contractions (means ± SEM) of peripheral cells when exposed to the myosin ATPase inhibitor, blebbistatin, showing that contractions are myosin-dependent. *n* = 10 cells each randomly selected from different clusters, *N* = 3 experiments. ***$P \leq 0.001$ (two-tailed Student's *t*-test). (**I and J**) Examples of neural crest cell mosaics with wild type (green) and CXCR4 morphant (red) cells. The circle at the top is the SDF1 bead. Percentage of clusters undergoing chemotaxis (means ± SEM) is quantified in J. *n* = 24 clusters, *N* = 3 experiments. ***$P \leq 0.001$ (one-way ANOVA); ns, not significant. (**K**) Diagram showing the proposed mechanism by which SDF1 inhibits front contractility during collective chemotaxis. At the front (bottom panel) SDF1 activates the CXCR4 receptor, which in turn activates RhoA leads to MLC phosphorylation and actomyosin contraction.

efficient in clusters in which control cells were at the front, rather than CXCR4 morphant cells, suggesting that SDF1 signals through the leaders (Fig. 4.9, I and J). Altogether, these data hint at a proposed mechanism in which SDF1 binds CXCR4, activates Rac1, which inhibits RhoA, myosin phosphorylation and consequently actomyosin contractility (Fig. 8I). In rear cells, or cells not exposed to an SDF1 gradient, Rac levels are low, whilst RhoA, phospho-myosin and contractility is high (Fig. 4.9K).

Cells at the periphery of an explant not exposed to SDF1 can therefore be considered to all act like 'rear' cells, and one of the effects of exposure to an SDF1 gradient is the transformation of a few rear cells into front cells.

An emergent question from this proposed mechanism is whether the cluster, and contractility is dependent on the absolute SDF1 levels that the cells are sensing, or whether it is dependent on relative levels sensed between the front and rear of the cluster. To assess this, contractility was measured in clusters exposed to uniform levels of SDF1. Unlike the SDF1 gradient, uniform SDF1 did not inhibit contractility (Fig. 4.10A), suggesting that the cluster responds to the chemotactic gradient instead of absolute SDF1 levels. To examine this further, contractility was quantified when clusters were far or near an SDF1 chemotactic source, where absolute levels are likely to be very different. Rear contractility and cluster speed were both unchanged during chemotaxis (Fig. 4.10, B and C), which hints that clusters respond to the gradient rather than to absolute levels of the chemoattractant, but given the low *p* value, this result remains somewhat inconclusive and would benefit from further analysis to increase *n* numbers. Also, how the differences between the front and rear of the cluster is communicated between the cells remains unclear, but may rely on communication via gap junction signals to allow for communication between the front and rear of the cell group.

To explore the connection between the asymmetric actomyosin contraction and collective chemotaxis, we simultaneously measured the position of front and rear cells of explants during migration, as well as the length of the actomyosin cable at the front and rear. Pulsatile contraction of the cable at the rear (Fig. 4.11, A and B, green lines) coincided with the forward movement of the rear (Fig. 4.11, A and B, blue lines). Both events immediately preceded the movement of the front of the cluster (Fig. 4.11, A and B, red lines). A similar local contraction precedes a short forward movement in the absence of SDF1, but with no long-range directed movement (Fig. 4.11, C and

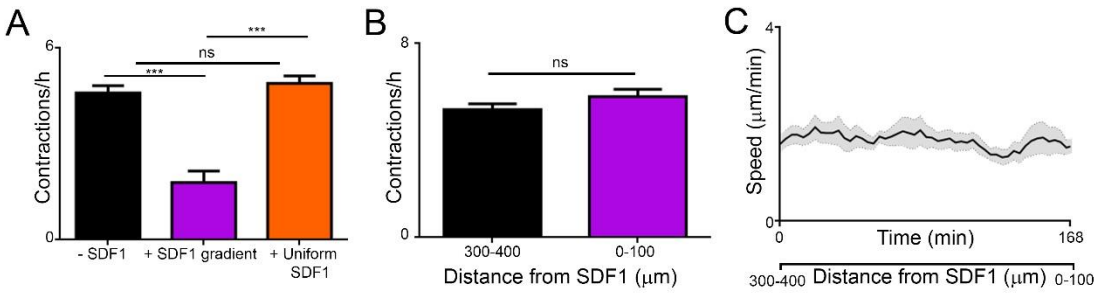

Fig. 4.10. Neural crest clusters respond to the SDF1 gradient. (**A**) Frequency of front cell contractions in the absence of SDF1, in the presence of an SDF1 gradient (+ SDF1) or exposed to uniform SDF1 (means ± SEM). *n* = 10 cells, each selected randomly from different clusters, *N* = 3 experiments. ****P* ≤ 0.001 (one-way ANOVA); ns, not significant. Note that a gradient of SDF1 but not uniform SDF1 can inhibit front contractions, indicating that the cluster responds to the gradient and not to an absolute value of SDF1. (**B**) Frequency of rear cell contractions when the cluster is at different distances from the SDF1 source. *n* = 10 cells from different clusters. (two-tailed Student's *t*-test); ns, not significant. As the SDF1 levels should be higher when the cluster is closer to the chemoattractant source, this observation suggests that the cluster does not respond to an absolute value of SDF, but to an SDF1 gradient. *p* = 0.16. *n* = 12 explants, *N* = 3 experiments. (two-tailed Student's t-test); ns, not significant. Note that *n* values are low, and the *p* value is close to 0.05, suggesting that with more data, there could be a significant data, so the conclusion that contractility does not change as the cluster gets closer to an SDF1 source is taken cautiously. (**C**) Rolling average of cluster speed during collective chemotaxis to SDF1. *n* = 7 clusters; *N* = 4 experiments. Like the above observation, the absence of a net acceleration/deceleration when the cluster is closer to the chemoattractant source suggests that it does not respond to the absolute SDF1 values.

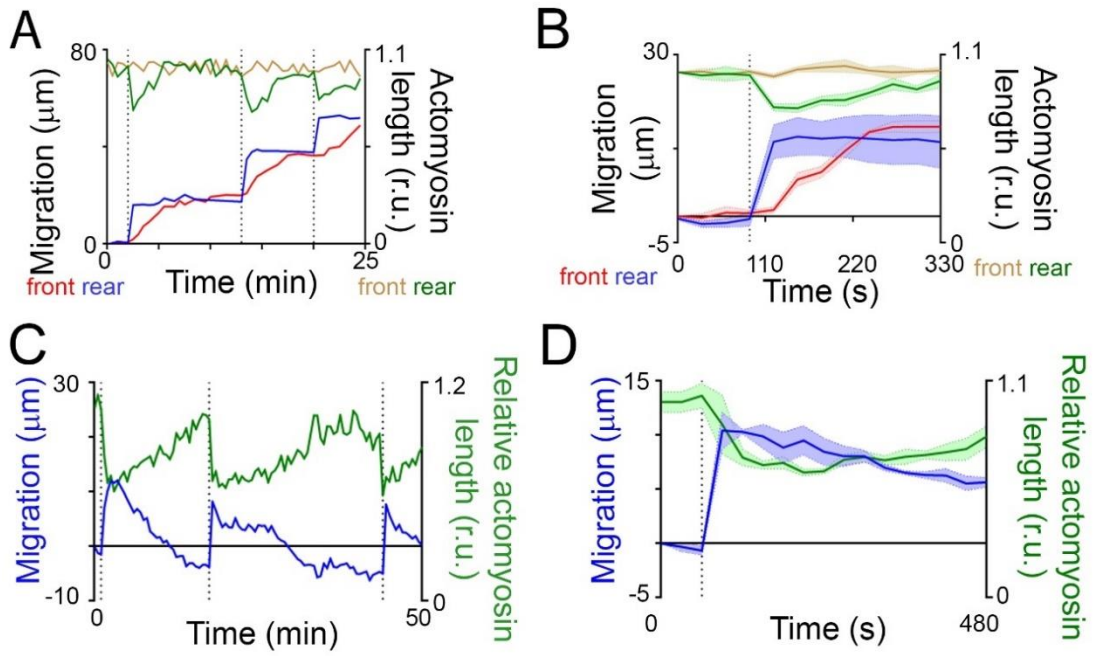

Fig. 4.11. Rear contraction coincides with a cluster's forward movement. (**A**) Relative actomyosin length at the front (brown line) and rear (green line) of a cluster, and the position of the front (red line) and rear (blue line) of the cluster. This shows a representative example that is quantified further in B. (**B**) Relative actomyosin length at the front (brown line) and rear (green line), and the position of the front (red line) and rear (blue line) of the cluster, averaged (means ± SEM) among many contractions from different clusters exposed to SDF1. An equivalent analysis, but for a single cluster, is shown in Fig. 4.11A. (**C and D**). Analysis of spontaneous contractions observed in absence of SDF1. (C) Position of the rear of the cluster (blue line) when a sequence of contractions is observed, analysed as actomyosin length (green line). (D) Similar to B but the average of many different contractions. Note that contractions without SDF1 are accompanied by forward movement of the rear of the cluster in the region where the contraction took place. *n* = 15 contractions (B) or 6 contractions (D) from different clusters (15 and 6, respectively), *N* = 3 experiments in each case.

D). Together, these results suggest that supracellular actomyosin contractility at the rear may drive collective cell chemotaxis.

4.2 Functional tests of actomyosin cable contractility *ex vivo*

We tested the role of rear contractility of the actomyosin ring on collective chemotaxis by performing laser ablation. Clusters were allowed to undergo chemotaxis to SDF1, before certain structures were ablated. Chemotaxis was impaired by ablation of the actomyosin ring in rear cells, but not by equivalent ablations in front cells, or by ablations to the cytoplasm of rear cells, or to cell-cell junctions of middle cells (Fig. 4.12). Repetitive ablations of the cable were performed in multiple cells due to the previously described dynamic reformation of the cable after it had been ablated (Fig. 4.6, C and D). By contrast, although ablation of the cell-cell junctions caused its full recoil, it did not reform within the imaging time so no repetitive ablations were required. This result suggests that the rear supracellular actomyosin cable is necessary for collective chemotaxis.

To test the requirement of rear contractility, we used an optogenetic system (Valon et al., 2017) to either increase (optoGEF-contract) or decrease (optoGEF-relax) contractility. The system is based on overexpressing a RhoA activator (DHPH domain of ARHGEF11) fused to the light-sensitive protein CRY2-mCherry. The resulting protein is called optoGEF-RhoA. In the absence of blue light, a fraction of the RhoA pool is active because of endogenous activity and overexpression of the RhoA activator. Upon illumination, CRY2 changes conformation and binds to its optogenetic partner, CIBN. To increase contractility, optoGEF-RhoA is translocated to the cell surface by co-injecting with CIBN-GFP-CAAX. To decrease contractility (relative to an unilluminated state), optoGEF-RhoA is sequestered at mitochondria by co-injecting with mito-CIBN-GFP. This system was optimised for *Xenopus* and optoGEF-RhoA could be correctly targeted (Fig. 4.13) as previously described (Valon et al., 2017).

In neural crest, the actomyosin cable is a medial-apical structure (Fig. 4.14A). The optogenetic tools were first successfully tested to, upon illumination with low doses of blue light, modulate the levels of phospho-myosin in the actomyosin cable without affecting the low levels of basal myosin (Fig. 4.14, B and C) that associates with focal adhesions. No effect was observed on cell protrusions (Fig. 4.15), focal adhesions

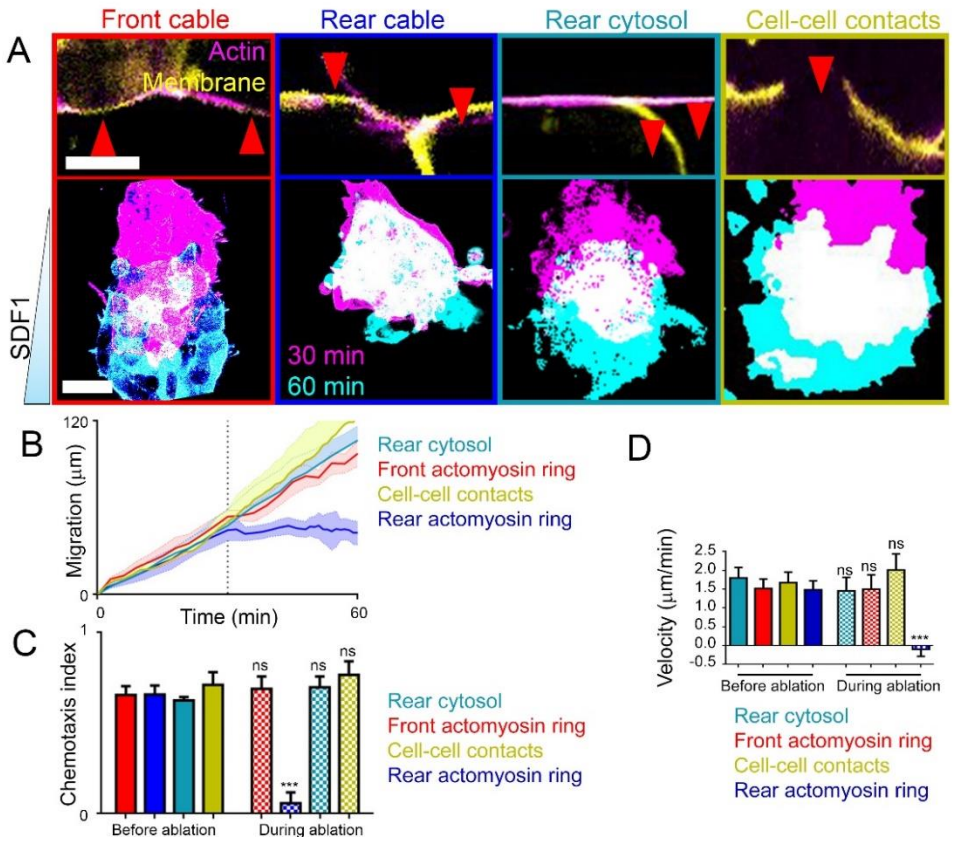

Fig. 4.12. Laser ablation of the rear actomyosin cable inhibits collective chemotaxis. (**A**) Above, examples of two neighbouring cells with ablations (red arrowheads). Scale bar, 10 μm. Below, images of explants exposed to SDF1 gradients during ablations between the indicated times. For A to C, red: front actomyosin cable ablation; blue: rear actomyosin cable ablation; turquoise: rear cell cytosol ablation; olive: centre cell-cell contact ablation. Repetitive ablations were performed in all positionally correct cells of clusters of similar sizes, except where cell-cell contacts were ablated as no recovery was observed (in this case, ablations were performed on 4-5 cell junctions). Scale bar, 50 μm. Note that cell-cell junction ablations do not affect chemotaxis. A shows examples that are quantified in B to D. (**B**) Position of the front of explants during chemotaxis (means ± SEM); dashed line indicates when ablations begin. *n* = 6-8 clusters, *N* = 3 experiments. (**C**) Chemotaxis index (means ± SEM) of clusters. *n* = 6-8 clusters, *N* = 3 experiments. ****P* ≤ 0.001 (one-way ANOVA); ****P* ≤ 0.001 (two-tailed Student's *t*-test); ns, not significant. (**D**) Velocity (means ± SEM) of the cluster during chemotaxis to SDF1 before or during ablation treatments. Note that the only ablation that impairs chemotaxis is the rear ablation of the actomyosin cable, whereas ablations in the rear cytosol, in the front actomyosin cable, or in the cell-cell junction do not interfere with chemotaxis. *n* = 6-8 clusters, *N* = 3 experiments. ****P* ≤ 0.001 (one-way ANOVA); ns, not significant.

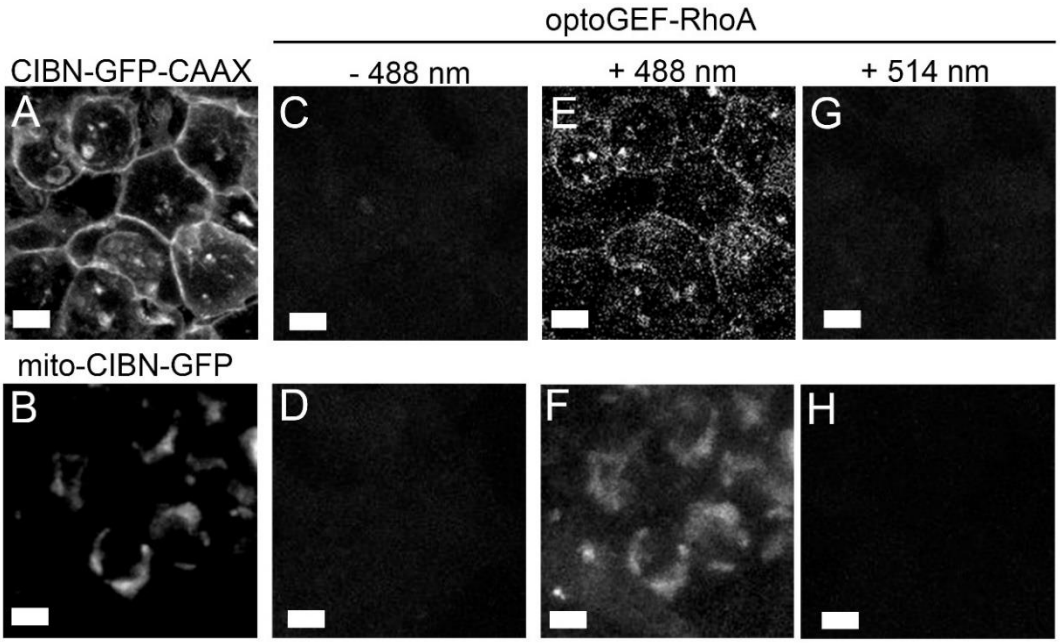

Fig. 4.13. optoGEF-RhoA translocates to the membrane or mitochondria upon blue light activation. (**A and B**) Representative images of CIBN-GFP-CAAX (A) or mito-CIBN-GFP (B). Note the membrane localization in A and the mitochondrial localization in B. These two constructs are tagged with GFP, for imaging purposes. Scale bar, 10 μm. (**C to H**) Representative images of optoGEF-RhoA (tagged with mCherry) in the absence of blue light (488-nm, C and D), in the presence of blue light (488-nm, E and F) or a control laser (514-nm, G and H), when co-expressed with CIBN-GFP-CAAX (C, E and G) or mito-CIBN-GFP (D, F and H). Note that only 488-nm is able to translocate the optoGEF-RhoA, as visualized by membrane and mitochondria localization in E and F, respectively. Scale bar, 10 μm. A and B show the GFP channel (CIBN-GFP-CAAX or mito-CIBN-GFP, respectively); C to H show the mCherry channel (optoGEF-RhoA-mCherry).

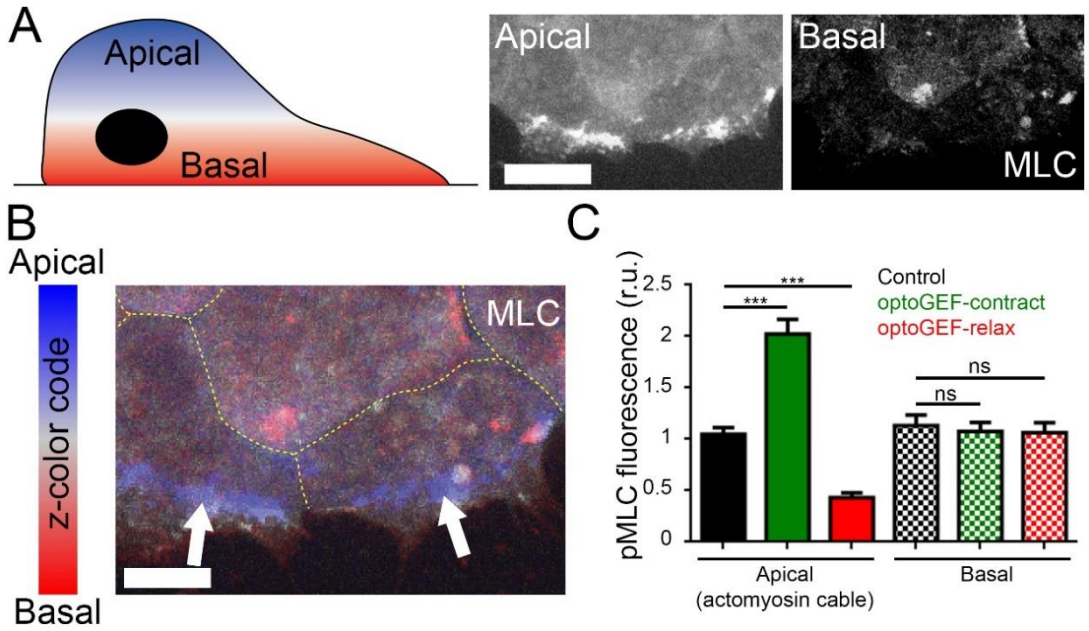

Fig. 4.14. Optogenetic activation method affects phospho-myosin levels on the actomyosin cable. (**A and B**) Diagram of a cell with apical (blue) and basal (red) regions, relative to the substrate, and pictures of the apical and basal myosin in neural crest cells (A). The edge of a neural crest cell cluster with myosin represented as different colors according to the z-plane (B). Note that two main populations of myosin are found in neural crest cells, an actomyosin cable located apically and a basal myosin population. MLC: myosin light chain. Scale bar, 20 μm. (**C**) Phospho-myosin levels using the optogenetic tools. Note that the tools affected the levels of phosphorylated myosin in the actomyosin cable (apical), but not the basal population. pMLC: phosho-myosin light chain. *n* = 40 cells from 18 explants, *N* = 3 experiments. ***$P \leq 0.001$ (one-way ANOVA); ns, not significant.

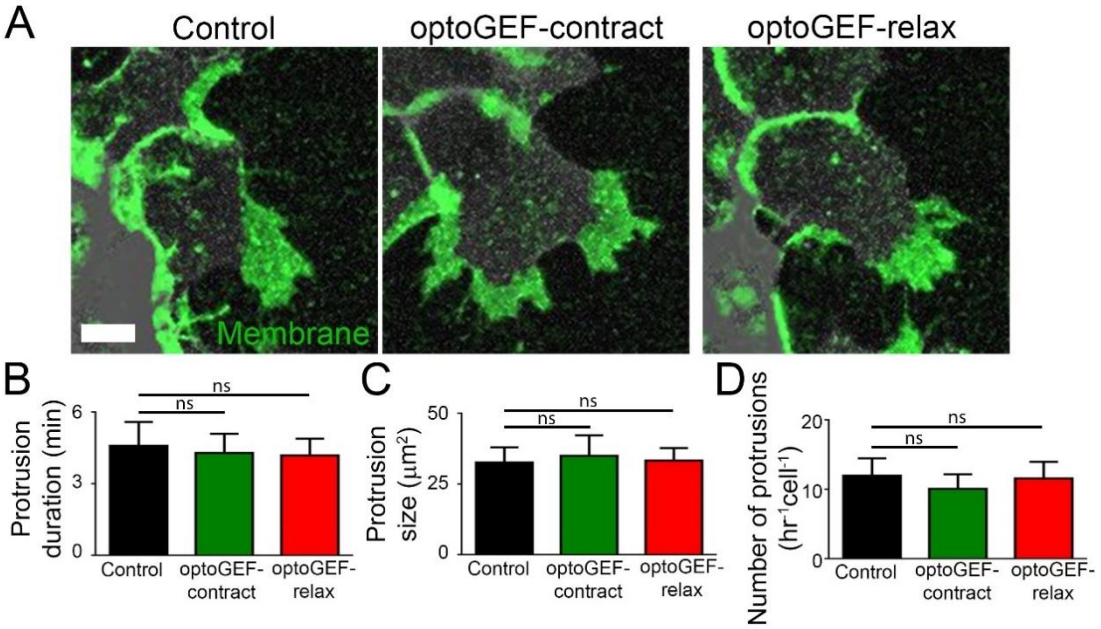

Fig. 4.15. Optogenetic tools do not affect protrusions in *Xenopus* neural crest. (**A**) Representative images of cell protrusions in control and after optoGEF-contract or optoGEF-relax photoactivation. Scale bar, 10 μm. (**B to D**) Protrusion duration (means ± SEM) (B), protrusion size (means ± SEM) (C) and number of protrusions (means ± SEM) (D). Note that optoGEF-contract and optoGEF-relax does not affect protrusion dynamics in the conditions used in our assay. *n* = 30 cells from 20 explants, *N* = 3 experiments. (one-way ANOVA); ns, not significant.

(Fig. 4.16), cell dispersion (Fig. 4.17) or phosphorylation of myosin located basally outside the cable upon illumination in the conditions of our assay (Fig. 4.14C).

We first tested whether high contractility at the rear is necessary for collective chemotaxis, by photoactivating optoGEF-relax at the rear of migrating clusters exposed to SDF1. Inhibition of contractility in rear cells impaired chemotaxis (Fig. 4.18, A to C). By contrast, inhibition of contractility in front cells failed to affect collective chemotaxis (Fig. 4.19). To determine whether rear contractility is sufficient to drive collective cell migration, we activated contractility in rear cells in the absence of SDF1. Whilst control neural crest did not exhibit directional migration, activated neural crest moved forward, away from the region of photoactivation (Fig. 4.18, D to F).

To test whether SDF1-dependent inhibition of contractility in front cells is required for collective chemotaxis, we activated contractility in front cells of migrating clusters exposed to SDF1; this repressed chemotaxis, suggesting that low front contractility is essential for collective chemotaxis (Fig. 4.18, G to I). Finally, we asked whether front inhibition of contractility by SDF1 was sufficient to generate directed migration. We inhibited front contractility in the absence of SDF1, which resulted in directional migration (Fig. 4.18, J to L). Moreover, preliminary data suggests cell explants could be forced to reverse their direction of migration using these optogenetic tools (Fig. 4.18, M and N). These optogenetic treatments affected contractility (Fig. 4.20) and seemed to not affect cell motility (Fig. 4.21). Together, these results suggest that collective migration requires greater contractility at the rear than at the front of the cell cluster.

4.3 Simulating anisotropic contractility during collective migration *in silico*

To understand how rear cell contractility might drive directed collective cell migration, a cell-centred computational model of a cell group with contractile edge cells (Fig. 4.22; Methods) was implemented. The model was developed by Dr. Andras Szabo, with input from myself regarding the design and data needed from it. Cells interact through a soft-core repulsion and mid-range attraction; to model contractions, cells at the edge (either around the cluster or at the rear) periodically attract one another with additional force (Fig. 4.22; Methods) to simulated actomyosin contractility.

In more detail: cells have a noise force (f_n), random polarisation force that determine the velocity vector (v) and an interaction force (f_i) that is based on the distance between it and its neighbour (Fig. 4.22A). This interaction force is repulsive at short-range and attractive at mid-range but does not exist at long-range (Fig. 22B).

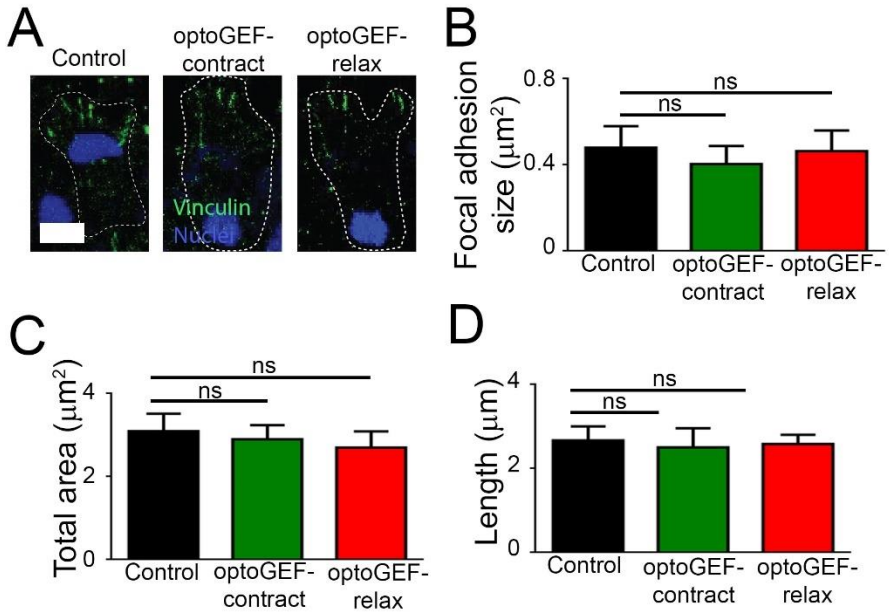

Fig. 4.16. Optogenetic tools do not affect focal adhesions in *Xenopus* neural crest. (**A**) Representative images of neural crest explants immunostained for vinculin in control and after optoGEF-contract or optoGEF-relax photoactivation. Scale bar, 5 μm. (**B to D**) Focal adhesion size (means ± SEM) (A), focal adhesion area (means ± SEM) (B) and focal adhesion length (means ± SEM) (C). Note that optoGEF-contract and optoGEF-relax does not affect focal adhesions in the conditions used in our assay. *n* = 20 cells from 16 explants, *N* = 3 experiments. (one-way ANOVA); ns, not significant.

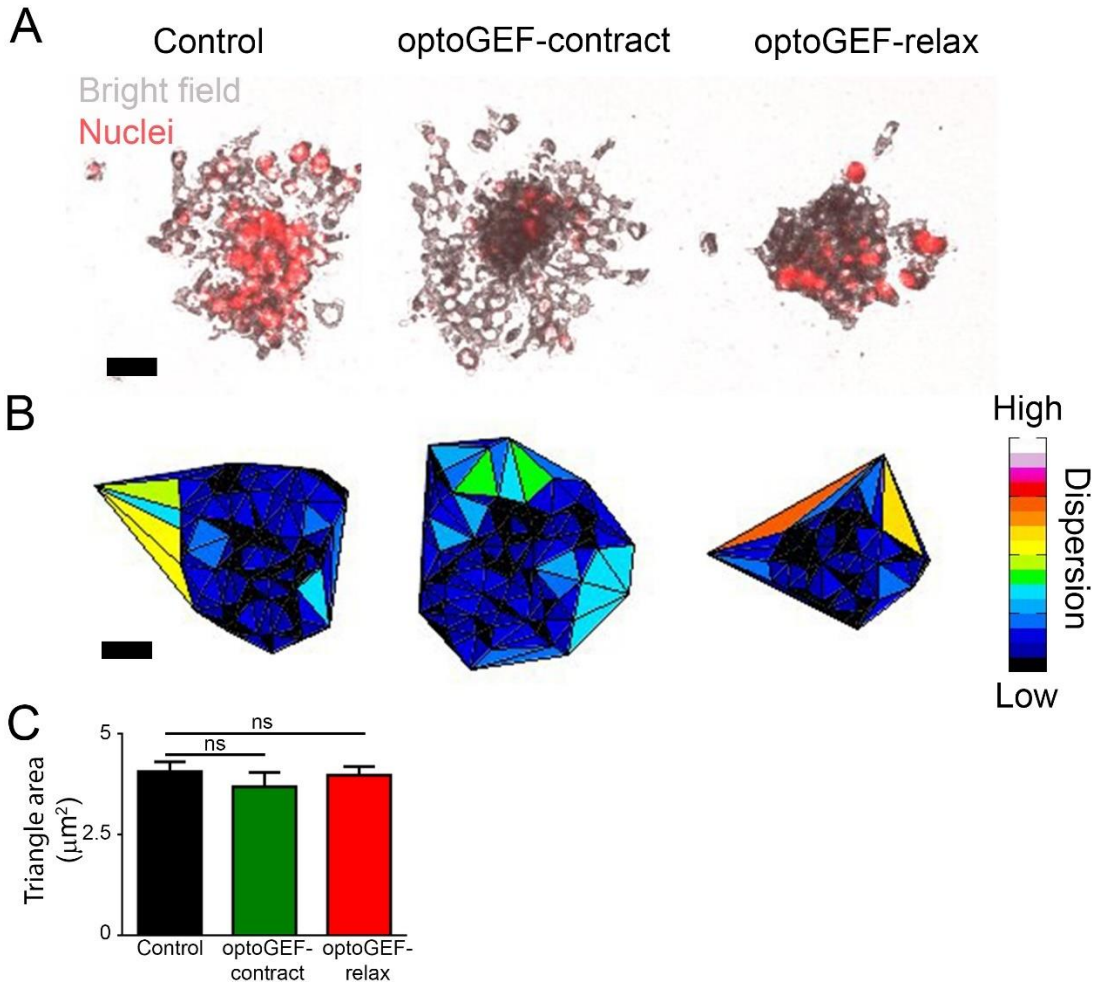

Fig. 4.17. Optogenetic tools do not affect cell-cell adhesions in *Xenopus* neural crest. (**A and B**) Representative images of cell positions in control and after optoGEF-contract or optoGEF-relax photoactivation (A), and diagrams of the associated Delaunay triangles to calculate cell dispersion (B). (**C**) Delaunay triangle area (means ± SEM). Note that optoGEF-contract and optoGEF-relax does not affect cell dispersion in the conditions used in our assay. Scale bar, 50 μm. *n* = 10 clusters, *N* = 3 experiments. (one-way ANOVA); ns, not significant.

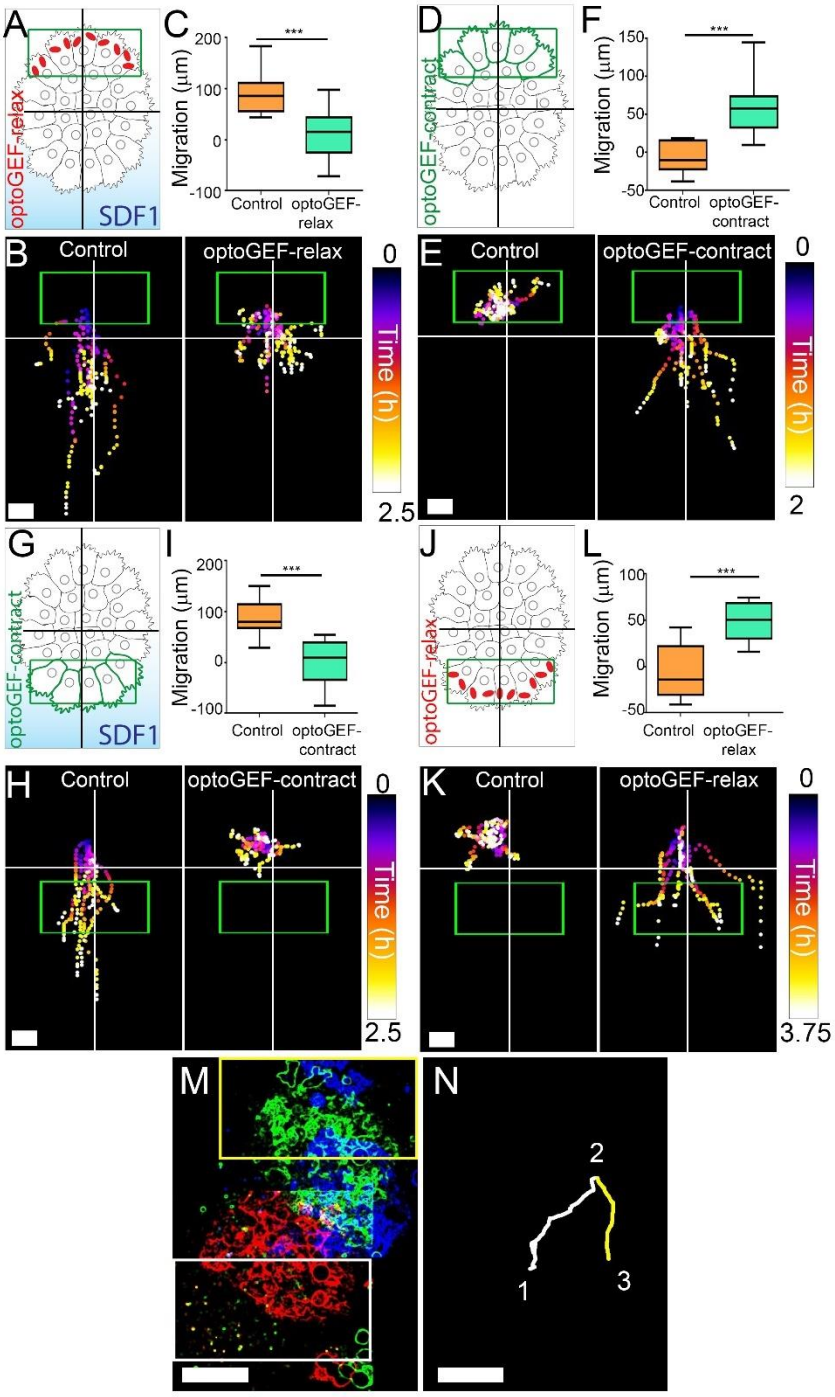

Fig. 4.18. Rear contractility is necessary and sufficient for collective chemotaxis of *Xenopus* neural crest. (**A to L**) Experimental setup for treated explants (A, D, G, J and M), representative cluster tracks (B, E, H, K and N) and the distance migrated (means ± SEM) over times as indicated in Methods (C, F, I , L and O). *n* = 10-23 clusters (F), *n* = 10-11 clusters (I), *n* = 14-18 clusters (L), *n* = 11-12 clusters (O). ****P* ≤ 0.001 (two-tailed Student's *t*-test). Scale bar, 40 µm (E and K); 20 µm (H and N). Green box: initial illumination area; cross: initial cluster position. Top of all pictures is the rear. All data are from *N* = 3 experiments. (**M**) Example of a cluster

in the absence of SDF1, membrane pseudocoloured a different time points: red, 0 min; green, 30 min; blue, 45 min. The white box represents the initial activation area at 0 min (optoGEF-contract), the yellow box representes the initial activation area at 30 min. Example M and N shows preliminary data (one example) from *n* = 3 explants from *N* = 1 experiment that shows control of directional migration with the optogenetic tools. This has not been quantified. Scale bar, 50 μm. (**N**) Cluster track. The white line represents the track between 0 and 30 min; the yellow line represents the track between 30 and 45 min. Note how the change in activation area from the rear to the front causes the cluster to switch directions. Scale bar, 50 μm.

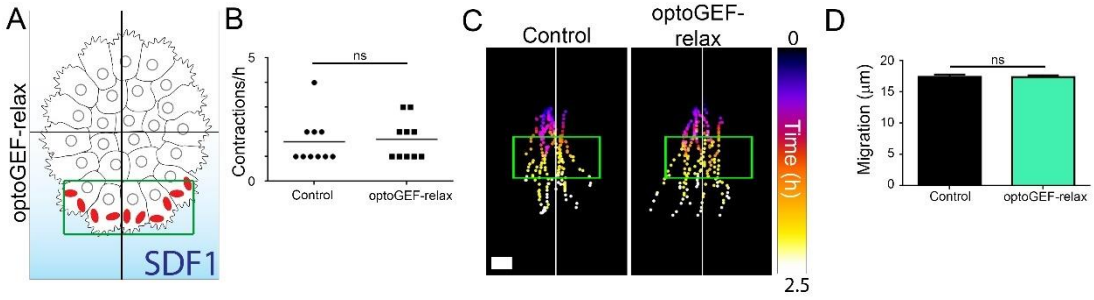

Fig. 4.19. Chemotaxis controls for optogenetic tool. (A) Diagram of the experimental setup; *Xenopus* neural crest explants expressing optoGEF-relax were exposed to a gradient of SDF1, followed by photoactivation in the front cells (red ovals indicate mitochondria). (**B**) Analysis of contractility as indicated (means ± SEM). (**C**) Representative cluster tracks. The green box (A and C) indicates the initial illumination area; the cross represents initial cluster position. (**D**) Distance migrated forward (means ± SEM) after time indicated in Methods. Note that photoactivation at the front does not affect collective chemotaxis. Scale bar, 40 μm. *n* = 35-36 clusters (B and D). (two-sided Mann-Whitney *U*-test); ns, not significant.

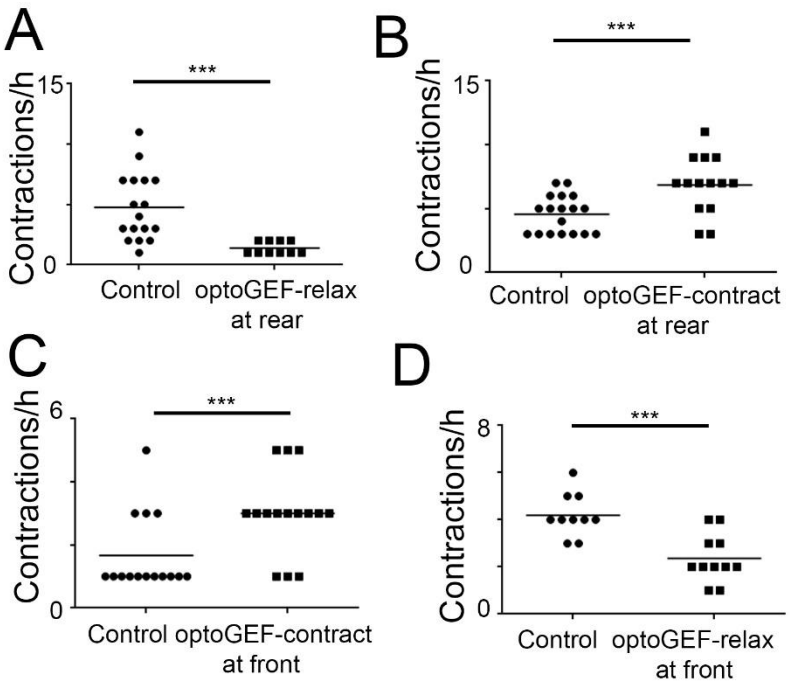

Fig. 4.20. Optogenetic tools control contractility. (**A to D**) Frequency of contractions (means ± SEM) in the indicated treatments during the experiments in Fig. 4.18: A corresponds to Fig. 4.18A, B to Fig. 4.18D, C to Fig.4.18G, D to Fig. 4.18J. *n* = 10 cells randomly selected from 10 different clusters. (two-tailed Student's *t*-test); ns, not significant.

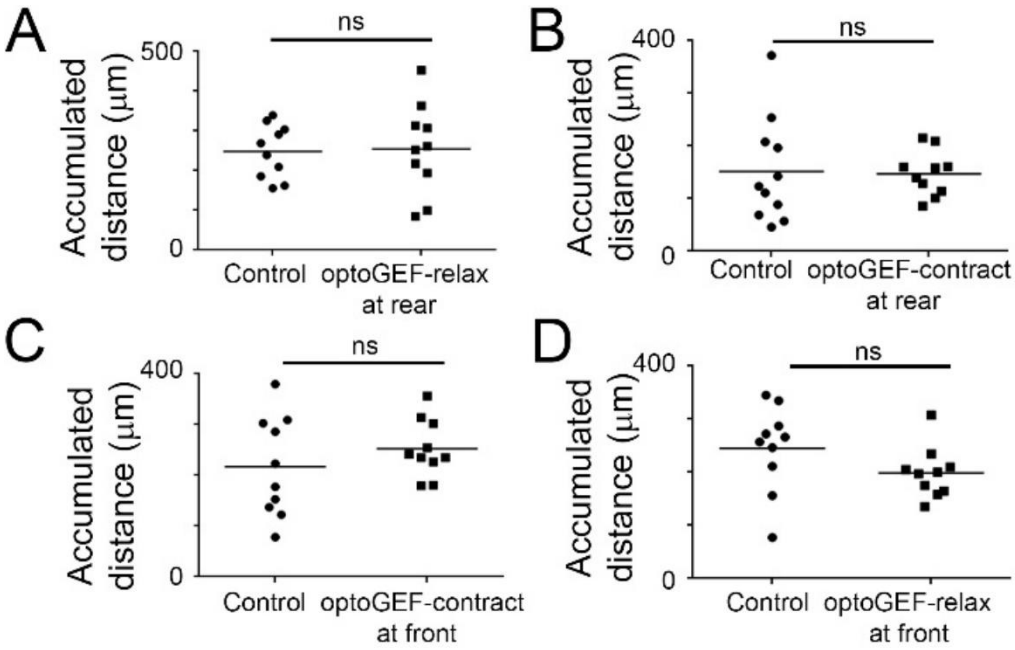

Fig. 4.21. Optogenetic tools do not affect cluster motility. (**A to D**) Accumulated distance (dot plot with mean line) of explants in the indicated treatments during the experiments in Fig. 4.18: A corresponds to Fig. 4.18A, B to Fig. 4.18D, C to Fig.4.18G, D to Fig. 4.18J. In all cases, *n* = 10-14 clusters, *N* = 3 experiments. (two-tailed Student's *t*-test); ns, not significant. These results show that the optogenetic treatments described here do not affect the motility of the cluster. A: $p = 0.87$ B: $p = 0.86$; C: $p = 0.33$ D: $p = 0.22$.

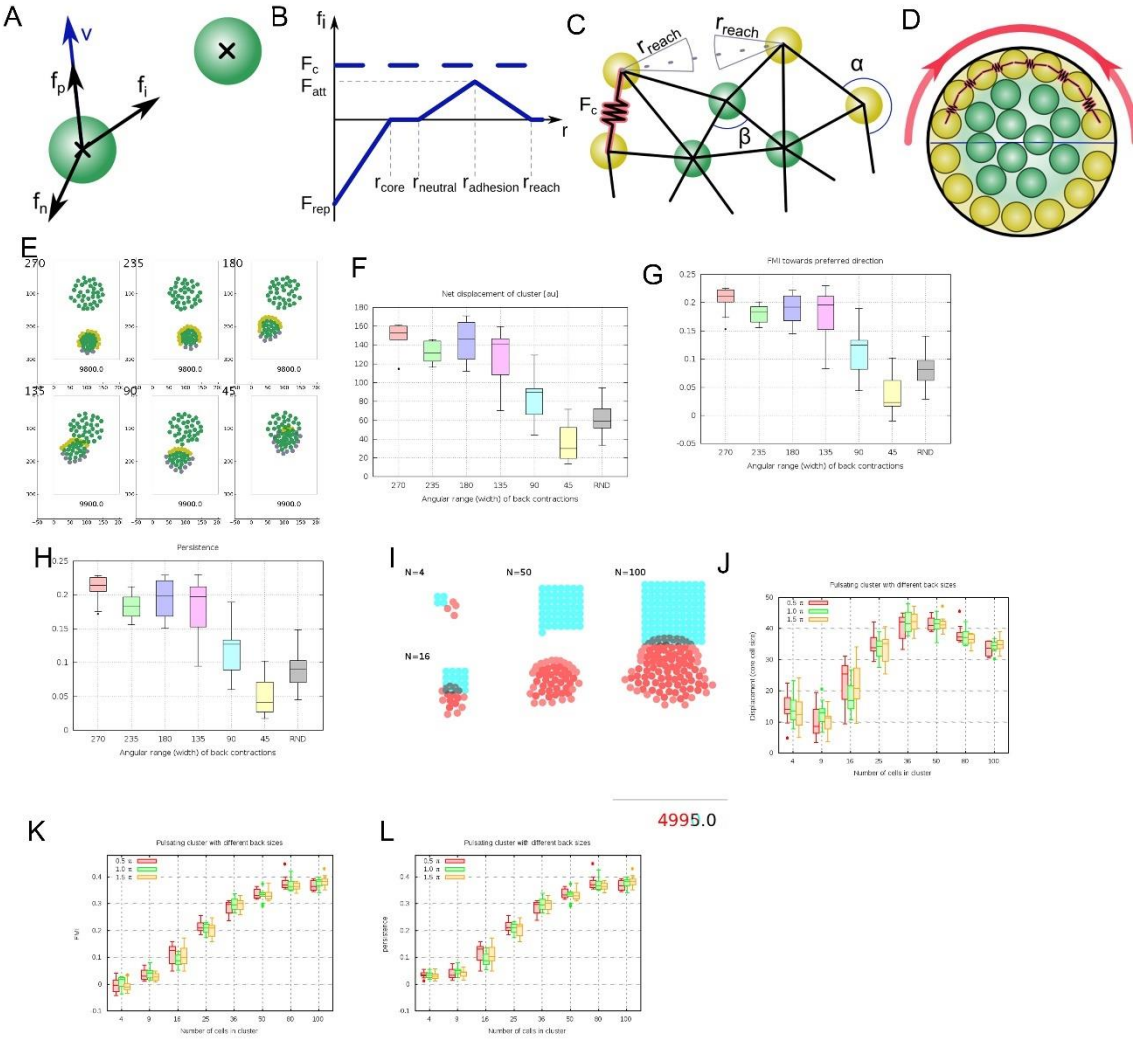

Fig. 4.22. Computational model of a cell cluster and testing parameters. This model was generated by Dr. Andras Szabo, with input from myself. (**A**) Cells are represented as disks on a 2D plane by their position and velocity, and with a central and symmetric interaction (f_i) amongst them. Cells are propelled by an internal polarization force (f_p) in the direction of their velocity vectors (v) and experience a noise factor (f_n). (**B**) Interaction profile of cells as a function of distance (r) from another cell. An additive contractile force (f_c) increases the interaction force uniformly (blue dashed line) between two contractile cells. (**C**) Representation of a cell cluster indicating neighbor relations. If the largest angle between neighbors is more than 135 degrees (for example: α), the cell is considered an outer cell (yellow); otherwise (β) it is an internal cell (green); red spring represents contraction. (**D**) Illustration of the computational model cluster. Yellow: edge cells; green: internal cells; red: contraction; horizontal line: distinction between front and rear, with rear outer cells contracting (red spring). (**E to H**) Pictures of example simulation clusters at start and end frames, with different rear regions, with quantification of displacement (F),

forward migration index (G) and persistence (H) (box plots for all). *n* = 50 simulations. Note that poor migration is only exhibited in clusters with a very small rear contractile region. (I to L) Pictures of example simulation clusters at start (blue) and end (red) time frames with clusters of different sizes. *N* on diagram is the number of cells in the cluster. Quantification of displacement (J), forward migration index (K) and persistence (L) (box plots for all) with different size contracting rears, *n* = 50 clusters. Note that migration is best (in the context of FMI, persistence, displacement) at a level similar to the size of *ex vivo* clusters (approximately 50 cells).

Contractility increases the interaction force (F_c) (Fig. 4.22B). Clusters are generated by Delaunay Triangulation from the Voronoi, and a contractile force (Fc, red spring) is periodically applied to contractile cells (yellow cells) are determined to be those that have a large angle (α) and not those (green cells) with a small angle (β) between cells (Fig. 22C). This does not apply to cells that have a large distance between them (r_{reach}). Regions of contractile cells are applied selectively (blue horizontal line) to either all valid cells, which reproduces control *ex vivo* clusters, in which all outer cells are contractile, or those just in the rear (Fig. 4.22D, red arrows) (like those *ex vivo* clusters undergoing chemotaxis). There is no chemotactic agents in the simulation, however. Some parameters were tested, examples of which are shown in Fig. 4.22. Modifying the region of rear contractility in simulations showed that migration was only strongly impaired when the region of rear contractility was very small (Fig. 4.22, E to H). Clusters migrated best when there were ~50 cells in the group, with low cell numbers resulting in poor migration and very high numbers causing a mild inhibition of migration (Fig. 4.22, I to L). Parameters are justified and explained in Section 3.7.

Similar to the *ex vivo* data, only simulations with rear but not with uniform contractility were able to migrate forward (Fig. 4.23A, and movie 2). Other migration outputs were comparable between *in silico* and *ex vivo* clusters (Fig. 4.23, B to D). Interestingly, these simulations supported the model that rear contractility may be sufficient for long-range directed collective cell migration, even in the absence of a chemotactic signal. To understand how this contractility-driven migration model might work, cell movements were carefully analysed in simulations. Unexpectedly, analysis of cell movements *in silico* revealed that rear cells in contractile regions intercalated forward, into the cell group (Fig. 4.24A, and movie 3). As predicted by the model, an equivalent intercalation at the rear of neural crest clusters was found (Fig. 4.24B), and this occurred at a high rate in clusters undergoing collective chemotaxis (Fig. 4.24C). To determine whether intercalation at the cluster rear causes a wave of cell movement forward, cells were tracked *in silico*. The simulations predicted that the effect of this local cell rearrangement is spread through the whole cell group such that when the cluster's rear contracts, the rear cells intercalate, triggering a wave of cell movement that propagates from the rear towards the front of the cluster (Fig. 4.25, A and B). Surprisingly, by analysing cell movement by PIV, a similar wave was observed *ex vivo*, as predicted by the model (Fig. 4.25, C and D). This suggests that rear cell intercalation might push cells forward progressively over time, following rear contractions. Cell intercalation likely causes a rearrangement of cells within the cluster. To understand what was happening, cell tracks from *in silico* simulations were

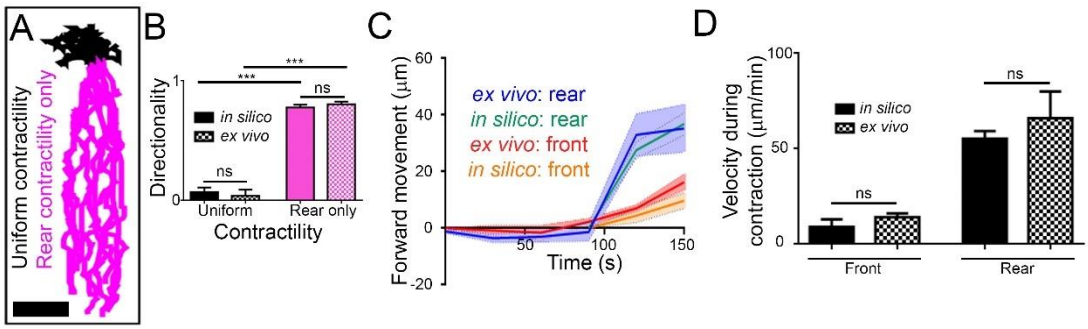

Fig. 4.23. *In silico* simulations generate directional migration that is similar to *ex vivo* cluster behaviour. (**A**) Simulated cluster tracks with uniform contractility (black tracks) or rear contractility (pink tracks). Note that only rear contractility promotes forward movement. Scale bar, 100 μm. (**B**) Directionality (means ± SEM) of clusters. n = 10 clusters. ***$P \leq 0.001$ (one-way ANOVA); ns, not significant. *ex vivo* clusters are from N = 4 experiments. (**C and D**) Positions (means ± SEM) of the front and rear of cell clusters during rear contractions (C) and velocity (means ± SEM) (D). n = 5-6 cells are randomly selected from different clusters (5-6 explants), N = 3 experiments. Note the fit between *ex vivo* and *in silico* data. (two-sided Mann-Whitney U-test); ns, not significant.

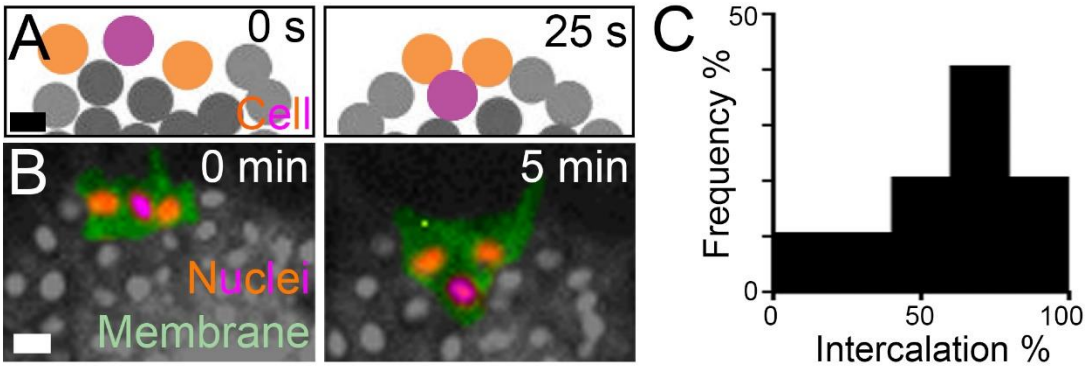

Fig. 4.24. Rear cells intercalate forward during directional migration. (**A and B**) Intercalation of a rear cell (purple) between two adjacent cells (orange) *in silico* (A) and *ex vivo* (B) during directional migration. Scale bar, 20 μm. Images are representative from imaging of 30 clusters. (**C**) Histogram of the frequency of rear cell intercalation during cluster directional migration *ex vivo*. Intercalation % refers to the percentage of cells intercalating into the cluster from the rear, while accounting for those cells moving in the reverse direction, described further in Methods Section 3.6.2. Frequency % refers to the % of clusters migrating at each level of intercalation percentage. *n* = 20 clusters, *N* = 5 experiments.

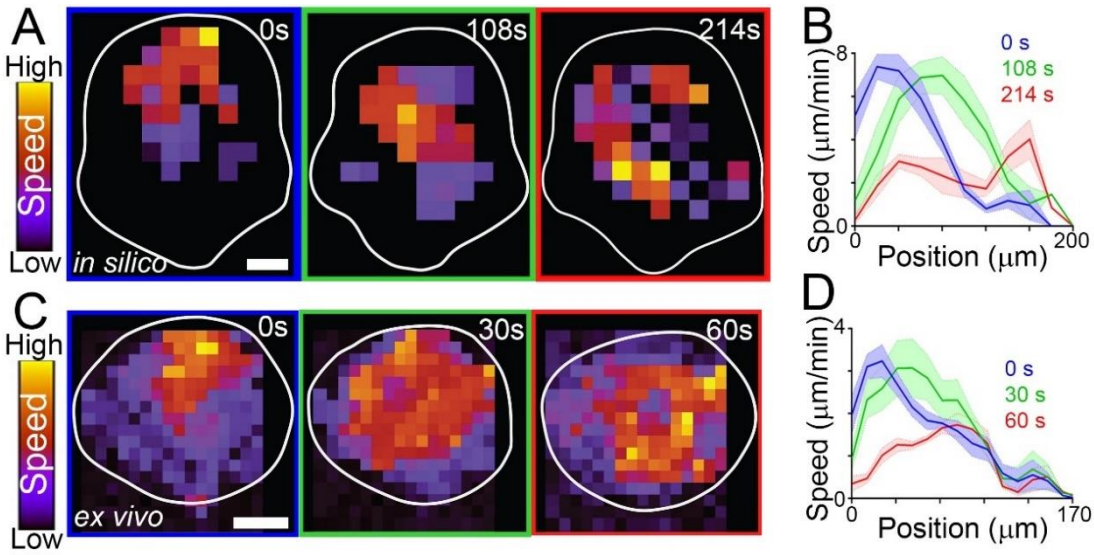

Fig. 4.25. A rear-to-front speed wave occurs after rear contraction. (**A to D**) Wave of contraction. Speed heat map during migration *in silico* (A) and *ex vivo* (C). Speed profile (means ± SEM) from clusters in *silico* (B) and *ex vivo* (D) at different times during directional migration. Position 0 μm represents the rear of the cluster; position 200 μm and 170 μm (B and D, respectively) represents the front of the cluster. *n* = 5 clusters. *ex vivo* data are from *N* = 4 experiments Scale bar, 40 μm.

used to average cell movement over time and subtract cluster movement. This revealed an intra-cluster flow of cells whereby rear cell intercalation causes a drift forwards through the middle of the group and cells at the front and sides move backwards, replacing rear cells (Fig. 4.26A). Using PIV from *ex vivo* clusters, this was then confirmed to occur experimentally too (Fig. 4.26B).

Consistent with this mechanism driving cluster movement, a positive correlation was found between the speed of *ex vivo* and *in silico* clusters during collective migration and the amount of rear cell intercalation (Fig. 4.27A). Furthermore, non-migratory *ex vivo* and *in silico* clusters had low intercalation, including during rear actomyosin ablation treatments (Fig. 4.27B). Migratory clusters *in silico* had comparable cluster speeds to *ex vivo* (Fig. 4.27B). It would be interesting to test this further by examining contractility and collective cell movement when intercalation is inhibited. LPAR2 inhibition (through use of a morpholino, MO) seems to prevent cell-cell exchange by blocking N-Cadherin endocytosis (Kuriyama et al., 2014); the same analysis (Fig. 27A, green dots) shows a fit to the trend of *ex vivo* wild type data. However, N-Cadherin also has functions in adhesion and cohesion (Scarpa et al., 2015) and CIL (Roycroft et al., 2018, Bahm et al., 2017) so this result might alternatively be explained by the effects of loss of LPAR2 on these features of collective neural crest migration, in addition to (or instead of) the effect on intercalation. Additionally, this LPAR2 data has low *n* values.

Actomyosin contractions were often preceded by relaxation by cells that do not intercalate. An alternative hypothesis is that relaxation of the rear actomyosin cable could be driving collective cell chemotaxis. However, under normal conditions, contractility and relaxation, if quantified by shortening and extension of the cable, respectively, are similar and intimately linked. To assess whether relaxation might be important for collective cell migration, the levels of contraction and relaxation were compared in different conditions. During normal chemotaxis, rear contractility and rear relaxation are both high (Fig. 4.28A). When not undergoing directed migration, clusters have low contractility and relaxation (Fig. 4.28A). However, activation of optoGEF-contract at the rear increases contractility and reduced relaxation (the latter because cells are intercalating), and these cluster still migrate forward (Fig. 4.28A). Thus, rear contractility is necessary for forward movement, whereas rear relaxation is not. This suggests that rear contraction, and not relaxation, drives directed migration. In support of this, simulations in which the rear continuously contracts (and does not relax at all) were able to migrate in a highly directional manner (Fig. 4.28B,

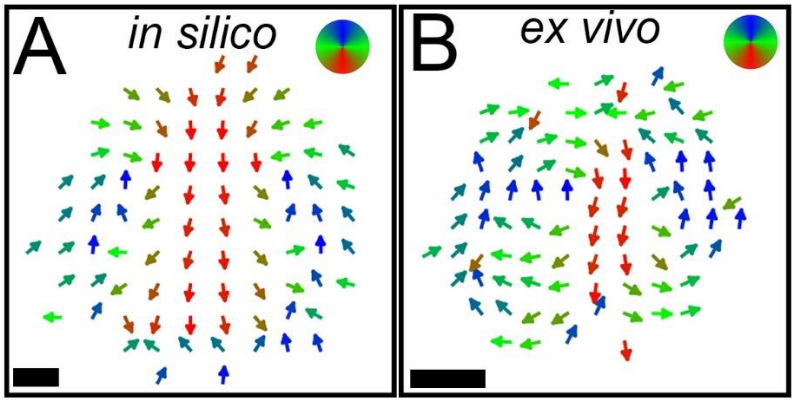

Fig. 4.26. Cluster movement arising from rear contraction. (**A and B**) Direction of intra-cluster cell movements shown from time-averaged cell tracks *in silico* (A) and particle image velocimetry (PIV) *ex vivo* (B) after subtracting cluster movement. Cells are tracked manually *in silico* and the bright field and membrane channels are used for PIV analysis *ex vivo*. These movements are an average from n = 5 clusters. Individual examples look similar. Scale bar, 40 μm.

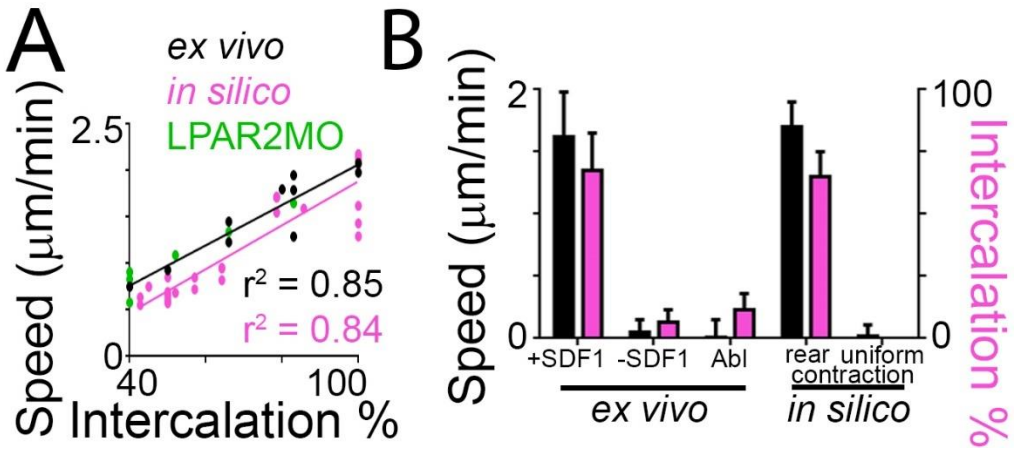

Fig. 4.27. Cluster speed positively correlates with rear cell intercalation (**A**) Cluster speed and rear cell intercalation during migration. *Ex vivo* (wild type, black) data are taken from *N* = 5 experiments; LPAR2MO (LPA receptor 2 morpholino, green) data are taken from *N* = 1 experiment. (**B**) Cluster speed (means ± SEM) and rear cell intercalation (means ± SEM) of clusters. Abl: laser ablation of the actomyosin ring in rear cells. *n* = 6-21 clusters, *N* = 3 experiments.

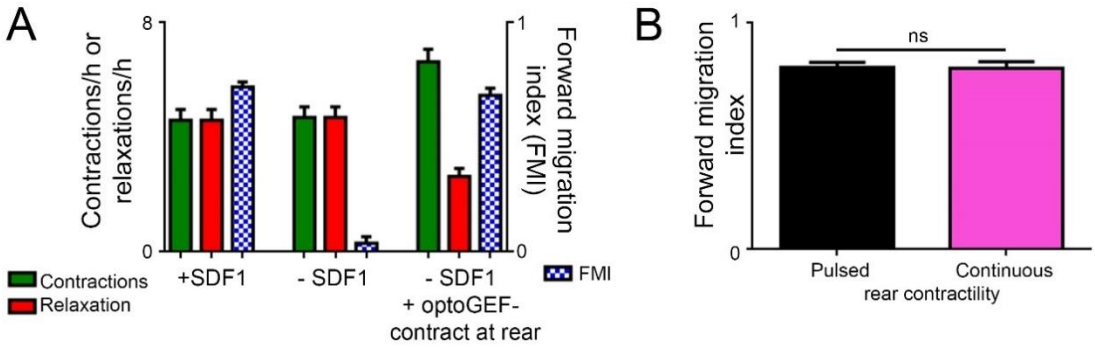

Fig. 4.28. Rear relaxation does not drive migration. (**A**) The frequency of rear contractions (green bars) (means ± SEM) and rear relaxations (red bars) (means ± SEM) of the actomyosin cable, and cluster forward migration (striped bars) (means ± SEM) when clusters are exposed to an SDF1 gradient, no SDF1 gradient, or no SDF1 gradient with optoGEF-contract activated at the cluster rear. Note that forward migration only occurs during high rear contraction but can occur during both high or low rear relaxation, suggesting high rear contraction, and not relaxation, drives collective chemotaxis. *n* = 10 cells randomly selected from 10 different clusters for contraction and relaxation, or clusters for forward migration index quantification. Data is from *N* = 5 experiments. (**B**) Forward migration (means ± SEM) of simulated clusters during pulsed rear contractions (clusters have both rear contraction and rear relaxation) and continuous rear contraction (no relaxation). Note that relaxation does not contribute to forward migration *in silico*. *n* = 10 clusters. (two-tailed Student's *t*-test); ns, not significant.

and Movie 4). Altogether, these results suggest that rear contractility drives collective cell migration by inducing cell intercalation which pushes the group forward.

4.4 Testing actomyosin contractility *in vivo*

The cumulative results of our *ex vivo* and *in silico* data suggest that rear contractility can drive collective cell migration. To test whether this model of collective cell chemotaxis explains *in vivo* migration of cranial neural crest in some species, we analysed neural crest migration in *Xenopus* and zebrafish embryos. Neural crest expressing fluorescently-tagged MLC were grafted into wild-type host *Xenopus* embryos and imaged. Similar to *ex vivo*, an actomyosin cable was present at the edge of the neural crest (Fig. 4.29, A to D).

To assess actomyosin in zebrafish, the transgenic line Tg(Sox10:nuclear-RFP-Gal4) was used. Sox10 is a promoter that is specifically active in the neural crest. The neural crest of this transgenic line is identified by nuclear-RFP expression driven by this promoter. Embryos were microinjected with a UAS-MLC-GFP, which causes MLC

expression specifically in neural crest cells upon Tamoxifen exposure. Imaging these embryos revealed a pluricellular actomyosin cable at the edge of the cranial neural crest (Fig. 4.29, E and F). Time-lapse imaging of the actomyosin showed that is a contractile structure *in vivo* in both *Xenopus* and zebrafish, with the cable reducing its length (Fig. 4.30, A to D) similar to *ex vivo*. Moreover, actomyosin contracts more frequently at the rear of the neural crest stream than at the front in *Xenopus* (Fig. 4.30E). Like *ex vivo*, rear contractility preceded forward movement of the cluster in *Xenopus* embryos (Fig. 4.30F).

Next, whole-mount immunostaining was performed on *Xenopus* and zebrafish embryos, and the front and rear of neural crest streams imaged (Fig. 4.31, A and E). For *Xenopus*, fibronectin was imaged to identify the neural crest stream; fibronectin is the substratum upon which the neural crest migrates. Less phospho-myosin was present at the front than at the rear at the beginning of migration (Fig. 4.31, A to D). In zebrafish, two different transgenic lines and two different pMLC antibodies were used. Tg(Sox10:nuclear-RFP-membrane-GFP), in which neural crest cells have fluorescently tagged nuclei and membrane markers, and Tg(Sox10:GFP), in which neural crest cells express GFP that is localised to the cytoplasm, were both used to identify neural crest cells. Actin cable-like structures were found at the front and rear of the neural crest in both lines (Fig. 4.31, F to I, middle panels), but phospho-myosin was primarily found on the rear cable and not the front cable (Fig. 4.31, E to J).

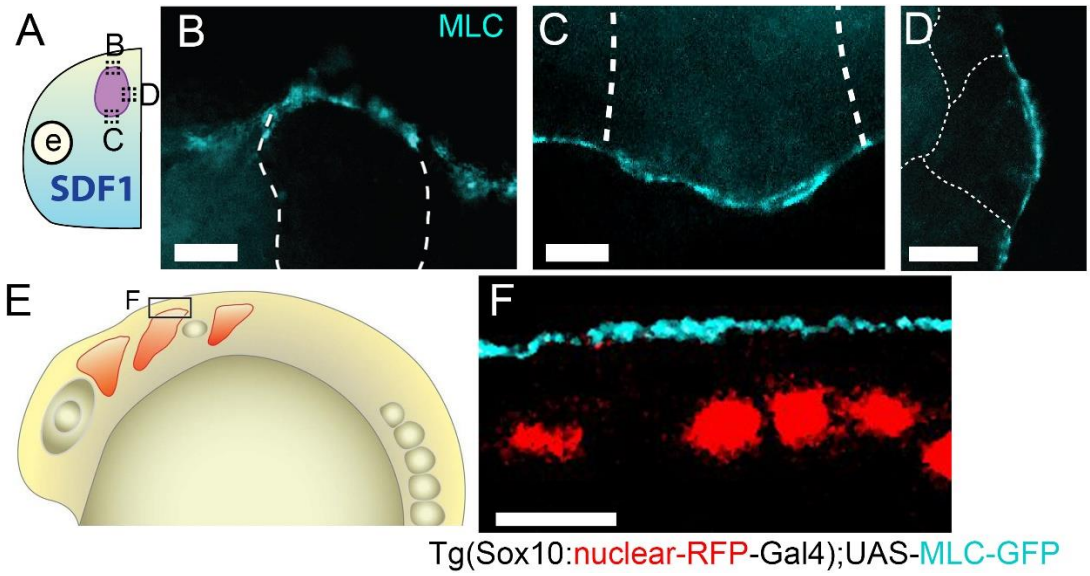

Fig. 4.29. *Xenopus* and zebrafish neural crest cluster have a rear actomyosin cable *in vivo*. (**A to D**) Diagram of a *Xenopus* embryo. Dashed boxes indicate the regions of the cephalic neural crest stream imaged in B to D; e, eye. Representative images of fluorescence of the rear (B), front (C) and side (D) of the *Xenopus* neural crest stream *in vivo*. MLC: myosin light chain; dashed lines: cell-cell contacts between neural crest cells. Scale bar, 10 μm. (B) White dashed lines indicate the junctions between neural crest cells. Scale bar, 10 μm. *n* = 10 embryos. *N* = 3 experiments. (**E**) A diagram of the zebrafish embryo. Red: neural crest. Boxes indicate the regions imaged in F. Rear (dorsal) is top of the pictures. (**F**) Immunofluoresence of neural crest cells expressing fluorescently-tagged nuclei Tg(Sox10:nuclearRFP-Gal4)) and myosin light chain (UAS:MLC-GFP). Note the formation of a neural crest-expressing myosin cable at the rear of the stream. Scale bar, 20 μm. *n* = 8 embryos. *N* = 3 experiments.

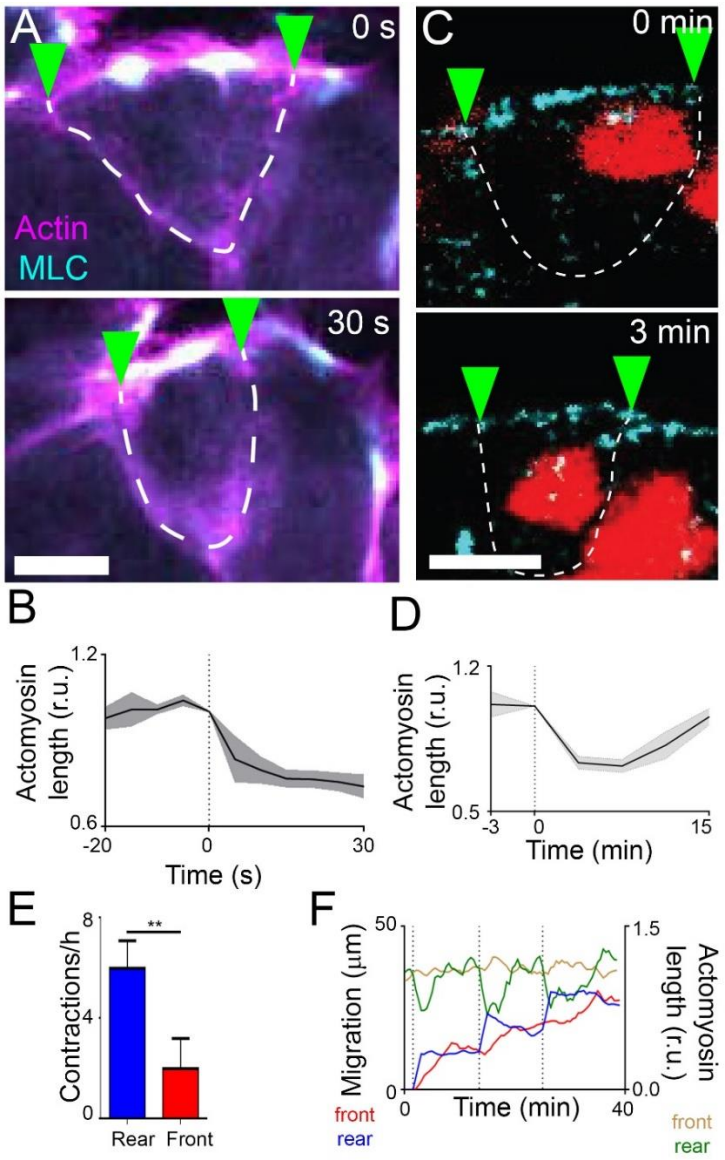

Fig. 4.30. The actomyosin cable is contractile in *Xenopus* and zebrafish. (**A**) Contraction of the actomyosin cable of *Xenopus* neural crest *in vivo*; green arrowheads: cell-cell contacts; dashed line: cell edges. Scale bar, 10 μm. (**B**) Relative actomyosin length (means ± SEM) during rear contraction. Dotted line at t = 0 is the contraction. *n* = 11 cells from different clusters (11 different clusters), *N* = 3 experiments. (**C and D**) Contraction of a rear cell during zebrafish neural crest migration in the transgenic line Tg(Sox10:nuclearRFP-Gal4); UAS:MLC-GFP was injected to visualize neural crest-expressing myosin. The white dashed line represents the cell-cell contacts between neural crest cells, identified using a membrane marker. Note the shortening of the rear actomyosin cable, which is quantified in D (means ± SEM). *n* = 10 cells from 10 different embryos, *N* = experiments. Scale bar, 10 μm. (**E**) Actomyosin contraction frequency (means ± SEM). *n* = 20 cells from different clusters (20 different clusters), *N* = 3 experiments.

$P \leq 0.01$ (two-tailed Student's *t*-test). (F**) Actomyosin length at the front (brown line) and rear (green line) of a *Xenopus* cluster *in vivo*, and the position of the front (red line) and rear (blue line) of the cluster.

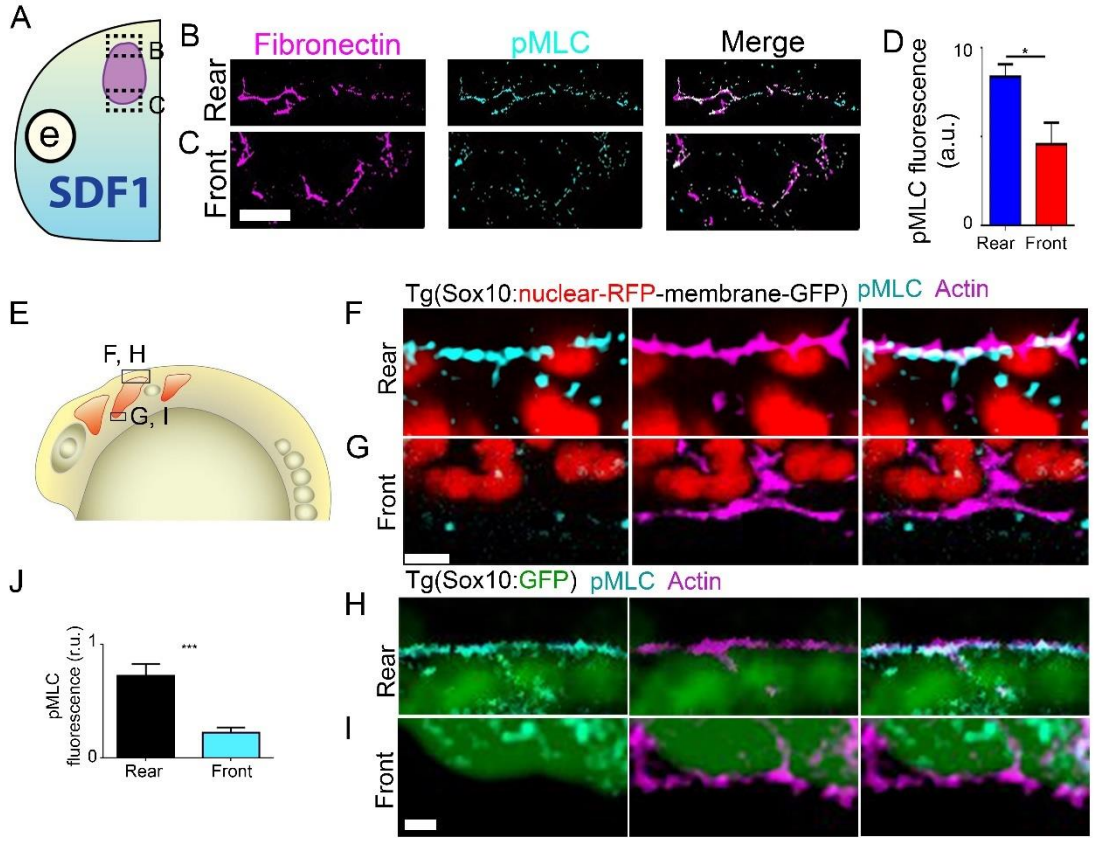

Fig. 4.31. Phospho-myosin is enhanced at the rear of neural crest clusters *in vivo*. (**A and D**) Diagram of a *Xenopus* embryo; e, eye (A) immunostained for phospho-myosin and fibronectin, the migratory substrate of the neural crest. Representative images of the rear (B) and front (C) of the neural crest stream *in vivo*. Note that this diagram is not a graft of the neural crest, the purple stream simply depicts the normal neural crest position. The images in B and C are from immunostained embryos. Scale bar, 20 μm. (D) Fluorescence (means ± SEM) of phospho-myosin light chain (pMLC) at the front and rear of neural crest streams after *in vivo* immunostaining. *n* = 20 cells from 12 different embryos, *N* = 4 experiments. **P* ≤ 0.05 (two-tailed Student's *t*-test). (**E**) A diagram of the zebrafish embryo. Red: neural crest. Boxes indicate the regions imaged in F to I. Rear (dorsal) is top of the pictures. (**F to I**) The rear and front of the neural crest cluster. Embryos from the zebrafish lines Tg(Sox10:nuclearRFP-membraneGFP) (F and G) and Tg(Sox10:GFP) (H and I) were immunostained against Phalloidin and phospho-myosin light chain (pMLC). Note the similarity of the staining in the two different transgenic systems and using two different phospho-myosin antibodies, and the presence of pMLC in the rear but not front of the cluster, which is quantified in F. *n* =

10 cells from 10 different clusters, N = 3 experiments. ***$P \leq 0.001$ (two-tailed Student's *t*-test). Scale bar, 10 μm.

Combined, these data suggest that there is rear contractility in neural crest cell groups *in vivo*.

To identify whether individual neural crest cells flowed through clusters, as predicted from *in silico* and *ex vivo* results, we tracked live cells during migration *in vivo*. In both *Xenopus* and zebrafish, cells that were initially at the rear of the group indeed intercalated forward during migration (Fig. 4.32, A to D). Similar to the *ex vivo* and *in silico* data, subtracting cluster movement to *in vivo* cell tracks reveals an intra-cluster flow in which rear cells intercalate inward, move forward and move backwards around the edges (Fig. 4.32, E and F). This suggests that rear contractility might be driving neural crest migration *in vivo*.

To test whether rear contractility is required for neural crest migration *in vivo*, we grafted neural crest expressing optoGEF-contract or optoGEF-relax into wild-type host *Xenopus* embryos. Activation of contractility at the front of the stream or inhibition at the rear impaired neural crest migration (Fig. 4.33, A to F, and movies 5 and 6), indicating that greater contractility at the rear than the front was necessary for migration in the embryo. Neural crest grafted into host embryos lacking SDF1, through the use an SDF1 morpholino, failed to migrate but activation of contractility at the rear of such grafts rescued migration, demonstrating that high actomyosin contractility at the rear can drive directed collective migration *in vivo* (Fig. 4.33, G and I, and movie 7).

The conclusion of these data is that rear contractility, as produced by a supracellular actomyosin cable, can drive collective cell chemotaxis *in vivo* (Fig. 4.34A). High Rho/ROCK levels at the cluster rear promotes myosin II phosphorylation (Fig. 4.34B) which results in high actomyosin cable contractility. Surpracellular contractility at the cluster rear causes cells to intercalate inward, which generates an anterograde flow of cells that makes the whole cluster move forward (Fig. 4.34A). Cells at the edge are mechanically coupled, and contractility pulls these cells rearward to replenish cells lost at the back (Fig. 4.34A). This system works thanks to the front/rear anisotropy in contractility that results from SDF1/CXCR4-induced inhibition of contractility in rear cells via activation of Rac1 and inhibition of Rho/ROCK/Myosin II.

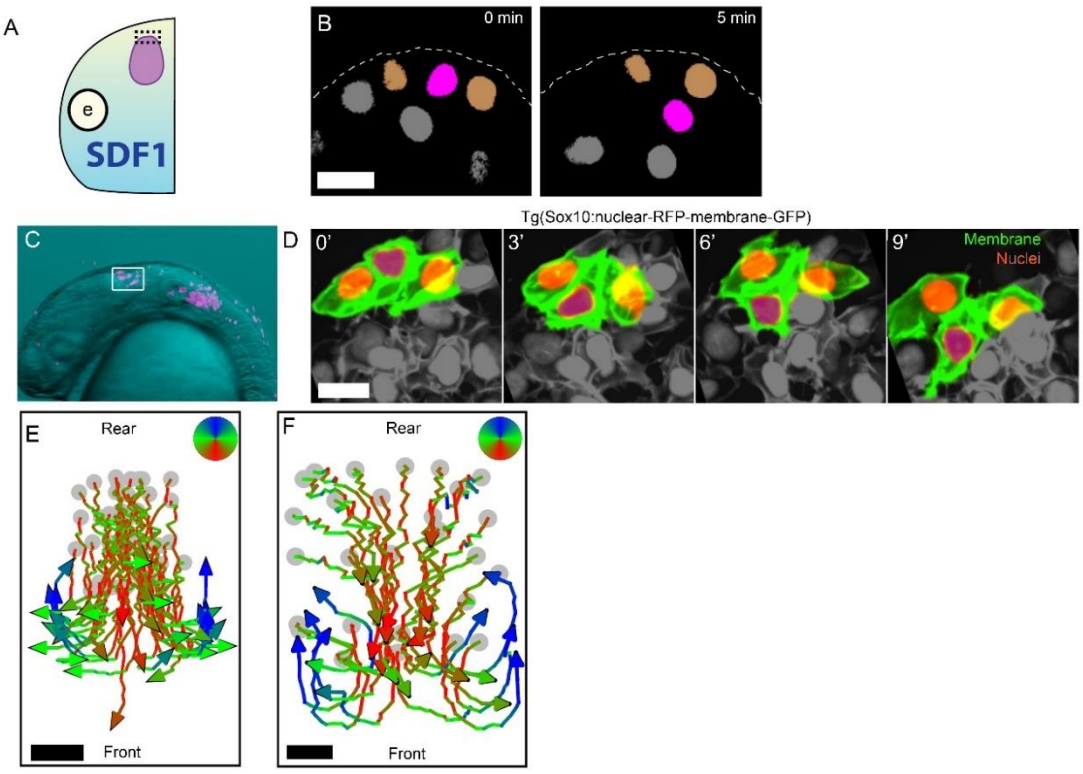

Fig. 4.32. Neural crest clusters have rear intercalation and flow of cells in *Xenopus* and zebrafish embryos. (**A**) Diagram of a *Xenopus* embryo used for imaging in B. (**B**) Intercalation of a rear cell (purple) between two adjacent cells (orange) in *in vivo* in *Xenopus*. Scale bar, 20 μm. (**C**) Picture of a zebrafish embryo Tg(Sox10:nuclearRFP-membraneGFP) with fluorescent neural crest cells. The white box indicates the cephalic neural crest. (**D**) Intercalation of a rear cell (purple) between two adjacent cells (orange) in *in vivo*. Scale bar, 20 μm. (**E**) Tracks of rear neural crest cells *in vivo* in Xenopus after subtracting the cluster movement. Scale bar, 30 μm. Grey dots: initial cell positions. Shows representative example from 5 embryos, *N* = 3 experiments. (**F**) Tracks of rear neural crest cells *in vivo* after subtracting the migration of the stream. Scale bar, 20 μm; grey disks: initial cell positions. Shows representative example from 5 embryos, *N* = 3 experiments.

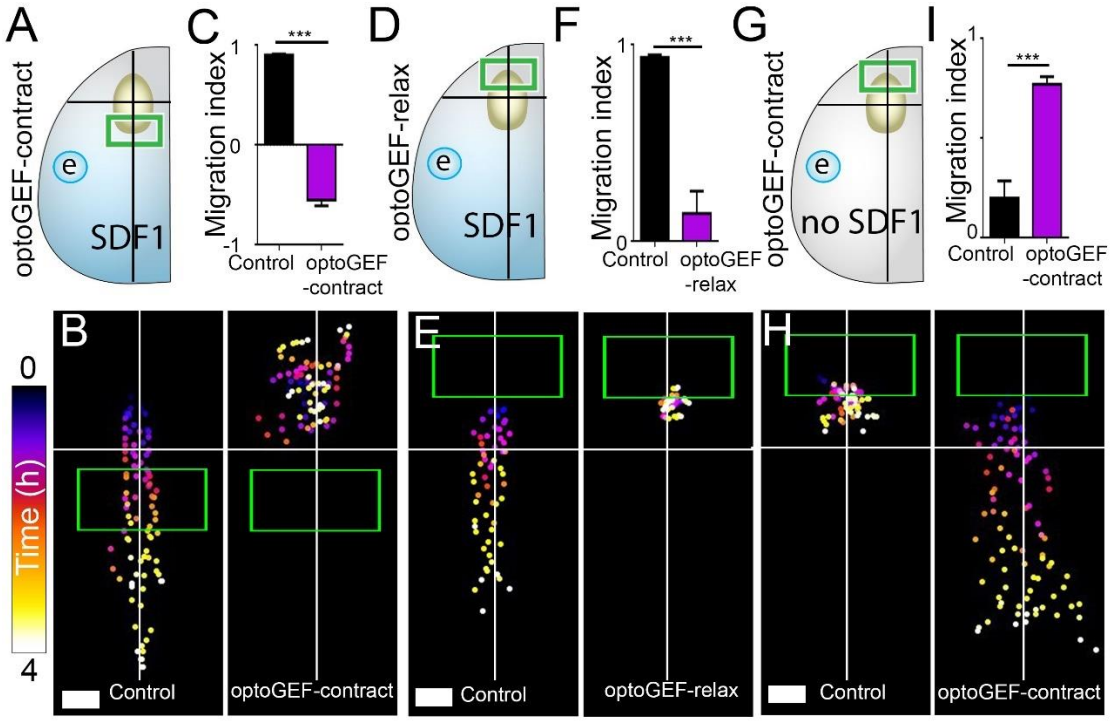

Fig. 4.33. Rear contractility is necessary and sufficient for *in vivo* collective neural crest cell chemotaxis. (**A to I**) Experimental design of treated *Xenopus* embryos (A, D and G), representative tracks of neural crest clusters (B, E and H) and migration index (means ± SEM) (C, F and I). Green box: initial illumination area; cross: starting position of the explant. *n* = 10 clusters (10 grafts, each in a different embryo), *N* = 3 embryos. ***$P \leq 0.001$ (two-tailed Student's *t*-test). Scale bar, 50 μm.

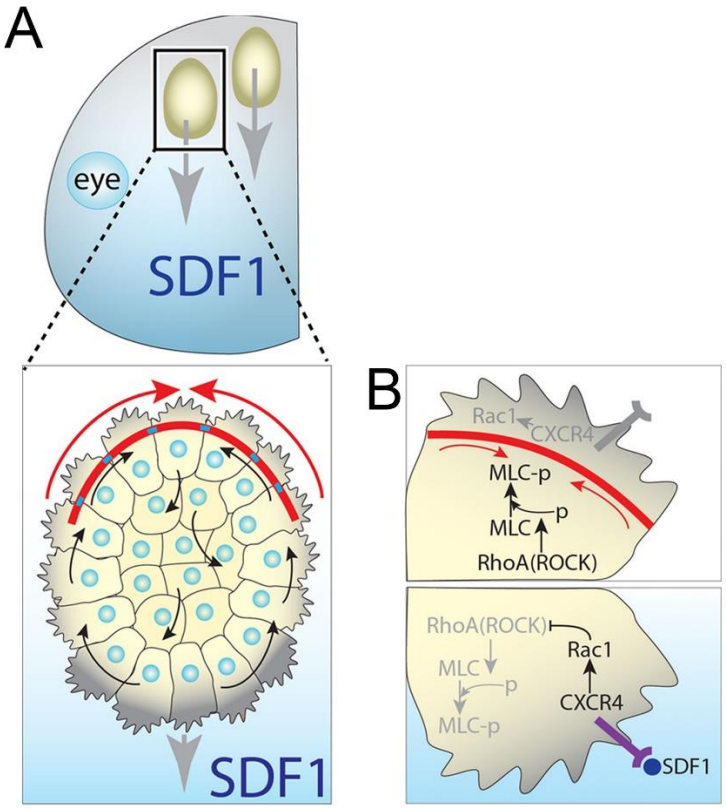

Fig. 4.34. The model. (**A**) Collective cell chemotaxis is driven by actomyosin contractility at the rear (red arrows) from an actomyosin cable (red band) which is connected to adjacent peripheral cells by N-Cadherin (blue squares). Rear contractility drives cells to reduce their cell width and intercalate into the cell group, which generates a flow of cells that move forward from the rear and then backwards around the sides (black arrows). This results in movement of the whole cell group forward (grey arrows). Anisotropic contractility is established by SDF1 inhibition of contractility in front cells. *In vivo*, rear contractility likely works with many other well described mechanisms, including contact inhibition of locomotion, co-attraction, confinement, focal adhesions and protrusions (grey edges). (**B**) In rear cells (top), high activity of Rho/ROCK causes high contractility via phosphorylation of myosin II. Front cells (bottom) are exposed to higher levels of SDF1, which binds to the receptor CXCR4 and activates Rac. Rac inhibits Rho/ROCK which reduces levels of active myosin.

Discussion

5.1 Rear-driven cellular motility

Diverse forms of life have always needed the ability to move. As is being increasing well-recognised, many modes of migration have evolved to address this, including cortical contractility-based adhesion-independent motility to adhesive crawling along surfaces. As previously discussed (Section 1.2), the best characterised mode of migration is based on polarised cells that have dynamic actin-based protrusions and focal adhesions that generate traction to pull the cell forward, with actomyosin contracting the cytoskeletal network to retract the cell rear (Ridley et al., 2003). More recently, however, alternative modes of cell motility have been characterised, such as those in which classical integrin-mediated adhesion is not required (Paluch et al., 2016). Although various examples of adhesion-independent migration are known (Bergert et al., 2015, Renkawitz and Sixt, 2010, Lammermann et al., 2008), their mechanistic basis is mostly unclear. Furthermore, neutrophils and *Dictyostelium* amoeba, classic modes of crawling cells, can also propel themselves by 'swimming' when suspended in liquid (Barry and Bretscher, 2010), and cells can migrate using friction on non-adhesive substrates to generate the forces required for migration (Bergert et al., 2015, Paluch et al., 2016). Ameboid migration tends to be controlled by active RhoA at the cell rear, which is sufficient to drive directional cellular motility in different contexts, such as on 2D surface, in liquid, and under confinement, and a common result of this is rearward membrane flow (Fig. 5.1, left) (O'Neill et al., 2018, Tanaka et al., 2017, Paluch et al., 2016). Experimental evidence for 'swimming' validates predictions made by physicists that cells can move by using tangential retrograde movement of their surfaces, which is more energetically efficient than other modes of migration because it minimises momentum transfer to the surrounding liquid, resulting in reduced viscous dissipation (Leshansky et al., 2007). Furthermore, the cell uses its endocytic machinery to traffic membrane forward from the rear, thereby not expending energy in synthesising new components. This suggests that the amoeboid migratory mode is highly efficient (Liu et al., 2015). In particular 'swimming' is reminiscent of Edward Purcell's toroidal swimmer model (Purcell, 1977) and subsequent models from Mark Bretscher based on surface treadmilling, in which retrograde membrane flow and anterograde vesicular trafficking drives cell migration (Bretscher, 1984, Bretscher, 1996, Bretscher, 2014).

This ameboid mode of individual cell migration is a process that has never been previously reported for collectives, though it has many similarities to the contractility-

driven model for collective chemotaxis described here (Fig. 5.1A). RhoA is highly active in rear cells of the neural crest cell cluster, and its activity results in rearward movement of the cells themselves (including their membrane, of course); an equivalent surface retrograde flow to ameboid cells. The anterograde vesicular trafficking that is part of ameboid migration in single cells to supply membrane to the front is analogous to the intercalation and anterograde movement of cells from the rear to the front. Furthermore, RhoA-stimulated actomyosin contractility at the rear generates the retrograde plasma membrane flow through the coupling of the plasma membrane to the flow of the actin cortex. This retrograde cortical actin flow, which is widely observed in amoeboid migration (Liu et al., 2015, Maiuri et al., 2015), could be considered equivalent to the actin cable, which mechanically couples cells at the edge of the cluster and pulls them rearward through its contractility. Indeed, faster actin flow in ameboid cells and higher intercalation in neural crest clusters both correlate with faster migration speeds (Maiuri et al., 2015) (Fig. 4.25A). Of course, this analogy is a false equivalency because the neural crest are known to generate integrin-dependent adhesion on the underlying fibronectin (Alfandari et al., 2003). Perhaps a better analogy is that the neural crest behaves as a single entity (a 'supracell') and reproduces the features of single cell crawling migration but across a larger scale (Fig. 5.1B). In this context, the retrograde flow of outer cells is akin to actin retrograde flow. The coupling of this rearward movement to myosin motor proteins in both cases is able to generate the forces for forward movement. In this manner, the supracellular cable acts almost like a long-scale molecular clutch that couples rearward flow and generates propulsive forces. In single cells, actin retrograde flow is coupled to cell-matrix adhesions to generate forces. In the collective neural crest, how the actin cable interacts with the substrate and across the tissue-scale is unclear. In the computational model, no mechanics were added, but such traction forces could be somewhat easily introduced, given our experimental knowledge that outer cells produce most of the traction forces (Scarpa et al., 2015). Introducing these forces, as well as the tensile forces underlying cell-cell adhesions (which are as of yet, unknown), would be beneficial to moving to a model that incorporates various mechanical aspects of collective chemotaxis together.

Interestingly, this is the first time it has been shown that cells at a group's rear are actively contributing to collective movement. This is, in part, due to frequent use of models where the rear cannot be studied, such as wound healing epithelial sheets which do not have a rear. One example of collective cell migration in which rear mechanical forces are known to be important is in ductal morphogenesis. Unlike most

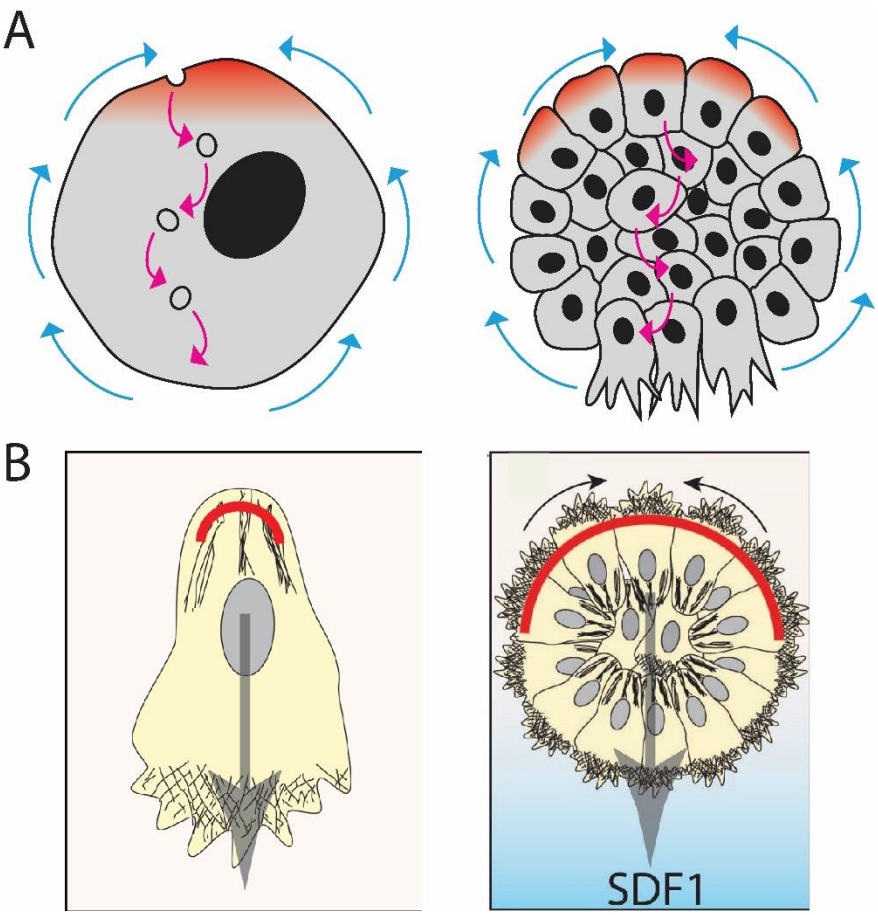

Figure 5.1. Rear-driven modes of solitary and collective cell migration. (A) Left, a single ameboid cell. Right, a neural crest cell cluster. High levels of RhoA (red) at the rear of the single cell or cell group (through the actomyosin cable) causes rear contraction. In single cells, this leads to rearward membrane flow (blue arrows). Forward movement is facilitated by anterograde trafficking of cell membrane (pink arrows). In clusters, contraction of the cable mechanically pulls edge cells around to the rear (blue arrows). Forward movement is facilitated by contractility-induced cell intercalation, which generates an anterograde flow of cells through the middle (pink arrows). (**B**) Left, single cell lamellipodial migration classically relies on rear actomyosin-driven forces. Rear contractility can initiate and even be sufficient for single cell motility in some cases. Right, collective neural crest cell chemotaxis also relies on rear actomyosin forces. Contractility is shared amongst whole of the cluster rear (i.e. amongst many rear cells) via an actomyosin cable whose contractility is necessary and sufficient for migration of the cluster.

other examples of collective movement, cells at the front of the migrating group do not extend protrusions or cellular extensions. Instead, myoepithelial cells form a stalk-like structure to seemingly push the whole structure forward, in the absence of apparent force generating-adhesion complexes (Ewald et al., 2008). Whether the internal flow forward of cells in neural crest is purely a supracellular pushing force, or also active through protrusive forces triggered by CIL remains unclear.

5.2 Supracellular migration

The equivalent behaviours between ameboid 'swimmers' and neural crest collectives, and the fact that this flow is reproduced *in silico* solely from having a contractile rear, suggests that the whole neural crest cluster behaves as 'supracell', an idea that has been suggested from some recent theoretical research (Friedl and Gilmour, 2009, Vedula et al., 2013). In fact, for more than a century, it has been proposed that groups of cells may behave as a supracellular unit, whereby the cell group could be considered as a giant 'supracell' (Ruth, 1911, Uhlenhuth, 1914, Vaughan and Trinkaus, 1966). This differs enormously from the collective migration of some epithelial cell groups, such as the *Drosophila* follicular epithelium, in which individual cells all behave identically and individual behaviour within the group is only minimally modified as a result of the formation of cell-cell contacts, which primarily act as anchor points. The supracellular behaviour that the neural crest display is evident through the necessity of each cell's contribution to the group's behaviour. Through CIL, a cluster is generated whose peripheral cells have larger, more stable protrusions and stronger forces than internal cells, whose protrusions are inhibited (Scarpa et al., 2015, Carmona-Fontaine et al., 2008b). A balance of CIL and short-range C3a-dependent chemotaxis (co-attraction) keeps the group held together but weakly enough that the outer cell-inner cell differential is achieved (Carmona-Fontaine et al., 2011), and the dynamic turnover of N-Cadherin, because the cells are mesenchymal, allows cells to act cohesively and exchange places (Kuriyama et al., 2014). A rear actomyosin cable that is formed in a supracellular manner, across multiple cells, and contracting many cells synchronously generates the cell flow that orients and drives long-range directed migration. The group's activity can therefore be considered highly 'supracellular' in that it behaves at a scale greater than that of the individual cell; simply 'sticking together' individual neural crest cells while maintaining their individual cell behaviour would not be sufficient to achieve the organisation and behaviour of the group for collective chemotaxis.

Whether the neural crest can be considered truly supracellular, however, is unclear, and there seems to be a spectrum of supracellularity that collectively migrating cells can exist upon (Fig. 5.2). 'True' supracellularity has been demonstrated in the collective movement arising from the *Drosophila* ventral furrow. Myosin-dependent apical constriction drives invagination of this epithelial sheet, which occurs even in acellular embryos (He et al., 2014), indicating that the entire tissue is behaving as if the individual cell components are irrelevant. Whether collective neural crest cell chemotaxis can occur through total loss of all internal cell junctions is an intriguing question that could be addressed with the laser ablation approach described in this thesis. Although CIL would be lost in such an experiment, the contractility model described here only requires for an anisotropic contractility to generate directed migration. Perhaps this enormous syncytium would behave like the ameboid that 'swim' – with retrograde membrane flow and anterograde trafficking of membrane components, in a manner similar to how the cellular neural crest behave.

5.3 The potential role of mechanical input into this model

The importance of mechanical signals to direct cell behaviour, including migration, is becoming well recognised (Roca-Cusachs et al., 2013, Lammermann and Sixt, 2009). The *ex vivo* assays used here plate neural crest on fibronectin-coated plastic or glass dishes, which are infinitely stiffer than the *in vivo* stiffness of ~120 Pa mesoderm upon which the neural crest migrate in *Xenopus* embryos *in vivo* (Barriga et al., 2018). *Ex vivo*, neural crest cells at the cluster's periphery have large, stable focal adhesions (relative to the internal cells). These focal adhesions, however, are proposed to be absent from ameboid migration (Liu et al., 2015) because integrin expression inhibits ameboid behaviour (Carragher et al., 2006). Focal adhesions and the cell cortex is thought to compete to recruit the actomyosin contractile machinery, leading to either contractile stress fibres, where cell-matrix adhesion is high, or a contractile/flowing cortex, where cell-matrix adhesion is low. In doing so, cells can adapt to their microenvironment and use different methods to move (Fig. 5.3). For this reason, the similarities between the single cell ameboid 'swimmer' migration model and the contractility-driven collective migration model described here are somewhat surprising. Swimmers are thought to behave in frictionless environments, yet it seems that the actomyosin cable can still exert a force to generate the 'swimmer'-type flow of cells in spite of its relatively strong adhesion to the substrate. Perhaps this emphasises the strength of the contractile cable and hints that the neural crest is possibly more ameboid-like than previously thought. Interestingly, the inner neural

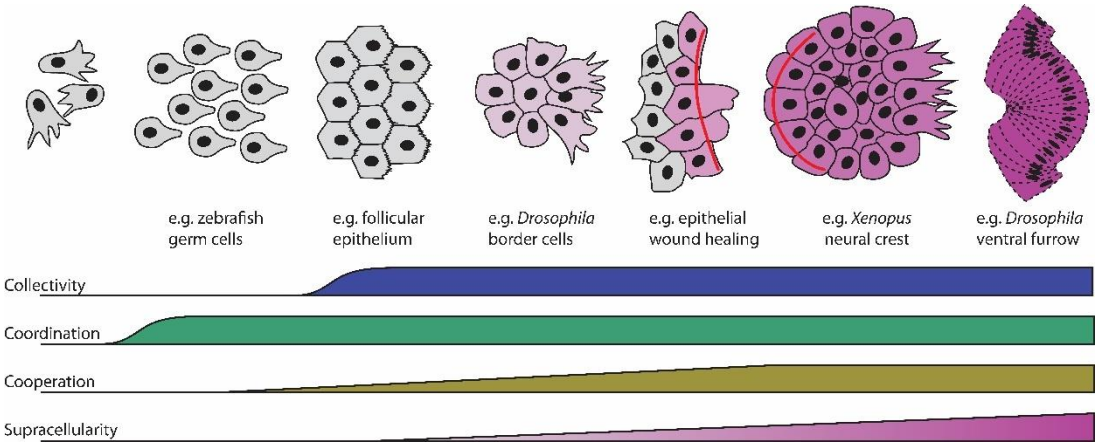

Figure 5.2. Supracellularity in collective cell migration. Examples of different modes of migration and movement by different cell types and in different morphogenetic events. Note how some types of movement display no supracellularity at all, such as collective migration of the *Drosophila* follicular epithelium, whose cells behave primarily as individuals despite having cell-cell junctions. By contrast, neural crest cells have a rear actomyosin cable whose supracellular contractions drive forward movement of the cluster through cell intercalation; and morphogenesis of the *Drosophila* ventral furrow can be explained through apical myosin contractility, which reproduces invagination even in acellularized embryos.

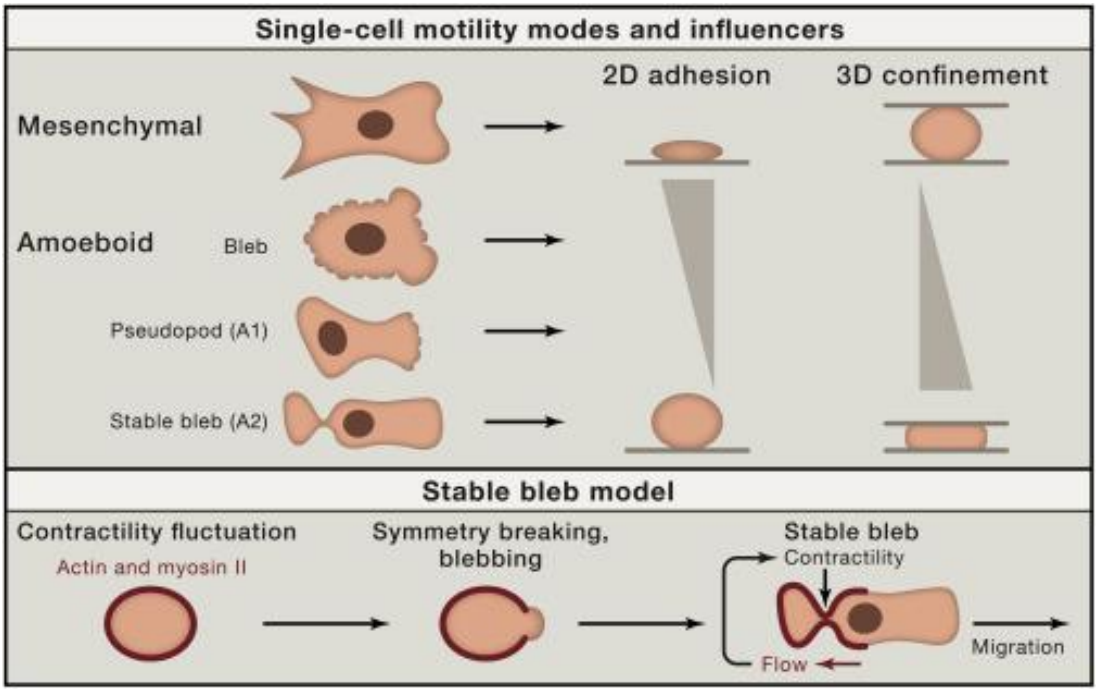

Fig. 5.3 Motility modes, influencing parameters and the initiation and maintenance of stable bleb motility. Motility modes include mesenchymal motility, or various forms of amoeboid motility characterized by blebs, pseudopods, or stable blebs. These are influenced by environmental factors, including the strength of adhesion to the substrate, or the extent of physical confinement and contractility. The formation of a stable bleb is theorized to involve fluctuations in cortical contractility, followed by symmetry breaking and the formation of a bleb. Cortical flow of actin and myosin II toward the cell rear then enhances contractility in this location, stabilizing the formation of a single bleb at the front and generating force that drives migration.

Adapted from (Welch, 2015).

crest cells tend to be more rounded, and have very small and transient focal adhesions, which is reminiscent of ameboid morphology.

In vivo, where ECM stiffness is comparatively low, neural crest cells at the edge of the stream might display more amoeboid-like behaviour *in vivo* and use internal contractile forces rather than stress fibres to move. This could explain why the effects of the optogenetic experiments were even more striking *in vivo* (Fig. 31) than *ex vivo* (Fig. 17). Indeed, integrin-mediated adhesions are not required for *in vivo* confined migration (Lammermann et al., 2008), and the neural crest migrates under confinement, which promotes its collective movement (Szabo et al., 2016). Whether the neural crest utilises the contraction mode of collective migration even more efficiently when integrin-mediated adhesion is reduced could be studied by plating neural crest explants on soft gels that reproduce *in vivo* mesodermal stiffness, as has been described previously (Barriga et al., 2018).

Despite the speculations made above, neural crest are known to produce protrusions *in vivo* (Carmona-Fontaine et al., 2008b), and collective migration is triggered by mesodermal stiffening *in vivo*, which is sensed by a complex composed of integrin, vinculin and talin (Barriga et al., 2018). This suggests that normal neural crest migration uses a combination of mechanisms, including rear actomyosin contraction, in addition to previously described mechanisms such as confinement (Szabo et al., 2016), CIL (Scarpa et al., 2015, Roycroft et al., 2018, Carmona-Fontaine et al., 2008b), protrusions (Theveneau et al., 2010), co-attraction (Carmona-Fontaine et al., 2011) and mechanical signals from the mesoderm (Barriga et al., 2018).

Interestingly, the mode of collective cell chemotaxis differs from collective cell durotaxis, which also involves long range force transmission but is based on differential substrate deformations at the cluster front and rear (Sunyer et al., 2016). Collective durotaxis occurs due to the ability of cells to deform the substrate more in the part of lower stiffness than in the stiffer part (Escribano et al., 2018). Both cases use anisotropic forces to generate directional movement, and suggests that the principals of cell movement *in vitro* could scale up to multicellular platforms. Collective durotaxis relies on cell-substrate adhesions forming, and the group is pulled in the direction of strongest force. This is an extension adhesion-based single cell motility, where the driving force is provided by cell-matrix. Although not tested in this thesis, the idea proposed here that contractility-driven migration could be more important in situations where there is less cell-matrix adhesions (and so the cluster is using its own contractile machinery) would be the equivalent of adhesion-free single cell

migration. Although these two collective mechanisms are tested separately, efficient *in vivo* migration is likely to be dictated by a combination of physical and chemical cues. For example, matrix elasticity regulates mesenchymal stem cell chemotaxis, meaning single cell chemotaxis speed it sum of a stiffness-dependent component and a chemokine concentration-dependent component (Saxena et al., 2018).

5.4 Implications for other models of collective migration

5.4.1 Border cells

Another highly tractable model system for collective chemotaxis are border cells, which are the gametes of the *Drosophila* embryo that migrate within the egg chamber in response to chemotactic gradients. Myosin II is highly expressed during border cell migration (Edwards and Kiehart, 1996) and, like the neural crest, actomyosin accumulates at the edge of the cell group, which is essential for normal chemotaxis (Combedazou et al., 2017, Lucas et al., 2013), suggesting that the contractility-driven collective chemotaxis mechanism described here may be applicable in other collective chemotaxis systems.

Border cells migrate in two phases. First, they undergo collective chemotaxis posteriorly toward PDGF/VEGF. They then migrate dorsally toward sources of EGF (Poukkula et al., 2011), which is required for their late phase migration (Duchek et al., 2001). The behaviour of the cluster is different in these two phases. Chemotaxis to PDGF/VEGF occurs in a more linear manner, in which one cell leads the others with external-facing protrusions, whereas the rotational (dorsal) phase of border cell chemotaxis to EGF is more disorganised; cells are more mobile and they exchange positions (Cliffe et al., 2017). Perhaps the two phases of border cell chemotaxis may represent two different styles/modes of collective migration. During the linear phase, cells behave in a more epithelial, and less supracellular manner. Unlike EGF, PVR activation, enhances Rac (Wang et al., 2010b, Prasad and Montell, 2007, Bianco et al., 2007), which in turn supresses myosin (Bianco et al., 2007, Fernandez-Espartero et al., 2013), meaning protrusions are more important for the group's migration, and cells tend to stick to the same positions in the cluster. This is redolent of epithelial-like behaviour. Indeed, border cells mutant for *spaghetti squash*, which encodes non-muscle myosin II light chain, form long, abnormal protrusions that phenocopies overexpression of actin (Fulga and Rorth, 2002), and myosin II is known to refine cellular protrusions (Majumder et al., 2012).

By contrast, chemotaxis during the rotational phase dorsally towards EGF is more mesenchymal-like, and the cluster behaves in a more supracellular manner. The

peripheral localisation of actomyosin is enhanced by EGF during the second phase of migration (Combedazou et al., 2017) and myosin II activity controls the linear-to-rotational switch (Combedazou et al., 2017), suggesting that a strong peripheral actomyosin localisation may be important in mesenchymal-like collective behaviour. This is alike to neural crest cells, which also have reduced peripheral actomyosin when they express more E-Cadherin or are pre-migratory (Fig. 4.5), having not yet gone through EMT. Moreover, suppression of myosin in border cell clusters causes them to migrate in a linear fashion regardless of their position in the egg chamber, and with reduced rotational speeds. Myosin activation is therefore necessary and might be sufficient to induce rotational border cell migration, and regulation of myosin is essential for linear-to-rotational switch as locking myosin in one state leads to a uniform mode of migration (linear when myosin is low, rotational when it's high). The rotational phase of collective border cell chemotaxis therefore seems comparable to collective neural crest cell chemotaxis. Despite the border cells being epithelial, perhaps the enhancement of actomyosin around the edge of the cluster, like in the neural crest, is important for them becoming more interchangeable.

The fact that PVR, unlike EGFR, inhibits myosin, implies that peripheral actomyosin organisation is more important for the rotational phase of migration than for the linear phase. However, the fact that linear migration efficiency is also affected when myosin is inhibited suggests that restricted activation of myosin is required for linear migration (Combedazou et al., 2017). The linear to rotational switch could thus be linked to a change in myosin activity from the single cell to the cluster level, which is reminiscent of a change in behaviour from individualistic to supracellular. Indeed, localised myosin signalling could be required during the initial polarised migration, whereas collective myosin regulation would dominate the later phase for more efficient migration through nurse cells (Majumder et al., 2012). The rotation of border cells remains quite a mysterious process, and little is known about the activation of myosin, but these changes could come about as a result of border cells meeting a different organisation of nurse cells, which would impact their morphology. Indeed, border cell-substrate adhesion activates a positive feedback loop of Rac and actin assembly to stabilise forward-directed protrusions and persistent migration (Cai et al., 2014).

Interestingly, at least one of the roles of peripheral actomyosin in border cells is to resist compression by nurse cells (Aranjuez et al., 2016). In doing so, they retain a round and cohesive cluster shape. Whether additional functions can be attributed to peripheral actomyosin remains an area for exploration.

5.4.2 Epithelial and cancer cells

Epithelial cells migrate collectively toward free surfaces created by a wound or the release of a physical barrier (Wood et al., 2002). MDCK fingers, studied as a model system of collective epithelial migration, behave as mechanical global entities, in which a giant leader cell drags the whole structure forward, and a peripheral actomyosin contractile cable mechanically inhibits the initiation of new leader cells (Reffay et al., 2014). Collective invasion by epithelial cancer cell lines also relies on peripheral actomyosin force being transmitted around the outside of the group to enable coordinated cell movement (Hidalgo-Carcedo et al., 2011). In this context, a reduction in actomyosin activity at cell-cell contacts through E-Cadherin/DDR1/Par3/Par6 is necessary for RhoA and pMLC inhibition and a subsequent reduction in tension on cell junctions (Hidalgo-Carcedo et al., 2011). For collective migration of these cancer cells, efficient transmission of force around the outside of the cell group prevents clusters from dissociating and avoids single cell motility. These examples of collective epithelial migration in 2D and 3D environments highlights the importance of pluricellular actomyosin contractile structures for cluster cohesion (Hidalgo-Carcedo et al., 2011, Omelchenko and Hall, 2012, Gaggioli et al., 2007). Moreover, it underlies the fact that a peripheral actomyosin cable can function in different ways for different systems. Although not tested, the role of peripheral actomyosin in driving collective cell migration for neural crest could occur in cancer cells alongside its known role in promoting cohesive behaviour. In some ways, the model described here is an extension of this idea; the neural crest's actomyosin ring promotes cohesiveness of the cluster at the supracellular level.

Interestingly, large clusters of colorectal cancer epithelial cells displaying a robust outward apical pole, termed tumour spheres with inverted polarity (TSIPs), use actomyosin contractility to collectively invade 3D extracellular matrices (Zajac et al., 2018). They do this in a seemingly adhesion-independent manner, as inhibition of FAK, Rac1 or integrins does not affect TSIP invasion. Therefore, at the apical pole of TSIPs, the contractility of the actomyosin cortex, and not the cell-ECM proteins, has a prevalent role in collective migration. These results indicate that TSIPs collectively invade tissues by, rather than involving formation of adhesion-based protrusions, as some most other collectively migrating systems do (Wang et al., 2010b, Hegerfeldt et al., 2002), relying on the high contractility of the apical peripheral actomyosin cortex resulting (Zajac et al., 2018). Mechanistically, contractility is regulated by non-canonical TGF-β signalling (Zajac et al., 2018), although not in a chemotactic manner.

This is highly reminiscent of propulsive amoeboid single-cell migration (Callan-Jones and Voituriez, 2016), and bares similarities to neural crest collectives.

The many above examples of collective migration, and the relationships shown between tension, actin superstructures and Rho activation are yet further examples of the transposition of concepts that have been validated on single cells to the multicellular scale (Vaezi et al., 2002), and suggests that other cell types may migrate under similar principles to the contractility-driven collective migration model described here.

5.5 Cell flows

The flow of cells during contractility-driven collective neural crest chemotaxis is essential to the mechanism of this model. It is not completely clear whether the flows observed in neural crest are active or passive. The actomyosin cable around the cluster periphery mechanically connects cell neighbours. Supracellular contraction therefore actively drives these cells from the front edge to the back edge. Likewise, intercalation is driven by contractility. However, the involvement of CIL forces in generating the forward flow of cells is unknown.

Cell flows seem to be a common feature of non-epithelial cell movements, as well as morphogenetic processes that require a mass of tissues. Cell flows have been described in other morphogenic processes, such as primitive streak formation (Rozbicki et al., 2015, Cui et al., 2005), morphological asymmetries in mammalian hair follicles (Cetera et al., 2018), and convergent extension (Simoes et al., 2014, Bertet et al., 2004). For example, placode epithelial cells engage in a counter-rotational pattern of cell flows that converts radially-symmetric epithelial clusters to planar polarised hair buds with anterior-directed growth (Fig. 5.4A) (Cetera et al., 2018). This flow pattern is identical to that of neural crest collectives during chemotaxis (Fig 5.4B) in both *Xenopus* and zebrafish. Moreover, neural crest movement shares features of other collective cell migration events such as cell intercalation during convergent extension (Guillot and Lecuit, 2013, Zallen and Blankenship, 2008) and ommatidia rotation in the *Drosophila* eye (Mlodzik, 1999), processes that depend on PCP, myosin II, Rho and ROCK (Keller, 2002, Tada and Heisenberg, 2012, Shindo, 2018, Zheng et al., 1995, Theisen et al., 1994, Wolff and Rubin, 1998, Winter et al., 2001, Fiehler and Wolff, 2007). Likewise, neural crest intercalation and cell flow is Rho and myosin II-dependent, and PCP contributes to CIL for directional migration. Cell intercalation allows cells to rearrange their positions, such as in the mouse visceral endoderm (Trichas et al., 2012), in the *Xenopus*

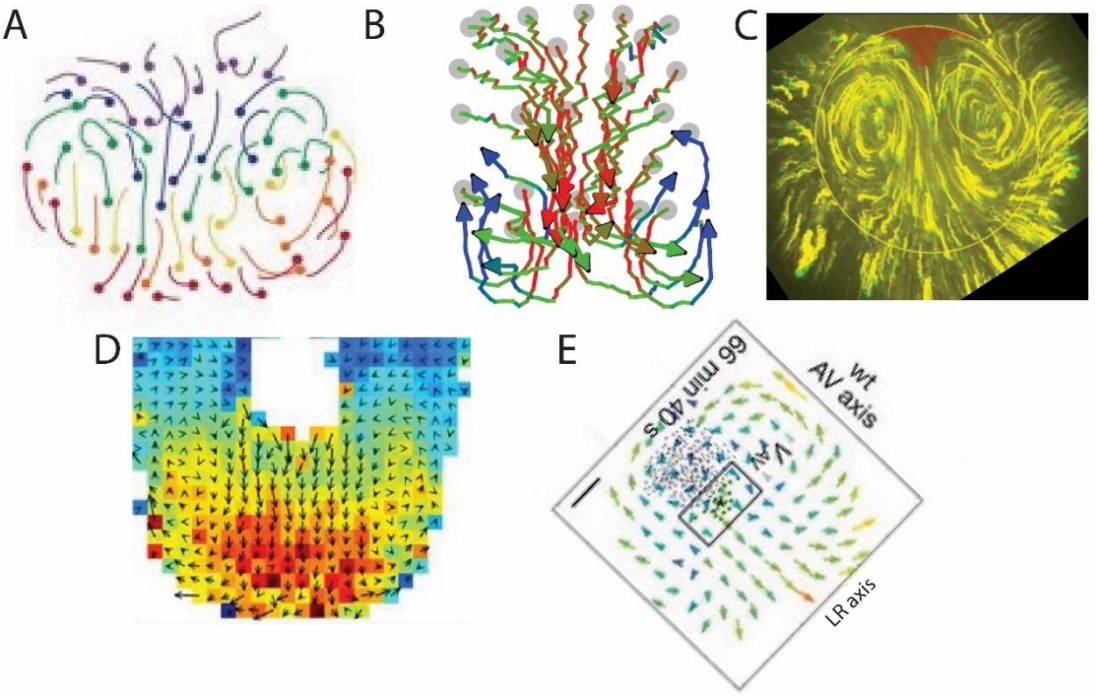

Fig. 5.4. Cells flows during collective movements. (A) Overall cell trajectories during placode polarisation. Cells at the centre of the placode move anteriorly, cells in the posterior converge towards the midline (blue and purple) and anterior cells move away from the midline and then posteriorly (red). Anterior is the bottom. **(B)** Neural crest cell tracks of rear cells in zebrafish embryos during collective cell migration. Front is the bottom. Grey disks indicate initial cell position. **(C)** Cell traces (GFP) of randomly scattered cells in the epiblast. Trajectories show the distance that the cells migrate over a 5 h. The trajectories are colour coded the distance migrated over the last hour of the experiment is shown in green and the colour coding thus indicates the direction of migration. The outline of the streak is shown in red. (**D**) Vector displacement map average of cell motion in the paraxial mesoderm of zebrafish embryos. Warm colours are higher speeds and arrows are averaged 3D velocity vectors (projected onto 2D). (**E**) Neuroectoderm cell movements in zebrafish embryos over the prechordal plate. Note how there is reoriented directed movement.

Adapted from (Cetera et al., 2018, Chuai and Weijer, 2008, Lawton et al., 2013, Smutny et al., 2017).

(Davidson and Keller, 1999) and chick neural tube (Nishimura et al., 2012), and in the *Drosophila* germ band (Bertet et al., 2004, Blankenship et al., 2006). Cell intercalation enables cell movement by changing the position for cell junctions in the tissue. Cell junctions are removed, bringing cells together, before new junctions are formed. Likewise, the massive junctional remodelling during neural crest migration is evident in their weak and dynamic cadherin-based contacts and high levels of cell-cell positional exchange. Moreover, asymmetric contractility is important not only for neural crest migration; likewise, directional contraction along cell boundaries driving cell intercalation has been shown previously in the primitive streak. Similar biased actin bundle contractions also drive Drosophila cell re-arrangements (Simoes et al., 2014, Cavey and Lecuit, 2009).

In several systems, cells locally produce the energy used to remodel contacts by forming planar-polarised actomyosin cables connecting two or more vertices together. This process is both active and to a certain degree collective, as it involves many cells that are connected by supracellular contractile cables. Junction shrinkage requires polarised phosphorylation of MLC, enrichment of myosin filaments, and polarised tension. The anisotropic contractility and cell movements bare similarity to collectively migrating neural crest, which likewise use polarised contractility and intercalation for complex cell re-arrangements.

Neural crest movements also resemble the ‘polonaise’ movements in avian embryos that occur during formation of the primitive streak, where epiblast cells undergo large-scale tissue flows organised in two counter-rotating streams (Fig. 5.4C) (Rozbicki et al., 2015, Voiculescu et al., 2007). However, whether the neural crest movements could also occur in such a large number of cells is not known. Interestingly, apical contraction and intercalation during primitive streak cell flows are myosin II dependent (Rozbicki et al., 2015), similar to the neural crest. In the case of hair follicles, PCP asymmetry may dictate the orientation of cell intercalations by localising myosin activity to induce junctional shrinkage (Nishimura et al., 2012, Shindo and Wallingford, 2014), which would initiate directional cell flow. Junction loss and assembly can cause rotation of neighbouring cell borders (Aigouy et al., 2010, Aw et al., 2016), just like in the more mesenchymal neural crest.

The tailbud in growing vertebrate embryos consists of motile progenitors for the musculoskeletal system. Cells of the posterior tail bud move rapidly, whereas there is less motion further back in the pre-somitic mesoderm. Although most of the cells from the dorsal medial zone, there are clear swirls of cells moving from the medial to

lateral progenitor zone (Fig. 5.4D) (Lawton et al., 2013). Interestingly, these morphogenetic flows are driven by persistent mediolateral supracellular stresses (Mongera et al., 2018). Thus, supracellular forces can guide collective movements in other systems. In this context, supracellular stresses generate these flows via restriction of lateral tissue expansion and posterior elongation (Mongera et al., 2018).A similar swirling pattern is observed in the tailbud of avian embryos, although in these cases it seems the flow pattern emerges from random collective cell motility (Benazeraf et al., 2010, Zamir et al., 2006). A similar flow pattern is observed in the collective movements of neurectoderm relative to the movement of the underlying prechordal plate cells. Most of the neuroectoderm cells undergo epiboly movements directed towards the vegetal pole, but cells located directly above and anterior to the leading edge of the prechordal plate slowed down their vegetal-directed movement and reoriented their direction of motion from vegetal to animal, resulting in high animal-directed movement alignment with the adjacent prechordal plate progenitors (Smutny et al., 2017). This local reorientation of neurectoderm cell movements close to the leading edged of the prechordal plate is accompanied by the formation of large-scale counter-rotating vortex-like cell flows within the neuroectoderm (Fig. 5.4E) (Smutny et al., 2017). In this context, cell flows are driven by friction forces between two collectively migrating cell populations moving in opposite directions in an E-Cadherin mediated manner (Smutny et al., 2017).

5.6 Molecular mechanism and gradient sensing

The proposed mechanism for establishing the front-rear anisotropy in contractility is based on differential exposure to SDF1. SDF1/CXCR4 signalling in front cells inhibits ROCK/Rho/Myosin II, whereas these downstream effectors are active in rear cells, meaning actomyosin contractility is high. This fits the data that shows, in the absence of SDF1, contractility is high in all edge cells irrespective of position, implying that the ‘default’ for edge cells is that they behave like the rear, and exposure to a chemoattractant like SDF1 generates a leading edge. Interestingly, PDGF-A, another known chemoattractant of the neural crest (Roycroft et al., 2018), has an identical effect on actomyosin contractility, suggesting this may be a common mechanism for collective cell chemotaxis.

Interestingly, the neural crest responds only to a chemoattractive gradient, and not to absolute values. Also, there seems to be a gradient of contractility from front to rear, rather discrete levels. To fit with the proposed mechanism, there would need to be at least two components. Firstly, there needs to be some form of intercellular

communication between cells of the cluster such that one side knows which is the front and the other knows to behave like the rear. In MDCK wound healing sheets, a propagating wave of ERK activation orients collective cell migration (Aoki et al., 2017). For neural crest, this may be some signalling pathway that act through gap junctions, which are well recognised as a means for intercellular communication, and indeed the gap junction component Cx43 is expressed specifically in the neural crest (Xu et al., 2006). The messaging would have to relay the relative levels of active (bound) CXCR4. Secondly, a factor would need to integrate into the signalling pathway to block the activity of SDF1/CXCR4 in the region where it is low (compared to other edge cells). These factors could potentially be the same molecule, although this regulation seems highly complex and likely involves many components.

An understanding of how single cells operate can only provide a partial understanding of the functions at a higher level of organisation (the collective). For example, mesoscale phenomena such as cell jamming, or collective gradient sensing cannot be explained by knowledge of the single cell or molecular scale (Good and Trepat). In the case of collective gradient sensing, the reconstitution of each individual element will not necessarily explain why groups move directionally but individual elements do not. Molecularly, long-range regulation of calcium, which regulates myosin activity, is a prime candidate for further investigation. Gap junctions, which permit intercellular ion flow including of calcium, have long been believed to be necessary for long-range communication in collective sensing although no clear evidence yet exists. Alternatively there may be a similar ERK wave propagation signal to that described above, which would communicate the region of SDF1 activation to prevent inhibition of contractility in the cells receiving the signal.

5.7 Pulsed contractions

The actomyosin cable of the neural crest display pulsatile contractions. This was first assessed by measuring the amplitude of contraction (by measuring cable length), laser ablation (to show the cable is under tension/contractile) and the frequency of contractions. Because we found no difference in the amplitude of contraction at the front and rear of the cluster independent of SDF1, we used frequency of contraction as a read-out of cable contractility for most experiments, such as the functional tests involving the optogenetic tools. However, pulsing frequencies are not necessarily a read-out of contractility. Ideally, laser ablations would be used as it is a more direct measurement of tension. This was avoided for technical reasons, but future experiments could test the recoil post-ablation at the front and rear of neural crest

clusters during chemotaxis, and the effect of the optogenetic tools on actomyosin recoil. Increasing contractility, for example, by using optoGEF-contract should increase the tension and lead to faster recoil. Importantly, actomyosin cable recoil post-ablation should be performed *in vivo* to more definitively show that it is under tension at the read of migratory cell groups.

The neural crest is not the first model system to show pulsed actomyosin contractions; actomyosin pulses is important for various morphogenic processes (Coravos et al., 2017). Examples include amnioserosa apical constriction at *Drosophila* dorsal closure (David et al., 2010), apical constriction of epithelial cells of the ventral furrow (Martin et al., 2009), salivary gland (Booth et al., 2014) and renal tubules (Saxena et al., 2014), during extension of the *Drosophila* germband (Rauzi et al., 2010) and in the follicular epithelium surrounding and shaping the developing oocytes (He et al., 2010). In all these examples, pulsatile contractions result from minifilaments dynamically assembling and contracting as a cytoskeletal network. Actomyosin pulses correspond with accumulation and dissipation of F-actin and can show oscillatory behaviour or act stochastically. Unlike this, the pulsed contraction in neural crest comes from a supracellular actin cable, rather than through a dynamically behaving actomyosin meshwork. However, in both cases, the tensile actomyosin cytoskeleton transmit force to cellular neighbours (Gardel et al., 2008, Roh-Johnson et al., 2012, Thievessen et al., 2013).

Mechanistically, pulsatile activity of ROCK, active RhoA, RhoGEF and RhoGAP have been observed in *Drosophila* epithelia (Mason et al., 2016, Vasquez et al., 2014, Munjal et al., 2015), suggesting that there is dynamic regulation of RhoA GTPase. In the ventral furrow, RhoGEF seems to initiate contraction pulses by increasing actomyosin assembly rate. To determine whether the actomyosin acts in a similar way, the levels of actin at the cable could be measured over time, and analysed as to whether it oscillates or not. Also, to elucidate the mechanism, the dynamics and activity of RhoA should be analysed. This could be achieved by using RhoA FRET, or, to visualise active RhoA, a construct in which the RhoA-binding domain of rhotekin (rGBD) is bound to GFP. These experiments would help determine whether the the mechanism is more akin to other previously describe actin cables, in which contractility is relatively constant but it structurally similar to the cable of neural crest, or more like the above describe actomyosin filament assemblies, which are more dynamic but contract in pulses (Röper, 2013). Interestingly, the contraction in neural crest is SDF1-independent, suggesting that actomyosin pulsing is a self-organised process. It has been previously proposed that this pulses could be initiated by low

level actomyosin activity driving flow of F-actin, myosin, and associated proteins (e.g. ROCK) and disassembly of pulses occurring through delayed negative-feedback (e.g. a myosin phosphatase) (Munjal et al., 2015).

Interestingly, at a transcriptional level, Snail initiates the actomyosin network contractions and Twist expression stabilises the constricted state of cells between pulsed contractions (Martin et al., 2009). The neural crest also express Snail and Twist during EMT, delamination and migration (Theveneau and Mayor, 2012b), and so may perform a similar role to regulate supracellular actomyosin contractility. Photo-activatable morpholinos to suppress their translation would be a good tool to use to investigate this, because Twist and Snail are required for neural crest development at stages earlier than migration, and thus normal morpholinos would not be appropriate; myosin contractility could be analysed in this respect.

5.8 *Ex vivo*/*in vivo* and *Xenopus*/zebrafish comparison

The results presented in this thesis are consistent between two different model organisms and between *in vivo* and *ex vivo*. But how does this data fit in with previous knowledge of cranial collective neural crest migration and what limitations should be considered? Firstly, the *ex vivo* experiments lacked confinement, which could have been introduced experimentally using tunnels. Confinement *in vivo* promotes collective migration (Szabo et al., 2016). The actomyosin cable is observed *in vivo*, suggesting that confinement does not affect the presence or contractility of the cable, but future would should examine this closer *ex vivo*. Also, the size of clusters used to analyse migration *ex vivo* is smaller than *in vivo* migration. The former uses <100 cells but the neural crest migrate *in vivo* in their 100s. Two important implications of this are: first, can a 'pushing' mechanism work over such a large distance; and second, at what stage of *in vivo* migration does the actomyosin contribute? In both models, the *in vivo* cell tracks were derived from the host tissue, not from grafts, suggesting that such large-scale movements do occur. However, contractility most likely contributes as one of several players toward *in vivo* chemotaxis, including traction generated by focal adhesions (Scarpa et al., 2015, Barriga et al., 2018), cell protrusions by leaders responding to SDF1 (Theveneau et al., 2010), and confinement (Szabo et al., 2016). Rear supracellular contraction is likely to be a complementary pushing force from the rear, to the pulling forces of leader cells at the front. This might be more achievable when the stream is less elongated, and therefore it is likely to play a more prominent role in early migration rather than late migration.

It is important to note, however, that although all the zebrafish data is consistent with that of *Xenopus*, no functional tests (i.e. optogenetics, laser ablation) were performed in zebrafish, so we cannot conclude that the function of the cable is the same. In zebrafish, it could have other roles, such as maintaining the group as a single entity, or providing mechanical support that prevents compression from the surrounding tissues. Using the optoGEF-RhoA optogenetic tools in zebrafish *in vivo* would help resolve this question.

In zebrafish (as well as chick), through careful analysis of cell movements *in vivo*, it has been previously shown that cranial neural crest does not require leader cells for migration (Richardson et al., 2016). The data from this thesis support this idea, because in our model leader cells are not permanent but instead are recycled as part of the supracellular rearrangements. The data from this previously published paper show continuous interchanging of cell positions. Although no mention of stereotypical or repeated cell movements is made (e.g. polonaise movements), our tracking to show this used the same transgenic zebrafish, and relied on specific tracking of rear cells, meaning the data is not necessarily contradictory, and can be compatible. The movements observed rely entirely on which cells are chosen to track, and knowing the dimensions of the migratory population, including cluster front and rear. Interestingly, it was shown that trunk neural crest movement works by a different process: leader and follower identities are specified before migration and remain fixed, so ablation of leader trunk cells impairs collective movement (Richardson et al., 2016). This further supports the idea that behaviour of the neural crest is highly subpopulation- and species-specific, so it is important to restrict our conclusions to the cranial *Xenopus*, and to a lesser degree, cranial zebrafish, cell populations.

The balance between CIL (to generate supracellular polarisation) and co-attraction (to maintain the cluster together) allows the cluster to move, but in this thesis we describe a mechanism to permit long-range highly directional migration (by chemotaxis). How does this fit together? Because CIL arises from cell-cell contacts, it will be important to determine how strong a role the increased N-Cadherin observed between adjacent peripheral cells contributes to CIL. Read-outs of CIL could be analysed through the assembly of mosaic clusters, either by reconstituting dissociated cells together, or by expression of DNA rather than mRNA. Similar experiments could be performed with manipulation of CIL (e.g. altered non-canonical Wnt/PCP signalling) to affect CIL in some edge cells and not others and analyse the actomyosin cable and its contractility. Likewise, it is important to know how CIL is involved in the flow of cell movement; for example, are the ‘pushing forces’ at the rear

solely driving the anterograde cell flow, or is each cells pushing on the its neighbour, thereby generating an increased cell-cell signalling and a wave of CIL that emanates forward from the rear, meaning each cell is contributing forces to moving forward. Analysis of cell protrusion orientation and cryptic protrusions would be useful in disguising between these options.

Concluding remarks

In conclusion, the results presented in this thesis demonstrate a novel mechanism for collective cell chemotaxis that can be explained by the activity of a peripheral actomyosin cable at the rear of the cell group. Supracellular contractility from this actomyosin cable causes rear edge cells to intercalate inward, which generates an anterograde cell flow that pushes the whole cluster forward. The mechanically coupled edge cells undergo retrograde movement to the rear to maintain cluster organisation. This mechanism works in collective cell chemotaxis because SDF1 inhibits front neural crest cell contractility, thereby establishing an anisotropy in front/rear contractility. The mechanism bares similarities to single cell motility. For example, individual mesenchymal motility can be driven by rear actomyosin activity, and ameboid cells can 'swim' in frictionless environments using high rear contractility which drives retrograde membrane flow and anterograde vesicular flow. Thus, the neural crest cell group can be considered as a 'supracell' in which in which coordinated contractility amongst multiple rear cells is responsible for the group's movement. Overall, this is the first demonstration that rear cells are actively involved in the migration of the group.

Moreover, these data suggest that, mechanistically, SDF1 inhibits front contractions through activation of CXCR4/Rac which inhibits ROCK/Rho/Myosin II, whereas myosin remains active in rear cells. The effect of a different chemoattractant, PDGF, also inhibits front contractility, indicating the downstream effectors regulating contractility could be activated by several pathways, which suggests contractility-driven migration could be a common and important general mechanism of collective cell chemotaxis. Indeed, most *in vivo* collective cell migration occurs by chemotaxis, and peripheral cluster contractility has been shown in various models of collective motility. These data also show that the neural crest cell group responds to a gradient, rather than absolute levels of chemoattractant, which suggests cell-cell communication and further supracellular activity is important for collective neural crest migration.

Perspectives

These results lead to many new and interesting questions. What role does N-Cadherin, the adhesion protein that couples the actomyosin cable between adjacent cells, play in mechanotransduction and force transmission between cells? Presumably, it plays a role in the supracellular nature of the contractility. What

chemical signals are involved in this? Gap junctions and calcium signalling, which permit rapid cell-cell communication and activation of myosin, respectively, are prime candidates to address this. How also does supracellular communication work to allow the cell group to read a gradient and how is it incorporated into the signalling pathway?

Publications

SHELLARD, A. & MAYOR, R. 2016. Chemotaxis during neural crest migration. *Seminars in Cell & Developmental Biology*, 55, 111-118

BARRIGA, E.*, **SHELLARD, A.*** & MAYOR, R. 2018. In vivo and in vitro analysis of neural crest cell migration. *Methods in Molecular Biology*. In press.

SHELLARD, A., SZABÓ, A., TREPAT, X. & MAYOR, R. 2018. Supracellular contraction at the rear of neural crest cell groups drives collective chemotaxis. *Science*, 362, 339-+.

Note: Most work presented in this thesis is from the above (Shellard et al., Supracellular contraction at the rear of neural crest cell groups drives collective chemotaxis. 2018. Science, 362, 339-+). Reprinted with permission from AAAS.

SHELLARD, A. & MAYOR, R. 2018. Supracellular motility: beyond collective cell migration. *Journal of Cell Science*. Under review.

* Joint first authors

References

ABERCROMBIE, M. 1970. CONTACT INHIBITION IN TISSUE CULTURE. *In Vitro-Journal of the Tissue Culture Association,* 6**,** 128-+.

ABERCROMBIE, M. & AMBROSE, E. J. 1958. INTERFERENCE MICROSCOPE STUDIES OF CELL CONTACTS IN TISSUE CULTURE. *Experimental Cell Research,* 15**,** 332-345.

ABERCROMBIE, M. & DUNN, G. A. 1975. ADHESIONS OF FIBROBLASTS TO SUBSTRATUM DURING CONTACT INHIBITION OBSERVED BY INTERFERENCE REFLECTION MICROSCOPY. *Experimental Cell Research,* 92**,** 57-62.

ABERCROMBIE, M. & HEAYSMAN, J. E. M. 1953. OBSERVATIONS ON THE SOCIAL BEHAVIOUR OF CELLS IN TISSUE CULTURE .1. SPEED OF MOVEMENT OF CHICK HEART FIBROBLASTS IN RELATION TO THEIR MUTUAL CONTACTS. *Experimental Cell Research,* 5**,** 111-131.

ABU-ISSA, R., SMYTH, G., SMOAK, I., YAMAMURA, K. & MEYERS, E. N. 2002. Fgf8 is required for pharyngeal arch and cardiovascular development in the mouse. *Development,* 129**,** 4613-4625.

ADAMS, R. H., DIELLA, F., HENNIG, S., HELMBACHER, F., DEUTSCH, U. & KLEIN, R. 2001. The cytoplasmic domain of the ligand ephrinB2 is required for vascular morphogenesis but not cranial neural crest migration. *Cell,* 104**,** 57-69.

AFFOLTER, M., BELLUSCI, S., ITOH, N., SHILO, B., THIERY, J. P. & WERB, Z. 2003. Tube or not tube: Remodeling epithelial tissues by branching morphogenesis. *Developmental Cell,* 4**,** 11-18.

AFFOLTER, M. & CAUSSINUS, E. 2008. Tracheal branching morphogenesis in Drosophila: new insights into cell behaviour and organ architecture. *Development,* 135**,** 2055-2064.

AGARWAL, P. & ZAIDEL-BAR, R. 2018. Principles of Actomyosin Regulation In Vivo. *Trends in Cell Biology*.

AIGOUY, B., FARHADIFAR, R., STAPLE, D. B., SAGNER, A., ROPER, J. C., JULICHER, F. & EATON, S. 2010. Cell Flow Reorients the Axis of Planar Polarity in the Wing Epithelium of Drosophila. *Cell,* 142**,** 773-786.

AIUTI, A., WEBB, I. J., BLEUL, C., SPRINGER, T. & GUTIERREZRAMOS, J. C. 1997. The chemokine SDF-1 is a chemoattractant for human CD34(+) hematopoietic progenitor cells and provides a new mechanism to explain the mobilization of CD34(+) progenitors to peripheral blood. *Journal of Experimental Medicine,* 185**,** 111-120.

ALEXANDER, S., KOEHL, G. E., HIRSCHBERG, M., GEISSLER, E. K. & FRIEDL, P. 2008. Dynamic imaging of cancer growth and invasion: a modified skin-fold chamber model. *Histochemistry and Cell Biology,* 130**,** 1147-1154.

ALEXANDROVA, A. Y., ARNOLD, K., SCHAUB, S., VASILIEV, J. M., MEISTER, J. J., BERSHADSKY, A. D. & VERKHOVSKY, A. B. 2008. Comparative Dynamics of Retrograde Actin Flow and Focal Adhesions: Formation of Nascent Adhesions Triggers Transition from Fast to Slow Flow. *Plos One,* 3.

ALFANDARI, D., COUSIN, H., GAULTIER, A., HOFFSTROM, B. G. & DESIMONE, D. W. 2003. Integrin alpha 5 beta 1 supports the migration of Xenopus cranial neural crest on fibronectin. *Developmental Biology,* 260**,** 449-464.

ALFANDARI, D., COUSIN, H., GAULTIER, A., SMITH, K., WHITE, J. M., DARRIBERE, T. & DESIMONE, D. W. 2001. Xenopus ADAM 13 is a metalloprotease required for cranial neural crest-cell migration. *Current Biology,* 11**,** 918-930.

ALFANDARI, D., WOLFSBERG, T. G., WHITE, J. M. & DESIMONE, D. W. 1997. ADAM 13: A novel ADAM expressed in somitic mesoderm and neural crest cells during Xenopus laevis development. *Developmental Biology,* 182**,** 314-330.

AMAN, A. & PIOTROWSKI, T. 2008. Wnt/beta-Catenin and Fgf Signaling Control Collective Cell Migration by Restricting Chemokine Receptor Expression. *Developmental Cell,* 15**,** 749-761.

AMAN, A. & PIOTROWSKI, T. 2010. Cell migration during morphogenesis. *Developmental Biology,* 341**,** 20-33.

ANANTHAKRISHNAN, R. & EHRLICHER, A. 2007. The forces behind cell movement. *International Journal of Biological Sciences,* 3**,** 303-317.

ANDERSON-BERRY, A., O'BRIEN, E. A., BLEYL, S. B., LAWSON, A., GUNDERSEN, N., RYSSMAN, D., SWEELEY, J., DAHL, M. J., DRAKE, C. J., SCHOENWOLF, G. C. & ALBERTINE, K. H. 2005. Vasculogenesis drives pulmonary vascular growth in the developing chick embryo. *Developmental Dynamics,* 233**,** 145-153.

ANGELA NIETO, M. 2013. Epithelial Plasticity: A Common Theme in Embryonic and Cancer Cells. *Science,* 342**,** 708-+.

AOKI, K., KONDO, Y., NAOKI, H., HIRATSUKA, T., ITOH, R. E. & MATSUDA, M. 2017. Propagating Wave of ERK Activation Orients Collective Cell Migration. *Developmental Cell,* 43**,** 305-+.

ARANJUEZ, G., BURTSCHER, A., SAWANT, K., MAJUMDER, P. & MCDONALD, J. A. 2016. Dynamic myosin activation promotes collective morphology and migration by locally balancing oppositional forces from surrounding tissue. *Molecular Biology of the Cell,* 27**,** 1898-1910.

ARATA, M., SUGIMURA, K. & UEMURA, T. 2017. Difference in Dachsous Levels between Migrating Cells Coordinates the Direction of Collective Cell Migration. *Developmental Cell,* 42**,** 479-+.

ASTIN, J. W., BATSON, J., KADIR, S., CHARLET, J., PERSAD, R. A., GILLATT, D., OXLEY, J. D. & NOBES, C. D. 2010. Competition amongst Eph receptors regulates contact inhibition of locomotion and invasiveness in prostate cancer cells. *Nature Cell Biology,* 12**,** 1194-U175.

AVRAHAM, H. K., LEE, T. H., KOH, Y. H., KIM, T. A., JIANG, S. X., SUSSMAN, M., SAMAREL, A. M. & AVRAHAM, S. 2003. Vascular endothelial growth factor regulates focal adhesion assembly in human brain microvascular endothelial cells through activation of the focal adhesion kinase and related adhesion focal tyrosine kinase. *Journal of Biological Chemistry,* 278**,** 36661-36668.

AW, W. Y., HECK, B. W., JOYCE, B. & DEVENPORT, D. 2016. Transient Tissue-Scale Deformation Coordinates Alignment of Planar Cell Polarity Junctions in the Mammalian Skin. *Current Biology,* 26**,** 2090-2100.

AYBAR, M. J., NIETO, M. A. & MAYOR, R. 2003. Snail precedes Slug in the genetic cascade required for the specification and migration of the Xenopus neural crest. *Development,* 130**,** 483-494.

BAHM, I., BARRIGA, E. H., FROLOV, A., THEVENEAU, E., FRANKEL, P. & MAYOR, R. 2017. PDGF controls contact inhibition of locomotion by regulating N-cadherin during neural crest migration. *Development,* 144**,** 2456-2468.
BAKER, M. D., WOLANIN, P. M. & STOCK, J. B. 2006. Signal transduction in bacterial chemotaxis. *Bioessays,* 28**,** 9-22.
BALZER, E. M., TONG, Z. Q., PAUL, C. D., HUNG, W. C., STROKA, K. M., BOGGS, A. E., MARTIN, S. S. & KONSTANTOPOULOS, K. 2012. Physical confinement alters tumor cell adhesion and migration phenotypes. *Faseb Journal,* 26**,** 4045-4056.
BARLAN, K., CETERA, M. & HORNE-BADOVINAC, S. 2017. Fat2 and Lar Define a Basally Localized Planar Signaling System Controlling Collective Cell Migration. *Developmental Cell,* 40**,** 467-477.
BARRIGA, E. H., FRANZE, K., CHARRAS, G. & MAYOR, R. 2018. Tissue stiffening coordinates morphogenesis by triggering collective cell migration in vivo. *Nature,* 554**,** 523-+.
BARRIGA, E. H., MAXWELL, P. H., REYES, A. E. & MAYOR, R. 2013. The hypoxia factor Hif-1 alpha controls neural crest chemotaxis and epithelial to mesenchymal transition. *Journal of Cell Biology,* 201**,** 759-776.
BARRIGA, E. H., TRAINOR, P. A., BRONNER, M. & MAYOR, R. 2015. Animal models for studying neural crest development: is the mouse different? *Development,* 142**,** 1555-1560.
BARRY, N. P. & BRETSCHER, M. S. 2010. Dictyostelium amoebae and neutrophils can swim. *Proceedings of the National Academy of Sciences of the United States of America,* 107**,** 11376-11380.
BARTHEL, S. R., GAVINO, J. D., DESCHENY, L. & DIMITROFF, C. J. 2007. Targeting selectins and selectin ligands in inflammation and cancer. *Expert Opinion on Therapeutic Targets,* 11**,** 1473-1491.
BASCH, M., GARCIA-CASTRO, M. & BRONNER-FRASER, M. 2004. Molecular mechanisms of neural crest induction. *Birth Defects Research Part C Today,* 72**,** 109-123.
BATSON, J., MACCARTHY-MORROGH, L., ARCHER, A., TANTON, H. & NOBES, C. D. 2014. EphA receptors regulate prostate cancer cell dissemination through Vav2-RhoA mediated cell-cell repulsion. *Biology Open,* 3**,** 453-462.
BAZELLIERES, E., CONTE, V., ELOSEGUI-ARTOLA, A., SERRA-PICAMAL, X., BINTANEL-MORCILLO, M., ROCA-CUSACHS, P., MUNOZ, J. J., SALES-PARDO, M., GUIMERA, R. & TREPAT, X. 2015. Control of cell-cell forces and collective cell dynamics by the intercellular adhesome. *Nature Cell Biology,* 17**,** 409-+.
BECKER, M. D., KRUSE, F. E., JOUSSEN, A. M., ROHRSCHNEIDER, K., NOBILING, R., GEBHARD, M. M. & VOLCKER, H. E. 1998. In vivo fluorescence microscopy of corneal neovascularization. *Graefes Archive for Clinical and Experimental Ophthalmology,* 236**,** 390-398.
BECKER, S. F. S., MAYOR, R. & KASHEF, J. 2013. Cadherin-11 Mediates Contact Inhibition of Locomotion during Xenopus Neural Crest Cell Migration. *Plos One,* 8.
BELL, C. D. & WAIZBARD, E. 1986. VARIABILITY OF CELL-SIZE IN PRIMARY AND METASTATIC HUMAN-BREAST CARCINOMA. *Invasion & Metastasis,* 6**,** 11-20.
BELMADANI, A., JUNG, H., REN, D. & MILLER, R. J. 2009. The chemokine SDF-1/CXCL12 regulates the migration of melanocyte progenitors in mouse hair follicles. *Differentiation,* 77**,** 395-411.
BELMADANI, A., TRAN, P. B., REN, D. J., ASSIMACOPOULOS, S., GROVE, E. A. & MILLER, R. J. 2005. The chemokine stromal cell-derived factor-1 regulates the migration of sensory neuron progenitors. *Journal of Neuroscience,* 25**,** 3995-4003.
BELVINDRAH, R., HANKEL, S., WALKER, J., PATTON, B. L. & MULLER, U. 2007. beta 1 integrins control the formation of cell chains in the adult rostral migratory stream. *Journal of Neuroscience,* 27**,** 2704-2717.
BENAZERAF, B., FRANCOIS, P., BAKER, R. E., DENANS, N., LITTLE, C. D. & POURQUIE, O. 2010. A random cell motility gradient downstream of FGF controls elongation of an amniote embryo. *Nature,* 466**,** 248-252.
BENINGO, K. A., DEMBO, M., KAVERINA, I., SMALL, J. V. & WANG, Y. L. 2001. Nascent focal adhesions are responsible for the generation of strong propulsive forces in migrating fibroblasts. *Journal of Cell Biology,* 153**,** 881-887.
BERGERT, M., CHANDRADOSS, S. D., DESAI, R. A. & PALUCH, E. 2012. Cell mechanics control rapid transitions between blebs and lamellipodia during migration. *Proceedings of the National Academy of Sciences of the United States of America,* 109**,** 14434-14439.
BERGERT, M., ERZBERGER, A., DESAI, R. A., ASPALTER, I. M., OATES, A. C., CHARRAS, G., SALBREUX, G. & PALUCH, E. K. 2015. Force transmission during adhesion-independent migration. *Nature Cell Biology,* 17**,** 524-+.
BERNDT, J. D., CLAY, M. R., LANGENBERG, T. & HALLORAN, M. C. 2008. Rho-kinase and myosin II affect dynamic neural crest cell behaviors during epithelial to mesenchymal transition in vivo. *Developmental Biology,* 324**,** 236-244.
BERTET, C., SULAK, L. & LECUIT, T. 2004. Myosin-dependent junction remodelling controls planar cell intercalation and axis elongation. *Nature,* 429**,** 667-671.
BHOWMICK, N. A., NEILSON, E. G. & MOSES, H. L. 2004. Stromal fibroblasts in cancer initiation and progression. *Nature,* 432**,** 332-337.
BIANCO, A., POUKKULA, M., CLIFFE, A., MATHIEU, J., LUQUE, C. M., FULGA, T. A. & RORTH, P. 2007. Two distinct modes of guidance signalling during collective migration of border cells. *Nature,* 448**,** 362-U12.
BILOZUR, M. E. & HAY, E. D. 1988. NEURAL CREST MIGRATION IN 3D EXTRACELLULAR-MATRIX UTILIZES LAMININ, FIBRONECTIN, OR COLLAGEN. *Developmental Biology,* 125**,** 19-33.
BIN-NUN, N., LICHTIG, H., MALYAROVA, A., LEVY, M., ELIAS, S. & FRANK, D. 2014. PTK7 modulates Wnt signaling activity via LRP6. *Development,* 141**,** 410-421.
BJERKE, M. A., DZAMBA, B. J., WANG, C. & DESIMONE, D. W. 2014. FAK is required for tension-dependent organization of collective cell movements in Xenopus mesendoderm. *Developmental Biology,* 394**,** 340-356.
BLANCHOIN, L., BOUJEMAA-PATERSKI, R., SYKES, C. & PLASTINO, J. 2014. ACTIN DYNAMICS, ARCHITECTURE, AND MECHANICS IN CELL MOTILITY. *Physiological Reviews,* 94**,** 235-263.
BLANKENSHIP, J. T., BACKOVIC, S. T., SANNY, J. S. P., WEITZ, O. & ZALLEN, J. A. 2006. Multicellular rosette formation links planar cell polarity to tissue morphogenesis. *Developmental Cell,* 11**,** 459-470.

BLEUL, C. C., FUHLBRIGGE, R. C., CASASNOVAS, J. M., AIUTI, A. & SPRINGER, T. A. 1996. A highly efficacious lymphocyte chemoattractant, stromal cell-derived factor 1 (SDF-1). *Journal of Experimental Medicine,* 184**,** 1101-1109.

BOETTIGER, D. 2012. Mechanical control of integrin-mediated adhesion and signaling. *Current Opinion in Cell Biology,* 24**,** 592-599.

BOGUSLAVSKY, S., GROSHEVA, I., LANDAU, E., SHTUTMAN, M., COHEN, M., ARNOLD, K., FEINSTEIN, E., GEIGER, B. & BERSHADSKY, A. 2007. p120 catenin regulates lamellipodial dynamics and cell adhesion in cooperation with cortactin. *Proceedings of the National Academy of Sciences of the United States of America,* 104**,** 10882-10887.

BOKEL, C. & BROWN, N. H. 2002. Integrins in development: Moving on, responding to, and sticking to the extracellular matrix. *Developmental Cell,* 3**,** 311-321.

BOLDAJIPOUR, B., MAHABALESHWAR, H., KARDASH, E., REICHMAN-FRIED, M., BLASER, H., MININA, S., WILSON, D., XU, Q. & RAZ, E. 2008. Control of chemokine-guided cell migration by ligand sequestration. *Cell,* 132**,** 463-473.

BOLOS, V., PEINADO, H., PEREZ-MORENO, M. A., FRAGA, M. F., ESTELLER, M. & CANO, A. 2003. The transcription factor Slug represses E-cadherin expression and induces epithelial to mesenchymal transitions: a comparison with Snail and E47 repressors. *Journal of Cell Science,* 116**,** 499-511.

BOOTH, A. J. R., BLANCHARD, G. B., ADAMS, R. J. & ROPER, K. 2014. A Dynamic Microtubule Cytoskeleton Directs Medial Actomyosin Function during Tube Formation. *Developmental Cell,* 29**,** 562-576.

BORCHERS, A., DAVID, R. & WEDLICH, D. 2001. Xenopus cadherin-11 restrains cranial neural crest migration and influences neural crest specification. *Development,* 128**,** 3049-3060.

BORCHERS, A., EPPERLEIN, H. H. & WEDLICH, D. 2000. An assay system to study migratory behavior of cranial neural crest cells in Xenopus. *Development Genes and Evolution,* 210**,** 217-222.

BORGHI, N., LOWNDES, M., MARUTHAMUTHU, V., GARDEL, M. L. & NELSON, W. J. 2010. Regulation of cell motile behavior by crosstalk between cadherin- and integrin-mediated adhesions. *Proceedings of the National Academy of Sciences of the United States of America,* 107**,** 13324-13329.

BRACHVOGEL, B., PAUSCH, F., FARLIE, P., GAIPL, U., ETICH, J., ZHOU, Z. G., CAMERONE, T., VON DER MARK, K., BATEMAN, J. F. & POSCHL, E. 2007. Isolated Anxa5(+)/Sca-1(+) perivascular cells from mouse meningeal vasculature retain their perivascular phenotype in vitro and in vivo. *Experimental Cell Research,* 313**,** 2730-2743.

BRAHMBHATT, A. A. & KLEMKE, R. L. 2003. ERK and RhoA differentially regulate pseudopodia growth and retraction during chemotaxis. *Journal of Biological Chemistry,* 278**,** 13016-13025.

BRAUN, M., WUNDERLIN, M., SPIETH, K., KNOCHEL, W., GIERSCHIK, P. & MOEPPS, B. 2002. Xenopus laevis stromal cell-derived factor 1: Conservation of structure and function during vertebrate development. *Journal of Immunology,* 168**,** 2340-2347.

BRETSCHER, M. S. 1984. ENDOCYTOSIS - RELATION TO CAPPING AND CELL LOCOMOTION. *Science,* 224**,** 681-686.

BRETSCHER, M. S. 1996. Getting membrane flow and the cytoskeleton to cooperate in moving cells. *Cell,* 87**,** 601-606.

BRETSCHER, M. S. 2014. Asymmetry of Single Cells and Where That Leads. *Annual Review of Biochemistry, Vol 83,* 83**,** 275-289.

BRON, R., EICKHOLT, B. J., VERMEREN, M., FRAGALE, N. & COHEN, J. 2004. Functional knockdown of neuropilin-1 in the developing chick nervous system by siRNA hairpins phenocopies genetic ablation in the mouse. *Developmental Dynamics,* 230**,** 299-308.

BRONNER-FRASER, M. 1986. Analysis of the early stages of trunk neural crest migration in avian embryos using monoclonal-antibody HNK-1. *Developmental Biology,* 115**,** 44-55.

BRONNER-FRASER, M. 2005. Gene-regulatory interactions in neural crest evolution and development. *Developmental Biology,* 283**,** 590-591.

BRONNERFRASER, M. 1994. NEURAL CREST CELL-FORMATION AND MIGRATION IN THE DEVELOPING EMBRYO. *Faseb Journal,* 8**,** 699-706.

BRONNERFRASER, M., WOLF, J. J. & MURRAY, B. A. 1992. EFFECTS OF ANTIBODIES AGAINST N-CADHERIN AND N-CAM ON THE CRANIAL NEURAL CREST AND NEURAL-TUBE. *Developmental Biology,* 153**,** 291-301.

BUCKLEY, C. D., TAN, J. Y., ANDERSON, K. L., HANEIN, D., VOLKMANN, N., WEIS, W. I., NELSON, W. J. & DUNN, A. R. 2014. The minimal cadherin-catenin complex binds to actin filaments under force. *Science,* 346**,** 600-+.

BURRIDGE, K. & MANGEAT, P. 1984. AN INTERACTION BETWEEN VINCULIN AND TALIN. *Nature,* 308**,** 744-746.

BURSTYN-COHEN, T., STANLEIGH, J., SELA-DONENFELD, D. & KALCHEIM, C. 2004. Canonical Wnt activity regulates trunk neural crest delamination linking BMP/noggin signaling with G1/S transition. *Development,* 131**,** 5327-5339.

BURUTE, M. & THERY, M. 2012. Spatial segregation between cell-cell and cell-matrix adhesions. *Current Opinion in Cell Biology,* 24**,** 628-636.

BUTLER, S. J. & DODD, J. 2003. A role for BMP heterodimers in roof plate-mediated repulsion of commissural axons. *Neuron,* 38**,** 389-401.

BYZOVA, T. V., GOLDMAN, C. K., PAMPORI, N., THOMAS, K. A., BETT, A., SHATTIL, S. J. & PLOW, E. F. 2000. A mechanism for modulation of cellular responses to VEGF: Activation of the integrins. *Molecular Cell,* 6**,** 851-860.

CAI, D., CHEN, S.-C., PRASAD, M., HE, L., WANG, X., CHOESMEL-CADAMURO, V., SAWYER, J. K., DANUSER, G. & MONTELL, D. J. 2014. Mechanical Feedback through E-Cadherin Promotes Direction Sensing during Collective Cell Migration. *Cell,* 157**,** 1146-1159.

CAI, D. & MONTELL, D. J. 2014. Diverse and dynamic sources and sinks in gradient formation and directed migration. *Current Opinion in Cell Biology,* 30**,** 91-98.

CAI, D. H. & BRAUER, P. R. 2002. Synthetic matrix metalloproteinase inhibitor decreases early cardiac neural crest migration in chicken embryos. *Developmental Dynamics,* 224**,** 441-449.

CAI, H., KRATZSCHMAR, J., ALFANDARI, D., HUNNICUTT, G. & BLOBEL, C. P. 1998. Neural crest-specific and general expression of distinct metalloprotease-disintegrins in early Xenopus laevis development. *Developmental Biology,* 204**,** 508-524.
CALLAN-JONES, A. C. & VOITURIEZ, R. 2016. Actin flows in cell migration: from locomotion and polarity to trajectories. *Current Opinion in Cell Biology,* 38**,** 12-17.
CAMAND, E., PEGLION, F., OSMANI, N., SANSON, M. & ETIENNE-MANNEVILLE, S. 2012. N-cadherin expression level modulates integrin-mediated polarity and strongly impacts on the speed and directionality of glial cell migration. *Journal of Cell Science,* 125**,** 844-857.
CANTEMIR, V., CAI, D. H., REEDY, M. V. & BRAUER, P. R. 2004. Tissue inhibitor of metalloproteinase-2 (TIMP-2) expression during cardiac neural crest cell migration and its role in proMMP-2 activation. *Developmental Dynamics,* 231**,** 709-719.
CAREY, D. J. 1997. Syndecans: Multifunctional cell-surface co-receptors. *Biochemical Journal,* 327**,** 1-16.
CARL, T. F., DUFTON, C., HANKEN, J. & KLYMKOWSKY, M. W. 1999. Inhibition of neural crest migration in Xenopus using antisense slug RNA. *Developmental Biology,* 213**,** 101-115.
CARMONA, G., PERERA, U., GILLETT, C., NABA, A., LAW, A. L., SHARMA, V. P., WANG, J., WYCKOFF, J., BALSAMO, M., MOSIS, F., DE PIANO, M., MONYPENNY, J., WOODMAN, N., MCCONNELL, R. E., MOUNEIMNE, G., VAN HEMELRIJCK, M., CAO, Y., CONDEELIS, J., HYNES, R. O., GERTLER, F. B. & KRAUSE, M. 2016. Lamellipodin promotes invasive 3D cancer cell migration via regulated interactions with Ena/VASP and SCAR/WAVE. *Oncogene,* 35**,** 5155-5169.
CARMONA-FONTAINE, C., MATTHEWS, H. & MAYOR, R. 2008a. Directional cell migration in vivo Wnt at the crest. *Cell Adhesion & Migration,* 2**,** 240-242.
CARMONA-FONTAINE, C., MATTHEWS, H. K., KURIYAMA, S., MORENO, M., DUNN, G. A., PARSONS, M., STERN, C. D. & MAYOR, R. 2008b. Contact inhibition of locomotion in vivo controls neural crest directional migration. *Nature,* 456**,** 957-961.
CARMONA-FONTAINE, C., THEVENEAU, E., TZEKOU, A., TADA, M., WOODS, M., PAGE, K. M., PARSONS, M., LAMBRIS, J. D. & MAYOR, R. 2011. Complement Fragment C3a Controls Mutual Cell Attraction during Collective Cell Migration. *Developmental Cell,* 21**,** 1026-1037.
CARNEY, T. J., DUTTON, K. A., GREENHILL, E., DELFINO-MACHIN, M., DUFOURCQ, P., BLADER, P. & KELSH, R. N. 2006. A direct role for Sox10 in specification of neural crest-derived sensory neurons. *Development,* 133**,** 4619-4630.
CARRAGHER, N. O., WALKER, S. M., CARRAGHER, L. S. A., HARRIS, F., SAWYER, T. K., BRUNTON, V. G., OZANNE, B. W. & FRAME, M. C. 2006. Calpain 2 and Src dependence distinguishes mesenchymal and amoeboid modes of tumour cell invasion: a link to integrin function. *Oncogene,* 25**,** 5726-5740.
CATTARUZZA, S. & PERRIS, R. 2005. Proteoglycan control of cell movement during wound healing and cancer spreading. *Matrix Biology,* 24**,** 400-417.
CATTIN, A. L., BURDEN, J. J., VAN EMMENIS, L., MACKENZIE, F. E., HOVING, J. J. A., CALAVIA, N. G., GUO, Y. P., MCLAUGHLIN, M., ROSENBERG, L. H., QUEREDA, V., JAMECNA, D., NAPOLI, I., PARRINELLO, S., ENVER, T., RUHRBERG, C. & LLOYD, A. C. 2015. Macrophage-Induced Blood Vessels Guide Schwann Cell-Mediated Regeneration of Peripheral Nerves. *Cell,* 162**,** 1127-1139.
CAUSSINUS, E., COLOMBELLI, J. & AFFOLTER, M. 2008. Tip-Cell Migration Controls Stalk-Cell Intercalation during Drosophila Tracheal Tube Elongation. *Current Biology,* 18**,** 1727-1734.
CAVANAUGH, A. M., HUANG, J. & CHEN, J.-N. 2015a. Two developmentally distinct populations of neural crest cells contribute to the zebrafish heart. *Developmental Biology,* 404**,** 103-112.
CAVANAUGH, A. M., HUANG, J. & CHEN, J. N. 2015b. Two developmentally distinct populations of neural crest cells contribute to the zebrafish heart. *Developmental Biology,* 404**,** 103-112.
CAVEY, M. & LECUIT, T. 2009. Molecular Bases of Cell-Cell Junctions Stability and Dynamics. *Cold Spring Harbor Perspectives in Biology,* 1.
CEBRA-THOMAS, J. A., TERRELL, A., BRANYAN, K., SHAH, S., RICE, R., GYI, L., YIN, M., HU, Y., MANGAT, G., SIMONET, J., BETTERS, E. & GILBERT, S. F. 2013. Late-Emigrating Trunk Neural Crest Cells in Turtle Embryos Generate an Osteogenic Ectomesenchyme in the Plastron. *Developmental Dynamics,* 242**,** 1223-1235.
CERNY, R., LWIGALE, P., ERICSSON, R., MEULEMANS, D., EPPERLEIN, H. H. & BRONNER-FRASER, M. 2004. Developmental origins and evolution of jaws: new interpretation of "maxillary" and "mandibular". *Developmental Biology,* 276**,** 225-236.
CETERA, M. & HORNE-BADOVINAC, S. 2015. Round and round gets you somewhere: collective cell migration and planar polarity in elongating Drosophila egg chambers. *Current Opinion in Genetics & Development,* 32**,** 10-15.
CETERA, M., LEYBOVA, L., JOYCE, B. & DEVENPORT, D. 2018. Counter-rotational cell flows drive morphological and cell fate asymmetries in mammalian hair follicles. *Nature Cell Biology,* 20**,** 541-+.
CHAFFER, C. L., THOMPSON, E. W. & WILLIAMS, E. D. 2007. Mesenchymal to epithelial transition in development and disease. *Cells Tissues Organs,* 185**,** 7-19.
CHANG, Y. C., WU, J. W., HSIEH, Y. C., HUANG, T. H., LIAO, Z. M., HUANG, Y. S., MONDO, J. A., MONTELL, D. & JANG, A. C. C. 2018. Rap1 Negatively Regulates the Hippo Pathway to Polarize Directional Protrusions in Collective Cell Migration. *Cell Reports,* 22**,** 2160-2175.
CHARRAS, G. & SAHAI, E. 2014. Physical influences of the extracellular environment on cell migration. *Nature Reviews Molecular Cell Biology,* 15**,** 813-824.
CHAUVET, S., BURK, K. & MANN, F. 2013. Navigation rules for vessels and neurons: cooperative signaling between VEGF and neural guidance cues. *Cellular and Molecular Life Sciences,* 70**,** 1685-1703.
CHEN, M. B., HAJAL, C., BENJAMIN, D. C., YU, C., AZIZGOLSHANI, H., HYNES, R. O. & KAMM, R. D. 2018. Inflamed neutrophils sequestered at entrapped tumor cells via chemotactic confinement promote tumor cell extravasation. *Proceedings of the National Academy of Sciences of the United States of America,* 115**,** 7022-7027.
CHEUNG, K. J. & EWALD, A. J. 2016. A collective route to metastasis: Seeding by tumor cell clusters. *Science,* 352**,** 167-169.

CHEUNG, M. & BRISCOE, J. 2003. Neural crest development is regulated by the transcription factor Sox9. *Development,* 130**,** 5681-5693.
CHEUNG, M., CHABOISSIER, M. C., MYNETT, A., HIRST, E., SCHEDL, A. & BRISCOE, J. 2005. The transcriptional control of trunk neural crest induction, survival, and delamination. *Developmental Cell,* 8**,** 179-192.
CHIDGEY, M. & DAWSON, C. 2007. Desmosomes: a role in cancer? *British Journal of Cancer,* 96**,** 1783-1787.
CHILTON, J. K. & GUTHRIE, S. 2003. Cranial expression of class 3 secreted semaphorins and their neuropilin receptors. *Developmental Dynamics,* 228**,** 726-733.
CHONG, S.-W., NGUYET, L.-M., JIANG, Y.-J. & KORZH, V. 2007. The chemokine Sdf-I and its receptor Cxcr4 are required for formation of muscle in zebrafish. *Bmc Developmental Biology,* 7.
CHONG, S. W., EMELYANOV, A., GONG, Z. Y. & KORZH, V. 2001. Expression pattern of two zebrafish genes, cxcr4a and cxcr4b. *Mechanisms of Development,* 109**,** 347-354.
CHRISTIANSEN, J. J. & RAJASEKARAN, A. K. 2006. Reassessing epithelial to mesenchymal transition as a prerequisite for carcinoma invasion and metastasis. *Cancer Research,* 66**,** 8319-8326.
CHUAI, M. & WEIJER, C. J. 2008. The mechanisms underlying primitive streak formation in the chick embryo. *Multiscale Modeling of Developmental Systems,* 81**,** 135-+.
CHUNG, C. Y., POTIKYAN, G. & FIRTEL, R. A. 2001. Control of cell polarity and chemotaxis by Akt/PKB and PI3 kinase through the regulation of PAKa. *Molecular Cell,* 7**,** 937-947.
CLARK, A. G., DIERKES, K. & PALUCH, E. K. 2013. Monitoring Actin Cortex Thickness in Live Cells. *Biophysical Journal,* 105**,** 570-580.
CLAY, M. R. & HALLORAN, M. C. 2010. Control of neural crest cell behavior and migration Insights from live imaging. *Cell Adhesion & Migration,* 4**,** 586-594.
CLAY, M. R. & HALLORAN, M. C. 2014. Cadherin 6 promotes neural crest cell detachment via F-actin regulation and influences active Rho distribution during epithelial-to-mesenchymal transition. *Development,* 141**,** 2506-2515.
CLIFFE, A., DOUPE, D. P., SUNG, H., LIM, I. K. H., ONG, K. H., CHENG, L. & YU, W. M. 2017. Quantitative 3D analysis of complex single border cell behaviors in coordinated collective cell migration. *Nature Communications,* 8.
CLUZEL, C., SALTEL, F., LUSSI, J., PAULHE, F., IMHOF, B. A. & WEHRLE-HALLER, B. 2005. The mechanisms and dynamics of alpha v beta 3 integrin clustering in living cells. *Journal of Cell Biology,* 171**,** 383-392.
COBURN, L., CERONE, L., TORNEY, C., COUZIN, I. D. & NEUFELD, Z. 2013. Tactile interactions lead to coherent motion and enhanced chemotaxis of migrating cells. *Physical Biology,* 10.
COLLAZO, A., BRONNERFRASER, M. & FRASER, S. E. 1993. Vital dye labeling of Xenopus-laevis trunk neural crest reveals multipotency and novel pathways of migration. *Development,* 118**,** 363-376.
COMBEDAZOU, A., CHOESMEL-CADAMURO, V., GAY, G., LIU, J. Y., DUPRE, L., RAMEL, D. & WANG, X. B. 2017. Myosin II governs collective cell migration behaviour downstream of guidance receptor signalling. *Journal of Cell Science,* 130**,** 97-103.
CORAVOS, J. S., MASON, F. M. & MARTIN, A. C. 2017. Actomyosin Pulsing in Tissue Integrity Maintenance during Morphogenesis. *Trends in Cell Biology,* 27**,** 276-283.
CORY, G. O. C., GARG, R., CRAMER, R. & RIDLEY, A. J. 2002. Phosphorylation of tyrosine enhances the ability of WASp to stimulate actin polymerization and filopodium formation. *Journal of Biological Chemistry,* 277**,** 45115-45121.
COSTANTINI, F. & KOPAN, R. 2010. Patterning a Complex Organ: Branching Morphogenesis and Nephron Segmentation in Kidney Development. *Developmental Cell,* 18**,** 698-712.
CRAMER 1997. Molecular mechanism of actin -dependent retrograde flow in lamellipodia of motile cells. *Frontiers in Bioscience***,** 2:d260-70.
CRAMER, L. P., KAY, R. R. & ZATULOVSKIY, E. 2018. Repellent and Attractant Guidance Cues Initiate Cell Migration by Distinct Rear-Driven and Front-Driven Cytoskeletal Mechanisms. *Current Biology,* 28**,** 995-+.
CREUZET, S., COULY, G., VINCENT, C. & LE DOUARIN, N. M. 2002. Negative effect of Hox gene expression on the development of the neural crest-derived facial skeleton. *Development,* 129**,** 4301-4313.
CREUZET, S., SCHULER, B., COULY, G. & LE DOUARIN, N. M. 2004. Reciprocal relationships between Fgf8 and neural crest cells in facial and forebrain development. *Proceedings of the National Academy of Sciences of the United States of America,* 101**,** 4843-4847.
CRUZ-MONSERRATE, Z. & O'CONNOR, K. L. 2008. Integrin alpha 6 beta 4 promotes migration, invasion through Tiam1 upregulation, and subsequent Rac activation. *Neoplasia,* 10**,** 408-U14.
CUI, C., YANG, X. S., CHUAI, M. L., GLAZIER, J. A. & WEIJER, C. J. 2005. Analysis of tissue flow patterns during primitive streak formation in the chick embryo. *Developmental Biology,* 284**,** 37-47.
CZYZ, J. 2008. The stage-specific function of gap junctions during tumourigenesis. *Cellular & Molecular Biology Letters,* 13**,** 92-102.
DABIRI, B. E., LEE, H. & PARKER, K. K. 2012. A potential role for integrin signaling in mechanoelectrical feedback. *Progress in Biophysics & Molecular Biology,* 110**,** 196-203.
DADY, A., BLAVET, C. & DUBAND, J. L. 2012. Timing and kinetics of E- to N-cadherin switch during neurulation in the avian embryo. *Developmental Dynamics,* 241**,** 1333-1349.
DAMBLY-CHAUDIERE, C., CUBEDO, N. & GHYSEN, A. 2007. Control of cell migration in the development of the posterior lateral line: antagonistic interactions between the chemokine receptors CXCR4 and CXCR7/RDC1. *Bmc Developmental Biology,* 7.
DAS, T., SAFFERLING, K., RAUSCH, S., GRABE, N., BOEHM, H. & SPATZ, J. P. 2015. A molecular mechanotransduction pathway regulates collective migration of epithelial cells. *Nature Cell Biology,* 17**,** 276-+.
DAVID, D. J. V., TISHKINA, A. & HARRIS, T. J. C. 2010. The PAR complex regulates pulsed actomyosin contractions during amnioserosa apical constriction in Drosophila. *Development,* 137**,** 1645-1655.
DAVID, N. B., SAPEDE, D., SAINT-ETIENNE, L., THISSE, C., THISSE, B., DAMBLY-CHAUDIERE, C., ROSA, F. M. & GHYSEN, A. 2002. Molecular basis of cell migration in the fish lateral line: Role of the chemokine receptor CXCR4 and of its ligand, SDF1. *Proceedings of the National Academy of Sciences of the United States of America,* 99**,** 16297-16302.

DAVIDSON, L. A. & KELLER, R. E. 1999. Neural tube closure in Xenopus laevis involves medial migration, directed protrusive activity, cell intercalation and convergent extension. *Development,* 126**,** 4547-4556.
DAVIS, F. M., AZIMI, I., FAVILLE, R. A., PETERS, A. A., JALINK, K., PUTNEY, J. W., GOODHILL, G. J., THOMPSON, E. W., ROBERTS-THOMSON, S. J. & MONTEITH, G. R. 2014. Induction of epithelial-mesenchymal transition (EMT) in breast cancer cells is calcium signal dependent. *Oncogene,* 33**,** 2307-2316.
DAVIS, J. R., LUCHICI, A., MOSIS, F., THACKERY, J., SALAZAR, J. A., MAO, Y. L., DUNN, G. A., BETZ, T., MIODOWNIK, M. & STRAMER, B. M. 2015. Inter-Cellular Forces Orchestrate Contact Inhibition of Locomotion. *Cell,* 161**,** 361-373.
DAVY, A., AUBIN, J. & SORIANO, P. 2004. Ephrin-B1 forward and reverse signaling are required during mouse development. *Genes & Development,* 18**,** 572-583.
DAVY, A. & SORIANO, P. 2007. Ephrin-B2 forward signaling regulates somite patterning and neural crest cell development. *Developmental Biology,* 304**,** 182-193.
DAY, C. L., SOBER, A. J., KOPF, A. W., LEW, R. A., MIHM, M. C., GOLOMB, F. M., POSTEL, A., HENNESSEY, P., HARRIS, M. N., GUMPORT, S. L., RAKER, J. W., MALT, R. A., COSIMI, A. B., WOOD, W. C., ROSES, D. F., GORSTEIN, F. & FITZPATRICK, T. B. 1981. A PROGNOSTIC MODEL FOR CLINICAL STAGE-I MELANOMA OF THE TRUNK - LOCATION NEAR THE MIDLINE IS NOT AN INDEPENDENT RISK FACTOR FOR RECURRENT DISEASE. *American Journal of Surgery,* 142**,** 247-251.
DE CALISTO, J., ARAYA, C., MARCHANT, L., RIAZ, C. F. & MAYOR, R. 2005. Essential role of non-canonical Wnt signalling in neural crest migration. *Development,* 132**,** 2587-2597.
DE PASCALIS, C., PÉREZ-GONZÁLEZ, C., SEETHARAMAN, S., BOËDA, B., VIANAY, B., BURUTE, M., LEDUC, C., BORGHI, N., TREPAT, X. & ETIENNE-MANNEVILLE, S. 2018. Intermediate filaments control collective migration by restricting traction forces and sustaining cell-cell contacts. *Journal of Cell Biology*.
DEFRANCO, B. H., NICKEL, B., BATY, C., MARTINEZ, J., GAY, V., SANDULACHE, V., HACKAM, D. & MURRAY, S. 2008. Migrating Cells Retain Gap Junction Plaque Structure and Function. *Cell Communication and Adhesion,* 15**,** 273-288.
DEL BARRIO, M. G. & NIETO, M. A. 2002. Overexpression of Snail family members highlights their ability to promote chick neural crest formation. *Development,* 129**,** 1583-1593.
DEL POZO, M. A., PRICE, L. S., ALDERSON, N. B., REN, X. D. & SCHWARTZ, M. A. 2000. Adhesion to the extracellular matrix regulates the coupling of the small GTPase Rac to its effector PAK. *Embo Journal,* 19**,** 2008-2014.
DENAIS, C. M., GILBERT, R. M., ISERMANN, P., MCGREGOR, A. L., TE LINDERT, M., WEIGELIN, B., DAVIDSON, P. M., FRIEDL, P., WOLF, K. & LAMMERDING, J. 2016. Nuclear envelope rupture and repair during cancer cell migration. *Science,* 352**,** 353-358.
DESAI, R. A., GAO, L., RAGHAVAN, S., LIU, W. F. & CHEN, C. S. 2009. Cell polarity triggered by cell-cell adhesion via E-cadherin. *Journal of Cell Science,* 122**,** 905-911.
DESAI, R. A., GOPAL, S. B., CHEN, S. & CHEN, C. S. 2013. Contact inhibition of locomotion probabilities drive solitary versus collective cell migration. *Journal of the Royal Society Interface,* 10.
DEVREOTES, P. & JANETOPOULOS, C. 2003. Eukaryotic chemotaxis: Distinctions between directional sensing and polarization. *Journal of Biological Chemistry,* 278**,** 20445-20448.
DING, H., WU, X. L., KIM, I., TAM, P. P. L., KOH, G. Y. & NAGY, A. 2000. The mouse Pdgfc gene: dynamic expression in embryonic tissues during organogenesis. *Mechanisms of Development,* 96**,** 209-213.
DING, X., ZHAO, Z., DUAN, W., WANG, S., JIN, X., XIANG, L. & JIN, X. 2013. Expression patterns of CXCR4 in different colon tissue segments of patients with Hirschsprung's disease. *Experimental and Molecular Pathology,* 95**,** 111-116.
DIZ-MUNOZ, A., THURLEY, K., CHINTAMEN, S., ALTSCHULER, S. J., WU, L. F., FLETCHER, D. A. & WEINER, O. D. 2016. Membrane Tension Acts Through PLD2 and mTORC2 to Limit Actin Network Assembly During Neutrophil Migration. *Plos Biology,* 14.
DONA, E., BARRY, J. D., VALENTIN, G., QUIRIN, C., KHMELINSKII, A., KUNZE, A., DURDU, S., NEWTON, L. R., FERNANDEZ-MINAN, A., HUBER, W., KNOP, M. & GILMOUR, D. 2013. Directional tissue migration through a self-generated chemokine gradient. *Nature,* 503**,** 285-+.
DOS REMEDIOS, C. G., CHHABRA, D., KEKIC, M., DEDOVA, I. V., TSUBAKIHARA, M., BERRY, D. A. & NOSWORTHY, N. J. 2003. Actin binding proteins: Regulation of cytoskeletal microfilaments. *Physiological Reviews,* 83**,** 433-473.
DUBAND, J.-L., DADY, A. & FLEURY, V. 2015. Resolving time and space constraints during neural crest formation and delamination. *Current topics in developmental biology,* 111**,** 27-67.
DUBAND, J. L. 2010. Diversity in the molecular and cellular strategies of epithelium-to-mesenchyme transitions Insights from the neural crest. *Cell Adhesion & Migration,* 4**,** 458-482.
DUBAND, J. L. & THIERY, J. P. 1982. DISTRIBUTION OF FIBRONECTIN IN THE EARLY PHASE OF AVIAN CEPHALIC NEURAL CREST CELL-MIGRATION. *Developmental Biology,* 93**,** 308-323.
DUCHEK, P., SOMOGYI, K., JEKELY, G., BECCARI, S. & RORTH, P. 2001. Guidance of cell migration by the Drosophila PDGF/VEGF receptor. *Cell,* 107**,** 17-26.
DUMORTIER, J. G., MARTIN, S., MEYER, D., ROSA, F. M. & DAVID, N. B. 2012. Collective mesendoderm migration relies on an intrinsic directionality signal transmitted through cell contacts. *Proceedings of the National Academy of Sciences of the United States of America,* 109**,** 16945-16950.
DUONG, T. D. & ERICKSON, C. A. 2004. MMP-2 plays an essential role in producing epithelial-mesenchymal transformations in the avian embryo. *Developmental Dynamics,* 229**,** 42-53.
DUPIN, E., CREUZET, S. & LE DOUARIN, N. M. 2006. The contribution of the neural crest to the vertebrate body. *Neural Crest Induction and Differentiation,* 589**,** 96-119.
DUPIN, I., CAMAND, E. & ETIENNE-MANNEVILLE, S. 2009. Classical cadherins control nucleus and centrosome position and cell polarity. *Journal of Cell Biology,* 185**,** 779-786.
EBERHART, J. K., HE, X., SWARTZ, M. E., YAN, Y.-L., SONG, H., BOLING, T. C., KUNERTH, A. K., WALKER, M. B., KIMMEL, C. B. & POSTLETHWAIT, J. H. 2008. MicroRNA Mirn140 modulates Pdgf signaling during palatogenesis. *Nature Genetics,* 40**,** 290-298.

EDWARDS, D. R., HANDSLEY, M. M. & PENNINGTON, C. J. 2008. The ADAM metalloproteinases. *Molecular Aspects of Medicine,* 29**,** 258-289.
EDWARDS, K. A. & KIEHART, D. P. 1996. Drosophila nonmuscle myosin II has multiple essential roles in imaginal disc and egg chamber morphogenesis. *Development,* 122**,** 1499-1511.
EICKHOLT, B. J., MACKENZIE, S. L., GRAHAM, A., WALSH, F. S. & DOHERTY, P. 1999. Evidence for collapsin-1 functioning in the control of neural crest migration in both trunk and hindbrain regions. *Development,* 126**,** 2181-2189.
ELISHA, Y., KALCHENKO, V., KUZNETSOV, Y. & GEIGER, B. 2018. Dual role of E-cadherin in the regulation of invasive collective migration of mammary carcinoma cells. *Scientific Reports,* 8.
ELLISON, D., MUGLER, A., BRENNAN, M. D., LEE, S. H., HUEBNER, R. J., SHAMIR, E. R., WOO, L. A., KIM, J., AMAR, P., NEMENMAN, I., EWALD, A. J. & LEVCHENKO, A. 2016. Cell-cell communication enhances the capacity of cell ensembles to sense shallow gradients during morphogenesis. *Proceedings of the National Academy of Sciences of the United States of America,* 113**,** E679-E688.
ENGELMANN, W. 1882. Ueber Assimilation von Haematococcus. Botanische Zeitung.
EPPERLEIN, H. H., HALFTER, W. & TUCKER, R. P. 1988. THE DISTRIBUTION OF FIBRONECTIN AND TENASCIN ALONG MIGRATORY PATHWAYS OF THE NEURAL CREST IN THE TRUNK OF AMPHIBIAN EMBRYOS. *Development,* 103**,** 743-756.
ERICKSON, C. A. 1985. Control of neural crest cell dispersion in the trunk of the avian embryos. *Developmental Biology,* 111**,** 138-157.
ERICKSON, C. A. & WESTON, J. A. 1983. AN SEM ANALYSIS OF NEURAL CREST MIGRATION IN THE MOUSE. *Journal of Embryology and Experimental Morphology,* 74**,** 97-118.
ESCOT, S., BLAVET, C., HAERTLE, S., DUBAND, J.-L. & FOURNIER-THIBAULT, C. 2013. Misregulation of SDF1-CXCR4 Signaling Impairs Early Cardiac Neural Crest Cell Migration Leading to Conotruncal Defects. *Circulation Research,* 113**,** 505-516.
ESCRIBANO, J., SUNYER, R., SANCHEZ, M. T., TREPAT, X., ROCA-CUSACHS, P. & GARCIA-AZNAR, J. M. 2018. A hybrid computational model for collective cell durotaxis. *Biomechanics and Modeling in Mechanobiology,* 17**,** 1037-1052.
ETCHEVERS, H. C., AMIEL, J. & LYONNET, S. 2007. Genetic and molecular bases of neurocristopathies. *Archives De Pediatrie,* 14**,** 668-672.
ETIENNE-MANNEVILLE, S. 2011. Control of polarized cell morphology and motility by adherens junctions. *Seminars in Cell & Developmental Biology,* 22**,** 850-857.
ETIENNE-MANNEVILLE, S. 2013. Microtubules in Cell Migration. *Annual Review of Cell and Developmental Biology, Vol 29,* 29**,** 471-499.
ETIENNE-MANNEVILLE, S. 2014. Neighborly relations during collective migration. *Current Opinion in Cell Biology,* 30**,** 51-59.
ETIENNE-MANNEVILLE, S. & HALL, A. 2001. Integrin-mediated activation of Cdc42 controls cell polarity in migrating astrocytes through PKC zeta. *Cell,* 106**,** 489-498.
ETIENNE-MANNEVILLE, S. & HALL, A. 2002. Rho GTPases in cell biology. *Nature,* 420**,** 629-635.
ETIENNE-MANNEVILLE, S. & HALL, A. 2003. Cell polarity: Par6, aPKC and cytoskeletal crosstalk. *Current Opinion in Cell Biology,* 15**,** 67-72.
EVEN-RAM, S. & YAMADA, K. M. 2005. Cell migration in 3D matrix. *Current Opinion in Cell Biology,* 17**,** 524-532.
EVERS, E. E., ZONDAG, G. C. M., MALLIRI, A., PRICE, L. S., TEN KLOOSTER, J. P., VAN DER KAMMEN, R. A. & COLLARD, J. G. 2000. Rho family proteins in cell adhesion and cell migration. *European Journal of Cancer,* 36**,** 1269-1274.
EWALD, A. J., BRENOT, A., DUONG, M., CHAN, B. S. & WERB, Z. 2008. Collective epithelial migration and cell rearrangements drive mammary branching morphogenesis. *Developmental Cell,* 14**,** 570-581.
FAROOQUI, R. & FENTEANY, G. 2005. Multiple rows of cells behind an epithelial wound edge extend cryptic lamellipodia to collectively drive cell-sheet movement. *Journal of Cell Science,* 118**,** 51-63.
FAWCETT, S. R. & KLYMKOWSKY, M. W. 2004. Embryonic expression of Xenopus laevis SOX7. *Gene Expression Patterns,* 4**,** 29-33.
FERNANDEZ-ESPARTERO, C. H., RAMEL, D., FARAGO, M., MALARTRE, M., LUQUE, C. M., LIMANOVICH, S., KATZAV, S., EMERY, G. & MARTIN-BERMUDO, M. D. 2013. GTP exchange factor Vav regulates guided cell migration by coupling guidance receptor signalling to local Rac activation. *Journal of Cell Science,* 126**,** 2285-2293.
FIEHLER, R. W. & WOLFF, T. 2007. Drosophila Myosin II, Zipper, is essential for ommatidial rotation. *Developmental Biology,* 310**,** 348-362.
FIRAT-KARALAR, E. N. & WELCH, M. D. 2011. New mechanisms and functions of actin nucleation. *Current Opinion in Cell Biology,* 23**,** 4-13.
FISCHER, R. S., GARDEL, M., MA, X. F., ADELSTEIN, R. S. & WATERMAN, C. M. 2009. Local Cortical Tension by Myosin II Guides 3D Endothelial Cell Branching. *Current Biology,* 19**,** 260-265.
FRANK, D. U., FOTHERINGHAM, L. K., BREWER, J. A., MUGLIA, L. J., TRISTANI-FIROUZI, M., CAPECCHI, M. R. & MOON, A. M. 2002. An Fgf8 mouse mutant phenocopies human 22q11 deletion syndrome. *Development,* 129**,** 4591-4603.
FRIEDL, P. 2004. Prespecification and plasticity: shifting mechanisms of cell migration. *Current Opinion in Cell Biology,* 16**,** 14-23.
FRIEDL, P., BORGMANN, S. & BROCKER, E. B. 2001. Amoeboid leukocyte crawling through extracellular matrix: lessons from the Dictyostelium paradigm of cell movement. *Journal of Leukocyte Biology,* 70**,** 491-509.
FRIEDL, P. & BROCKER, E. B. 2000. The biology of cell locomotion within three-dimensional extracellular matrix. *Cellular and Molecular Life Sciences,* 57**,** 41-64.
FRIEDL, P. & GILMOUR, D. 2009. Collective cell migration in morphogenesis, regeneration and cancer. *Nature Reviews Molecular Cell Biology,* 10**,** 445-457.
FRIEDL, P., HEGERFELDT, Y. & TUSCH, M. 2004. Collective cell migration in morphogenesis and cancer. *International Journal of Developmental Biology,* 48**,** 441-449.

FRIEDL, P., NOBLE, P. B., WALTON, P. A., LAIRD, D. W., CHAUVIN, P. J., TABAH, R. J., BLACK, M. & ZANKER, K. S. 1995. MIGRATION OF COORDINATED CELL CLUSTERS IN MESENCHYMAL AND EPITHELIAL CANCER EXPLANTS IN-VITRO. *Cancer Research,* 55**,** 4557-4560.
FRIEDL, P., SAHAI, E., WEISS, S. & YAMADA, K. M. 2012. New dimensions in cell migration. *Nature Reviews Molecular Cell Biology,* 13**,** 743-747.
FRIEDL, P. & WEIGELIN, B. 2008. Interstitial leukocyte migration and immune function. *Nature Immunology,* 9**,** 960-969.
FRIEDL, P. & WOLF, K. 2003. Tumour-cell invasion and migration: Diversity and escape mechanisms. *Nature Reviews Cancer,* 3**,** 362-374.
FRIEDL, P. & WOLF, K. 2008. Tube travel: The role of proteases in individual and collective a cancer cell invasion. *Cancer Research,* 68**,** 7247-7249.
FRIEDL, P. & WOLF, K. 2009. Proteolytic interstitial cell migration: a five-step process. *Cancer and Metastasis Reviews,* 28**,** 129-135.
FU, X., KATO, S., LONG, J., MATTINGLY, H. H., HE, C., VURAL, D. C., ZUCKER, S. W. & EMONET, T. 2018. Spatial self-organization resolves conflicts between individuality and collective migration. *Nature Communications,* 9.
FUENTEALBA, J., TORO-TAPIA, G., ARRIAGADA, C., RIQUELME, L., BEYER, A., HENRIQUEZ, J. P., CAPRILE, T., MAYOR, R., MARCELLINI, S., HINRICHS, M. V., OLATE, J. & TORREJON, M. 2013. Ric-8A, a guanine nucleotide exchange factor for heterotrimeric G proteins, is critical for cranial neural crest cell migration. *Developmental Biology,* 378**,** 74-82.
FULGA, T. A. & RORTH, P. 2002. Invasive cell migration is initiated by guided growth of long cellular extensions. *Nature Cell Biology,* 4**,** 715-719.
GAGGIOLI, C., HOOPER, S., HIDALGO-CARCEDO, C., GROSSE, R., MARSHALL, J. F., HARRINGTON, K. & SAHAI, E. 2007. Fibroblast-led collective invasion of carcinoma cells with differing roles for RhoGTPases in leading and following cells. *Nature Cell Biology,* 9**,** 1392-U92.
GALBRAITH, C. G., YAMADA, K. M. & SHEETZ, M. P. 2002. The relationship between force and focal complex development. *Journal of Cell Biology,* 159**,** 695-705.
GALLIK, K. L., TREFFY, R. W., NACKE, L. M., AHSAN, K., ROCHA, M., GREEN-SAXEN, A. & SAXENA, A. 2017. Neural crest and cancer: Divergent travelers on similar paths. *Mechanisms of Development,* 148**,** 89-99.
GAMMILL, L. S., GONZALEZ, C. & BRONNER-FRASER, M. 2007. Neuropilin 2/semaphorin 3F signaling is essential for cranial neural crest migration and trigeminal ganglion condensation. *Developmental Neurobiology,* 67**,** 47-56.
GAMMILL, L. S., GONZALEZ, C., GU, C. H. & BRONNER-FRASER, M. 2006. Guidance of trunk neural crest migration requires neuropilin 2/semaphorin 3F signaling. *Development,* 133**,** 99-106.
GAMMILL, L. S. & ROFFERS-AGARWAL, J. 2010. Division of labor during trunk neural crest development. *Developmental Biology,* 344**,** 555-565.
GANS, C. & NORTHCUTT, R. G. 1983. NEURAL CREST AND THE ORIGIN OF VERTEBRATES - A NEW HEAD. *Science,* 220**,** 268-273.
GARDEL, M. L., SABASS, B., JI, L., DANUSER, G., SCHWARZ, U. S. & WATERMAN, C. M. 2008. Traction stress in focal adhesions correlates biphasically with actin retrograde flow speed. *Journal of Cell Biology,* 183**,** 999-1005.
GARDEL, M. L., SCHNEIDER, I. C., ARATYN-SCHAUS, Y. & WATERMAN, C. M. 2010. Mechanical Integration of Actin and Adhesion Dynamics in Cell Migration. *Annual Review of Cell and Developmental Biology, Vol 26,* 26**,** 315-333.
GARDINER, E. M., PESTONJAMASP, K. N., BOHL, B. P., CHAMBERLAIN, C., HAHN, K. M. & BOKOCH, G. M. 2002. Spatial and temporal analysis of Rac activation during live neutrophil chemotaxis. *Current Biology,* 12**,** 2029-2034.
GAVERT, N., BEN-SHMUEL, A., RAVEH, S. & BEN-ZE'EV, A. 2008. L1-CAM in cancerous tissues. *Expert Opinion on Biological Therapy,* 8**,** 1749-1757.
GEIGER, B., BERSHADSKY, A., PANKOV, R. & YAMADA, K. M. 2001. Transmembrane extracellular matrix-cytoskeleton crosstalk. *Nature Reviews Molecular Cell Biology,* 2**,** 793-805.
GEISBRECHT, E. R. & MONTELL, D. J. 2002. Myosin VI is required for E-cadherin-mediated border cell migration. *Nature Cell Biology,* 4**,** 616-620.
GHABRIAL, A. S. & KRASNOW, M. A. 2006. Social interactions among epithelial cells during tracheal branching morphogenesis. *Nature,* 441**,** 746-749.
GHIGLIONE, C., JOUANDIN, P., CEREZO, D. & NOSELLI, S. 2018. The Drosophila insulin pathway controls Profilin expression and dynamic actin-rich protrusions during collective cell migration. *Development,* 145.
GIAMBERNARDI, T. A., SAKAGUCHI, A. Y., GLUHAK, J., PAVLIN, D., TROYER, D. A., DAS, G., RODECK, U. & KLEBE, R. J. 2001. Neutrophil collagenase (MMP-8) is expressed during early development in neural crest cells as well as in adult melanoma cells. *Matrix Biology,* 20**,** 577-587.
GILBERT, S. F., BENDER, G., BETTERS, E., YIN, M. & CEBRA-THOMAS, J. A. 2007. The contribution of neural crest cells to the nuchal bone and plastron of the turtle shell. *Integrative and Comparative Biology,* 47**,** 401-408.
GILMOUR, D., REMBOLD, M. & LEPTIN, M. 2017. From morphogen to morphogenesis and back. *Nature,* 541**,** 311-320.
GIOVANNONE, D., REYES, M., REYES, R., CORREA, L., MARTINEZ, D., RA, H., GOMEZ, G., KAISER, J., MA, L., STEIN, M. P. & DE BELLARD, M. E. 2012. Slits affect the timely migration of neural crest cells via robo receptor. *Developmental Dynamics,* 241**,** 1274-1288.
GITTES, F., MICKEY, B., NETTLETON, J. & HOWARD, J. 1993. FLEXURAL RIGIDITY OF MICROTUBULES AND ACTIN-FILAMENTS MEASURED FROM THERMAL FLUCTUATIONS IN SHAPE. *Journal of Cell Biology,* 120**,** 923-934.
GLADING, A., LAUFFENBURGER, D. A. & WELLS, A. 2002. Cutting to the chase: calpain proteases in cell motility. *Trends in Cell Biology,* 12**,** 46-54.
GOLDING, J. P., TRAINOR, P., KRUMLAUF, R. & GASSMANN, M. 2000. Defects in pathfinding by cranial neural crest cells in mice lacking the neuregulin receptor ErbB4. *Nature Cell Biology,* 2**,** 103-109.

GOOD, M. & TREPAT, X. Cell parts to complex processes, from the bottom up. *Nature,* 563.
GOPAL, S., VERACINI, L., GRALL, D., BUTORI, C., SCHAUB, S., AUDEBERT, S., CAMOIN, L., BAUDELET, E., RADWANSKA, A., DIVONNE, S. B. D., VIOLETTE, S. M., WEINREB, P. H., REKIMA, S., ILIE, M., SUDAKA, A., HOFMAN, P. & VAN OBBERGHEN-SCHILLING, E. 2017. Fibronectin-guided migration of carcinoma collectives. *Nature Communications,* 8.
GOTO, A., SUMIYAMA, K., KAMIOKA, Y., NAKASYO, E., ITO, K., IWASAKI, M., ENOMOTO, H. & MATSUDA, M. 2013. GDNF and Endothelin 3 Regulate Migration of Enteric Neural Crest-Derived Cells via Protein Kinase A and Rac1. *Journal of Neuroscience,* 33**,** 4901-4912.
GRAHAM, A. & SMITH, A. 2001. Patterning the pharyngeal arches. *Bioessays,* 23**,** 54-61.
GRASSIE, M. E., MOFFAT, L. D., WALSH, M. P. & MACDONALD, J. A. 2011. The myosin phosphatase targeting protein (MYPT) family: A regulated mechanism for achieving substrate specificity of the catalytic subunit of protein phosphatase type 1 delta. *Archives of Biochemistry and Biophysics,* 510**,** 147-159.
GROEGER, G. & NOBES, C. D. 2007. Co-operative Cdc42 and Rho signalling mediates ephrinB-triggered endothelial cell retraction. *Biochemical Journal,* 404**,** 23-29.
GRUNERT, S., JECHLINGER, M. & BEUG, H. 2003. Diverse cellular and molecular mechanisms contribute to epithelial plasticity and metastasis. *Nature Reviews Molecular Cell Biology,* 4**,** 657-665.
GUDJONSSON, T., RONNOV-JESSEN, L., VILLADSEN, R., RANK, F., BISSELL, M. J. & PETERSEN, O. W. 2002. Normal and tumor-derived myoepithelial cells differ in their ability to interact with luminal breast epithelial cells for polarity and basement membrane deposition. *Journal of Cell Science,* 115**,** 39-50.
GUILLOT, C. & LECUIT, T. 2013. Mechanics of Epithelial Tissue Homeostasis and Morphogenesis. *Science,* 340**,** 1185-1189.
GUO, W. J. & GIANCOTTI, F. G. 2004. Integrin signalling during tumour progression. *Nature Reviews Molecular Cell Biology,* 5**,** 816-826.
HAAS, P. & GILMOUR, D. 2006. Chemokine signaling mediates self-organizing tissue migration in the zebrafish lateral line. *Developmental Cell,* 10**,** 673-680.
HADEBALL, B., BORCHERS, A. & WEDLICH, D. 1998. Xenopus cadherin-11 (Xcadherin-11) expression requires the Wg/Wnt signal. *Mechanisms of Development,* 72**,** 101-113.
HAEGER, A., WOLF, K., ZEGERS, M. M. & FRIEDL, P. 2015. Collective cell migration: guidance principles and hierarchies. *Trends in Cell Biology,* 25**,** 556-566.
HALL, B. K. 2008. The neural crest and neural crest cells: discovery and significance for theories of embryonic organization. *Journal of Biosciences,* 33**,** 781-793.
HARLAND, R. M. 1991. IN-SITU HYBRIDIZATION - AN IMPROVED WHOLE-MOUNT METHOD FOR XENOPUS-EMBRYOS. *Methods in Cell Biology,* 36**,** 685-695.
HAWKINS, R. J., PIEL, M., FAURE-ANDRE, G., LENNON-DUMENIL, A. M., JOANNY, J. F., PROST, J. & VOITURIEZ, R. 2009. Pushing off the Walls: A Mechanism of Cell Motility in Confinement. *Physical Review Letters,* 102.
HAY, E. D. 1995. An overview of epithelio-mesenchymal transformation. *Acta Anatomica,* 154**,** 8-20.
HAYER, A., SHAO, L., CHUNG, M. Y., JOUBERT, L. M., YANG, H. W., TSAI, F. C., BISARIA, A., BETZIG, E. & MEYER, T. 2016. Engulfed cadherin fingers are polarized junctional structures between collectively migrating endothelial cells. *Nature Cell Biology,* 18**,** 1311-+.
HAYES, M., NAITO, M., DAULAT, A., ANGERS, S. & CIRUNA, B. 2013. Ptk7 promotes non-canonical Wnt/PCP-mediated morphogenesis and inhibits Wnt/beta-catenin-dependent cell fate decisions during vertebrate development. *Development,* 140**,** 1807-1818.
HE, B., DOUBROVINSKI, K., POLYAKOV, O. & WIESCHAUS, E. 2014. Apical constriction drives tissue-scale hydrodynamic flow to mediate cell elongation. *Nature,* 508**,** 392-+.
HE, F. & SORIANO, P. 2013. A Critical Role for PDGFR alpha Signaling in Medial Nasal Process Development. *Plos Genetics,* 9.
HE, L., WANG, X. B., TANG, H. L. & MONTELL, D. J. 2010. Tissue elongation requires oscillating contractions of a basal actomyosin network. *Nature Cell Biology,* 12**,** 1133-U40.
HEASMAN, S. J., CARLIN, L. M., COX, S., NG, T. & RIDLEY, A. J. 2010. Coordinated RhoA signaling at the leading edge and uropod is required for T cell transendothelial migration. *Journal of Cell Biology,* 190**,** 553-563.
HEGERFELDT, Y., TUSCH, M., BROCKER, E. B. & FRIEDL, P. 2002. Collective cell movement in primary melanoma explants: Plasticity of cell-cell interaction, ss 1-integrin function, and migration strategies. *Cancer Research,* 62**,** 2125-2130.
HELLSTROM, M., PHNG, L. K., HOFMANN, J. J., WALLGARD, E., COULTAS, L., LINDBLOM, P., ALVA, J., NILSSON, A. K., KARLSSON, L., GAIANO, N., YOON, K., ROSSANT, J., IRUELA-ARISPE, M. L., KALEN, M., GERHARDT, H. & BETSHOLTZ, C. 2007. Dll4 signalling through Notch1 regulates formation of tip cells during angiogenesis. *Nature,* 445**,** 776-780.
HENDEY, B., KLEE, C. B. & MAXFIELD, F. R. 1992. INHIBITION OF NEUTROPHIL CHEMOKINESIS ON VITRONECTIN BY INHIBITORS OF CALCINEURIN. *Science,* 258**,** 296-299.
HENDRIX, M. J. C., SEFTOR, E. A., HESS, A. R. & SEFTOR, R. E. B. 2003. Molecular plasticity of human melanoma cells. *Oncogene,* 22**,** 3070-3075.
HIDALGO-CARCEDO, C., HOOPER, S., CHAUDHRY, S. I., WILLIAMSON, P., HARRINGTON, K., LEITINGER, B. & SAHAI, E. 2011. Collective cell migration requires suppression of actomyosin at cell-cell contacts mediated by DDR1 and the cell polarity regulators Par3 and Par6. *Nature Cell Biology,* 13**,** 49-U123.
HIGGS, H. N. & POLLARD, T. D. 2001. Regulation of actin filament network formation through Arp2/3 complex: Activation by a diverse array of proteins. *Annual Review of Biochemistry,* 70**,** 649-676.
HIGH, F. A., JAIN, R., STOLLER, J. Z., ANTONUCCI, N. B., LU, M. M., LOOMES, K. M., KAESTNER, K. H., PEAR, W. S. & EPSTEIN, J. A. 2009. Murine Jagged1/Notch signaling in the second heart field orchestrates Fgf8 expression and tissue-tissue interactions during outflow tract development. *Journal of Clinical Investigation,* 119**,** 1986-1996.
HIS, W. 1868. Untersuchungen über die erste Anlage des Wirbelthierleibes: die erste Entwickelung des Hühnchens im Ei. FCW Vogel.

HO, L., SYMES, K., YORDAN, C., GUDAS, L. J. & MERCOLA, M. 1994. Localization of PDGF-A and PDGFR-alpha messenger-RNA in Xenopus embryos suggests signaling from neural ectoderm and pharyngeal endoderm to neural crest cells. *Mechanisms of Development,* 48**,** 165-174.
HOELZINGER, D. B., DEMUTH, T. & BERENS, M. E. 2007. Autocrine factors that sustain glioma invasion and paracrine biology in the brain microenvironment. *Journal of the National Cancer Institute,* 99**,** 1583-1593.
HONORE, S. M., AYBAR, M. J. & MAYOR, R. 2003. Sox10 is required for the early development of the prospective neural crest in Xenopus embryos. *Developmental Biology,* 260**,** 79-96.
HOPWOOD, N. D., PLUCK, A. & GURDON, J. B. 1989. A XENOPUS MESSENGER-RNA RELATED TO DROSOPHILA TWIST IS EXPRESSED IN RESPONSE TO INDUCTION IN THE MESODERM AND THE NEURAL CREST. *Cell,* 59**,** 893-903.
HORWITZ, A., DUGGAN, K., BUCK, C., BECKERLE, M. C. & BURRIDGE, K. 1986. INTERACTION OF PLASMA-MEMBRANE FIBRONECTIN RECEPTOR WITH TALIN - A TRANSMEMBRANE LINKAGE. *Nature,* 320**,** 531-533.
HOUK, A. R., JILKINE, A., MEJEAN, C. O., BOLTYANSKIY, R., DUFRESNE, E. R., ANGENENT, S. B., ALTSCHULER, S. J., WU, L. F. & WEINER, O. D. 2012. Membrane Tension Maintains Cell Polarity by Confining Signals to the Leading Edge during Neutrophil Migration. *Cell,* 148**,** 175-188.
HUANG, G. Y., COOPER, E. S., WALDO, K., KIRBY, M. L., GILULA, N. B. & LO, C. W. 1998. Gap junction-mediated cell-cell communication modulates mouse neural crest migration. *Journal of Cell Biology,* 143**,** 1725-1734.
HUANG, X. & SAINT-JEANNET, J. P. 2004. Induction of the neural crest and the opportunities of life on the edge. *Developmental Biology,* 275**,** 1-11.
HUSSAIN, N. K., JENNA, S., GLOGAUER, M., QUINN, C. C., WASIAK, S., GUIPPONI, M., ANTONARAKIS, S. E., KAY, B. K., STOSSEL, T. P., LAMARCHE-VANE, N. & MCPHERSON, P. S. 2001. Endocytic protein intersectin-l regulates actin assembly via Cdc42 and N-WASP. *Nature Cell Biology,* 3**,** 927-932.
HÖRSTADIUS , S. 1950. *The Neural Crest: Its Properties and Derivatives in the Light of Experimental Research*. Oxford University Press, London.
IKEYA, T. & HAYASHI, S. 1999. Interplay of Notch and FGF signaling restricts cell fate and MAPK activation in the Drosophila trachea. *Development,* 126**,** 4455-4463.
ITO, A., KOMA, Y., UCHINO, K., OKADA, T., OHBAYASHI, C., TSUBOTA, N. & OKADA, M. 2006. Increased expression of connexin 26 in the invasive component of lung squamous cell carcinoma: Significant correlation with poor prognosis. *Cancer Letters,* 234**,** 239-248.
ITOH, R. E., KUROKAWA, K., OHBA, Y., YOSHIZAKI, H., MOCHIZUKI, N. & MATSUDA, M. 2002. Activation of Rac and Cdc42 video imaged by fluorescent resonance energy transfer-based single-molecule probes in the membrane of living cells. *Molecular and Cellular Biology,* 22**,** 6582-6591.
JACINTO, A., WOOD, W., WOOLNER, S., HILEY, C., TURNER, L., WILSON, C., MARTINEZ-ARIAS, A. & MARTIN, P. 2002. Dynamic analysis of actin cable function during Drosophila dorsal closure. *Current Biology,* 12**,** 1245-1250.
JACOBELLI, J., FRIEDMAN, R. S., CONTI, M. A., LENNON-DUMENIL, A. M., PIEL, M., SORENSEN, C. M., ADELSTEIN, R. S. & KRUMMEL, M. F. 2010. Confinement-optimized three-dimensional T cell amoeboid motility is modulated via myosin IIA-regulated adhesions. *Nature Immunology,* 11**,** 953-U110.
JECHLINGER, M., SOMMER, A., MORIGGL, R., SEITHER, P., KRAUT, N., CAPODIECCI, P., DONOVAN, M., CORDON-CARDO, C., BEUG, H. & GRUNERT, S. 2006. Autocrine PDGFR signaling promotes mammary cancer metastasis. *Journal of Clinical Investigation,* 116**,** 1561-1570.
JIA, L., CHENG, L. & RAPER, J. 2005. Slit/Robo signaling is necessary to confine early neural crest cells to the ventral migratory pathway in the trunk. *Developmental Biology,* 282**,** 411-421.
JOHNSON, R. P. & CRAIG, S. W. 1995. F-ACTIN BINDING-SITE MASKED BY THE INTRAMOLECULAR ASSOCIATION OF VINCULIN HEAD AND TAIL DOMAINS. *Nature,* 373**,** 261-264.
KAMETANI, Y. & TAKEICHI, M. 2007. Basal-to-apical cadherin flow at cell junctions. *Nature Cell Biology,* 9**,** 92-U118.
KAMPOURAKIS, T. & IRVING, M. 2015. Phosphorylation of myosin regulatory light chain controls myosin head conformation in cardiac muscle. *Journal of Molecular and Cellular Cardiology,* 85**,** 199-206.
KANDEL, E. 2013. *Principles of Neural Science*, New York: The McGraw-Hill Companies, Inc.
KANG, Y. B. & MASSAGUE, J. 2004. Epithelial-mesenchymal transitions: Twist in development and metastasis. *Cell,* 118**,** 277-279.
KARDASH, E., REICHMAN-FRIED, M., MAITRE, J. L., BOLDAJIPOUR, B., PAPUSHEVA, E., MESSERSCHMIDT, E. M., HEISENBERG, C. P. & RAZ, E. 2010. A role for Rho GTPases and cell-cell adhesion in single-cell motility in vivo. *Nature Cell Biology,* 12**,** 47-U112.
KASEMEIER-KULESA, J. C., MCLENNAN, R., ROMINE, M. H., KULESA, P. M. & LEFCORT, F. 2010. CXCR4 Controls Ventral Migration of Sympathetic Precursor Cells. *Journal of Neuroscience,* 30**,** 13078-13088.
KASHEF, J., KOHLER, A., KURIYAMA, S., ALFANDARI, D., MAYOR, R. & WEDLICH, D. 2009. Cadherin-11 regulates protrusive activity in Xenopus cranial neural crest cells upstream of Trio and the small GTPases. *Genes & Development,* 23**,** 1393-1398.
KAWAKAMI, M., UMEDA, M., NAKAGATA, N., TAKEO, T. & YAMAMURA, K.-I. 2011. Novel migrating mouse neural crest cell assay system utilizing P0-Cre/EGFP fluorescent time-lapse imaging. *Bmc Developmental Biology,* 11.
KAY, R. R., LANGRIDGE, P., TRAYNOR, D. & HOELLER, O. 2008. Changing directions in the study of chemotaxis. *Nature Reviews Molecular Cell Biology,* 9**,** 455-463.
KELLER, R. 2002. Shaping the vertebrate body plan by polarized embryonic cell movements. *Science,* 298**,** 1950-1954.
KELSH, R. N., HARRIS, M. L., COLANESI, S. & ERICKSON, C. A. 2009. Stripes and belly-spots-A review of pigment cell morphogenesis in vertebrates. *Seminars in Cell & Developmental Biology,* 20**,** 90-104.
KEROSUO, L. & BRONNER-FRASER, M. 2012. What is bad in cancer is good in the embryo: Importance of EMT in neural crest development. *Seminars in Cell & Developmental Biology,* 23**,** 320-332.
KHAN, K., HARDY, R., HAQ, A., OGUNBIYI, O., MORTON, O. & CHIDGEY, M. 2006. Desmocollin switching in colorectal cancer. *British Journal of Cancer,* 95**,** 1367-1370.

KIBBEY, M. C., GRANT, D. S. & KLEINMAN, H. K. 1992. ROLE OF THE SIKVAV SITE OF LAMININ IN PROMOTION OF ANGIOGENESIS AND TUMOR-GROWTH - AN INVIVO MATRIGEL MODEL. *Journal of the National Cancer Institute,* 84**,** 1633-1638.
KILLIAN, E. C. O., BIRKHOLZ, D. A. & ARTINGER, K. B. 2009. A role for chemokine signaling in neural crest cell migration and craniofacial development. *Developmental Biology,* 333**,** 161-172.
KIMMEL, C. B., BALLARD, W. W., KIMMEL, S. R., ULLMANN, B. & SCHILLING, T. F. 1995. STAGES OF EMBRYONIC-DEVELOPMENT OF THE ZEBRAFISH. *Developmental Dynamics,* 203**,** 253-310.
KIMMEL, C. B., MILLER, C. T. & KEYNES, R. J. 2001. *Neural crest patterning and the evolution of the jaw*.
KINBARA, K., GOLDFINGER, L. E., HANSEN, M., CHOU, F. L. & GINSBERG, M. H. 2003. Ras GTPases: Integrins' friends or foes? *Nature Reviews Molecular Cell Biology,* 4**,** 767-776.
KIOSSES, W. B., SHATTIL, S. J., PAMPORI, N. & SCHWARTZ, M. A. 2001. Rac recruits high-affinity integrin alpha v beta 3 to lamellipodia in endothelial cell migration. *Nature Cell Biology,* 3**,** 316-320.
KIRBY, M. L., GALE, T. F. & STEWART, D. E. 1983. Neural crest cells contribute to normal aorticopulmonary septation. *Science,* 220**,** 1059-1061.
KIRBY, M. L. & HUTSON, M. R. 2010. Factors controlling cardiac neural crest cell migration. *Cell Adhesion & Migration,* 4**,** 609-621.
KLINGHOFFER, R. A., SACHSENMAIER, C., COOPER, J. A. & SORIANO, P. 1999. Src family kinases are required for integrin but not PDGFR signal transduction. *Embo Journal,* 18**,** 2459-2471.
KNAUT, H., WERZ, C., GEISLER, R., NUSSLEIN-VOLHARD, C. & TUBINGEN SCREEN, C. 2003. A zebrafish homologue of the chemokine receptor Cxcr4 is a germ-cell guidance receptor. *Nature,* 421**,** 279-282.
KNIGHT, B., LAUKAITIS, C., AKHTAR, N., HOTCHIN, N. A., EDLUND, M. & HORWITZ, A. R. 2000. Visualizing muscle cell migration in situ. *Current Biology,* 10**,** 576-585.
KOESTNER, U., SHNITSAR, I., LINNEMANNSTONS, K., HUFTON, A. L. & BORCHERS, A. 2008. Semaphorin and Neuropilin Expression During Early Morphogenesis of Xenopus laevis. *Developmental Dynamics,* 237**,** 3853-3863.
KOLEGA, J. 1981. THE MOVEMENT OF CELL CLUSTERS INVITRO - MORPHOLOGY AND DIRECTIONALITY. *Journal of Cell Science,* 49**,** 15-32.
KOLSCH, V., CHAREST, P. G. & FIRTEL, R. A. 2008. The regulation of cell motility and chemotaxis by phospholipid signaling. *Journal of Cell Science,* 121**,** 551-559.
KRAUSE, M. & GAUTREAU, A. 2014. Steering cell migration: lamellipodium dynamics and the regulation of directional persistence. *Nature Reviews Molecular Cell Biology,* 15**,** 577-590.
KRAUSE, M., LESLIE, J. D., STEWART, M., LAFUENTE, E. M., VALDERRAMA, F., JAGANNATHAN, R., STRASSER, G. A., RUBINSON, D. A., LIU, H., WAY, M., YAFFE, M. B., BOUSSIOTIS, V. A. & GERTIER, F. B. 2004. Lamellipodin, an EnaNASP ligand, is implicated in the regulation of lamellipodial dynamics. *Developmental Cell,* 7**,** 571-583.
KUBOTA, Y. & ITO, K. 2000. Chemotactic migration of mesencephalic neural crest cells in the mouse. *Developmental Dynamics,* 217**,** 170-179.
KULESA, P., ELLIES, D. L. & TRAINOR, P. A. 2004. Comparative analysis of neural crest cell death, migration, and function during vertebrate embryogenesis. *Developmental Dynamics,* 229**,** 14-29.
KULESA, P. M., BAILEY, C. M., KASEMEIER-KULESA, J. C. & MCLENNAN, R. 2010. Cranial neural crest migration: New rules for an old road. *Developmental Biology,* 344**,** 543-554.
KULESA, P. M. & FRASER, S. E. 1998. Neural crest cell dynamics revealed by time-lapse video microscopy of whole embryo chick explant cultures. *Developmental Biology,* 204**,** 327-344.
KULESA, P. M. & FRASER, S. E. 2000. In ovo time-lapse analysis of chick hindbrain neural crest cell migration shows cell interactions during migration to the branchial arches. *Development,* 127**,** 1161-1172.
KULESA, P. M. & MCLENNAN, R. 2015. Neural crest migration: trailblazing ahead. *F1000prime reports,* 7**,** 02-02.
KULESA, P. M., MORRISON, J. A. & BAILEY, C. M. 2013. The Neural Crest and Cancer: A Developmental Spin on Melanoma. *Cells Tissues Organs,* 198**,** 12-21.
KUO, B. R. & ERICKSON, C. A. 2010. Regional differences in neural crest morphogenesis. *Cell Adhesion & Migration,* 4**,** 567-585.
KURIYAMA, S. & MAYOR, R. 2008. Molecular analysis of neural crest migration. *Philosophical Transactions of the Royal Society B-Biological Sciences,* 363**,** 1349-1362.
KURIYAMA, S., THEVENEAU, E., BENEDETTO, A., PARSONS, M., TANAKA, M., CHARRAS, G., KABLA, A. & MAYOR, R. 2014. In vivo collective cell migration requires an LPAR2-dependent increase in tissue fluidity. *Journal of Cell Biology,* 206**,** 113-127.
KUWADA, S. K. & LI, X. F. 2000. Integrin alpha 5/beta 1 mediates fibronectin-dependent epithelial cell proliferation through epidermal growth factor receptor activation. *Molecular Biology of the Cell,* 11**,** 2485-2496.
LABERNADIE, A., KATO, T., BRUGUES, A., SERRA-PICAMAL, X., DERZSI, S., ARWERT, E., WESTON, A., GONZALEZ-TARRAGO, V., ELOSEGUI-ARTOLA, A., ALBERTAZZI, L., ALCARAZ, J., ROCA-CUSACHS, P., SAHAI, E. & TREPAT, X. 2017. A mechanically active heterotypic E-cadherin/N-cadherin adhesion enables fibroblasts to drive cancer cell invasion. *Nature Cell Biology,* 19**,** 224-237.
LABONNE, C. & BRONNER-FRASER, M. 2000. Snail-related transcriptional repressors are required in Xenopus for both the induction of the neural crest and its subsequent migration. *Developmental Biology,* 221**,** 195-205.
LADOUX, B. & MEGE, R. M. 2017. Mechanobiology of collective cell behaviours. *Nature Reviews Molecular Cell Biology,* 18**,** 743-757.
LADOUX, B., MEGE, R. M. & TREPAT, X. 2016. Front-Rear Polarization by Mechanical Cues: From Sincle Cells to Tissues. *Trends in Cell Biology,* 26**,** 420-433.
LADOUX, B. & NICOLAS, A. 2012. Physically based principles of cell adhesion mechanosensitivity in tissues. *Reports on Progress in Physics,* 75.
LAMALICE, L., LE BOEUF, F. & HUOT, J. 2007. Endothelial cell migration during angiogenesis. *Circulation Research,* 100**,** 782-794.
LAMMERMANN, T., AFONSO, P. V., ANGERMANN, B. R., WANG, J. M., KASTENMULLER, W., PARENT, C. A. & GERMAIN, R. N. 2013. Neutrophil swarms require LTB4 and integrins at sites of cell death in vivo. *Nature,* 498**,** 371-+.

LAMMERMANN, T., BADER, B. L., MONKLEY, S. J., WORBS, T., WEDLICH-SOLDNER, R., HIRSCH, K., KELLER, M., FORSTER, R., CRITCHLEY, D. R., FASSLER, R. & SIXT, M. 2008. Rapid leukocyte migration by integrin-independent flowing and squeezing. *Nature,* 453**,** 51-+.

LAMMERMANN, T. & SIXT, M. 2009. Mechanical modes of 'amoeboid' cell migration. *Current Opinion in Cell Biology,* 21**,** 636-644.

LAMOUILLE, S., XU, J. & DERYNCK, R. 2014. Molecular mechanisms of epithelial-mesenchymal transition. *Nature Reviews Molecular Cell Biology,* 15**,** 178-196.

LANGBEIN, L., PAPE, U. F., GRUND, C., KUHN, C., PRAETZEL, S., MOLL, I., MOLL, R. & FRANKE, W. W. 2003. Tight junction-related structures in the absence of a lumen: Occludin, claudins and tight junction plaque proteins in densely packed cell formations of stratified epithelia and squamous cell carcinomas. *European Journal of Cell Biology,* 82**,** 385-400.

LARSEN, M., TREMBLAY, M. L. & YAMADA, K. M. 2003. Phosphatases in cell-matrix adhesion and migration. *Nature Reviews Molecular Cell Biology,* 4**,** 700-711.

LARUE, L. & BELLACOSA, A. 2005. Epithelial-mesenchymal transition in development and cancer: role of phosphatidylinositol 3 ' kinase/AKT pathways. *Oncogene,* 24**,** 7443-7454.

LAUFFENBURGER, D. A. & HORWITZ, A. F. 1996. Cell migration: A physically integrated molecular process. *Cell,* 84**,** 359-369.

LAUTSCHAM, L. A., KAMMERER, C., LANGE, J. R., KOLB, T., MARK, C., SCHILLING, A., STRISSEL, P. L., STRICK, R., GLUTH, C., ROWAT, A. C., METZNER, C. & FABRY, B. 2015. Migration in Confined 3D Environments Is Determined by a Combination of Adhesiveness, Nuclear Volume, Contractility, and Cell Stiffness. *Biophysical Journal,* 109**,** 900-913.

LAW, A. L., VEHLOW, A., KOTINI, M., DODGSON, L., SOONG, D., THEVENEAU, E., BODO, C., TAYLOR, E., NAVARRO, C., PERERA, U., MICHAEL, M., DUNN, G. A., BENNETT, D., MAYOR, R. & KRAUSE, M. 2013. Lamellipodin and the Scar/WAVE complex cooperate to promote cell migration in vivo. *Journal of Cell Biology,* 203**,** 673-689.

LAWTON, A. K., NANDI, A., STULBERG, M. J., DRAY, N., SNEDDON, M. W., PONTIUS, W., EMONET, T. & HOLLEY, S. A. 2013. Regulated tissue fluidity steers zebrafish body elongation. *Development,* 140**,** 573-582.

LE BOEUF, F., HOULE, F., SUSSMAN, M. & HUOT, J. 2006. Phosphorylation of focal adhesion kinase (FAK) on Ser732 is induced by Rho-dependent kinase and is essential for proline-rich tyrosine kinase-2-mediated phosphorylation of FAK on Tyr407 in response to vascular endothelial growth factor. *Molecular Biology of the Cell,* 17**,** 3508-3520.

LE DOUARIN, N. 1969. Particularités du noyau interphasique chez la Caille japonaise (Coturnix coturnix japonica). Utilisation de ces particularités comme "marquage biologique" dans les recherches sur les interactions tissulaires et les migrations cellulaires au cours de l'ontogenèse. *Bulletin biologique de la France et de la Belgique,* 103**,** 435-452.

LE DOUARIN, N. M. 2004. The avian embryo as a model to study the development of the neural crest: a long and still ongoing story. *Mechanisms of Development,* 121**,** 1089-1102.

LE DOUARIN, N. M. & TEILLET, M. A. M. 1974. Experimental analysis of migration and differentiation of neuroblasts of autonomic nervous-system and of neurectodermal mesenchymal derivatives, using a biological cell marking technique. *Developmental Biology,* 41**,** 162-184.

LE DOUARIN, N. M., ZILLER, C. & COULY, G. F. 1993. Patterning of neural crest derivatives in the avian embryo - in-vivo and in-vitro studies. *Developmental Biology,* 159**,** 24-49.

LE NOBLE, F., KLEIN, C., TINTU, A., PRIES, A. & BUSCHMANN, I. 2008. Neural guidance molecules, tip cells, and mechanical factors in vascular development. *Cardiovascular Research,* 78**,** 232-241.

LECAUDEY, V. & GILMOUR, D. 2006. Organizing moving groups during morphogenesis. *Current Opinion in Cell Biology,* 18**,** 102-107.

LECKBAND, D. E. & DE ROOIJ, J. 2014. Cadherin Adhesion and Mechanotransduction. *Annual Review of Cell and Developmental Biology, Vol 30,* 30**,** 291-315.

LEE, G. Y., KENNY, P. A., LEE, E. H. & BISSELL, M. J. 2007. Three-dimensional culture models of normal and malignant breast epithelial cells. *Nature Methods,* 4**,** 359-365.

LEE, J., ISHIHARA, A., OXFORD, G., JOHNSON, B. & JACOBSON, K. 1999. Regulation of cell movement is mediated by stretch-activated calcium channels. *Nature,* 400**,** 382-386.

LEE, J. M., DEDHAR, S., KALLURI, R. & THOMPSON, E. W. 2006. The epithelial-mesenchymal transition: new insights in signaling, development, and disease. *Journal of Cell Biology,* 172**,** 973-981.

LEHEMBRE, F., YILMAZ, M., WICKI, A., SCHOMBER, T., STRITTMATTER, K., ZIEGLER, D., KREN, A., WENT, P., DERKSEN, P. W. B., BERNS, A., JONKERS, J. & CHRISTOFORI, G. 2008. NCAM-induced focal adhesion assembly: a functional switch upon loss of E-cadherin. *Embo Journal,* 27**,** 2603-2615.

LESHANSKY, A. M., KENNETH, O., GAT, O. & AVRON, J. E. 2007. A frictionless microswimmer. *New Journal of Physics,* 9.

LI, J. F. & LOWENGRUB, J. 2014. The effects of cell compressibility, motility and contact inhibition on the growth of tumor cell clusters using the Cellular Potts Model. *Journal of Theoretical Biology,* 343**,** 79-91.

LI, L., HARTLEY, R., REISS, B., SUN, Y. H., PU, J., WU, D., LIN, F., HOANG, T., YAMADA, S., JIANG, J. X. & ZHAO, M. 2012. E-cadherin plays an essential role in collective directional migration of large epithelial sheets. *Cellular and Molecular Life Sciences,* 69**,** 2779-2789.

LI, Z., HANNIGAN, M., MO, Z. C., LIU, B., LU, W., WU, Y., SMRCKA, A. V., WU, G. Q., LI, L., LIU, M. Y., HUANG, C. K. & WU, D. Q. 2003. Directional sensing requires G beta gamma-mediated PAK1 and PIX alpha-dependent activation of cdc42. *Cell,* 114**,** 215-227.

LIM, F. Y., KOON, Y. L. & CHIAM, K. H. 2013. A computational model of amoeboid cell migration. *Computer Methods in Biomechanics and Biomedical Engineering,* 16**,** 1085-1095.

LIN, C. H., ESPREAFICO, E. M., MOOSEKER, M. S. & FORSCHER, P. 1997. Myosin drives retrograde F-actin flow in neuronal growth cones. *Biological Bulletin,* 192**,** 183-185.

LIU, J. A., RAO, Y. X., CHEUNG, M. P. L., HUI, M. N., WU, M. H., CHAN, L. K., NG, I. O. L., NIU, B., CHEAH, K. S. E., SHARMA, R., HODGSON, L. & CHEUNG, M. 2017. Asymmetric localization of DLC1 defines avian trunk neural crest polarity for directional delamination and migration. *Nature Communications,* 8.

LIU, Q., DALMAN, M. R., SARMAH, S., CHEN, S., CHEN, Y., HURLBUT, A. K., SPENCER, M. A., PANCOE, L. & MARRS, J. A. 2011. Cell Adhesion Molecule Cadherin-6 Function in Zebrafish Cranial and Lateral Line Ganglia Development. *Developmental Dynamics,* 240**,** 1716-1726.
LIU, S., THOMAS, S. M., WOODSIDE, D. G., ROSE, D. M., KIOSSES, W. B., PFAFF, M. & GINSBERG, M. H. 1999. Binding of paxillin to alpha(4) integrins modifies integrin-dependent biological responses. *Nature,* 402**,** 676-681.
LIU, Y. J., LE BERRE, M., LAUTENSCHLAEGER, F., MAIURI, P., CALLAN-JONES, A., HEUZE, M., TAKAKI, T., VOITURIEZ, R. & PIEL, M. 2015. Confinement and Low Adhesion Induce Fast Amoeboid Migration of Slow Mesenchymal Cells. *Cell,* 160**,** 659-672.
LO, C. W., COHEN, M. F., HUANG, G. Y., LAZATIN, B. O., PATEL, N., SULLIVAN, R., PAUKEN, C. & PARK, S. M. J. 1997. Cx43 gap junction gene expression and gap junctional communication in mouse neural crest cells. *Developmental Genetics,* 20**,** 119-132.
LORING, J. F. & ERICKSON, C. A. 1987. Neural crest cell migratory pathways in the trunk of the chick-embryo. *Developmental Biology,* 121**,** 220-236.
LUCAS, E. P., KHANAL, I., GASPAR, P., FLETCHER, G. C., POLESELLO, C., TAPON, N. & THOMPSON, B. J. 2013. The Hippo pathway polarizes the actin cytoskeleton during collective migration of Drosophila border cells. *Journal of Cell Biology,* 201**,** 875-885.
LUMB, R., WISZNIAK, S., KABBARA, S., SCHERER, M., HARVEY, N. & SCHWARZ, Q. 2014. Neuropilins define distinct populations of neural crest cells. *Neural Development,* 9.
LUO, T., MATSUO-TAKASAKI, M., THOMAS, M. L., WEEKS, D. L. & SARGENT, T. D. 2002. Transcription factor AP-2 is an essential and direct regulator of epidermal development in Xenopus. *Developmental Biology,* 245**,** 136-144.
MACATEE, T. L., HAMMOND, B. P., ARENKIEL, B. R., FRANCIS, L., FRANK, D. U. & MOON, A. M. 2003. Ablation of specific expression domains reveals discrete functions of ectoderm- and endoderm-derived FGF8 during cardiovascular and pharyngeal development. *Development,* 130**,** 6361-6374.
MADSEN, C. D. & SAHAI, E. 2010. Cancer Dissemination-Lessons from Leukocytes. *Developmental Cell,* 19**,** 13-26.
MAIURI, P., RUPPRECHT, J. F., WIESER, S., RUPRECHT, V., BENICHOU, O., CARPI, N., COPPEY, M., DE BECO, S., GOV, N., HEISENBERG, C. P., CRESPO, C. L., LAUTENSCHLAEGER, F., LE BERRE, M., LENNON-DUMENIL, A. M., RAAB, M., THIAM, H. R., PIEL, M., SIXT, M. & VOITURIEZ, R. 2015. Actin Flows Mediate a Universal Coupling between Cell Speed and Cell Persistence. *Cell,* 161**,** 374-386.
MAJUMDAR, R., SIXT, M. & PARENT, C. A. 2014. New paradigms in the establishment and maintenance of gradients during directed cell migration. *Current Opinion in Cell Biology,* 30**,** 33-40.
MAJUMDER, P., ARANJUEZ, G., AMICK, J. & MCDONALD, J. A. 2012. Par-1 Controls Myosin-II Activity through Myosin Phosphatase to Regulate Border Cell Migration. *Current Biology,* 22**,** 363-372.
MALET-ENGRA, G., YU, W. M., OLDANI, A., REY-BARROSO, J., GOV, N. S., SCITA, G. & DUPRE, L. 2015. Collective Cell Motility Promotes Chemotactic Prowess and Resistance to Chemorepulsion. *Current Biology,* 25**,** 242-250.
MANCILLA, A. & MAYOR, R. 1996. Neural crest formation in Xenopus laevis: Mechanisms of Xs1ug induction. *Developmental Biology,* 177**,** 580-589.
MANDA, B., MIR, H., GANGWAR, R., MEENA, A. S., AMIN, S., SHUKLA, P. K., DALAL, K., SUZUKI, T. & RAO, R. 2018. Phosphorylation hotspot in the C-terminal domain of occludin regulates the dynamics of epithelial junctional complexes. *Journal of Cell Science,* 131.
MARCHANT, L., LINKER, C., RUIZ, P., GUERRERO, N. & MAYOR, R. 1998. The inductive properties of mesoderm suggest that the neural crest cells are specified by a BMP gradient. *Developmental Biology,* 198**,** 319-329.
MARSHALL, A. M. 1879. The morphology of the vertebrate olfactory organ. *Quarterly journal of microscopical science,* 18**,** 300-340.
MARTIK, M. L. & BRONNER, M. E. 2017. Regulatory Logic Underlying Diversification of the Neural Crest. *Trends in Genetics,* 33**,** 715-727.
MARTIN, A. C., KASCHUBE, M. & WIESCHAUS, E. F. 2009. Pulsed contractions of an actin-myosin network drive apical constriction. *Nature,* 457**,** 495-U11.
MARTIN, K., VILELA, M., JEON, N. L., DANUSER, G. & PERTZ, O. 2014. A Growth Factor-Induced, Spatially Organizing Cytoskeletal Module Enables Rapid and Persistent Fibroblast Migration. *Developmental Cell,* 30**,** 701-716.
MASON, F. M., XIE, S. C., VASQUEZ, C. G., TWOROGER, M. & MARTIN, A. C. 2016. RhoA GTPase inhibition organizes contraction during epithelial morphogenesis. *Journal of Cell Biology,* 214**,** 603-617.
MASSOUMI, R., KUPHAL, S., HELLERBRAND, C., HAAS, B., WILD, P., SPRUSS, T., PFEIFER, A., FASSLER, R. & BOSSERHOFF, A. K. 2009. Down-regulation of CYLD expression by Snail promotes tumor progression in malignant melanoma. *Journal of Experimental Medicine,* 206**,** 221-232.
MATSUZAWA, K., HIMOTO, T., MOCHIZUKI, Y. & IKENOUCHI, J. 2018. alpha-Catenin Controls the Anisotropy of Force Distribution at Cell-Cell Junctions during Collective Cell Migration. *Cell Reports,* 23**,** 3447-3456.
MATTHEWS, H. K., MARCHANT, L., CARMONA-FONTAINE, C., KURIYAMA, S., LARRAIN, J., HOLT, M. R., PARSONS, M. & MAYOR, R. 2008. Directional migration of neural crest cells in vivo is regulated by Syndecan-4/Rac1 and non-canonical Wnt signaling/RhoA. *Development,* 135**,** 1771-1780.
MATTILA, P. K. & LAPPALAINEN, P. 2008. Filopodia: molecular architecture and cellular functions. *Nature Reviews Molecular Cell Biology,* 9**,** 446-454.
MAYOR, R. & CARMONA-FONTAINE, C. 2010. Keeping in touch with contact inhibition of locomotion. *Trends in Cell Biology,* 20**,** 319-328.
MAYOR, R. & ETIENNE-MANNEVILLE, S. 2016. The front and rear of collective cell migration. *Nature Reviews Molecular Cell Biology,* 17**,** 97-109.
MAYOR, R., GUERRERO, N., YOUNG, R. M., GOMEZ-SKARMETA, J. L. & CUELLAR, C. 2000. A novel function for the Xslug gene: control of dorsal mesendoderm development by repressing BMP-4. *Mechanisms of Development,* 97**,** 47-56.
MAYOR, R. & THEVENEAU, E. 2013. The neural crest. *Development,* 140**,** 2247-2251.
MAYOR, R. & THEVENEAU, E. 2014. The role of the non-canonical Wnt-planar cell polarity pathway in neural crest migration. *Biochemical Journal,* 457**,** 19-26.

MCLENNAN, R., BAILEY, C. M., SCHUMACHER, L. J., TEDDY, J. M., MORRISON, J. A., KASEMEIER-KULESA, J. C., WOLFE, L. A., GOGOL, M. M., BAKER, R. E., MAINI, P. K. & KULESA, P. M. 2017. DAN (NBL1) promotes collective neural crest migration by restraining uncontrolled invasion. *Journal of Cell Biology,* 216**,** 3339-3354.
MCLENNAN, R., DYSON, L., PRATHER, K. W., MORRISON, J. A., BAKER, R. E., MAINI, P. K. & KULESA, P. M. 2012. Multiscale mechanisms of cell migration during development: theory and experiment. *Development,* 139**,** 2935-2944.
MCLENNAN, R. & KULESA, P. M. 2007. In vivo analysis reveals a critical role for neuropilin-1 in cranial neural crest cell migration in chick. *Developmental Biology,* 301**,** 227-239.
MCLENNAN, R. & KULESA, P. M. 2010. Neuropilin-1 Interacts With the Second Branchial Arch Microenvironment to Mediate Chick Neural Crest Cell Dynamics. *Developmental Dynamics,* 239**,** 1664-1673.
MCLENNAN, R., LJ, S., JA, M., JM, T., DA, R., AC, B., CL, S., H, L., W, M., D, K., PK, M., RE, B. & PM, K. 2015. VEGF signals induce trailblazer cell identity that drives neural crest migration. Developmental Biology.
MCLENNAN, R., TEDDY, J. M., KASEMEIER-IULESA, J. C., ROMINE, M. H. & KULESA, P. M. 2010. Vascular endothelial growth factor (VEGF) regulates cranial neural crest migration in vivo. *Developmental Biology,* 339**,** 114-125.
MCLIN, V. A., HU, C.-H., SHAH, R. & JAMRICH, M. 2008. Expression of complement components coincides with early patterning and organogenesis in Xenopus laevis. *International Journal of Developmental Biology,* 52**,** 1123-1133.
MELLOTT, D. O. & BURKE, R. D. 2008. Divergent roles for Eph and Ephrin in Avian Cranial Neural Crest. *Bmc Developmental Biology,* 8.
MERLOT, S. & FIRTEL, R. A. 2003. Leading the way: directional sensing through phosphatidylinositol 3-kinase and other signaling pathways. *Journal of Cell Science,* 116**,** 3471-3478.
MEULEMANS, D. & BRONNER-FRASER, M. 2004. Gene-regulatory interactions in neural crest evolution and development. *Developmental Cell,* 7**,** 291-299.
MILET, C. & MONSORO-BURQ, A. H. 2012. Neural crest induction at the neural plate border in vertebrates. *Developmental Biology,* 366**,** 22-33.
MITRA, S. K., HANSON, D. A. & SCHLAEPFER, D. D. 2005. Focal adhesion kinase: In command and control of cell motility. *Nature Reviews Molecular Cell Biology,* 6**,** 56-68.
MLODZIK, M. 1999. Planar polarity in the Drosophila eye: a multifaceted view of signaling specificity and cross-talk. *Embo Journal,* 18**,** 6873-6879.
MONGERA, A., ROWGHANIAN, P., GUSTAFSON, H. J., SHELTON, E., KEALHOFER, D. A., CARN, E. K., SERWANE, F., LUCIO, A. A., GIAMMONA, J. & CAMPAS, O. 2018. A fluid-to-solid jamming transition underlies vertebrate body axis elongation. *Nature*.
MONTELL, D. J. 2003. Border-cell migration: The race is on. *Nature Reviews Molecular Cell Biology,* 4**,** 13-24.
MONTELL, D. J. 2008. Morphogenetic Cell Movements: Diversity from Modular Mechanical Properties. *Science,* 322**,** 1502-1505.
MONTELL, D. J., YOON, W. H. & STARZ-GAIANO, M. 2012. Group choreography: mechanisms orchestrating the collective movement of border cells. *Nature Reviews Molecular Cell Biology,* 13**,** 631-645.
MONZO, P., CHONG, Y. K., GUETTA-TERRIER, C., KRISHNASAMY, A., SATHE, S. R., YIM, E. K. F., NG, W. H., ANG, B. T., TANG, C., LADOUX, B., GAUTHIER, N. C. & SHEETZ, M. P. 2016. Mechanical confinement triggers glioma linear migration dependent on formin FHOD3. *Molecular Biology of the Cell,* 27**,** 1246-1261.
MOORE, R., THEVENEAU, E., POZZI, S., ALEXANDRE, P., RICHARDSON, J., MERKS, A., PARSONS, M., KASHEF, J., LINKER, C. & MAYOR, R. 2013. Par3 controls neural crest migration by promoting microtubule catastrophe during contact inhibition of locomotion. *Development,* 140**,** 4763-+.
MOREAU, V., FRISCHKNECHT, F., RECKMANN, I., VINCENTELLI, R., RABUT, G., STEWART, D. & WAY, M. 2000. A complex of N-WASP and WIP integrates signalling cascades that lead to actin polymerization. *Nature Cell Biology,* 2**,** 441-448.
MORRISON-GRAHAM, K., SCHATTEMAN, G. C., BORK, T., BOWENPOPE, D. F. & WESTON, J. A. 1992. A PDGF receptor mutation in the mouse (Patch) perturbs the development ofa nonneuronal subset of neural crest-derived cells. *Development,* 115**,** 133-142.
MSEKA, T. & CRAMER, L. P. 2011. Actin Depolymerization-Based Force Retracts the Cell Rear in Polarizing and Migrating Cells. *Current Biology,* 21**,** 2085-2091.
MUELLER, J., SZEP, G., NEMETHOVA, M., DE VRIES, I., LIEBER, A. D., WINKLER, C., KRUSE, K., SMALL, J. V., SCHMEISER, C., KEREN, K., HAUSCHILD, R. & SIXT, M. 2017. Load Adaptation of Lamellipodial Actin Networks. *Cell,* 171**,** 188-+.
MUGLER, A., LEVCHENKO, A. & NEMENMAN, I. 2016. Limits to the precision of gradient sensing with spatial communication and temporal integration. *Proceedings of the National Academy of Sciences of the United States of America,* 113**,** E689-E695.
MUINONEN-MARTIN, A. J., SUSANTO, O., ZHANG, Q. F., SMETHURST, E., FALLER, W. J., VELTMAN, D. M., KALNA, G., LINDSAY, C., BENNETT, D. C., SANSOM, O. J., HERD, R., JONES, R., MACHESKY, L. M., WAKELAM, M. J. O., KNECHT, D. A. & INSALL, R. H. 2014. Melanoma Cells Break Down LPA to Establish Local Gradients That Drive Chemotactic Dispersal. *Plos Biology,* 12.
MUNJAL, A., PHILIPPE, J. M., MUNRO, E. & LECUIT, T. 2015. A self-organized biomechanical network drives shape changes during tissue morphogenesis. *Nature,* 524**,** 351-+.
MUNOZ, W. A. & TRAINOR, P. A. 2015. Neural Crest Cell Evolution: How and When Did a Neural Crest Cell Become a Neural Crest Cell. *Neural Crest and Placodes,* 111**,** 3-26.
MURRELL, M., OAKES, P. W., LENZ, M. & GARDEL, M. L. 2015. Forcing cells into shape: the mechanics of actomyosin contractility. *Nature Reviews Molecular Cell Biology,* 16**,** 486-498.
MWIZERWA, O., DAS, P., NAGY, N., AKBAREIAN, S. E., MABLY, J. D. & GOLDSTEIN, A. M. 2011. Gdnf Is Mitogenic, Neurotrophic, and Chemoattractive to Enteric Neural Crest Cells in the Embryonic Colon. *Developmental Dynamics,* 240**,** 1402-1411.
NABESHIMA, K., INOUE, T., SHIMAO, Y., OKADA, Y., ITOH, Y., SEIKI, M. & KOONO, M. 2000. Front-cell-specific expression of membrane-type 1 matrix metalloproteinase and gelatinase a during cohort migration of colon carcinoma cells induced by hepatocyte growth factor/scatter factor. *Cancer Research,* 60**,** 3364-3369.

NABESHIMA, K., SHIMAO, Y., INOUE, T., ITOH, H., KATAOKA, H. & KOONO, M. 1998. Hepatocyte growth factor/scatter factor induces not only scattering but also cohort **migration** of human colorectal-adenocarcinoma cells. *International Journal of Cancer,* 78**,** 750-9.
NAGASAWA, T., HIROTA, S., TACHIBANA, K., TAKAKURA, N., NISHIKAWA, S., KITAMURA, Y., YOSHIDA, N., KIKUTANI, H. & KISHIMOTO, T. 1996. Defects of B-cell lymphopoiesis and bone-marrow myelopoiesis in mice lacking the CXC chemokine PBSF/SDF-1. *Nature,* 382**,** 635-638.
NAKAGAWA, M., FUKATA, M., YAMAGA, M., ITOH, N. & KAIBUCHI, K. 2001. Recruitment and activation of Rac1 by the formation of E-cadherin-mediated cell-cell adhesion sites. *Journal of Cell Science,* 114**,** 1829-1838.
NAKAGAWA, S. & TAKEICHI, M. 1995. Neural crest cell-cell adhesion controlled by sequential and subpopulation-specific expression of novel cadherins. *Development,* 121**,** 1321-1332.
NANDADASA, S., TAO, Q., MENON, N. R., HEASMAN, J. & WYLIE, C. 2009. N- and E-cadherins in Xenopus are specifically required in the neural and non-neural ectoderm, respectively, for F-actin assembly and morphogenetic movements. *Development,* 136**,** 1327-1338.
NETOTEA, S., BERTANI, I., STEINDLER, L., KERENYI, A., VENTURI, V. & PONGOR, S. 2009. A simple model for the early events of quorum sensing in Pseudomonas aeruginosa: modeling bacterial swarming as the movement of an "activation zone". *Biology Direct,* 4.
NGUYEN, B. P., RYAN, M. C., GIL, S. G. & CARTER, W. G. 2000. Deposition of laminin 5 in epidermal wounds regulates integrin signaling and adhesion. *Current Opinion in Cell Biology,* 12**,** 554-562.
NGUYEN, V. H., SCHMID, B., TROUT, J., CONNORS, S. A., EKKER, M. & MULLINS, M. C. 1998. Ventral and lateral regions of the zebrafish gastrula, including the neural crest progenitors, are established by a bmp2b/swirl pathway of genes. *Developmental Biology,* 199**,** 93-110.
NICHOLS, D. H. 1981. NEURAL CREST FORMATION IN THE HEAD OF THE MOUSE EMBRYO AS OBSERVED USING A NEW HISTOLOGICAL TECHNIQUE. *Journal of Embryology and Experimental Morphology,* 64**,** 105-120.
NICHOLS, D. H. 1987. ULTRASTRUCTURE OF NEURAL CREST FORMATION IN THE MIDBRAIN ROSTRAL HINDBRAIN AND PREOTIC HINDBRAIN REGIONS OF THE MOUSE EMBRYO. *American Journal of Anatomy,* 179**,** 143-154.
NIESSEN, C. M. 2007. Tight junctions/adherens junctions: Basic structure and function. *Journal of Investigative Dermatology,* 127**,** 2525-2532.
NIETO, M. A. & CANO, A. 2012. The epithelial-mesenchymal transition under control: Global programs to regulate epithelial plasticity. *Seminars in Cancer Biology,* 22**,** 361-368.
NIETO, M. A., SARGENT, M. G., WILKINSON, D. G. & COOKE, J. 1994. CONTROL OF CELL BEHAVIOR DURING VERTEBRATE DEVELOPMENT BY SLUG, A ZINC-FINGER GENE. *Science,* 264**,** 835-839.
NIEUWKOOP, P. & FABER, J. 1967. *Normal table of Xenopus laevis (Daudin) : a systematical and chronological survey of the development from the fertilized egg till the end of metamorphosis*, North-Holland.
NIEWIADOMSKA, P., GODT, D. & TEPASS, U. 1999. DE-cadherin is required for intercellular motility during Drosophila oogenesis. *Journal of Cell Biology,* 144**,** 533-547.
NIKITINA, N., SAUKA-SPENGLER, T. & BRONNER-FRASER, M. 2008. Dissecting early regulatory relationships in the lamprey neural crest gene network. *Proceedings of the National Academy of Sciences of the United States of America,* 105**,** 20083-20088.
NISCHT, R., SCHMIDT, C., MIRANCEA, N., BARANOWSKY, A., MOKKAPATI, S., SMYTH, N., WOENNE, E. C., STARK, H. J., BOUKAMP, P. & BREITKREUTZ, D. 2007. Lack of nidogen-1 and -2 prevents basement membrane assembly in skin-organotypic coculture. *Journal of Investigative Dermatology,* 127**,** 545-554.
NISHIMURA, T., HONDA, H. & TAKEICHI, M. 2012. Planar Cell Polarity Links Axes of Spatial Dynamics in Neural-Tube Closure. *Cell,* 149**,** 1084-1097.
NOBES, C. D. & HALL, A. 1999. Rho GTPases control polarity, protrusion, and adhesion during cell movement. *Journal of Cell Biology,* 144**,** 1235-1244.
NOGARE, D. D., SOMERS, K., RAO, S., MATSUDA, M., REICHMAN-FRIED, M., RAZ, E. & CHITNIS, A. B. 2014. Leading and trailing cells cooperate in collective migration of the zebrafish posterior lateral line primordium. *Development,* 141**,** 3188-3196.
NOGUERA-TROISE, I., DALY, C., PAPADOPOULOS, N. J., COETZEE, S., BOLAND, P., GALE, N. W., LIN, H. C., YANCOPOULOS, G. D. & THURSTON, G. 2006. Blockade of Dll4 inhibits tumour growth by promoting non-productive angiogenesis. *Nature,* 444**,** 1032-1037.
NORTHCUTT, R. G. & GANS, C. 1983. THE GENESIS OF NEURAL CREST AND EPIDERMAL PLACODES - A REINTERPRETATION OF VERTEBRATE ORIGINS. *Quarterly Review of Biology,* 58**,** 1-28.
O'NEILL, P. R., CASTILLO-BADILLO, J. A., MESHIK, X., KALYANARAMAN, V., MELGAREJO, K. & GAUTAM, N. 2018. Membrane Flow Drives an Adhesion-Independent Amoeboid Cell Migration Mode. *Developmental Cell,* 46**,** 9-+.
OMELCHENKO, T. & HALL, A. 2012. Myosin-IXA Regulates Collective Epithelial Cell Migration by Targeting RhoGAP Activity to Cell-Cell Junctions. *Current Biology,* 22**,** 278-288.
OMELCHENKO, T., VASILIEV, J. M., GELFAND, I. M., FEDER, H. H. & BONDER, E. M. 2003. Rho-dependent formation of epithelial "leader" cells during wound healing. *Proceedings of the National Academy of Sciences of the United States of America,* 100**,** 10788-10793.
ORIMO, A., GUPTA, P. B., SGROI, D. C., ARENZANA-SEISDEDOS, F., DELAUNAY, T., NAEEM, R., CAREY, V. J., RICHARDSON, A. L. & WEINBERG, R. A. 2005. Stromal fibroblasts present in invasive human breast carcinomas promote tumor growth and angiogenesis through elevated SDF-1/CXCL12 secretion. *Cell,* 121**,** 335-348.
ORRURTREGER, A., BEDFORD, M. T., DO, M. S., EISENBACH, L. & LONAI, P. 1992. Developmental expression of the alpha receptor for platelet-derived growth-factor, which is deleted in the embryonic lethal patch mutation. *Development,* 115**,** 289-303.
OSBORNE, N. J., BEGBIE, J., CHILTON, J. K., SCHMIDT, H. & EICKHOLT, B. J. 2005. Semaphorin/neuropilin signaling influences the positioning of migratory neural crest cells within the hindbrain region of the chick. *Developmental Dynamics,* 232**,** 939-949.
OTA, K. G., KURAKU, S. & KURATANI, S. 2007. Hagfish embryology with reference to the evolution of the neural crest. *Nature,* 446**,** 672-675.

OTEY, C. A., PAVALKO, F. M. & BURRIDGE, K. 1990. AN INTERACTION BETWEEN ALPHA-ACTININ AND THE BETA-1 INTEGRIN SUBUNIT INVITRO. *Journal of Cell Biology,* 111**,** 721-729.
OVERSTREET, M. G., GAYLO, A., ANGERMANN, B. R., HUGHSON, A., HYUN, Y. M., LAMBERT, K., ACHARYA, M., BILLROTH-MACLURG, A. C., ROSENBERG, A. F., TOPHAM, D. J., YAGITA, H., KIM, M., LACY-HULBERT, A., MEIER-SCHELLERSHEIM, M. & FOWELL, D. J. 2013. Inflammation-induced interstitial migration of effector CD4(+) T cells is dependent on integrin alpha(V). *Nature Immunology,* 14**,** 949-+.
PALMIERI, D., ASTIGIANO, S., BARBIERI, O., FERRARI, N., MARCHISIO, S., ULIVI, V., VOLTA, C. & MANDUCA, P. 2008. Procollagen ICOOH-terminal fragment induces VEGF-A and CXCR4 expression in breast carcinoma cells. *Experimental Cell Research,* 314**,** 2289-2298.
PALUCH, E. K., ASPALTER, I. M. & SIXT, M. 2016. Focal Adhesion-Independent Cell Migration. *Annual Review of Cell and Developmental Biology, Vol 32,* 32**,** 469-490.
PALUCH, E. K. & RAZ, E. 2013. The role and regulation of blebs in cell migration. *Current Opinion in Cell Biology,* 25**,** 582-590.
PANDYA, P., ORGAZ, J. L. & SANZ-MORENO, V. 2017. Actomyosin contractility and collective migration: may the force be with you. *Current Opinion in Cell Biology,* 48**,** 87-96.
PANKOVA, K., ROSEL, D., NOVOTNY, M. & BRABEK, J. 2010. The molecular mechanisms of transition between mesenchymal and amoeboid invasiveness in tumor cells. *Cellular and Molecular Life Sciences,* 67**,** 63-71.
PARK, K. S. & GUMBINER, B. M. 2012. Cadherin-6B stimulates an epithelial mesenchymal transition and the delamination of cells from the neural ectoderm via LIMK/cofilin mediated non-canonical BMP receptor signaling. *Developmental Biology,* 366**,** 232-243.
PARSONS, J. T., HORWITZ, A. R. & SCHWARTZ, M. A. 2010. Cell adhesion: integrating cytoskeletal dynamics and cellular tension. *Nature Reviews Molecular Cell Biology,* 11**,** 633-643.
PEGLION, F., LLENSE, F. & ETIENNE-MANNEVILLE, S. 2014. Adherens junction treadmilling during collective migration. *Nature Cell Biology,* 16**,** 639-+.
PENG, H. S., ONG, Y. M., SHAH, W. A., HOLLAND, P. C. & CARBONETTO, S. 2013. Integrins regulate centrosome integrity and astrocyte polarization following a wound. *Developmental Neurobiology,* 73**,** 333-353.
PERADZIRYI, H., KAPLAN, N. A., PODLESCHNY, M., LIU, X. P., WEHNER, P., BORCHERS, A. & TOLWINSKI, N. S. 2011. PTK7/Otk interacts with Wnts and inhibits canonical Wnt signalling. *Embo Journal,* 30**,** 3729-3740.
PEREZ-ALCALA, S., NIETO, M. A. & BARBAS, J. A. 2004. LSox5 regulates RhoB expression in the neural tube and promotes generation of the neural crest. *Development,* 131**,** 4455-4465.
PERRIS, R. 1997. The extracellular matrix in neural crest-cell migration. *Trends in Neurosciences,* 20**,** 23-31.
PERTZ, O., HODGSON, L., KLEMKE, R. L. & HAHN, K. M. 2006. Spatiotemporal dynamics of RhoA activity in migrating cells. *Nature,* 440**,** 1069-1072.
PETRIE, R. J., DOYLE, A. D. & YAMADA, K. M. 2009. Random versus directionally persistent cell migration. *Nature Reviews Molecular Cell Biology,* 10**,** 538-549.
PFEFFER, W. 1884. Locomotorische Richtungsbewegungen durch chemische Reize. Untersuch. Bot. Inst. Tübingen.
PIETRAS, K. & OSTMAN, A. 2010. Hallmarks of cancer: Interactions with the tumor stroma. *Experimental Cell Research,* 316**,** 1324-1331.
PLA, P., MOORE, R., MORALI, O. G., GRILLE, S., MARTINOZZI, S., DELMAS, V. & LARUE, L. 2001. Cadherins in neural crest cell development and transformation. *Journal of Cellular Physiology,* 189**,** 121-132.
PLOU, J., JUSTE-LANAS, Y., V, O., DEL AMO, C., BORAU, C. & GARCÍA-AZNAR, J. 2018. From individual to collective 3D cancer dissemination: roles of collagen concentration and TGF-β. *Scientific Reports,* 8.
PLUTONI, C., BAZELLIERES, E., LE BORGNE-ROCHET, M., COMUNALE, F., BRUGUES, A., SEVENO, M., PLANCHON, D., THUAULT, S., MORIN, N., BODIN, S., TREPAT, X. & GAUTHIER-ROUVIERE, C. 2016. P-cadherin promotes collective cell migration via a Cdc42-mediated increase in mechanical forces. *Journal of Cell Biology,* 212**,** 199-217.
POCHA, S. M. & MONTELL, D. J. 2014. Cellular and Molecular Mechanisms of Single and Collective Cell Migrations in Drosophila: Themes and Variations. *Annual Review of Genetics, Vol 48,* 48**,** 295-318.
POINCLOUX, R., COLLIN, O., LIZARRAGA, F., ROMAO, M., DEBRAY, M., PIEL, M. & CHAVRIER, P. 2011. Contractility of the cell rear drives invasion of breast tumor cells in 3D Matrigel. *Proceedings of the National Academy of Sciences of the United States of America,* 108**,** 1943-1948.
POLLARD, T. D. & BORISY, G. G. 2003. Cellular motility driven by assembly and disassembly of actin filaments. *Cell,* 112**,** 453-465.
POUKKULA, M., CLIFFE, A., CHANGEDE, R. & RORTH, P. 2011. Cell behaviors regulated by guidance cues in collective migration of border cells. *Journal of Cell Biology,* 192**,** 513-524.
POWELL, D. R., BLASKY, A. J., BRITT, S. G. & ARTINGER, K. B. 2013. Riding the crest of the wave: parallels between the neural crest and cancer in epithelial-to-mesenchymal transition and migration. *Wiley Interdisciplinary Reviews-Systems Biology and Medicine,* 5**,** 511-522.
PRASAD, M. & MONTELL, D. J. 2007. Cellular and molecular mechanisms of border cell migration analyzed using time-lapse live-cell Imaging. *Developmental Cell,* 12**,** 997-1005.
PRASAD, M. S., SAUKA-SPENGLER, T. & LABONNE, C. 2012. Induction of the neural crest state: Control of stem cell attributes by gene regulatory, post-transcriptional and epigenetic interactions. *Developmental Biology,* 366**,** 10-21.
PRIYA, M. K., SAHU, G., SOTO-PANTOJA, D. R., GOLDY, N., SUNDARESAN, A. M., JADHAV, V., BARATHKUMAR, T. R., SARAN, U., ALI, B. M., ROBERTS, D. D., BERA, A. K. & CHATTERJEE, S. 2015. Tipping off endothelial tubes: nitric oxide drives tip cells. *Angiogenesis,* 18**,** 175-189.
PRUITT, B. L., DUNN, A. R., WEIS, W. I. & NELSON, W. J. 2014. Mechano-Transduction: From Molecules to Tissues. *Plos Biology,* 12.
PURCELL, E. M. 1977. LIFE AT LOW REYNOLDS-NUMBER. *American Journal of Physics,* 45**,** 3-11.
RABADAN, M. A., HERRERA, A., FANLO, L., USIETO, S., CARMONA-FONTAINE, C., BARRIGA, E. H., MAYOR, R., PONS, S. & MARTI, E. 2016. Delamination of neural crest cells requires transient and reversible Wnt inhibition mediated by Dact1/2. *Development,* 143**,** 2194-2205.
RANGARAJAN, J., LUO, T. & SARGENT, T. D. 2006. PCNS: A novel protocadherin required for cranial neural crest migration and somite morphogenesis in Xenopus. *Developmental Biology,* 295**,** 206-218.

RAUCHER, D. & SHEETZ, M. P. 2000. Cell spreading and lamellipodial extension rate is regulated by membrane tension. *Journal of Cell Biology,* 148**,** 127-136.
RAUZI, M., LENNE, P. F. & LECUIT, T. 2010. Planar polarized actomyosin contractile flows control epithelial junction remodelling. *Nature,* 468**,** 1110-U515.
RAWLES, M. E. 1948. Origin of melanophores and their role in development of color patterns in vetebrates. *Physiological Reviews,* 28**,** 383-408.
REFFAY, M., PARRINI, M. C., COCHET-ESCARTIN, O., LADOUX, B., BUGUIN, A., COSCOY, S., AMBLARD, F., CAMONIS, J. & SILBERZAN, P. 2014. Interplay of RhoA and mechanical forces in collective cell migration driven by leader cells. *Nature Cell Biology,* 16**,** 217-+.
REHIM, R., KHALIDA, N., YUSUF, F., DAI, F., MOROSAN-PUOPOLO, G. & BRAND-SABER, B. 2008. Stromal-derived factor-1 (SDF-1) expression during early chick development. *International Journal of Developmental Biology,* 52**,** 87-92.
RENKAWITZ, J. & SIXT, M. 2010. Mechanisms of force generation and force transmission during interstitial leukocyte migration. *Embo Reports,* 11**,** 744-750.
REVENU, C., STREICHAN, S., DONA, E., LECAUDEY, V., HUFNAGEL, L. & GILMOUR, D. 2014. Quantitative cell polarity imaging defines leader-to-follower transitions during collective migration and the key role of microtubule-dependent adherens junction formation. *Development,* 141**,** 1282-U195.
REZZOUG, F., SEELAN, R. S., BHATTACHERJEE, V., GREENE, R. M. & PISANO, M. M. 2011. Chemokine-mediated migration of mesencephalic neural crest cells. *Cytokine,* 56**,** 760-768.
RIAHI, R., SUN, J., WANG, S., LONG, M., ZHANG, D. D. & WONG, P. K. 2015. Notch1-Dll4 signalling and mechanical force regulate leader cell formation during collective cell migration. *Nature Communications,* 6.
RIBEIRO, C., EBNER, A. & AFFOLTER, M. 2002. In vivo Imaging reveals different cellular functions for FGF and Dpp signaling in tracheal branching morphogenesis. *Developmental Cell,* 2**,** 677-683.
RICHARDSON, B. E., BECKETT, K., NOWAK, S. J. & BAYLIES, M. K. 2007. SCAR/WAVE and Arp2/3 are crucial for cytoskeletal remodeling at the site of myoblast fusion. *Development,* 134**,** 4357-4367.
RICHARDSON, J., GAUERT, A., MONTECINOS, L. B., FANLO, L., ALHASHEM, Z. M., ASSAR, R., MARTI, E., KABLA, A., HARTEL, S. & LINKER, C. 2016. Leader Cells Define Directionality of Trunk, but Not Cranial, Neural Crest Cell Migration. *Cell Reports,* 15**,** 2076-2088.
RICHARTE, A. M., MEAD, H. B. & TALLQUIST, M. D. 2007. Cooperation between the PDGF receptors in cardiac neural crest cell migration. *Developmental Biology,* 306**,** 785-796.
RICKMANN, M., FAWCETT, J. W. & KEYNES, R. J. 1985. The migration of neural crest cells and the growth of motor axons through the rostral half of the chick somite. *Journal of Embryology and Experimental Morphology,* 90**,** 437-455.
RICOULT, S. G., KENNEDY, T. E. & JUNCKER, D. 2015. Substrate-bound protein gradients to study haptotaxis. *Frontiers in bioengineering and biotechnology,* 3**,** 40-40.
RIDGWAY, J., ZHANG, G., WU, Y., STAWICKI, S., LIANG, W. C., CHANTHERY, Y., KOWALSKI, J., WATTS, R. J., CALLAHAN, C., KASMAN, I., SINGH, M., CHIEN, M., TAN, C., HONGO, J. A. S., DE SAUVAGE, F., PLOWMAN, G. & YAN, M. H. 2006. Inhibition of Dll4 signalling inhibits tumour growth by deregulating angiogenesis. *Nature,* 444**,** 1083-1087.
RIDLEY, A. J. 2015. Rho GTPase signalling in cell migration. *Current Opinion in Cell Biology,* 36**,** 103-112.
RIDLEY, A. J., SCHWARTZ, M. A., BURRIDGE, K., FIRTEL, R. A., GINSBERG, M. H., BORISY, G., PARSONS, J. T. & HORWITZ, A. R. 2003. Cell migration: Integrating signals from front to back. *Science,* 302**,** 1704-1709.
RIENTO, K. & RIDLEY, A. J. 2003. Rocks: Multifunctional kinases in cell behaviour. *Nature Reviews Molecular Cell Biology,* 4**,** 446-456.
RINON, A., MOLCHADSKY, A., NATHAN, E., YOVEL, G., ROTTER, V., SARIG, R. & TZAHOR, E. 2011. p53 coordinates cranial neural crest cell growth and epithelial-mesenchymal transition/delamination processes. *Development,* 138**,** 1827-1838.
RIZZA, A., WALIA, A., LANQUAR, V., FROMMER, W. B. & JONES, A. M. 2017. In vivo gibberellin gradients visualized in rapidly elongating tissues. *Nature Plants,* 3**,** 803-813.
ROBBINS, J. R., MCGUIRE, P. G., WEHRLE-HALLER, B. & ROGERS, S. L. 1999. Diminished matrix metalloproteinase 2 (MMP-2) in ectomesenchyme-derived tissues of the Patch mutant mouse: Regulation of MMP-2 by PDGF and effects on mesenchymal cell migration. *Developmental Biology,* 212**,** 255-263.
ROCA-CUSACHS, P., SUNYER, R. & TREPAT, X. 2013. Mechanical guidance of cell migration: lessons from chemotaxis. *Current Opinion in Cell Biology,* 25**,** 543-549.
RODRIGUEZ, O. C., SCHAEFER, A. W., MANDATO, C. A., FORSCHER, P., BEMENT, W. M. & WATERMAN-STORER, C. M. 2003. Conserved microtubule-actin interactions in cell movement and morphogenesis. *Nature Cell Biology,* 5**,** 599-609.
ROGERS, C. D., JAYASENA, C. S., NIE, S. & BRONNER, M. E. 2012. Neural crest specification: tissues, signals, and transcription factors. *Wiley Interdisciplinary Reviews-Developmental Biology,* 1**,** 52-68.
ROGERS, C. D., SAXENA, A. & BRONNER, M. E. 2013. Sip1 mediates an E-cadherin-to-N-cadherin switch during cranial neural crest EMT. *Journal of Cell Biology,* 203**,** 835-847.
ROH-JOHNSON, M., SHEMER, G., HIGGINS, C. D., MCCLELLAN, J. H., WERTS, A. D., TULU, U. S., GAO, L., BETZIG, E., KIEHART, D. P. & GOLDSTEIN, B. 2012. Triggering a Cell Shape Change by Exploiting Preexisting Actomyosin Contractions. *Science,* 335**,** 1232-1235.
RORTH, P. 2009. Collective Cell Migration. *Annual Review of Cell and Developmental Biology,* 25**,** 407-429.
ROSZIK, J., LISBOA, D., SZOLLOSI, J. & VEREB, G. 2009. Evaluation of Intensity-Based Ratiometric FRET in Image Cytometry-Approaches and a Software Solution. *Cytometry Part A,* 75A**,** 761-767.
ROUSSOS, E. T., CONDEELIS, J. S. & PATSIALOU, A. 2011. Chemotaxis in cancer. *Nature Reviews Cancer,* 11**,** 573-587.
ROVASIO, R. A., FAAS, L. & BATTIATO, N. L. 2012. Insights into Stem Cell Factor chemotactic guidance of neural crest cells revealed by a real-time directionality-based assay. *European Journal of Cell Biology,* 91**,** 375-390.
ROYCROFT, A. & MAYOR, R. 2016. Molecular basis of contact inhibition of locomotion. *Cellular and Molecular Life Sciences,* 73**,** 1119-1130.

ROYCROFT, A., SZABO, A., BAHM, I., DALY, L., CHARRAS, G., PARSONS, M. & MAYOR, R. 2018. Redistribution of Adhesive Forces through Src/FAK Drives Contact Inhibition of Locomotion in Neural Crest. *Developmental Cell,* 45**,** 565-+.
ROZBICKI, E., CHUAI, M., KARJALAINEN, A. I., SONG, F. F., SANG, H. M., MARTIN, R., KNOLKER, H. J., MACDONALD, M. P. & WEIJER, C. J. 2015. Myosin-II-mediated cell shape changes and cell intercalation contribute to primitive streak formation. *Nature Cell Biology,* 17**,** 397-+.
RUPRECHT, V., WIESER, S., CALLAN-JONES, A., SMUTNY, M., MORITA, H., SAKO, K., BARONE, V., RITSCH-MARTE, M., SIXT, M., VOITURIEZ, R. & HEISENBERG, C. P. 2015. Cortical Contractility Triggers a Stochastic Switch to Fast Amoeboid Cell Motility. *Cell,* 160**,** 673-685.
RUTH, E. S. 1911. Cicatrization of wounds in vitro. *Journal of Experimental Medicine,* 13**,** 422-U28.
RÖPER, K. 2013. Supracellular actomyosin assemblies during development. *Bioarchitecture,* 3**,** 45-49.
SADAGHIANI, B. & THIEBAUD, C. H. 1987. NEURAL CREST DEVELOPMENT IN THE XENOPUS-LAEVIS EMBRYO, STUDIED BY INTERSPECIFIC TRANSPLANTATION AND SCANNING ELECTRON-MICROSCOPY. *Developmental Biology,* 124**,** 91-110.
SAIKA, S., LIU, C. Y., AZHAR, M., SANFORD, L. P., DOETSCHMAN, T., GENDRON, R. L., KAO, C. W. C. & KAO, W. W. Y. 2001. TGF beta 2 in corneal morphogenesis during mouse embryonic development. *Developmental Biology,* 240**,** 419-432.
SAITO, D., TAKASE, Y., MURAI, H. & TAKAHASHI, Y. 2012. The Dorsal Aorta Initiates a Molecular Cascade That Instructs Sympatho-Adrenal Specification. *Science,* 336**,** 1578-1581.
SALMENPERA, P., KANKURI, E., BIZIK, J., SIREN, V., VIRTANEN, I., TAKAHASHI, S., LEISS, M., FASSLER, R. & VAHERI, A. 2008. Formation and activation of fibroblast spheroids depend on fibronectin-integrin interaction. *Experimental Cell Research,* 314**,** 3444-3452.
SANES, D. 2012. *Development of the Nervous System*, Oxford: ELSEVIER INC.
SANTIAGO, A. & ERICKSON, C. A. 2002. Ephrin-B ligands play a dual role in the control of neural crest cell migration. *Development,* 129**,** 3621-3632.
SASAHARA, Y., RACHID, R., BYRNE, M. J., DE LA FUENTE, M. A., ABRAHAM, R. T., RAMESH, N. & GEHA, R. S. 2002. Mechanism of recruitment of WASP to the immunological synapse and of its activation following TCR ligation. *Molecular Cell,* 10**,** 1269-1281.
SASAI, N., MIZUSEKI, K. & SASAI, Y. 2001. Requirement of FoxD3-class signaling for neural crest determination in Xenopus. *Development,* 128**,** 2525-2536.
SATO, A., SCHOLL, A. M., KUHN, E. B., STADT, H. A., DECKER, J. R., PEGRAM, K., HUTSON, M. R. & KIRBY, M. L. 2011. FGF8 signaling is chemotactic for cardiac neural crest cells. *Developmental Biology,* 354**,** 18-30.
SAUKA-SPENGLER, T. & BRONNER-FRASER, M. 2008. A gene regulatory network orchestrates neural crest formation. *Nature Reviews Molecular Cell Biology,* 9**,** 557-568.
SAXENA, A., DENHOLM, B., BUNT, S., BISCHOFF, M., VIJAYRAGHAVAN, K. & SKAER, H. 2014. Epidermal Growth Factor Signalling Controls Myosin II Planar Polarity to Orchestrate Convergent Extension Movements during Drosophila Tubulogenesis. *Plos Biology,* 12.
SAXENA, N., MOGHA, P., DASH, S., MAJUMDER, A., JADHAV, S. & SEN, S. 2018. Matrix elasticity regulates mesenchymal stem cell chemotaxis. *Journal of Cell Science,* 131.
SCARPA, E. & MAYOR, R. 2016. Collective cell migration in development. *The Journal of cell biology,* 212**,** 143-55.
SCARPA, E., SZABO, A., BIBONNE, A., THEVENEAU, E., PARSONS, M. & MAYOR, R. 2015. Cadherin Switch during EMT in Neural Crest Cells Leads to Contact Inhibition of Locomotion via Repolarization of Forces. *Developmental Cell,* 34**,** 421-434.
SCHATTEMAN, G. C., MORRISONGRAHAM, K., VANKOPPEN, A., WESTON, J. A. & BOWENPOPE, D. F. 1992. Regulation and role of PDGF receptor alpha-subunit expression during embryogenesis. *Development,* 115**,** 123-131.
SCHILLING, T. F. & KIMMEL, C. B. 1994. SEGMENT AND CELL-TYPE LINEAGE RESTRICTIONS DURING PHARYNGEAL ARCH DEVELOPMENT IN THE ZEBRAFISH EMBRYO. *Development,* 120**,** 483-494.
SCHMIDT, M., PAES, K., DE MAZIERE, A., SMYCZEK, T., YANG, S., GRAY, A., FRENCH, D., KASMAN, I., KLUMPERMAN, J., RICE, D. S. & YE, W. L. 2007. EGFL7 regulates the collective migration of endothelial cells by restricting their spatial distribution. *Development,* 134**,** 2913-2923.
SCHREIBER, S. C., GIEHL, K., KASTILAN, C., HASEL, C., MUHLENHOFF, M., ADLER, G., WEDLICH, D. & MENKE, A. 2008. Polysialylated NCAM represses E-cadherin-mediated cell-cell adhesion in pancreatic tumor cells. *Gastroenterology,* 134**,** 1555-1566.
SEDDIKI, R., NARAYANA, G., STRALE, P. O., BALCIOGLU, H. E., PEYRET, G., YAO, M. X., LE, A. P., LIM, C. T., YAN, J., LADOUX, B. & MEGE, R. M. 2018. Force-dependent binding of vinculin to alpha-catenin regulates cell-cell contact stability and collective cell behavior. *Molecular Biology of the Cell,* 29**,** 380-388.
SELA-DONENFELD, D. & KALCHEIM, C. 2000. Inhibition of noggin expression in the dorsal neural tube by somitogenesis: a mechanism for coordinating the timing of neural crest emigration. *Development,* 127**,** 4845-4854.
SELLECK, M. A. J. & BRONNER-FRASER, M. 1995. Origins of the avian neural crest - the role of enural plate-epidermal interactions. *Development,* 121**,** 525-538.
SHARMA, A., HALDER, S., FELIX, M., NISAA, K., DESHPANDE, G. & PRASAD, M. 2018. Insulin signaling modulates border cell movement in Drosophila oogenesis. *Development,* 145.
SHATTIL, S. J. 1995. FUNCTION AND REGULATION OF THE BETA(3) INTEGRINS IN HEMOSTASIS AND VASCULAR BIOLOGY. *Thrombosis and Haemostasis,* 74**,** 149-155.
SHELLARD, A. & MAYOR, R. 2016. Chemotaxis during neural crest migration. *Seminars in Cell & Developmental Biology,* 55**,** 111-118.
SHEN, B., DELANEY, M. K. & DU, X. P. 2012. Inside-out, outside-in, and inside-outside-in: G protein signaling in integrin-mediated cell adhesion, spreading, and retraction. *Current Opinion in Cell Biology,* 24**,** 600-606.
SHI, J. L., SEVERSON, C., YANG, J. X., WEDLICH, D. & KLYMKOWSKY, M. W. 2011. Snail2 controls mesodermal BMP/Wnt induction of neural crest. *Development,* 138**,** 3135-3145.
SHINDO, A. 2018. Models of convergent extension during morphogenesis. *Wiley Interdisciplinary Reviews-Developmental Biology,* 7.

SHINDO, A. & WALLINGFORD, J. B. 2014. PCP and Septins Compartmentalize Cortical Actomyosin to Direct Collective Cell Movement. *Science,* 343**,** 649-652.
SHINTANI, Y., FUKUMOTO, Y., CHAIKA, N., SVOBODA, R., WHEELOCK, M. J. & JOHNSON, K. R. 2008. Collagen I-mediated up-regulation of N-cadherin requires cooperative signals from integrins and discoidin domain receptor 1. *Journal of Cell Biology,* 180**,** 1277-1289.
SHNITSAR, I. & BORCHERS, A. 2008. PTK7 recruits dsh to regulate neural crest migration. *Development,* 135**,** 4015-4024.
SHONE, V. & GRAHAM, A. 2014. Endodermal/ectodermal interfaces during pharyngeal segmentation in vertebrates. *Journal of Anatomy,* 225**,** 479-491.
SIEG, D. J., HAUCK, C. R., ILIC, D., KLINGBEIL, C. K., SCHAEFER, E., DAMSKY, C. H. & SCHLAEPFER, D. D. 2000. FAK integrates growth-factor and integrin signals to promote cell migration. *Nature Cell Biology,* 2**,** 249-256.
SIEKMANN, A. F. & LAWSON, N. D. 2007. Notch signalling limits angiogenic cell behaviour in developing zebrafish arteries. *Nature,* 445**,** 781-784.
SILVER, D. L. & MONTELL, D. J. 2001. Paracrine signaling through the JAK/STAT pathway activates invasive behavior of ovarian epithelial cells in Drosophila. *Cell,* 107**,** 831-841.
SIMKIN, J. E., ZHANG, D. C., ROLLO, B. N. & NEWGREEN, D. F. 2013. Retinoic Acid Upregulates Ret and Induces Chain Migration and Population Expansion in Vagal Neural Crest Cells to Colonise the Embryonic Gut. *Plos One,* 8.
SIMOES, S. D., MAINIERI, A. & ZALLEN, J. A. 2014. Rho GTPase and Shroom direct planar polarized actomyosin contractility during convergent extension. *Journal of Cell Biology,* 204**,** 575-589.
SIMOES-COSTA, M. & BRONNER, M. E. 2015. Establishing neural crest identity: a gene regulatory recipe. *Development,* 142**,** 242-257.
SIMPSON, K. J., SELFORS, L. M., BUI, J., REYNOLDS, A., LEAKE, D., KHVOROVA, A. & BRUGGE, J. S. 2008. Identification of genes that regulate epithelial cell migration using an siRNA screening approach. *Nature Cell Biology,* 10**,** 1027-1038.
SMALL, J. V. & KAVERINA, I. 2003. Microtubules meet substrate adhesions to arrange cell polarity. *Current Opinion in Cell Biology,* 15**,** 40-47.
SMALLEY, K. S. M., BRAFFORD, P., HAASS, N. K., BRANDNER, J. M., BROWN, E. & HERLYN, M. 2005. Up-regulated expression of zonula occludens protein-1 in human melanoma associates with N-cadherin and contributes to invasion and adhesion. *American Journal of Pathology,* 166**,** 1541-1554.
SMITH, A., ROBINSON, V., PATEL, K. & WILKINSON, D. G. 1997. The EphA4 and EphB1 receptor tyrosine kinases and ephrin-B2 ligand regulate targeted migration of branchial neural crest cells. *Current Biology,* 7**,** 561-570.
SMOLA, H., STARK, H. J., THIEKOTTER, G., MIRANCEA, N., KRIEG, T. & FUSENIG, N. E. 1998. Dynamics of basement membrane formation by keratinocyte-fibroblast interactions in organotypic skin culture. *Experimental Cell Research,* 239**,** 399-410.
SMUTNY, M., AKOS, Z., GRIGOLON, S., SHAMIPOUR, S., RUPRECHT, V., CAPEK, D., BEHRNDT, M., PAPUSHEVA, E., TADA, M., HOF, B., VICSEK, T., SALBREUX, G. & HEISENBERG, C. P. 2017. Friction forces position the neural anlage. *Nature Cell Biology,* 19**,** 306-+.
SODERLING, S. H., BINNS, K. L., WAYMAN, G. A., DAVEE, S. M., ONG, S. H., PAWSON, T. & SCOTT, J. D. 2002. The WRP component of the WAVE-1 complex attenuates Rac-mediated signalling. *Nature Cell Biology,* 4**,** 970-975.
SORIANO, P. 1997. The PDGF alpha receptor is required for neural crest cell development and for normal patterning of the somites. *Development,* 124**,** 2691-2700.
SQUARR, A. J., BRINKMANN, K., CHEN, B. Y., STEINBACHER, T., EBNET, K., ROSEN, M. K. & BOGDAN, S. 2016. Fat2 acts through the WAVE regulatory complex to drive collective cell migration during tissue rotation. *Journal of Cell Biology,* 212**,** 591-603.
SRINIVASAN, S., WANG, F., GLAVAS, S., OTT, A., HOFMANN, F., AKTORIES, K., KALMAN, D. & BOURNE, H. R. 2003. Rac and Cdc42 play distinct roles in regulating PI(3,4,5)P-3 and polarity during neutrophil chemotaxis. *Journal of Cell Biology,* 160**,** 375-385.
STEHBENS, S. & WITTMANN, T. 2012. Targeting and transport: How microtubules control focal adhesion dynamics. *Journal of Cell Biology,* 198**,** 481-489.
STEMPLE, D. L. & ANDERSON, D. J. 1993. Lineage diversification of the neural crest - in-vitro investigations. *Developmental Biology,* 159**,** 12-23.
STERNLICHT, M. D. & WERB, Z. 2001. How matrix metalloproteinases regulate cell behavior. *Annual Review of Cell and Developmental Biology,* 17**,** 463-516.
STEVENTON, B., ARAYA, C., LINKER, C., KURIYAMA, S. & MAYOR, R. 2009. Differential requirements of BMP and Wnt signalling during gastrulation and neurulation define two steps in neural crest induction. *Development,* 136**,** 771-779.
STEVENTON, B., CARMONA-FONTAINE, C. & MAYOR, R. 2005. Genetic network during neural crest induction: From cell specification to cell survival. *Seminars in Cell & Developmental Biology,* 16**,** 647-654.
STEVENTON, B., MAYOR, R. & STREIT, A. 2014. Neural crest and placode interaction during the development of the cranial sensory system. *Developmental Biology,* 389**,** 28-38.
STRAMER, B. M., DUNN, G. A., DAVIS, J. R. & MAYOR, R. 2013. Rediscovering contact inhibition in the embryo. *Journal of Microscopy,* 251**,** 206-211.
STREIT, A. & STERN, C. D. 1999. Establishment and maintenance of the border of the neural plate in the chick: involvement of FGF and BMP activity. *Mechanisms of Development,* 82**,** 51-66.
SUETSUGU, S., HATTORI, M., MIKI, H., TEZUKA, T., YAMAMOTO, T., MIKOSHIBA, K. & TAKENAWA, T. 2002. Sustained activation of N-WASP through phosphorylation is essential for neurite extension. *Developmental Cell,* 3**,** 645-658.
SUFFOLETTO, K., JETTA, D. & HUA, S. Z. 2018. E-cadherin mediated lateral interactions between neighbor cells necessary for collective migration. *Journal of Biomechanics,* 71**,** 159-166.

SUNYER, R., CONTE, V., ESCRIBANO, J., ELOSEGUI-ARTOLA, A., LABERNADIE, A., VALON, L., NAVAJAS, D., GARCIA-AZNAR, J. M., MUNOZ, J. J., ROCA-CUSACHS, P. & TREPAT, X. 2016. Collective cell durotaxis emerges from long-range intercellular force transmission. *Science,* 353**,** 1157-1161.

SVETIC, V., HOLLWAY, G. E., ELWORTHY, S., CHIPPERFIELD, T. R., DAVISON, C., ADAMS, R. J., EISEN, J. S., INGHAM, P. W., CURRIE, P. D. & KELSH, R. N. 2007. Sdf1a patterns zebrafish melanophores and links the somite and melanophore pattern defects in choker mutants. *Development,* 134**,** 1011-1022.

SWANEY, K. F., HUANG, C.-H. & DEVREOTES, P. N. 2010. Eukaryotic Chemotaxis: A Network of Signaling Pathways Controls Motility, Directional Sensing, and Polarity. *Annual Review of Biophysics, Vol 39,* 39**,** 265-289.

SZABO, A. & MAYOR, R. 2015. Cell traction in collective cell migration and morphogenesis: The chase and run mechanism. *Cell Adhesion & Migration,* 9**,** 380-383.

SZABO, A., MELCHIONDA, M., NASTASI, G., WOODS, M. L., CAMPO, S., PERRIS, R. & MAYOR, R. 2016. In vivo confinement promotes collective migration of neural crest cells. *Journal of Cell Biology,* 213**,** 543-555.

TACHIBANA, K., HIROTA, S., IIZASA, H., YOSHIDA, H., KAWABATA, K., KATAOKA, Y., KITAMURA, Y., MATSUSHIMA, K., YOSHIDA, N., NISHIKAWA, S., KISHIMOTO, T. & NAGASAWA, T. 1998. The chemokine receptor CXCR4 is essential for vascularization of the gastrointestinal tract. *Nature,* 393**,** 591-594.

TADA, M. & HEISENBERG, C. P. 2012. Convergent extension: using collective cell migration and cell intercalation to shape embryos. *Development,* 139**,** 3897-3904.

TAKAKURA, N., YOSHIDA, H., OGURA, Y., KATAOKA, H., NISHIKAWA, S. & NISHIKAWA, S. I. 1997. PDGFR alpha expression during mouse embryogenesis: Immunolocalization analyzed by whole-mount immunohistostaining using the monoclonal anti-mouse PDGFR alpha antibody APA5. *Journal of Histochemistry & Cytochemistry,* 45**,** 883-893.

TALLQUIST, M. D. & SORIANO, P. 2003. Cell autonomous requirement for PDGFR alpha in populations of cranial and cardiac neural crest cells. *Development,* 130**,** 507-518.

TALLQUIST, M. D., WEISMANN, K. E., HELLSTROM, M. & SORIANO, P. 2000. Early myotome specification regulates PDGFA expression and axial skeleton development. *Development,* 127**,** 5059-5070.

TAMBE, D. T., HARDIN, C. C., ANGELINI, T. E., RAJENDRAN, K., PARK, C. Y., SERRA-PICAMAL, X., ZHOU, E. H., ZAMAN, M. H., BUTLER, J. P., WEITZ, D. A., FREDBERG, J. J. & TREPAT, X. 2011. Collective cell guidance by cooperative intercellular forces. *Nature Materials,* 10**,** 469-475.

TAMKUN, J. W., DESIMONE, D. W., FONDA, D., PATEL, R. S., BUCK, C., HORWITZ, A. F. & HYNES, R. O. 1986. STRUCTURE OF INTEGRIN, A GLYCOPROTEIN INVOLVED IN THE TRANSMEMBRANE LINKAGE BETWEEN FIBRONECTIN AND ACTIN. *Cell,* 46**,** 271-282.

TANAKA, M., KIKUCHI, T., UNO, H., OKITA, K., KITANISHI-YUMURA, T. & YUMURA, S. 2017. Turnover and flow of the cell membrane for cell migration. *Scientific Reports,* 7.

TANEYHILL, L. A. 2008. To adhere or not to adhere The role of Cadherins in neural crest development. *Cell Adhesion & Migration,* 2**,** 223-230.

TANEYHILL, L. A., COLES, E. G. & BRONNER-FRASER, M. 2007. Snail2 directly represses cadherin6B during epithelial-tomesenchymal transitions of the neural crest. *Development,* 134**,** 1481-1490.

TEDDER, T. F., STEEBER, D. A., CHEN, A. & ENGEL, P. 1995. THE SELECTINS - VASCULAR ADHESION MOLECULES. *Faseb Journal,* 9**,** 866-873.

TEDDY, J. M. & KULESA, P. M. 2004. In vivo evidence for short- and long-range cell communication in cranial neural crest cells. *Development,* 131**,** 6141-6151.

TEILLET, M. A., KALCHEIM, C. & LEDOUARIN, N. M. 1987. Formation of the dorsal-root ganglia in the avian embryo - segmenteal origin and migratory behavior of neural crest progenitor cells. *Developmental Biology,* 120**,** 329-347.

TESTAZ, S. & DUBAND, J. L. 2001. Central role of the alpha 4 beta 1 integrin in the coordination of avian truncal neural crest cell adhesion, migration, and survival. *Developmental Dynamics,* 222**,** 127-140.

THEISEN, H., PURCELL, J., BENNETT, M., KANSAGARA, D., SYED, A. & MARSH, J. L. 1994. DISHEVELLED IS REQUIRED DURING WINGLESS SIGNALING TO ESTABLISH BOTH CELL POLARITY AND CELL IDENTITY. *Development,* 120**,** 347-360.

THEVENEAU, E., DUBAND, J. L. & ALTABEF, M. 2007. Ets-1 Confers Cranial Features on Neural Crest Delamination. *Plos One,* 2.

THEVENEAU, E. & LINKER, C. 2017. Leaders in collective migration : are front cells really endowed with a particular set of skills ? *F1000Research,* 6.

THEVENEAU, E., MARCHANT, L., KURIYAMA, S., GULL, M., MOEPPS, B., PARSONS, M. & MAYOR, R. 2010. Collective Chemotaxis Requires Contact-Dependent Cell Polarity. *Developmental Cell,* 19**,** 39-53.

THEVENEAU, E. & MAYOR, R. 2011a. Beads on the Run: Beads as Alternative Tools for Chemotaxis Assays. *Cell Migration: Developmental Methods and Protocols, Second Edition,* 769**,** 449-460.

THEVENEAU, E. & MAYOR, R. 2011b. Can mesenchymal cells undergo collective cell migration? The case of the neural crest. *Cell Adhesion & Migration,* 5**,** 490-498.

THEVENEAU, E. & MAYOR, R. 2011c. Collective Cell Migration of the Cephalic Neural Crest: The Art of Integrating Information. *Genesis,* 49**,** 164-176.

THEVENEAU, E. & MAYOR, R. 2012a. Cadherins in collective cell migration of mesenchymal cells. *Current Opinion in Cell Biology,* 24**,** 677-684.

THEVENEAU, E. & MAYOR, R. 2012b. Neural crest delamination and migration: From epithelium-to-mesenchyme transition to collective cell migration. *Developmental Biology,* 366**,** 34-54.

THEVENEAU, E. & MAYOR, R. 2012c. Neural crest migration: interplay between chemorepellents, chemoattractants, contact inhibition, epithelial-mesenchymal transition, and collective cell migration. *Wiley Interdisciplinary Reviews-Developmental Biology,* 1**,** 435-445.

THEVENEAU, E., STEVENTON, B., SCARPA, E., GARCIA, S., TREPAT, X., STREIT, A. & MAYOR, R. 2013. Chase-and-run between adjacent cell populations promotes directional collective migration. *Nature Cell Biology,* 15**,** 763-+.

THIERY, J. P., ACLOQUE, H., HUANG, R. Y. J. & ANGELA NIETO, M. 2009. Epithelial-Mesenchymal Transitions in Development and Disease. *Cell,* 139**,** 871-890.

THIERY, J. P. & MORGAN, M. 2004. Breast cancer progression with a Twist. *Nature Medicine,* 10**,** 777-778.
THIEVESSEN, I., THOMPSON, P. M., BERLEMONT, S., PLEVOCK, K. M., PLOTNIKOV, S. V., ZEMLJIC-HARPF, A., ROSS, R. S., DAVIDSON, M. W., DANUSER, G., CAMPBELL, S. L. & WATERMAN, C. M. 2013. Vinculin-actin interaction couples actin retrograde flow to focal adhesions, but is dispensable for focal adhesion growth. *Journal of Cell Biology,* 202**,** 163-177.
THOMPSON, E. W. & WILLIAMS, E. D. 2008. EMT and MET in carcinoma - clinical observations, regulatory pathways and new models. *Clinical & Experimental Metastasis,* 25**,** 591-592.
TOMLINSON, M. L., GUAN, P. P., MORRIS, R. J., FIDOCK, M. D., REJZEK, M., GARCIA-MORALES, C., FIELD, R. A. & WHEELER, G. N. 2009. A Chemical Genomic Approach Identifies Matrix Metalloproteinases as Playing an Essential and Specific Role in Xenopus Melanophore Migration. *Chemistry & Biology,* 16**,** 93-104.
TOSNEY, K. W. 1982. The segregation and early migration of cranial neural crest cells in the avian embryo. *Developmental Biology,* 89**,** 13-24.
TOYJANOVA, J., FLORES-CORTEZ, E., REICHNER, J. S. & FRANCK, C. 2015. Matrix Confinement Plays a Pivotal Role in Regulating Neutrophil-generated Tractions, Speed, and Integrin Utilization. *Journal of Biological Chemistry,* 290**,** 3752-3763.
TOYOFUKU, T., YOSHIDA, J., SUGIMOTO, T., YAMAMOTO, M., MAKINO, N., TAKAMATSU, H., TAKEGAHARA, N., SUTO, F., HORI, M., FUJISAWA, H., KUMANOGOH, A. & KIKUTANI, H. 2008. Repulsive and attractive semaphorins cooperate to direct the navigation of cardiac neural crest cells. *Developmental Biology,* 321**,** 251-262.
TOZLUOGLU, M., TOURNIER, A. L., JENKINS, R. P., HOOPER, S., BATES, P. A. & SAHAI, E. 2013. Matrix geometry determines optimal cancer cell migration strategy and modulates response to interventions. *Nature Cell Biology,* 15**,** 751-+.
TREPAT, X. & FREDBERG, J. J. 2011. Plithotaxis and emergent dynamics in collective cellular migration. *Trends in Cell Biology,* 21**,** 638-646.
TREPAT, X., WASSERMAN, M. R., ANGELINI, T. E., MILLET, E., WEITZ, D. A., BUTLER, J. P. & FREDBERG, J. J. 2009. Physical forces during collective cell migration. *Nature Physics,* 5**,** 426-430.
TRIBULO, C., AYBAR, M. J., NGUYEN, V. H., MULLINS, M. C. & MAYOR, R. 2003. Regulation of Msx genes by a Bmp gradient is essential for neural crest specification. *Development,* 130**,** 6441-6452.
TRIBULO, C., AYBAR, M. J., SANCHEZ, S. S. & MAYOR, R. 2004. A balance between the anti-apoptotic activity of Slug and the apoptotic activity of msx1 is required for the proper development of the neural crest. *Developmental Biology,* 275**,** 325-342.
TRICHAS, G., SMITH, A. M., WHITE, N., WILKINS, V., WATANABE, T., MOORE, A., JOYCE, B., SUGNASEELAN, J., RODRIGUEZ, T. A., KAY, D., BAKER, R. E., MAINI, P. K. & SRINIVAS, S. 2012. Multi-Cellular Rosettes in the Mouse Visceral Endoderm Facilitate the Ordered Migration of Anterior Visceral Endoderm Cells. *Plos Biology,* 10.
TROKOVIC, N., TROKOVIC, R., MAI, P. & PARTANEN, J. 2003. Fgfr1 regulates patterning of the pharyngeal region. *Genes & Development,* 17**,** 141-153.
TROKOVIC, N., TROKOVIC, R. & PARTANEN, J. 2005. Fibroblast growth factor signalling and regional specification of the pharyngeal ectoderm. *International Journal of Developmental Biology,* 49**,** 797-805.
TSAI, F. C. & MEYER, T. 2012. Ca2+ Pulses Control Local Cycles of Lamellipodia Retraction and Adhesion along the Front of Migrating Cells. *Current Biology,* 22**,** 837-842.
TSUJI, T., ISHIZAKI, T., OKAMOTO, M., HIGASHIDA, C., KIMURA, K., FURUYASHIKI, T., ARAKAWA, Y., BIRGE, R. B., NAKAMOTO, T., HIRAI, H. & NARUMIYA, S. 2002. ROCK and mDia1 antagonize in Rho-dependent Rac activation in Swiss 3T3 fibroblasts. *Journal of Cell Biology,* 157**,** 819-830.
TUCKER, R. P. 2001. Abnormal neural crest cell migration after the in vivo knockdown of tenascin-C expression with morpholino antisense oligonucleotides. *Developmental Dynamics,* 222**,** 115-119.
TURNER, C. E., WEST, K. A. & BROWN, M. C. 2001. Paxillin-ARF GAP signaling and the cytoskeleton. *Current Opinion in Cell Biology,* 13**,** 593-599.
UHLENHUTH, E. 1914. Cultivation of the skin epithelium of the adult frog, Rana pipiens. *Journal of Experimental Medicine,* 20**,** 614-635.
ULMER, B., HAGENLOCHER, C., SCHMALHOLZ, S., KURZ, S., SCHWEICKERT, A., KOHL, A., ROTH, L., SELA-DONENFELD, D. & BLUM, M. 2013. Calponin 2 Acts As an Effector of Noncanonical Wnt-Mediated Cell Polarization during Neural Crest Cell Migration. *Cell Reports,* 3**,** 615-621.
VAEZI, A., BAUER, C., VASIOUKHIN, V. & FUCHS, E. 2002. Actin cable dynamics and Rho/Rock orchestrate a polarized cytoskeletal architecture in the early steps of assembling a stratified epithelium. *Developmental Cell,* 3**,** 367-381.
VALENTIN, G., HAAS, P. & GILMOUR, D. 2007. The chemokine SDF1a coordinates tissue migration through the spatially restricted activation of Cxcr7 and Cxcr4b. *Current Biology,* 17**,** 1026-1031.
VALLIN, J., GIRAULT, J. M., THIERY, J. P. & BRODERS, F. 1998. Xenopus cadherin-11 is expressed in different populations of migrating neural crest cells. *Mechanisms of Development,* 75**,** 171-174.
VALON, L., MARIN-LLAURADO, A., WYATT, T., CHARRAS, G. & TREPAT, X. 2017. Optogenetic control of cellular forces and mechanotransduction. *Nature Communications,* 8.
VAN DE PUTTE, T., MARUHASHI, M., FRANCIS, A., NELLES, L., KONDOH, H., HUYLEBROECK, D. & HIGASHI, Y. 2003. Mice lacking Zfhx1b, the gene that codes for Smad- interacting protein-1, reveal a role for multiple neural crest cell defects in the etiology of Hirschsprung disease-mental retardation syndrome. *American Journal of Human Genetics,* 72**,** 465-470.
VAN GRUNSVEN, L. A., TAELMAN, V., MICHIELS, C., VERSTAPPEN, G., SOUOPGUI, J., NICHANE, M., MOENS, E., OPDECAMP, K., VANHOMWEGEN, J., KRICHA, S., HUYLEBROECK, D. & BELLEFROID, E. J. 2007. XSip1 neuralizing activity involves the co-repressor CtBP and occurs through BMP dependent and independent mechanisms. *Developmental Biology,* 306**,** 34-49.
VAN KEMPEN, L., VAN DEN OORD, J. J., VAN MUIJEN, G. N. P., WEIDLE, U. H., BLOEMERS, H. P. J. & SWART, G. W. M. 2000. Activated leukocyte cell adhesion molecule/CD166, a marker of tumor progression in primary malignant melanoma of the skin. *American Journal of Pathology,* 156**,** 769-774.

VANDEWALLE, C., COMIJN, J., DE CRAENE, B., VERMASSEN, P., BRUYNEEL, E., ANDERSEN, H., TULCHINSKY, E., VAN ROY, F. & BERX, G. 2005. SIP1/ZEB2 induces EMT by repressing genes of different epithelial cell-cell junctions. *Nucleic Acids Research,* 33**,** 6566-6578.
VASIOUKHIN, V., BAUER, C., YIN, M. & FUCHS, E. 2000. Directed actin polymerization is the driving force for epithelial cell-cell adhesion. *Cell,* 100**,** 209-219.
VASQUEZ, C. G., TWOROGER, M. & MARTIN, A. C. 2014. Dynamic myosin phosphorylation regulates contractile pulses and tissue integrity during epithelial morphogenesis. *Journal of Cell Biology,* 206**,** 435-450.
VASSILEV, V., PLATEK, A., HIVER, S., ENOMOTO, H. & TAKEICHI, M. 2017. Catenins Steer Cell Migration via Stabilization of Front-Rear Polarity. *Developmental Cell,* 43**,** 463-+.
VASTRIK, I., EICKHOLT, B. J., WALSH, F. S., RIDLEY, A. & DOHERTY, P. 1999. Sema3A-induced growth-cone collapse is mediated by Rac1 amino acids 17-32. *Current Biology,* 9**,** 991-998.
VAUGHAN, R. B. & TRINKAUS, J. P. 1966. MOVEMENTS OF EPITHELIAL CELL SHEETS IN VITRO. *Journal of Cell Science,* 1**,** 407-&.
VEDULA, S. R. K., RAVASIO, A., LIM, C. T. & LADOUX, B. 2013. Collective Cell Migration: A Mechanistic Perspective. *Physiology,* 28**,** 370-379.
VEGA, S., MORALES, A. V., OCANA, O. H., VALDES, F., FABREGAT, I. & NIETO, M. A. 2004. Snail blocks the cell cycle and confers resistance to cell death. *Genes & Development,* 18**,** 1131-1143.
VEITCH, E., BEGBIE, J., SCHILLING, T. F., SMITH, M. M. & GRAHAM, A. 1999. Pharyngeal arch patterning in the absence of neural crest. *Current Biology,* 9**,** 1481-1484.
VENKITESWARAN, G., LEWELLIS, S. W., WANG, J., REYNOLDS, E., NICHOLSON, C. & KNAUT, H. 2013. Generation and Dynamics of an Endogenous, Self-Generated Signaling Gradient across a Migrating Tissue. *Cell,* 155**,** 674-687.
VENTRE, M., CAUSA, F. & NETTI, P. A. 2012. Determinants of cell-material crosstalk at the interface: towards engineering of cell instructive materials. *Journal of the Royal Society Interface,* 9**,** 2017-2032.
VICENTE-MANZANARES, M., MA, X. F., ADELSTEIN, R. S. & HORWITZ, A. R. 2009. Non-muscle myosin II takes centre stage in cell adhesion and migration. *Nature Reviews Molecular Cell Biology,* 10**,** 778-790.
VIG, D. K., HAMBY, A. E. & WOLGEMUTH, C. W. 2017. Cellular Contraction Can Drive Rapid Epithelial Flows. *Biophysical Journal,* 113**,** 1613-1622.
VIKTORINOVA, I. & DAHMANN, C. 2013. Microtubule Polarity Predicts Direction of Egg Chamber Rotation in Drosophila. *Current Biology,* 23**,** 1472-1477.
VILLAR-CERVINO, V., MOLANO-MAZON, M., CATCHPOLE, T., VALDEOLMILLOS, M., HENKEMEYER, M., MARTINEZ, L. M., BORRELL, V. & MARIN, O. 2013. Contact Repulsion Controls the Dispersion and Final Distribution of Cajal-Retzius Cells. *Neuron,* 77**,** 457-471.
VINCENT, S., WILSON, R., COELHO, C., AFFOLTER, M. & LEPTIN, M. 1998. The Drosophila protein Dof is specifically required for FGF signaling. *Molecular Cell,* 2**,** 515-525.
VISHWAKARMA, M., DI RUSSO, J., PROBST, D., SCHWARZ, U. S., DAS, T. & SPATZ, J. P. 2018. Mechanical interactions among followers determine the emergence of leaders in migrating epithelial cell collectives. *Nature Communications,* 9.
VITORINO, P. & MEYER, T. 2008. Modular control of endothelial sheet migration. *Genes & Development,* 22**,** 3268-3281.
VOICULESCU, O., BERTOCCHINI, F., WOLPERT, L., KELLER, R. E. & STERN, C. D. 2007. The amniote primitive streak is defined by epithelial cell intercalation before gastrulation. *Nature,* 449**,** 1049-1052.
WALKER, A. S., BURRONE, J. & MEYER, M. P. 2013. Functional imaging in the zebrafish retinotectal system using RGECO. *Frontiers in Neural Circuits,* 7.
WALSHE, J. & MASON, I. 2003. Unique and combinatorial functions of Fgf3 and Fgf8 during zebrafish forebrain development. *Development,* 130**,** 4337-4349.
WANG, C. L., CHOWDHURY, S., DRISCOLL, M., PARENT, C. A., GUPTA, S. K. & LOSERT, W. 2014. The interplay of cell-cell and cell-substrate adhesion in collective cell migration. *Journal of the Royal Society Interface,* 11.
WANG, H. U. & ANDERSON, D. J. 1997. Eph family transmembrane ligands can mediate repulsive guidance of trunk neural crest migration and motor axon outgrowth. *Neuron,* 18**,** 383-396.
WANG, Q., UHLIROVA, M. & BOHMANN, D. 2010a. Spatial Restriction of FGF Signaling by a Matrix Metalloprotease Controls Branching Morphogenesis. *Developmental Cell,* 18**,** 157-164.
WANG, X. B., HE, L., WU, Y. I., HAHN, K. M. & MONTELL, D. J. 2010b. Light-mediated activation reveals a key role for Rac in collective guidance of cell movement in vivo. *Nature Cell Biology,* 12**,** 591-U154.
WATANABE, N. & MITCHISON, T. J. 2002. Single-molecule speckle analysis of Aactin filament turnover in lamellipodia. *Science,* 295**,** 1083-1086.
WAXMAN, N. M. 2018. CaM Kinases: Contribution for Biomedical Sciences. *Reference Module in Biomedical Sciences*.
WEBB, D. J., PARSONS, J. T. & HORWITZ, A. F. 2002. Adhesion assembly, disassembly and turnover in migrating cells - over and over and over again. *Nature Cell Biology,* 4**,** E97-E100.
WEBER, G. F., BJERKE, M. A. & DESIMONE, D. W. 2012. A Mechanoresponsive Cadherin-Keratin Complex Directs Polarized Protrusive Behavior and Collective Cell Migration. *Developmental Cell,* 22**,** 104-115.
WEDLICH-SOLDNER, R. & LI, R. 2003. Spontaneous cell polarization: undermining determinism. *Nature Cell Biology,* 5**,** 267-270.
WEHRLE-HALLER, B. 2012. Assembly and disassembly of cell matrix adhesions. *Current Opinion in Cell Biology,* 24**,** 569-581.
WEI, J., HORTSCH, M. & GOODE, S. 2004. Neuroglian stabilizes epithelial structure during Drosophila oogenesis. *Developmental Dynamics,* 230**,** 800-808.
WEI, S. C., FATTET, L., TSAI, J. H., GUO, Y. R., PAI, V. H., MAJESKI, H. E., CHEN, A. C., SAH, R. L., TAYLOR, S. S., ENGLER, A. J. & YANG, J. 2015. Matrix stiffness drives epithelial mesenchymal transition and tumour metastasis through a TWIST1-G3BP2 mechanotransduction pathway. *Nature Cell Biology,* 17**,** 678-U306.
WEIJER, C. J. 2009. Collective cell migration in development. *Journal of Cell Science,* 122**,** 3215-3223.
WELCH, H. C. E., COADWELL, W. J., STEPHENS, L. R. & HAWKINS, P. T. 2003. Phosphoinositide 3-kinase-dependent activation of Rac. *Febs Letters,* 546**,** 93-97.

WELCH, M. D. 2015. Cell Migration, Freshly Squeezed. *Cell,* 160**,** 581-582.
WELCH, M. D. & MULLINS, R. D. 2002. Cellular control of actin nucleation. *Annual Review of Cell and Developmental Biology,* 18**,** 247-288.
WESTERFIELD, M. 2000. *The Zebrafish Book. A Guide for The Laboratory Use of Zebrafish (Danio rerio)*.
WILSON, A. L., SHEN, Y. C., BABB-CLENDENON, S. G., ROSTEDT, J., LIU, B., BARALD, K. F., MARRS, J. A. & LIU, Q. 2007. Cadherin-4 plays a role in the development of zebrafish cranial ganglia and lateral line system. *Developmental Dynamics,* 236**,** 893-902.
WINKLBAUER, R., SELCHOW, A., NAGEL, M. & ANGRES, B. 1992. CELL-INTERACTION AND ITS ROLE IN MESODERM CELL-MIGRATION DURING XENOPUS GASTRULATION. *Developmental Dynamics,* 195**,** 290-302.
WINNING, R. S., SCALES, J. B. & SARGENT, T. D. 1996. Disruption of cell adhesion in Xenopus embryos by Pagliaccio, an Eph-class receptor tyrosine kinase. *Developmental Biology,* 179**,** 309-319.
WINTER, C. G., WANG, B., BALLEW, A., ROYOU, A., KARESS, R., AXELROD, J. D. & LUO, L. Q. 2001. Drosophila Rho-associated kinase (Drok) links frizzled-mediated planar cell polarity signaling to the actin cytoskeleton. *Cell,* 105**,** 81-91.
WISZNIAK, S., MACKENZIE, F. E., ANDERSON, P., KABBARA, S., RUHRBERG, C. & SCHWARZ, Q. 2015. Neural crest cell-derived VEGF promotes embryonic jaw extension. *Proceedings of the National Academy of Sciences of the United States of America,* 112**,** 6086-6091.
WITZEL, S., ZIMYANIN, V., CARREIRA-BARBOSA, F., TADA, M. & HEISENBERG, C. P. 2006. Wnt11 controls cell contact persistence by local accumulation of Frizzled 7 at the plasma membrane. *Journal of Cell Biology,* 175**,** 791-802.
WODA, J. M., PASTAGIA, J., MERCOLA, M. & ARTINGER, K. B. 2003. Dix proteins position the neural plate border and determine adjacent cell fates. *Development,* 130**,** 331-342.
WOLF, K. & FRIEDL, P. 2006. Molecular mechanisms of cancer cell invasion and plasticity. *British Journal of Dermatology,* 154**,** 11-15.
WOLF, K., WU, Y. I., LIU, Y., GEIGER, J., TAM, E., OVERALL, C., STACK, M. S. & FRIEDL, P. 2007. Multi-step pericellular proteolysis controls the transition from individual to collective cancer cell invasion. *Nature Cell Biology,* 9**,** 893-U39.
WOLFENSON, H., LAVELIN, I. & GEIGER, B. 2013. Dynamic Regulation of the Structure and Functions of Integrin Adhesions. *Developmental Cell,* 24**,** 447-458.
WOLFF, T. & RUBIN, G. M. 1998. strabismus, a novel gene that regulates tissue polarity and cell fate decisions in Drosophila. *Development,* 125**,** 1149-1159.
WOOD, W., JACINTO, A., GROSE, R., WOOLNER, S., GALE, J., WILSON, C. & MARTIN, P. 2002. Wound healing recapitulates morphogenesis in Drosophila embryos. *Nature Cell Biology,* 4**,** 907-912.
WOODS, A. & COUCHMAN, J. R. 2001. Syndecan-4 and focal adhesion function. *Current Opinion in Cell Biology,* 13**,** 578-583.
WOODS, A., LONGLEY, R. L., TUMOVA, S. & COUCHMAN, J. R. 2000. Syndecan-4 binding to the high affinity heparin-binding domain of fibronectin drives focal adhesion formation in fibroblasts. *Archives of Biochemistry and Biophysics,* 374**,** 66-72.
WOODS, M. L., CARMONA-FONTAINE, C., BARNES, C. P., COUZIN, I. D., MAYOR, R. & PAGE, K. M. 2014. Directional Collective Cell Migration Emerges as a Property of Cell Interactions. *Plos One,* 9.
WOOLF, E., GRIGOROVA, I., SAGIV, A., GRABOVSKY, V., FEIGELSON, S. W., SHULMAN, Z., HARTMANN, T., SIXT, M., CYSTER, J. G. & ALON, R. 2007. Lymph node chemokines promote sustained T lymphocyte motility without triggering stable integrin adhesiveness in the absence of shear forcesm. *Nature Immunology,* 8**,** 1076-1085.
WORTHYLAKE, R. A. & BURRIDGE, K. 2003. RhoA and ROCK promote migration by limiting membrane protrusions. *Journal of Biological Chemistry,* 278**,** 13578-13584.
WOZNIAK, M. A., MODZELEWSKA, K., KWONG, L. & KEELY, P. J. 2004. Focal adhesion regulation of cell behavior. *Biochimica Et Biophysica Acta-Molecular Cell Research,* 1692**,** 103-119.
XI, W., SONAM, S., SAW, T. B., LADOUX, B. & LIM, C. T. 2017. Emergent patterns of collective cell migration under tubular confinement. *Nature Communications,* 8.
XU, H., YE, D., BEHRA, M., BURGESS, S., CHEN, S. H. & LIN, F. 2014. G beta 1 controls collective cell migration by regulating the protrusive activity of leader cells in the posterior lateral line primordium. *Developmental Biology,* 385**,** 316-327.
XU, J. S., WANG, F., VAN KEYMEULEN, A., HERZMARK, P., STRAIGHT, A., KELLY, K., TAKUWA, Y., SUGIMOTO, N., MITCHISON, T. & BOURNE, H. R. 2003. Divergent signals and cytoskeletal assemblies regulate self-organizing polarity in neutrophils. *Cell,* 114**,** 201-214.
XU, X., FRANCIS, R., WEI, C. J., LINASK, K. L. & LO, C. W. 2006. Connexin 43-mediated modulation of polarized cell movement and the directional migration of cardiac neural crest cells. *Development,* 133**,** 3629-3639.
XU, X., LI, W. E. I., HUANG, G. Y., MEYER, R., CHEN, T., LUO, Y., THOMAS, M. P., RADICE, G. L. & LO, C. W. 2001a. Modulation of mouse neural crest cell motility by N-cadherin and connexin 43 gap junctions. *Journal of Cell Biology,* 154**,** 217-229.
XU, X., LI, W. E. I., HUANG, G. Y., MEYER, R., CHEN, T., LUO, Y., THOMAS, M. P., RADICE, G. L. & LO, C. W. 2001b. N-cadherin and Cx43 alpha 1 gap junctions modulates mouse neural crest cell motility via distinct pathways. *Cell Communication and Adhesion,* 8**,** 321-+.
YAM, P. T., WILSON, C. A., JI, L., HEBERT, B., BARNHART, E. L., DYE, N. A., WISEMAN, P. W., DANUSER, G. & THERIOT, J. A. 2007. Actin-myosin network reorganization breaks symmetry at the cell rear to spontaneously initiate polarized cell motility. *Journal of Cell Biology,* 178**,** 1207-1221.
YAMADA, S. & NELSON, W. J. 2007. Localized zones of Rho and Rac activities drive initiation and expansion of epithelial cell-cell adhesion. *Journal of Cell Biology,* 178**,** 517-527.
YANA, I., SAGARA, H., TAKAKI, S., TAKATSU, K., NAKAMURA, K., NAKAO, K., KATSUKI, M., TANIGUCHI, S. I., AOKI, T., SATO, H., WEISS, S. J. & SEIKI, M. 2007. Crosstalk between neovessels and mural cells directs the site-specific expression of MT1-MMP to endothelial tip cells. *Journal of Cell Science,* 120**,** 1607-1614.

YANG, X. S., DORMANN, D., MUNSTERBERG, A. E. & WEIJER, C. J. 2002. Cell movement patterns during gastrulation in the chick are controlled by chemotaxis mediated by positive and negative FGF4 and FGF8. *Developmental Cell,* 3**,** 425-437.

YONEMURA, S., WADA, Y., WATANABE, T., NAGAFUCHI, A. & SHIBATA, M. 2010. alpha-Catenin as a tension transducer that induces adherens junction development. *Nature Cell Biology,* 12**,** 533-U35.

YOUNG, H. M., HEARN, C. J., FARLIE, P. G., CANTY, A. J., THOMAS, P. Q. & NEWGREEN, D. F. 2001. GDNF is a chemoattractant for enteric neural cells. *Developmental Biology,* 229**,** 503-516.

YU, C. H., LAW, J. B. K., SURYANA, M., LOW, H. Y. & SHEETZ, M. P. 2011. Early integrin binding to Arg-Gly-Asp peptide activates actin polymerization and contractile movement that stimulates outward translocation. *Proceedings of the National Academy of Sciences of the United States of America,* 108**,** 20585-20590.

YU, H. H. & MOENS, C. B. 2005. Semaphorin signaling guides cranial neural crest cell migration in zebrafish. *Developmental Biology,* 280**,** 373-385.

YUE, W., MOUSTAFA, R. K. A., BIN, D., TIEGANG, H., KUANGCAI, C., JIN, C., YAN, T., NING, F., FANGJUN, W. & MOSTAFA, A. E.-S. 2018. Gold Nanorod Photothermal Therapy Alters Cell Junctions and Actin Network in Inhibiting Cancer Cell Collective Migration. *ACS Nano*.

ZAIDEL-BAR, R., ITZKOVITZ, S., MA'AYAN, A., IYENGAR, R. & GEIGER, B. 2007. Functional atlas of the integrin adhesome. *Nature Cell Biology,* 9**,** 858-868.

ZAJAC, O., RAINGEAUD, J., LIBANJE, F., LEFEBVRE, C., SABINO, D., MARTINS, I., ROY, P., BENATAR, C., CANET-JOURDAN, C., AZORIN, P., POLROT, M., GONIN, P., BENBARCHE, S., SOUQUERE, S., PIERRON, G., NOWAK, D., BIGOT, L., DUCREUX, M., MALKA, D., LOBRY, C., SCOAZEC, J. Y., EVENO, C., POCARD, M., PERFETTINI, J. L., ELIAS, D., DARTIGUES, P., GOERE, D. & JAULIN, F. 2018. Tumour spheres with inverted polarity drive the formation of peritoneal metastases in patients with hypermethylated colorectal carcinomas. *Nature Cell Biology,* 20**,** 296-+.

ZALLEN, J. A. & BLANKENSHIP, J. T. 2008. Multicellular dynamics during epithelial elongation. *Seminars in Cell & Developmental Biology,* 19**,** 263-270.

ZAMIR, E. A., CZIROK, A., CUI, C., LITTLE, C. D. & RONGISH, B. J. 2006. Mesodermal cell displacements during avian gastrulation are due to both individual cell-autonomous and convective tissue movements. *Proceedings of the National Academy of Sciences of the United States of America,* 103**,** 19806-19811.

ZANIN, J. P., LAURA BATTIATO, N. & ROVASIO, R. A. 2013. Neurotrophic factor NT-3 displays a non-canonical cell guidance signaling function for cephalic neural crest cells. *European Journal of Cell Biology,* 92**,** 264-279.

ZHENG, L., ZHANG, J. J. & CARTHEW, R. W. 1995. FRIZZLED REGULATES MIRROR-SYMMETRICAL PATTERN-FORMATION IN THE DROSOPHILA EYE. *Development,* 121**,** 3045-3055.